Investigating conjugative transfer of carbapenem resistance plasmids in *Klebsiella pneumoniae* planktonic and biofilm populations

by

Sarah Jane Element

A thesis submitted to the University of Birmingham for the degree of DOCTOR OF PHILOSOPHY

Institute of Microbiology and Infection
College of Medical and Dental Sciences
University of Birmingham

April 2022

Abstract

Horizontal gene transfer via conjugative plasmids has a large impact on the dissemination of antimicrobial resistance genes. This work focused on studying the transfer of multidrug resistance plasmids in planktonic and biofilm populations of *Klebsiella pneumoniae*. Firstly, a flow cytometry fluorescence reporter system was evaluated for monitoring transfer of the pKpQIL plasmid. Next, plasmid transfer from a set of carbapenemase-producing clinical isolate donors was determined. Isolate CPE16 transferred its carbapenenmase plasmid at high frequency in both planktonic and biofilm populations, with a higher transfer frequency in a biofilm. In some cases, multiple plasmids were transferred from the donors into the recipient. There was no obvious growth impact on transconjugants upon plasmid acquisition. Transconjugant gene expression was investigated to establish any effect of the plasmid on the host transcriptome across three planktonic and biofilm conditions. The effect of lifestyle on plasmid gene expression was also determined. This revealed that plasmid carriage in the biofilm lifestyle had the largest impact on the host transcriptome, and that lifestyle affected plasmid gene expression.

Acknowledgements

I would like to thank my supervisors, Dr Michelle Buckner and Professor Willem van Schaik, for their encouragement and support throughout.

I feel incredibly privileged to have had the chance to work with several fantastic scientists during this project. For flow cytometry and confocal microscopy technical assistance respectively, thank you to Dr Adriana Flores-Langarica and Dr Alessandro Di Maio. For access to clinical isolates, thank you to Dr Claire McMurray and staff at the Queen Elizabeth Hospital. For assistance with recombineering protocols, thank you to Dr Jack Bryant and Dr Jessica Gray. For assistance with cloning protocols, thank you to Dr Helen McNeil. For Bioinformatics assistance, thank you to all members of the ARM and McNally groups.

Thank you to the University of Birmingham for funding this project, and to the Wellcome Trust Doctoral Training Programme.

Thank you to all members (past and present) of the Buckner lab, ARM, the McNally lab, the Blair lab and ARG for always being willing to help.

Thank you to Dr Beth Grimsey, Dr Georgina Lloyd and Onalenna Neo for all their support.

To Mum, Dad, Nicola and Pete, thank you for being my biggest supporters. Without you this wouldn't have been possible. Thank you so much for all that you do.

Clarification of collaborative work

The agar MIC experiment was prepared and performed by Elizabeth Darby. Sarah Jane Element grew up strains to add to the experiment and read the resulting MIC values for those strains. The data are presented in Table 5.1.

Contents

1 Introduction **1**

1.1 Antimicrobial resistance 1

1.2 Antibiotic resistance 2

1.2.1 Resistance mechanisms 3

1.3 Mechanisms of carbapenem resistance 4

1.3.1 Treatment of carbapenem-resistant infections 5

1.4 *K. pneumoniae* 6

1.4.1 *K. pneumoniae* colonisation and disease 7

1.4.2 Drug-resistant *K. pneumoniae* infections 8

1.4.3 Epidemic clones and plasmids 9

1.5 Horizontal gene transfer in Gram-negative bacteria 10

1.5.1 Conjugation 12

1.5.2 Studying conjugation 14

1.5.3 Conjugative plasmids 16

1.5.4 Plasmid mobilisation 18

1.5.5 F-type plasmids: classification 19

1.5.6 Genetic organisation of F-type conjugation modules 19

1.6 Plasmid features 21

1.6.1 Plasmid carriage and fitness 21

1.7 Mobilisation of resistance genes 22

1.8 Insights from genome sequencing 24

1.8.1 Combining short- and long-read WGS technologies 26

1.8.2 Linking genotype to phenotype 27

1.8.3 RNA-sequencing 28

1.9 Bacterial lifestyles 28

1.9.1 Biofilm and planktonic populations are distinct 30

1.9.2 A method to study biofilms 30

1.10 Importance 31

1.11 Aims, hypotheses and objectives 32

2 Materials and Methods **34**

2.1 Bacterial strains, plasmids and primers 34

2.2 Crystal violet biofilm assays 39

2.3 Growth kinetics 39

2.4 Viable counts . . . 40

2.5 Fluorescence reporter system for flow cytometry and microscopy . . . 40

2.6 Flow cytometry . . . 41

2.6.1 Preparation of biofilm growth plates in 6-well format for flow cytometry . . . 41

2.6.2 Sample preparation for flow cytometry . . . 42

2.6.3 Experiment settings . . . 42

2.7 Microscopy . . . 43

2.8 Construction of KP16 control strain . . . 44

2.9 Conjugation assays . . . 45

2.9.1 Planktonic conjugation assays (plating method) . . . 45

2.9.2 Biofilm conjugation assays (plating method) . . . 46

2.10 Colony PCR . . . 47

2.11 Gel electrophoresis . . . 48

2.12 Construction of a hygromycin-resistant KP1 recipient strain . . . 48

2.12.1 Method overview . . . 48

2.12.2 Method details . . . 49

2.13 Whole Genome Sequencing . . . 53

2.14 RNA-sequencing . . . 54

2.14.1 Evaluating plasmid persistence . . . 55

2.14.2 Processing cell pellets 56

2.15 Bioinformatics 56

2.15.1 Manual annotation 56

2.15.2 Characterisation 56

2.15.3 Phylogenetic tree 57

2.15.4 Strain validation 57

2.15.5 RNA-Seq analysis 57

2.15.6 Statistical analyses and data analyses 58

3 Monitoring conjugation in planktonic and biofilm populations using a fluorescence reporter system 59

3.1 Background 59

3.1.1 Aims and hypotheses 61

3.2 Strain characterisation 61

3.3 Development of a biofilm model 66

3.4 Evaluating plasmid transmission in *K. pneumoniae* using flow cytometry 71

3.4.1 Evaluating the contribution of coincident events 73

3.4.2 Adjusting the acquisition setup 78

3.5 Discussion 80

3.6 Conclusions 88

3.6.1 Key findings 89

4 Investigating the plasmid and AMR gene content of five carbapenemase-producing *K. pneumoniae* (CPE) clinical isolates 90

4.1 Background 90

4.2 Core genome phylogenetic analysis 92

4.3 Investigating the accessory genome 98

4.4 Carbapenem resistance plasmids 102

4.5 Discussion 109

4.6 Limitations and future work 114

4.7 Conclusions 115

4.7.1 Key findings 115

5 Conjugation of carbapenem resistance plasmids in planktonic and biofilm lifestyles 117

5.1 Background 117

5.1.1 Aims and hypotheses 120

5.2 Initial characterisation 120

5.3 Strain construction and validation: KP20 124

5.4 KP20 characterisation 127

5.5 Planktonic conjugation assays 129

5.6 Transconjugant characterisation 134

5.7 Biofilm conjugation assays 136

5.8 Discussion 140

5.9 Conclusion 147

5.9.1 Key findings 148

6 Investigating the impact of plasmid acquisition and lifestyle on gene expression 150

6.1 Background 150

6.2 Selection of a suitable transconjugant 151

6.3 Lifestyle impact on chromosomal gene expression 153

6.4 Plasmid impact on chromosomal gene expression 158

6.5 Evaluating a chromosomal plasmid signature 166

6.6 Lifestyle impact on plasmid gene expression 168

6.7 Discussion 173

6.8 Conclusion 179

6.8.1 Key findings 179

7 Discussion 181

7.1 **The application of flow cytometry to study conjugation in bacterial populations** 181

7.2 **Conjugation monitoring in *K. pneumoniae* populations using clinical isolate donors** 182

7.3 **The evaluation of plasmid and lifestyle impacts on gene expression** 184

7.4 References 185

8 Appendices **254**

8.1 Appendix 1 - Chapter 2 254

8.2 Appendix 2 - Chapter 3 258

8.3 Appendix 3 - Chapter 4 260

8.4 Appendix 4 - Chapter 5 262

8.5 Appendix 5 - Chapter 6 267

List of Tables

2.1 Bacterial strains 36

2.2 Plasmids 37

2.3 Primers and colony PCR annealing temperatures 38

2.4 Reaction components for colony PCR 47

2.5 Colony PCR conditions 48

2.6 PCR conditions for DNA donor molecule preparation 51

2.7 Reaction components for DNA donor molecule preparation 51

2.8 DpnI digestion 52

4.1 Plasmid replicons and AMR profiles 101

4.2 CPE01 and CPE25 Flye plasmid replicons and AMR profiles 105

4.3 GenBank sequences similar to carbapenem resistance plasmids 109

5.1 CPE isolates agar MIC 121

5.2 Plasmids in transconjugants 133

6.1 pCPE16_3 plasmid persistence 153

S1 Antibiotic stock preparation 254

S2 Agar MIC 262

List of Figures

1.1 The evolution of antimicrobial resistance 2

1.2 Virulence factors 7

1.3 Pathotypes 8

1.4 Mechanisms of horizontal gene transfer 12

1.5 Conjugation overview in Gram-negative bacteria 14

1.6 Flow cytometer schematic 16

1.7 Structure of mobilisable and conjugative plasmids 18

1.8 F-type plasmid conjugation module regulation overview 20

1.9 Insertion Sequence structure 23

1.10 Phylogenetic tree of *K. pneumoniae* species complex and relatives . . 25

1.11 Hybrid genome assembly method 27

1.12 Biofilm and planktonic lifestyles 29

2.1 Flow cytometry fluorescence reporter system 41

2.2 RNA-Sequencing condition comparisons 55

3.1 Crystal violet biofilm formation 62

3.2 Growth kinetics 64

3.3 *mcherry* fragment schematic 65

3.4 *mcherry* mRNA secondary structure 65

3.5 Viable counts for OD-corrected cultures 67

3.6 Ratio-corrected biofilm crystal violet assays 68

3.7 Confocal microscopy of biofilm 70

3.8 Flow cytometry gating by fluorescence (planktonic and biofilm populations) 72

3.9 Sample dilution controls for planktonic and biofilm flow cytometry samples 74

3.10 Flow cytometry gating by fluorescence (non-conjugative control) . . . 76

3.11 Sample dilution controls for non-conjugative control flow cytometry samples 78

3.12 Increasing total events acquired using volume-based sample acquisition 80

4.1 CPE isolate phylogenetic tree 93

4.2 Pathogenwatch examples and CPE isolates *K. pneumoniae* world maps 94

4.3 CPE01 and CPE25 alongside ST147 Pathogenwatch collection sequences 96

4.4 CPE16 alongside ST14 Pathogenwatch collection sequences 97

4.5 Unicycler hybrid assembly graphs 99

4.6 Annotated putative carbapenem resistance plasmids from CPE isolates (AMR, replicon(s) & transfer genes) 103

4.7 CPE01 and CPE25 Flye assembly graphs 104

4.8 Annotated putative carbapenem resistance plasmids from CPE isolates (Insertion Sequences) 107

4.9 Genetic context of the CPE carbapenem resistance genes 108

5.1 CPE isolate growth kinetics in LB 122

5.2 CPE isolate biofilm formation 122

5.3 CPE isolate growth kinetics in TSBs 123

5.4 Validation of candidate KP20 125

5.5 Check for loss of recombineering plasmid pACBSCE 126

5.6 Annotated cassette sequence from KP20 127

5.7 KP20 biofilm and growth profiles 128

5.8 Planktonic conjugation frequencies 129

5.9 Donor:recipient ratios 130

5.10 Transconjugant colony PCR check 132

5.11 Transconjugant growth kinetics 135

5.12 CPE16 and KP20 24 h biofilm 137

5.13 CPE16 and KP20 biofilm conjugation frequency 138

6.1 KP20/pCPE16 transconjugants replicon check 152

6.2 Multidimensional scaling plot comparing lifestyles 155

6.3 Differential expression of chromosomal genes heatmap 157

6.4 Multidimensional scaling plot comparing transconjugant samples against KP20 reference genome 159

6.5 Biofilm COG categories 161

6.6 Exponential planktonic COG categories 162

6.7 Heatmap of differentially-expressed chromosomal genes (biofilm condition) 164

6.8 Heatmap of differentially-expressed chromosomal genes (planktonic exponential condition) 165

6.9 Heatmap of common differentially-expressed chromosomal genes across lifestyles 167

6.10 Multidimensional scaling plot comparing transconjugant samples against KP20/pCPE16_3 reference genome 169

6.11 Heatmap of common differentially-expressed plasmid genes across lifestyles 170

6.12 Heatmap of differentially-expressed plasmid genes 172

S1 Spectra for GFP and mCherry 254

S2 'Total bacteria' gate 255

S3 bla_{SHV} chromosomal sequence in KP1 256

S4 Hygromycin resistance cassette from pSIM18 257

S5 Predicted final sequence of inserted cassette 258

S6 Flow cytometry gating by fluorescence (volume parameter) 259

S7 Predicted final sequence of inserted cassette 260

S8 CPE24 contig 4 match to chromosomal sequence 261

S9 Amplified pSIM18 cassette 263

S10 KP20 candidate on agar plates 263

S11 Biofilm transconjugants PCR validation 264

S12 Biofilm conjugation assays (donor:recipient ratio) 264

S13 Biofilm conjugation assays mixed populations CFU/mL 265

S14 Morphology comparisons of CPE16 and KP20 266

S15 Percentage variance MDS plots (lifestyle comparison) 267

Abbreviations

+/-	With/without
µg	Micrograms
µL	Microlitre
µM	Micromolar
µs	Microseconds
AMR	Antimicrobial resistance
ANOVA	Analysis of variance
A	Absorbance
bp	Base pair
CFU	Colony forming units
COG	Clusters of orthologous genes
CV	Crystal violet
dNTP	Deoxynucleotide triphosphate
DNA	Deoxyribonucleic acid
dsDNA	double stranded DNA
EDTA	Ethylenediaminetetraacetic acid
FSC	Forward scatter
g	grams
x g	Multiplied by gravity
GFP	Green fluorescent protein
h	Hours
Kb	Kilobase
L	Litre
LBB	Lysogeny broth
LBA	Lysogeny broth agar
Mb	megabases
mg	miligram
MIC	Minimum inhibitory concentration
min	minute(s)
mL	millilitre
mm	milimetre
mM	millimolar
MDS	Multidimensional scaling
nm	nanometre
OD	Optical density
PBS	Phosphate buffered saline
PCR	Polymerase chain reaction
RNA	Ribonucleic acid
rpm	Revolutions per minute
s	second(s)
SD	Standard deviation
SDW	Sterile distilled water
SNP	Single nucleotide polymorphism
SSC	Side scatter
ssDNA	single stranded DNA
TAE	Tris acetate-EDTA
TC	Transconjugant
TSBs	Tryptic soy broth supplemented
T4SS	Type 4 secretion system
V	volt(s)
WGS	Whole genome sequencing
WT	Wild-type

Chapter 1

Introduction

1.1 Antimicrobial resistance

Antimicrobial resistance (AMR) is the ability of viruses, parasites, fungi and bacteria to overcome the effects of antimicrobial drugs. In a population exposed to antimicrobials, resistant organisms are more likely to survive and reproduce than susceptible organisms, thus leading to the resistant population becoming the majority (Figure 1.1). AMR remains an urgent unresolved international public health issue because it limits treatment options for infections and impacts the effectiveness of prophylaxis for other medical applications (O'Neill, 2016; Prestinaci *et al.*, 2015). Acknowledgement of the problem is increasingly reflected in focused public research, development funding and action plans, along with campaigns to improve public knowledge on AMR (CDC, 2020; Department of Health and Social Care, 2020; Kelly *et al.*, 2016; World Health Organization, 2015). Despite this, drug-resistant infections continue to cause significant morbidity and mortality (Dadgostar, 2019). Predictions indicate that this problem will have a major impact on routine medical procedures and on mortality rates if the spread of resistance is not reduced (O'Neill, 2016).

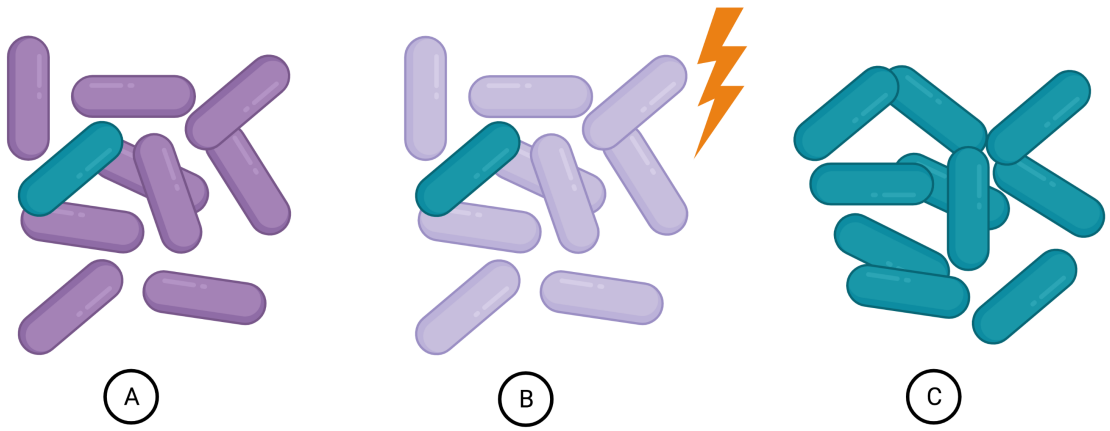

Figure 1.1: The evolution of antimicrobial resistance, using bacterial cells as an example. A: Mixed population of susceptible (dark purple) and resistant (teal) bacterial cells. B: Upon encountering antibiotic stress (lightning bolt), the susceptible population dies (now indicated in light purple). C: The resistant population can proliferate and becomes the majority. Note: some cells may be tolerant to antibiotic stress and exist in a dormant state (not shown) (Gollan *et al.*, 2019). Created with BioRender.com.

1.2 Antibiotic resistance

Resistance to antibiotics, a subgroup of antimicrobial agents which target bacteria (O'Neill, 2016), has been a concern since these drugs were first introduced clinically. However, for a period, new agents were developed at such a rate that the impact of AMR was not in the public consciousness (Ventola, 2015). Now there is a lack of new drugs, especially against Gram-negative organisms (Hawkey *et al.*; Kmietowicz, 2017). AMR has become critical due to an increased incidence of resistant infections and treatment failures (Currie *et al.*, 2014; Smith *et al.*, 2015). Clinicians are increasingly forced to treat patients with toxic antibiotic drugs because infecting organisms are resistant to previously-effective treatment options (Dookie *et al.*, 2016). Human actions and behaviour provides strong selective pressure for maintenance or development of resistance, above that present in nature (Bengtsson-Palme *et al.*, 2018; Fair and Tor, 2014; Holmes *et al.*, 2016). This includes overuse of antibiotics (Ventola, 2015), release of antibiotics into the environment (Davies and Davies,

2010) and use of these agents in agriculture and food production (Ayukekbong *et al.*, 2017), although controlled use will still provide selective pressure for resistance evolution (Bell and MacLean, 2018). There is a need for behavioural change to reduce resistance, such as an overhaul of prescribing practices using antimicrobial stewardship programmes (Doron and Davidson, 2011). In addition, the development of new drugs to treat resistant infections is urgently required (O'Neill, 2016). History indicates that the evolution of resistance to antibiotics is likely inevitable (Ventola, 2015), and some researchers argue that the development of evolution-proof antibiotics is unlikely (Bell and MacLean, 2018). Alternative methods to treat infectious diseases are thus needed (Stanton, 2013). Long-term solutions to the problem of AMR will require a combined approach of new antibiotics, improved infrastructure for waste management, access to clean water and better hygiene practices (O'Neill, 2016; Stanton, 2013).

1.2.1 Resistance mechanisms

Mechanisms of resistance to antibiotics can be acquired or intrinsic. For example, a bacterium can acquire a resistance gene from another bacterium or may lack a particular drug target (Blair *et al.*, 2015). Intrinsic mechanisms relate to existing features that act to reduce drug susceptibility. Examples include the outer membrane present on the Gram-negative bacterial cell wall, which is a structural barrier that prevents some drugs from entering the cell (Blair *et al.*, 2011), or the presence of efflux pumps, which can remove unwanted agents from the cell such that a greater environmental antibiotic concentration is required for inhibition (Blair *et al.*, 2014, 2015). Antimicrobial resistance mechanisms can vary between species and there may be multiple routes leading to resistance to a given drug class (Munita and Arias, 2016).

Acquired resistance is thought to contribute more to clinical treatment challenges (Munita and Arias, 2016). This resistance relates to chromosomal mutations and

resistance genes, the products of which can induce gene expression changes (e.g. to cause de-repression), modify drug targets (e.g. by methylation), inactivate drugs (e.g. by hydrolysis) and bypass metabolic pathways (e.g. by overproduction of target sites so there are more target sites than drug molecules to act on them) (Blair *et al.*, 2015; Munita and Arias, 2016). One of the most notable and problematic examples of resistance resulting from drug inactivation involves carbapenemase enzymes (Meletis, 2016).

1.3 Mechanisms of carbapenem resistance

Carbapenems are frequently-used, well-tolerated beta-lactam drugs effective against a wide range of bacterial pathogens (Hawkey and Livermore, 2012; Papp-Wallace *et al.*, 2011; Ur Rahman *et al.*, 2018). These antibiotics are especially valuable when resistance has arisen to alternative drugs like the penicillins, and cephalosporins, and as such are viewed as a last-resort against otherwise resistant Gram-negative bacterial infections (Papp-Wallace *et al.*, 2011). The carbapenems, like the other beta-lactams, exert their bactericidal effect through binding to the penicillin binding proteins on the bacterial cell wall and inhibiting cell wall synthesis (Bush and Bradford, 2016). Unfortunately, resistance to carbapenems is increasingly reported (De Oliveira *et al.*, 2020). This is mostly attributed to the carriage of carbapenem resistance genes, which encode enzymes that hydrolyse the beta-lactam ring and render the antibiotics inactive (Bush and Bradford, 2016; Cui *et al.*, 2019), but target modification and other routes can also result in resistance (Zeng and Lin, 2013).

Beta-lactamases, of which carbapenemases are a sub-group (Queenan and Bush, 2007), can be classified based on their sequence into Ambler groups A-D, although additional classification systems based on function may be used (Bush and Jacoby, 2010). Carbapenemases are encoded by a variety of beta-lactamase (*bla*) genes such as bla_{NDM} (New Delhi Metallo-beta-lactamase), bla_{KPC} (*Klebsiella pneumoniae* car-

bapenemase) and $bla_{\text{OXA-48}}$-like (oxacillinase), the products of which can be grouped on the basis of the co-factor they use for drug hydrolysis (Cui *et al.*, 2019; Lisa *et al.*, 2017; Nordmann *et al.*, 2011; Papp-Wallace *et al.*, 2011; Sheu *et al.*, 2019; Yang *et al.*, 2021). Newly identified homologous enzymes are named using consecutive numbering (Bush and Bradford, 2019). First reported more than 20 years ago in the United States (Yigit *et al.*, 2001), KPC carbapenemases, which use a serine in the active site for hydrolysis, are now found worldwide in Gram-negative bacteria, particularly in *K. pneumoniae*. KPC enzymes are currently the most widespread of the serine co-factor group (Bush and Bradford, 2019; Kazmierczak *et al.*, 2016).The NDM enzymes, which use a zinc co-factor, were recently identified. The first member of this group was reported in 2008 from a *K. pneumoniae* urine isolate from India (Yong *et al.*, 2009). Unlike the more restricted spread of some of the other metallo-beta-lactamases, NDM enzymes are now found worldwide (Bush and Bradford, 2019). The degree of resistance is dependent on the enzyme (its activity and expression) as well as host-specific factors (Queenan and Bush, 2007). Carbapenem resistance genes can be present on the chromosome and on plasmids, leading to diverse means of spread within bacterial populations (David *et al.*, 2020).

1.3.1 Treatment of carbapenem-resistant infections

Treatment of infections caused by organisms carrying carbapenem resistance genes can sometimes only be achieved by using toxic drugs of last resort such as polymyxins (Rodríguez-Baño *et al.*, 2018). This is because beta-lactamase-producing (including carbapenemase-producing) organisms often carry genes conferring resistance to other drug classes (Paterson and Bonomo, 2005; Rodríguez-Baño *et al.*, 2018). The mortality rate associated with infections caused by carbapenem-resistant *Enterobacteriaceae* (CRE) is high. For example, for bloodstream infections in particular, in one study in a hospital in the United States CRE was reported to cause death in approximately 50% of cases (Patel *et al.*, 2008). This problem is compounded if

initial treatment is inappropriate due to the multidrug resistance of the infecting organism(s) (Livermore, 2009). One CRE which causes significant global disease burden is *K. pneumoniae* (Wyres and Holt, 2022).

1.4 *K. pneumoniae*

Multidrug resistant *K. pneumoniae* has been listed as a 'priority pathogen' by The World Health Organization, indicating that research into this organism is of high importance (Tacconelli *et al.*, 2017). *K. pneumoniae* often carries multiple AMR genes and contributes to their spread by transferring these genes to other Gram-negative bacteria (Wyres and Holt, 2018). This is a ubiquitous rod-shaped organism which can act as an opportunistic pathogen in both human and other animal hosts (Martin and Bachman, 2018; Wyres *et al.*, 2020a; Yang *et al.*, 2019). This usually non-motile bacterium is a facultative anaerobe and is found to colonise the intestines, mouth and skin in its role as a commensal in humans (Carabarin-Lima *et al.*, 2016; Guo *et al.*, 2012; Martin and Bachman, 2018; Pope *et al.*, 2019). For its infectious lifestyle, *K. pneumoniae* makes use of a set of factors including a capsule (a protective polysaccharide coating around the cell which aids immune evasion), fimbriae (proteins arranged in a filament which aid adhesion), lipopolysaccharide (LPS) and iron-capturing siderophores to facilitate pathogenicity (Figure 1.2) (Clegg and Murphy, 2016; Gomes *et al.*, 2021; Hsieh *et al.*, 2012; Mol and Oudega, 1996; Struve and Krogfelt, 2003). In an infection context, some or all of these factors facilitate *K. pneumoniae* survival as it infects its host (Paczosa and Mecsas, 2016).

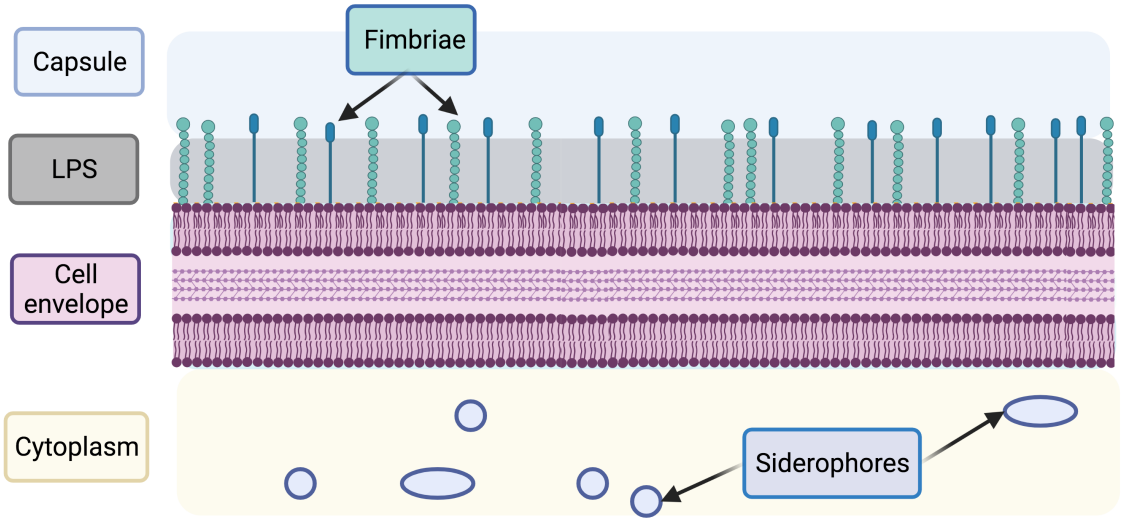

Figure 1.2: Section of the *K. pneumoniae* cell envelope and cytoplasm. The main virulence factors that may be used by *K. pneumoniae* are indicated: capsule, fimbriae, LPS (lipopolysaccharide) and siderophores, where the text box fill colours correspond to the colour of the feature in the figure. Created with BioRender.com.

1.4.1 *K. pneumoniae* colonisation and disease

K. pneumoniae strains can be split into two pathotypes on the basis of the infections they tend to cause (Figure 1.3) (Russo *et al.*, 2018). Classical *K. pneumoniae* generally cause infections in hospitals such as urinary tract infections (UTI) and pneumonia in the immunocompromised (Choby *et al.*, 2020; Holt *et al.*, 2015). In contrast, hypervirulent *K. pneumoniae* strains, so defined because they usually produce extensively mucoid colonies and show a greater ability than classical strains to withstand killing in 'virulence' assays (Russo *et al.*, 2018), ordinarily cause invasive infections such as liver abscesses in the immunocompetent (Choby *et al.*, 2020). The spread of pathogenic *K. pneumoniae* adds to a challenging disease burden from this organism. For example, *K. pneumoniae* is a leading cause of UTI. These common infections impact millions of people globally, both in terms of health and economic consequences. Recurrence may be frequent and AMR strains complicate treatment (Flores-Mireles *et al.*, 2015). Intestinal colonisation by *K. pneumoniae* is reported as a pre-disposing factor for development of subsequent infection (Struve *et al.*,

2009). Indeed, intestinal colonisation was associated with later disease in a recent nosocomial outbreak of bloodstream infections caused by multidrug resistant *K. pneumoniae*, where second-line antibiotics were required. Closely-related isolates to those from the outbreak have been detected internationally (Martin *et al.*, 2021). Community-acquired (usually antibiotic-sensitive (Martin and Bachman, 2018)) and antimicrobial-resistant infections are reported with increasing frequency (Paczosa and Mecsas, 2016).

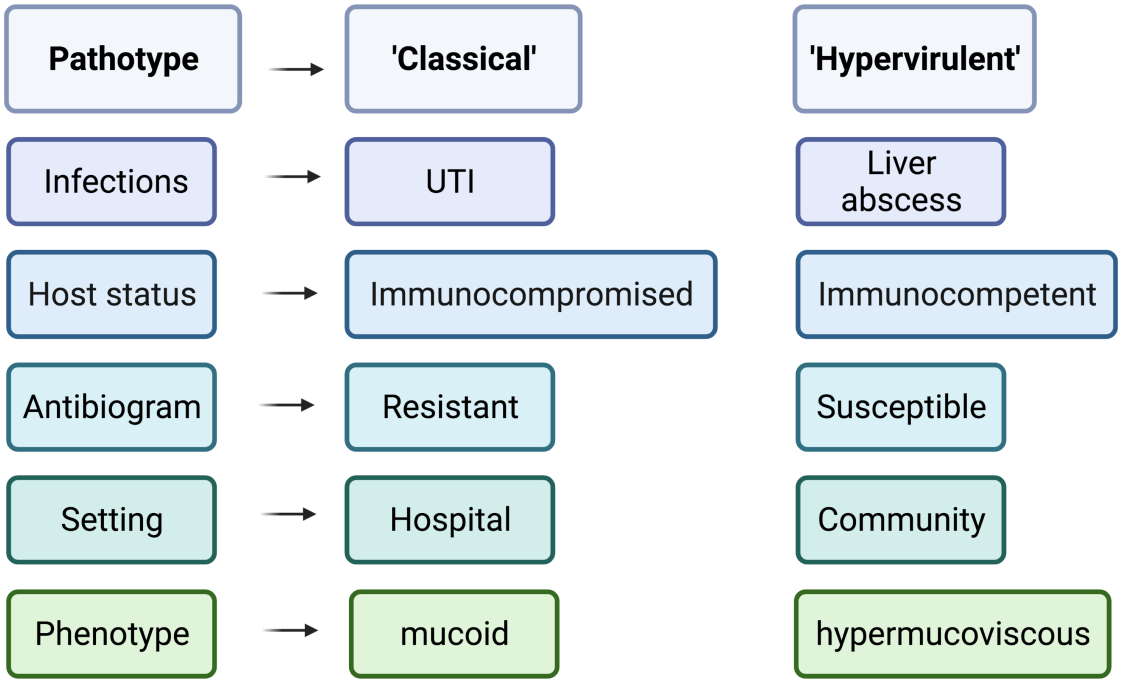

Figure 1.3: Examples of typical features of 'classical' and 'hypervirulent' *K. pneumoniae*. Created with BioRender.com.

1.4.2 Drug-resistant *K. pneumoniae* infections

A challenging aspect of treating hospital-acquired *K. pneumoniae* infections is that they are often resistant to multiple antimicrobial drugs, mirrored in the large number of AMR genes carried by circulating strains (Bassetti *et al.*, 2019; Wyres *et al.*, 2020a). The effect of AMR gene carriage is reflected in patient outcomes. For exam-

ple, pooled mortality rates for patients infected with carbapenem-resistant strains can be higher than 40% according to a recent estimate (Xu *et al.*, 2017). Although hypervirulent strains are usually susceptible to antimicrobials, there are reports of hypervirulent-AMR strains leading to hybrid phenotypes (Gu *et al.*, 2018; Shankar *et al.*, 2020). Recent evidence suggests that virulent strains are more likely to acquire AMR than AMR strains are to acquire virulence determinants (Lam *et al.*, 2021). Although relatively rare at the moment, convergence of these phenotypes has been found internationally (Lam *et al.*, 2021). In addition, reports of plasmids carrying both virulence and AMR determinants raises the possibility of horizontal transfer (Wyres *et al.*, 2020b). This trend is concerning because it may increase the risk of treatment failure (Lam *et al.*, 2021; Xu *et al.*, 2019). Globally, drug resistant *K. pneumoniae* is a growing problem, which has led to work to understand the phylogenetic relatedness of this species (Holt *et al.*, 2015).

1.4.3 Epidemic clones and plasmids

Some clones of *K. pneumoniae* have been more successful than others at spreading AMR internationally, for example via animals, medical settings and the environment (Navon-Venezia *et al.*, 2017). These 'high-risk' clones can be described by their sequence type (assigned by Multilocus Sequence Typing, MLST), which facilitates use of this existing classification system for comparative studies (Wyres *et al.*, 2020a). Current examples include ST258 (and its close relative ST512), ST147 and ST14 amongst others, which have all been reported to carry AMR genes and be implicated in outbreaks. For example, a multidrug resistant clone of ST147 was recently implicated in an outbreak in Italy (Martin *et al.*, 2021). However, some clones may provide a large disease burden without being multidrug-resistant, or may be problematic locally. It is thought that the expansion of clones, rather than horizontal gene transfer (HGT), is principally responsible for the spread of AMR *K. pneumoniae*. However, the impact of HGT is nonetheless a contributing factor

(Navon-Venezia *et al.*, 2017; Wyres *et al.*, 2020a).

Potentiating the high-risk clones are mobile genetic elements such as plasmids, which can associate with them and contribute multiple AMR genes. For example, ST258 has been reported to stably carry the epidemic plasmid pKpQIL, which itself carries $bla_{\text{KPC-3}}$ on a transposon (Tn*4401a*) (Navon-Venezia *et al.*, 2017). Indeed, it has been demonstrated in a recent study of patient-isolated *K. pneumoniae* genomes that a small number of clones are responsible for the majority of *K. pneumoniae* carbapenem resistance gene carriage in Europe, and that hospitals provide a route for dissemination (David *et al.*, 2019). However, the picture is not clear cut. Using the same set of genome sequences in a parallel study, David *et al.* showed that in addition to via clonal spread (e.g. bla_{KPC}), carbapenem resistance genes can also be transferred through carriage on a single plasmid (e.g. pOXA-48) or via multiple plasmid transfer events to diverse *K. pneumoniae* hosts (David *et al.*, 2020). This further highlights that plasmids have a key role in the dissemination of carbapenem resistance genes. In combination, horizontal and vertical transmission of carbapenem resistance genes has led to the current carbapenem-resistance problem (Ferreira *et al.*, 2021), and it is therefore vital that all of the processes and settings contributing to carbapenem resistance gene transmission are studied. One prominent process that can lead to carbapenem resistance is HGT (Potter *et al.*, 2016).

1.5 Horizontal gene transfer in Gram-negative bacteria

Cell division is responsible for the vertical transmission of genetic information from a parent cell to offspring (Reyes-Lamothe and Sherratt, 2019; Rothfield and Justice, 1997). In bacteria, mechanisms for DNA transfer between cells, known as HGT, significantly contribute to adaptation and evolution (Lorenzo-Díaz *et al.*, 2017).

For example, HGT can deliver genes within and between species, can occur quickly and facilitate responses to new environmental conditions (Dimitriu *et al.*, 2019; Król *et al.*, 2013; Nolivos *et al.*, 2019; Norman *et al.*, 2009; Vogan and Higgs, 2011; Woods *et al.*, 2020). Nonetheless, most occurrences of horizontal transfer are not likely to provide a benefit (Hall *et al.*, 2020; Vogan and Higgs, 2011). Several mechanisms of HGT have been reported including transduction (DNA uptake facilitated by bacterial viruses (bacteriophage)), transformation (DNA uptake from the environment), conjugation (pilus-mediated DNA transfer between neighbouring cells) and other routes (such as via vesicles) (Figure 1.4) (Thomas and Nielsen, 2005; Tran and Boedicker, 2019). Despite this variety of HGT routes, not all bacterial species use all of these mechanisms (Thomas and Nielsen, 2005). Although acquiring chromosomal mutations can lead to drug resistance, the rapid global spread of AMR has been mainly attributed to HGT of plasmids carrying resistance determinants (Knopp and Andersson, 2018; Pornsukarom and Thakur, 2017). For *K. pneumoniae*, both bacteriophage and plasmid-mediated HGT are thought to be common (Wyres *et al.*, 2019). Due to its large impact on the transmission of plasmids and AMR genes (Cabezón *et al.*, 2015; Carattoli, 2013; San Millan and MacLean, 2017), plasmid transfer by conjugation will be the focus of this work.

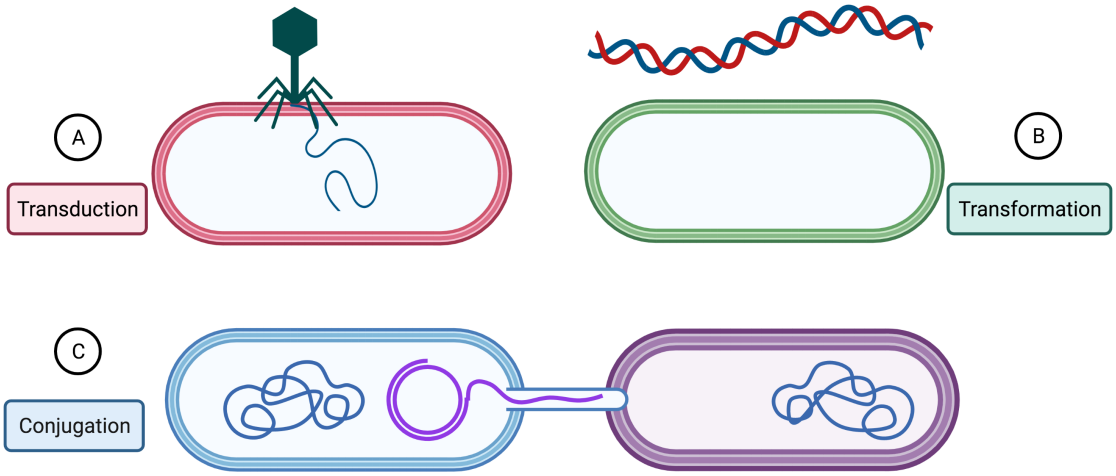

Figure 1.4: Overview of the main horizontal gene transfer mechanisms. A: Transduction mediated by a bacteriophage which injects DNA into a host cell. B: Transformation, where naked DNA (here illustrated by a red and blue helix) is taken up from the environment. C: Conjugation, where DNA is transferred from a donor to a recipient cell via a pilus. Here a Gram-negative bacterial cell is shown, and a single strand of plasmid DNA is transferred to the recipient cell. See Figure 1.5 for more information on conjugation. Created with BioRender.com.

1.5.1 Conjugation

Although conjugative elements are not limited to plasmids (Burrus *et al.*, 2002), other elements are beyond the scope of this work. While much is still undetermined about the precise order and steps of conjugation, the general process can be described (Figure 1.5) (Waksman, 2019). Conjugation in Gram-negative bacteria involves the transfer of single-stranded DNA (ssDNA) from a donor to a recipient cell (De La Cruz *et al.*, 2010). To transfer by conjugation, plasmids must carry genes encoding products for mating pair formation (the coming together of the donor and recipient cells (Schröder and Lanka, 2005)) and subsequent DNA transport via a Type 4 Secretion System (T4SS) (Norman *et al.*, 2009; Ramsay and Firth, 2017), which assembles to produce a pilus/channel (Waksman, 2019). Conjugation requires energy (De La Cruz *et al.*, 2010), and close cell proximity or cell-cell contact effected by a pilus which, depending on the type, may extend and retract dynamically (Clarke *et al.*, 2008; Waksman, 2019).

A donor cell containing a plasmid to be transferred attaches via a pilus to a recipient cell (Arutyunov and Frost, 2013; Hu *et al.*, 2019). The plasmid DNA is nicked by the relaxase (part of the relaxosome nucleoprotein complex which also contains some additional proteins) at the *nic* site at the origin of transfer (*oriT*) and split into two single strands (De La Cruz *et al.*, 2010; Ilangovan *et al.*, 2017). The relaxase attaches to the 5' end of a DNA strand (Arutyunov and Frost, 2013; Graf *et al.*, 2019) and this complex is transferred through the T4SS channel into the recipient cell (Álvarez-Rodríguez *et al.*, 2020; Dostál *et al.*, 2011; Gruber *et al.*, 2016). Mating pair formation and DNA transport processes are linked by a coupling protein via delivery to and interaction with the relaxosome-DNA complex at the T4SS channel (Álvarez-Rodríguez *et al.*, 2020; Ramsay and Firth, 2017). Once transferred the ssDNA is circularised by the relaxase and replicated to form dsDNA (replication also occurs in the donor cell) (Graf *et al.*, 2019). The recipient is now known as a transconjugant and may be able to donate the plasmid on to new recipient cells (Alderliesten *et al.*, 2020; Graf *et al.*, 2019). In a new cell, plasmid genes might be expressed to a higher or lower level (e.g. accessory AMR genes (Guiney *et al.*, 1984)) due to strain background differences (Miyakoshi *et al.*, 2009), so a phenotype may not be maintained to the same degree in a new host.

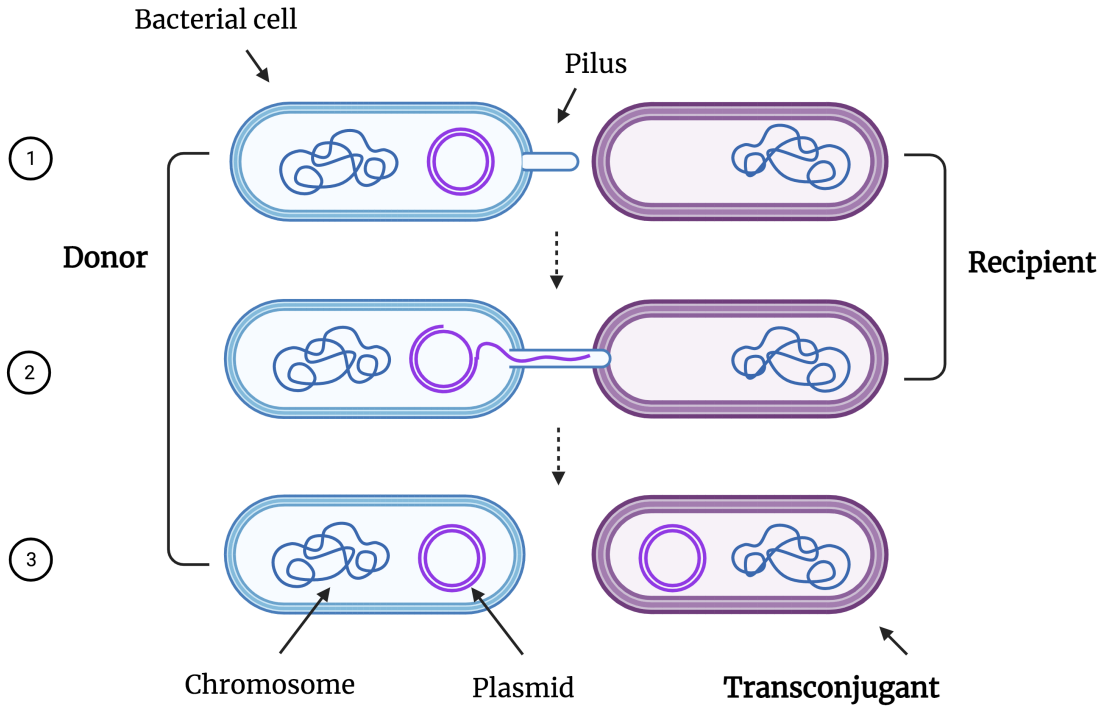

Figure 1.5: Conjugation overview in Gram-negative bacteria. 1: A donor cell (blue) contacts a recipient cell (purple) via a pilus. 2: Plasmid DNA is nicked by the relaxase at the origin of transfer. A single strand is transferred by the relaxosome nucleoprotein complex to the recipient cell. 3: The ssDNA is circularised by the relaxase and replicated to dsDNA in the donor and the recipient. The recipient containing the transferred plasmid is known as a transconjugant, which may pass on the plasmid to a new recipient cell. Created with BioRender.com.

1.5.2 Studying conjugation

Conjugation has traditionally been studied using plating assays where transconjugants are selected on antibiotic-containing media (Bethke *et al.*, 2020). To perform these experiments, the donor and recipient strain must have different drug resistance profiles, such that the donor will be inhibited by the antibiotic used to select the recipient, and vice versa. Resulting transconjugants can then be selected for and counted on dual antibiotic agar, and mixed populations can be plated on single antibiotics to select and quantify donors and recipients. Although colony forming units (CFU)/mL determination is considered the 'gold-standard' approach,

these assays are restricted by the need to use donors and recipients with distinct resistance profiles. Suitable donors/recipients can be challenging to find when using multidrug-resistant strains as this may limit the available selective antibiotics. In addition, these assays provide a relatively slow and low-throughput method for transconjugant quantification, as culturing of resultant transconjugant colonies is required before counting (Alderliesten *et al.*, 2020). It is also possible that colonies may result from overlapping cells on an agar plate, leading to an underestimation of the number of transconjugant, donor and recipient colonies. The need for serial dilution of culture may also contribute error (Chase and Hoel, 1975; Hazan *et al.*, 2012).

Alternative methods for studying conjugation, for example those using microscopy (Carranza *et al.*, 2021) or high-throughput genetic screening (Alalam *et al.*, 2020), have been developed to complement plating assays, which are still required for validation (Alalam *et al.*, 2020; Carranza *et al.*, 2021). Techniques such as flow cytometry, which employs a stream of fluid to separate samples into single cells before passing them through a laser beam and collecting information about their properties (Wilkinson, 2018), are also promising for this application (Figure 1.6). Flow cytometry can provide multiparametric information about thousands of individual cells and allow sub-populations to be identified without the need for culture (Álvarez-Barrientos *et al.*, 2000). Flow cytometry has been used successfully in the past to monitor conjugation in bacterial populations, for example using donors containing fluorescently-tagged conjugative plasmids (Buckner *et al.*, 2020; Sørensen *et al.*, 2003).

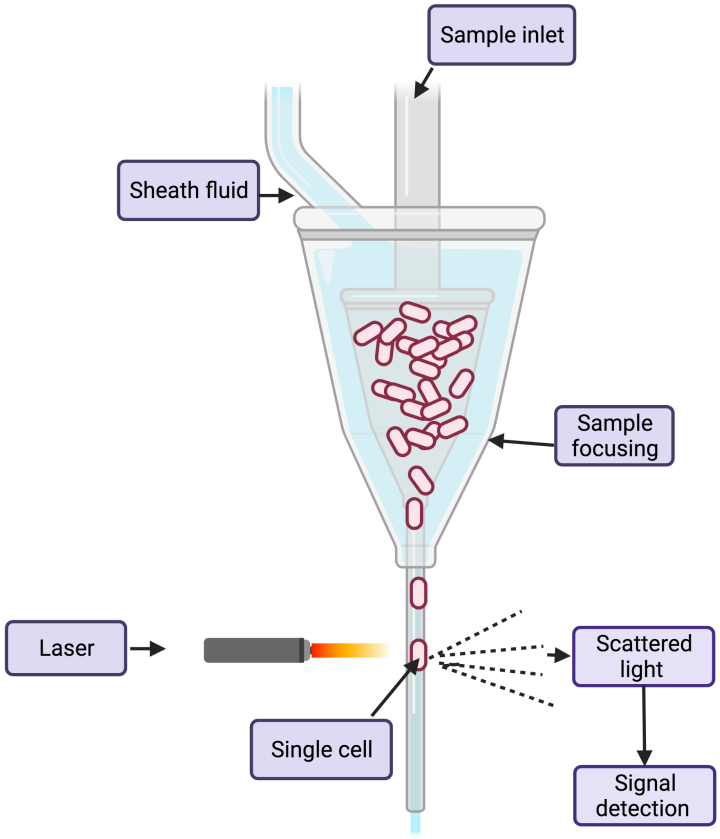

Figure 1.6: Simplified flow cytometer schematic. Cell suspensions are focused to single cells before they pass the laser interrogation point. Here, cells scatter the light. This information can be detected to give information about individual cells. Created with BioRender.com.

1.5.3 Conjugative plasmids

Plasmids are semi-autonomously replicating, typically circular DNA elements which are distinct from the bacterial chromosome (Carroll and Wong, 2018; Norman *et al.*, 2009). They form part of the accessory genome (Jackson *et al.*, 2011; Tazzyman and Bonhoeffer, 2015), and genes they carry may provide an advantage to the host under certain conditions (Wein *et al.*, 2021). Plasmids themselves carry a set of core genes which facilitate their continued proliferation and can be used for classification (Orlek *et al.*, 2017).

Conjugative plasmids carry a 'backbone' of genes encoding essential functions (Figure 1.7). These can be broadly divided into three categories: genes for replication,

stability and propagation. Replication genes include those for low copy-number (<10 copies/cell) maintenance to reduce the metabolic burden of plasmid carriage (Ni *et al.*, 2021; Norman *et al.*, 2009). Considering plasmid stability, active partitioning (*par*) genes are needed to ensure that a copy of the plasmid remains present in daughter cells (Baxter and Funnell, 2014). Addiction/post-segregational killing systems, such as toxin-antitoxin systems where a toxin will kill any daughter cells without the antitoxin, may also be present to prevent plasmid-free cell survival (Kroll *et al.*, 2010; Norman *et al.*, 2009). This is in contrast to cells containing high copy number, non-conjugative plasmids, where the random distribution of plasmids within the cell before division may be sufficient to ensure plasmid maintenance in daughter cells (Norman *et al.*, 2009). Propagation genes refer to those genes required for production of conjugative transfer machinery. Conjugative plasmids may also carry additional features via accessory genes that, when present in a host cell, may confer a benefit in particular environmental conditions (Norman *et al.*, 2009). For example, the conjugative plasmid pQBR103 in *Pseudomonas* provides resistance to mercury (Kottara *et al.*, 2018), and the conjugative plasmid pKpQIL provides resistance to carbapenem antibiotics in species including *K. pneumoniae* (Doumith *et al.*, 2017; Leavitt *et al.*, 2010).

Conjugative plasmids contribute to evolution by facilitating HGT across species boundaries which permits widespread gene sharing and environmental adaptation. These plasmids are usually large (>30 kb) and can be costly to carry although host-plasmid co-evolution can contribute to fitness cost reduction (Harrison and Brockhurst, 2012; Ni *et al.*, 2021; Norman *et al.*, 2009). Other HGT mechanisms, transformation and transduction, are restricted by requirement for competence and a narrow host-range respectively (Norman *et al.*, 2009). Although many cells in a population may contain a particular conjugative plasmid, signals indicating favourable conditions, such as sufficient population density, are required for transfer competence of (some) donors. Even with an induction signal, the majority of donor cells will not become competent for conjugation (Bingle and Thomas, 2001; Koraimann

and Wagner, 2014). Plasmids can be transferred into new hosts by conjugation, but not all plasmids have the required transfer machinery (Prensky *et al.*, 2021).

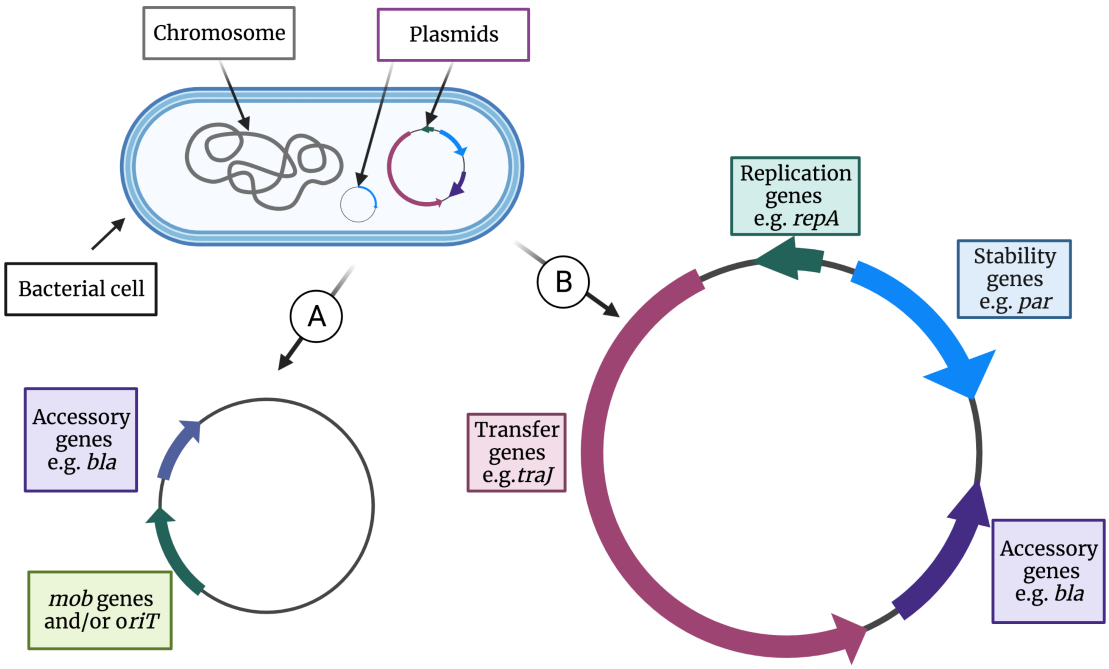

Figure 1.7: Schematic of the structure of mobilisable and conjugative plasmids. A bacterial cell containing a chromosome and two plasmids is shown. Larger scale (A) mobilisable and (B) conjugative plasmids are indicated. Plasmid genes can be classified on the basis of their function. For mobilisable plasmids, the minimum requirement for transfer is an *oriT* sequence, although mobilisation (*mob*) genes may be present. Conjugative plasmids generally contain genes for replication, stability and transfer. Both plasmid types may contain accessory genes such as AMR genes which may be beneficial in some environments. Created with BioRender.com.

1.5.4 Plasmid mobilisation

Non-conjugative plasmids can transfer by making use of machinery from a conjugative plasmid present in the same cell (Orlek *et al.*, 2017). In this case, the plasmid is known as mobilisable. The minimum requirement for mobilisation of a plasmid is now thought to be the presence of an *oriT* sequence (Ramsay and Firth, 2017). In fact, there is increasing appreciation for the lesser-studied small mobilisable plasmids, for example in co-transfer with conjugative plasmids carrying antimicrobial resistance genes (Barry *et al.*, 2019) or themselves as vectors of AMR gene spread

(Moran and Hall, 2017). Indeed, traditional conjugation experiments may miss transfer of mobilisable plasmids if they are selecting only for a conjugative plasmid of interest. The contribution of plasmid mobilisation to bacterial evolution may be underestimated (Rodríguez-Beltrán *et al.*, 2021).

1.5.5 F-type plasmids: classification

Of the different types of plasmids, F-type conjugative plasmids are perhaps some of the best-studied (Fernandez-Lopez *et al.*, 2016). The prototypical F plasmid was first identified by Lederberg and Tatum as a "fertility factor" in 1946 (Hu *et al.*, 2019; Lederberg and Tatum, 1946), and it later emerged that unlike the other F-type plasmids studied to date (Koraimann, 2018), conjugative transfer of this plasmid is de-repressed due to a mutation in a negative regulator of the process, FinO (Yoshioka *et al.*, 1987). The F-type plasmids were originally grouped together on the basis of their experimentally-determined incompatibility profile but remain clustered when updated grouping, for example using signature plasmid PCR targets or relaxase (*mob*) gene similarity, is used for classification. F-type plasmids can be further sub-divided based on plasmid multilocus sequence typing (pMLST) which classifies using allele differences (Rozwandowicz *et al.*, 2018). As well as shared features, F-type plasmids exhibit diversity, such as in their accessory gene content (Fernandez-Lopez *et al.*, 2016). They may also carry multiple replicons of different types, which is thought to aid in their dissemination and in overcoming incompatibility (Rozwandowicz *et al.*, 2018; Villa *et al.*, 2010).

1.5.6 Genetic organisation of F-type conjugation modules

In F-type plasmids, conjugation genes are typically present on a discrete module (Norman *et al.*, 2009), generally arranged in an approximately 33 kb operon (Frost *et al.*, 1994) under the control of the Py promoter (Figure 1.8). Regulators of this

promoter include the plasmid-encoded activator protein TraJ (which is itself negatively regulated post-transcriptionally by FinP (anti-sense RNA) and its chaperone FinO (Fernandez-Lopez *et al.*, 2016) and the positively-acting chromosomal regulator ArcA (Lu *et al.*, 2019). Although there are approximately 40 conjugation genes on the prototypical F plasmid conjugation module, not all are essential for conjugation or conserved across F-type plasmids (Fernandez-Lopez *et al.*, 2016; Frost *et al.*, 1994). Perhaps due to the energy requirement for expression of the conjugation machinery, the operon is ordinarily repressed (Frost *et al.*, 1994; Norman *et al.*, 2009). When the operon is expressed (which happens due to an as-yet-undefined signal), conjugation is thought to happen in a small proportion of the population (Koraimann and Wagner, 2014). However, temporary de-repression of conjugation module genes may occur in new donor cells (transconjugants) (Frost *et al.*, 1994).

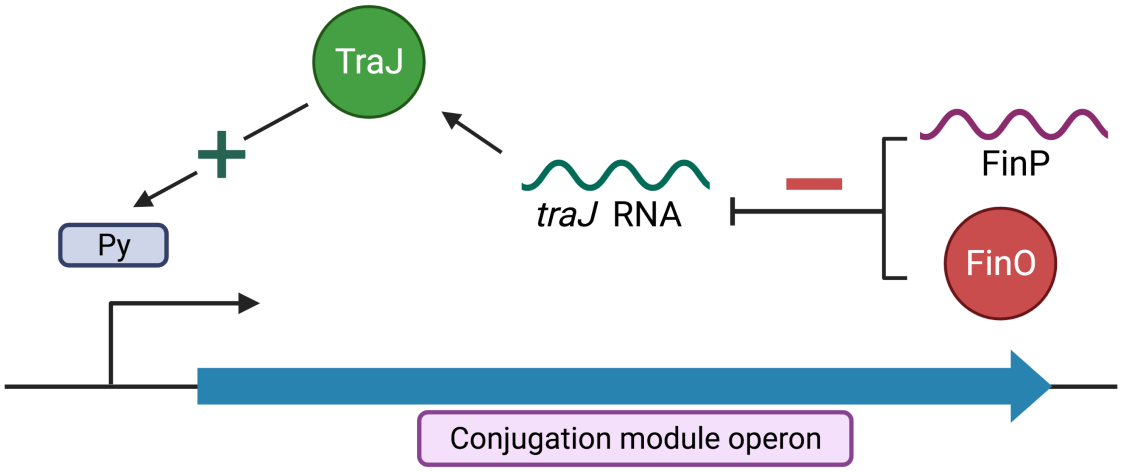

Figure 1.8: Overview of the regulation of conjugation modules in F-type plasmids. The Py promoter controls expression of the conjugation module which contains genes required for plasmid transfer. The TraJ protein activates Py upon induction by an unknown signal (indicated by a plus sign). TraJ itself is negatively regulated post-transcriptionally (indicated by a 'minus' sign) by the antisense RNA FinP, which is accompanied by its chaperone FinO. The default state of the Py promoter is 'off'. Created with BioRender.com.

1.6 Plasmid features

In addition to performing specific functions for the plasmid, genes carried on plasmids may affect expression of chromosomal genes (and vice versa) or act directly or indirectly to alter host cell phenotypes (Gama *et al.*, 2020; Hall *et al.*, 2021; Madsen *et al.*, 2016). For example, some reports identify a positive association with biofilm formation and carriage of plasmids with conjugation modules (Gama *et al.*, 2020; Ghigo, 2001). This is thought to relate to the potential for conjugative pili to facilitate adhesion (Gama *et al.*, 2020). Additionally, plasmid genes conferring resistance to, for example, antimicrobials or heavy metals may permit host survival in the presence of these substances (Carroll and Wong, 2018). Genes on plasmids are also subject to the effect of the increased copy number of plasmids compared to the chromosome. Multiple plasmid copies produce multiple gene copies which can amplify gene expression to impact phenotype (Rodríguez-Beltrán *et al.*, 2021). For example, higher copy number of a plasmid encoding $bla_{\text{OXA-232}}$ was determined to be a plausible cause of increased carbapenem resistance in a *K. pneumoniae* clinical isolate (Shen *et al.*, 2020). Plasmid sequences are also more likely to recombine compared to the chromosome, in part due to the presence of transposable elements and their action (discussed further in section 1.7). This may explain the large proportion of publicly available plasmid sequences that are hybrids of more than one original sequence, and the difficulty in using phylogenetic trees to illustrate plasmid evolutionary relationships (Matlock *et al.*, 2021; Rodríguez-Beltrán *et al.*, 2021).

1.6.1 Plasmid carriage and fitness

It has been suggested that a beneficial plasmid gene will be integrated into the host chromosome and that costly plasmids will be lost without selection (Dorado-Morales *et al.*, 2021). Nonetheless, plasmids are widespread and, as discussed above, there may be additional (e.g. recombination or expression) benefits to carrying genes on a

plasmid (Dorado-Morales *et al.*, 2021; Matlock *et al.*, 2021; Rodríguez-Beltrán *et al.*, 2021).

Although plasmids can benefit their host cell, plasmid carriage is frequently reported to be energetically costly. Despite this, some plasmids can be maintained without positive selection, calling into question the 'metabolic burden' argument. This cost-benefit conflict has been termed the 'plasmid paradox' (Carroll and Wong, 2018; Harrison and Brockhurst, 2012) and explanations for this phenomenon are currently incomplete (Carroll and Wong, 2018). Compensatory evolution through mutation may act to reduce cost-of-carriage. Recent work has introduced the idea that fitness costs (here defined as causing a reduction in successful reproduction and survival (Orr, 2009)) may relate to gene conflicts (Hall *et al.*, 2021), putting into question the broader 'metabolic burden' explanation (Hall *et al.*, 2021; San Millan and MacLean, 2017). However, not all plasmids produce a fitness cost for the host, and some plasmids may increase fitness without selection (Carroll and Wong, 2018). For example, a recent study determined that carriage of the pOXA-48_K8 plasmid was of benefit for some patient gut microbiota isolates on the basis of competition experiments and growth assays (Alonso-del Valle *et al.*, 2021). Another recent study found that some *E. coli* strains which acquired the pLL35 plasmid had enhanced growth versus the plasmid-free recipient (Dunn *et al.*, 2021). In work comparing two pKpQIL-like plasmids, gene expression changes rather than mutations were sufficient to reduce plasmid carriage costs (Buckner *et al.*, 2018). The cost-benefit balance may switch quickly upon encountering new environmental conditions (Heuer *et al.*, 2008), and host background can have a large impact on fitness (Alonso-del Valle *et al.*, 2021).

1.7 Mobilisation of resistance genes

Horizontal transfer of resistance genes is a major route of AMR transmission (Vrancianu *et al.*, 2020). These genes (and others) are often associated with intracellular

mobile genetic elements like Insertion Sequences (IS) (Partridge *et al.*, 2018; Razavi *et al.*, 2020; Vrancianu *et al.*, 2020). IS are simple transposable elements usually carrying only a transposase gene (for their own transfer) and generally flanked by inverted repeat sequences (containing the target for the transposase enzyme) (Figure 1.9). Direct target DNA repeats which result from target site duplications of a given (characteristic) length may also be present outside of the inverted repeats due to the mechanism of DNA insertion (Mahillon and Chandler, 1998; Siguier *et al.*, 2014).

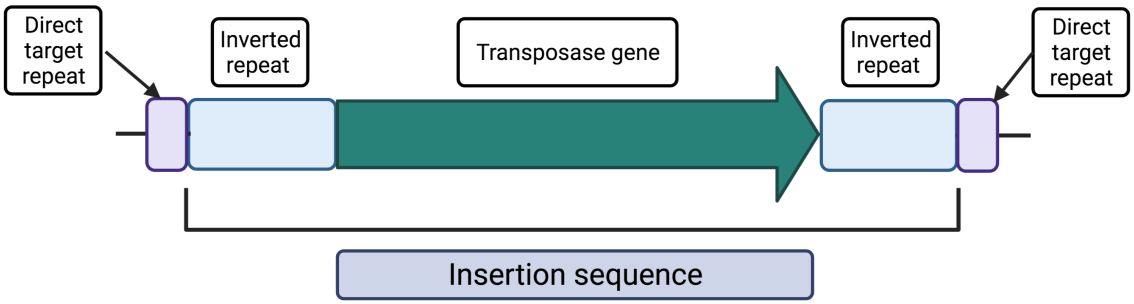

Figure 1.9: General structure of an Insertion Sequence (IS). A transposase gene, for transport of the IS, is flanked by a pair of inverted repeat sequences. Direct target repeats, which result from duplication of the IS target site, may also be present. Created with BioRender.com.

IS are likely the most common intracellular mobile genetic elements (Siguier *et al.*, 2014). They can facilitate the transfer of resistance genes either to new locations between or within intercellular mobile genetic elements such as plasmids, between intercellular mobile genetic elements and the chromosome (and vice versa), or within the chromosome (Consuegra *et al.*, 2021; Razavi *et al.*, 2020; Vandecraen *et al.*, 2017; Vrancianu *et al.*, 2020). Flanking of an AMR gene(s) by a pair of IS (forming a structure called a composite transposon), or in some cases a single IS, can be sufficient for mobilisation of cargo gene(s) (Partridge *et al.*, 2018; Vandecraen *et al.*, 2017).

Interestingly, it appears that IS*26*, which is often found clustered around AMR genes in Gram-negative bacteria, may be more likely to transfer into locations where an

existing copy is already present. This may indicate a target preference where many IS do not appear to have one (Harmer *et al.*, 2014; Partridge *et al.*, 2018). Apart from transferring genes, IS can also exert other effects. For example, IS insertion can inactivate a gene through interrupting its sequence, positively affect gene expression by providing an upstream promoter sequence (Vandecraen *et al.*, 2017), or delete regions of sequence (Siguier *et al.*, 2014). Gene copy number (e.g. due to carriage on a multicopy plasmid) as well as the variant of a gene (e.g. $bla_{\text{KPC-2}}$ versus $_{\text{KPC-3}}$ may also affect level of phenotypic resistance (Dimitriu *et al.*, 2021; Stoesser *et al.*, 2017). Overall, plasmids, in concert with other mobile genetic elements like IS contribute significantly to AMR gene spread (Partridge *et al.*, 2018).

1.8 Insights from genome sequencing

A deeper insight into the biology of *K. pneumoniae*, such as tracking of resistance genes and infection monitoring and management, is aided by tools such as whole genome sequencing (WGS). WGS has enabled an in-depth look at *K. pneumoniae* population structure, and revealed large diversity within the species' accessory genome (defined as the genes that are not shared by all *K. pneumoniae*) (Wyres *et al.*, 2020a). It has also permitted closely-related species within the *K. pneumoniae* species complex to be identified where otherwise these would be indistinguishable by standard laboratory tests (Figure 1.10) (Rodrigues *et al.*, 2019).

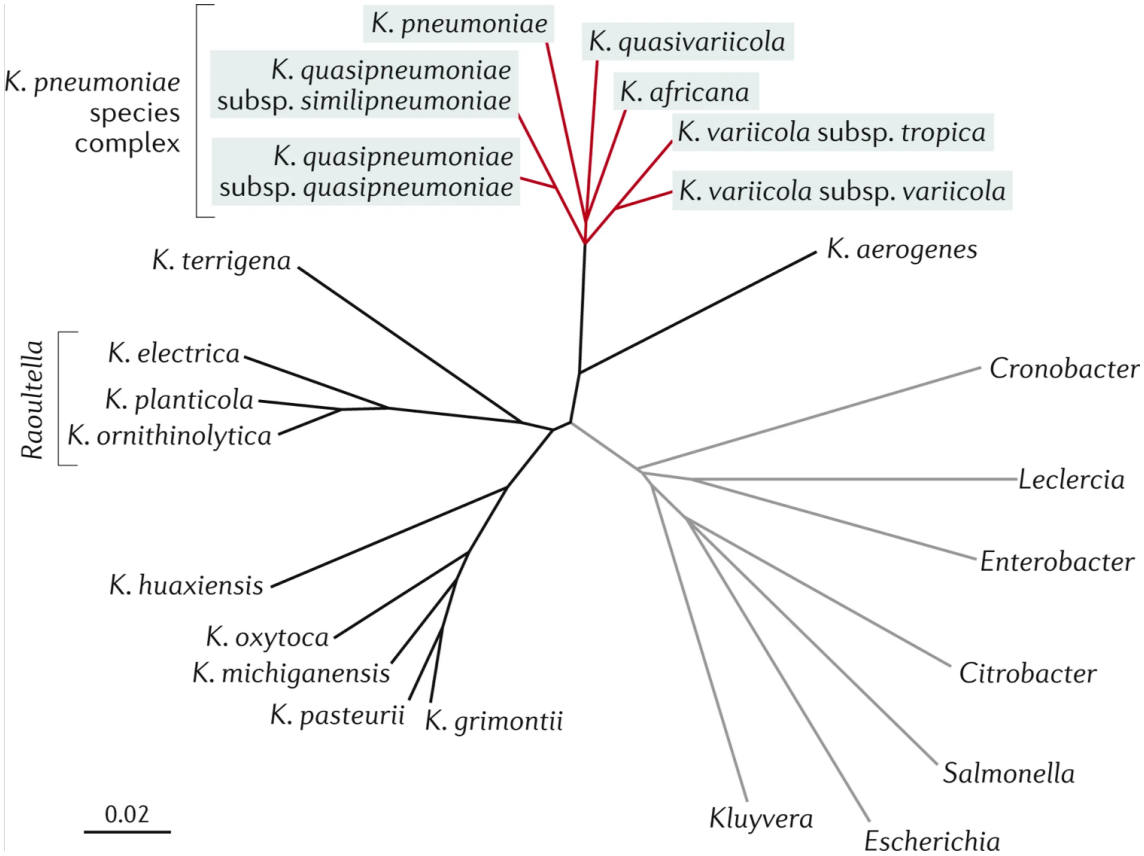

Figure 1.10: Whole-genome-based tree showing the phylogenetic relationships between *K. pneumoniae*, its close relatives in the *K. pneumoniae* species complex (red branches), other select members of the *Klebsiella* genus (black branches) and family *Enterobacteriaceae* (grey branches). The tree was inferred from mash distances of representative whole genome sequences. Scale bar is the estimated average nucleotide divergence. Figure and shortened legend reproduced with permission from Wyres *et al.* (2020a).

Large-scale genomic studies investigating *K. pneumoniae* have facilitated identification of dominant lineages, resistance profiles and distribution (Wyres *et al.*, 2020a). Typing schemes have been applied or developed to aid this process and provide a common starting point for comparison between studies. Examples include MLST, where each allele of seven housekeeping genes is assigned a number and the allele combination has a unique number signature (Diancourt *et al.*, 2005), and core genome MLST, which makes use of a set of highly conserved core genes (cgMLST) (Bialek-Davenet *et al.*, 2014). cgMLST also uses number assignment for alleles, but uses a far larger number of genes to improve the resolution (de Sales *et al.*, 2020). In conjunction with curated databases such as ResFinder (for known AMR genes)

(Bortolaia *et al.*, 2020) and PlasmidFinder (for known plasmid replicons) (Carattoli *et al.*, 2014) isolates can be sequenced, classified and interrogated for features of interest. As tools are built upon and improved, existing sequences can be re-queried and conclusions updated to reflect any new findings (Anjum *et al.*, 2017). With ever-increasing numbers of publicly-available bacterial genomes (Land *et al.*, 2015), alongside community-driven development of a variety of open-source analysis pipelines, such as Unicycler for genome assembly (Wick *et al.*, 2017b) and comparative visualisation tools such as Microreact (Argimón *et al.*, 2016), sequencing data continues to provide a rich data source (Argimón *et al.*, 2016).

1.8.1 Combining short- and long-read WGS technologies

An accurate and cost-effective WGS technology is Illumina short-read sequencing (Wick *et al.*, 2017a). However, one limitation of this method is that it cannot decipher repetitive regions of sequence and therefore struggles to resolve plasmid sequences (De Maio *et al.*, 2019). The creation of hybrid genome assemblies, which combine short-read and long-read (such as Oxford Nanopore) sequencing data, is a suitable method for resolving plasmids (Figure 1.11). The long-read data aids in resolving genome structure as it can create reads longer than repetitive regions, whilst the accuracy of the short-read data is retained (Wick *et al.*, 2017a). Such data can provide information on the presence of AMR genes and plasmids in clinical isolates (George *et al.*, 2017). This is important because, for example, a single plasmid can provide a reservoir of multiple resistance genes (Darphorn *et al.*, 2021). Therefore, identification of plasmid sequences is essential to the successful monitoring of antimicrobial resistance.

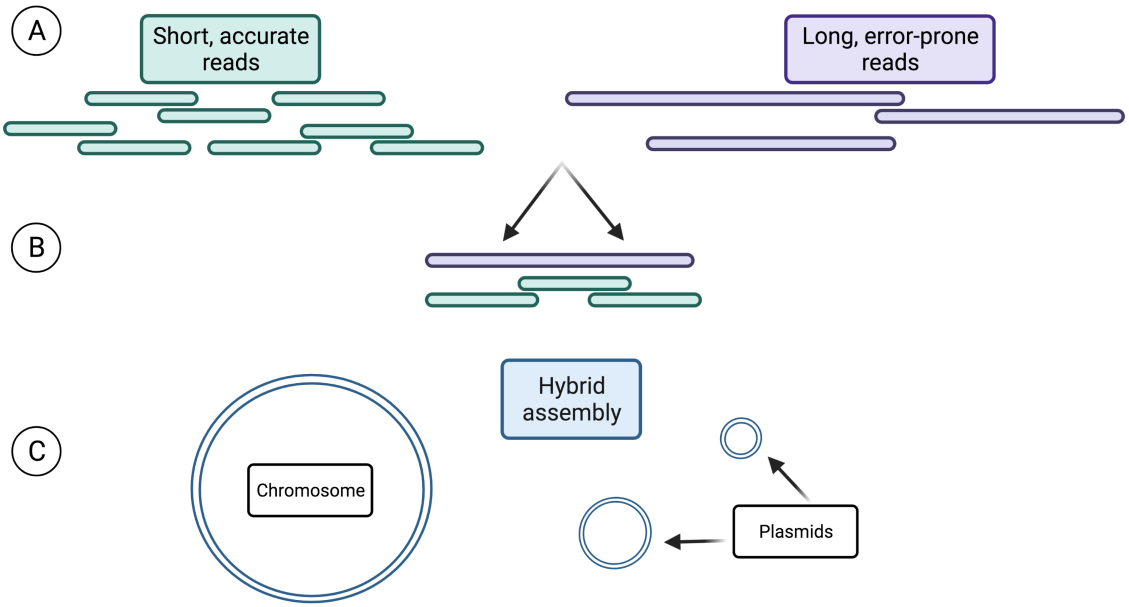

Figure 1.11: Schematic of hybrid genome assembly methods. (A) WGS is carried out using two methods to produce short and long reads. (B) Long-read data can be used to determine genome structure and bridge repeats. Short reads can be used to improve accuracy. (C) Combining these approaches can resolve plasmids to give a complete circularised genome. Created with BioRender.com.

1.8.2 Linking genotype to phenotype

Accurate annotation can be challenging as genomes annotated on the basis of experimental data are infrequently available for reference (Baric *et al.*, 2016). Homology methods are often used to predict gene presence and functionality, but can be unreliable if reference sequences are not well-validated (Pearson, 2013; Richardson and Watson, 2013). Therefore, phenotypic studies are important to determine how well genomic data reflects the biology (Baric *et al.*, 2016). Smaller-scale studies facilitate a detailed assessment of both genomic data (e.g. via thorough annotation) and phenotypic profiles (e.g. through experimentation), therefore enabling linking of genotype to phenotype (e.g. Liu *et al.* (2021)). For conjugation studies, phenotypic assessment can reveal whether annotated genes are functional and plasmids are conjugative.

1.8.3 RNA-sequencing

WGS is a powerful tool which can inform on, for example, gene presence/absence (Gabrielaite and Marvig, 2020), and variation by comparison to reference sequences (Marco-Puche *et al.*, 2019; Uelze *et al.*, 2020). RNA-sequencing (RNA-seq) permits gene expression to be studied and reveals functional sequence in a given condition (Wang *et al.*, 2009). RNA-seq is becoming a popular technique in studies of bacterial populations as it can provide substantial insight into the biological processes that are important in a given environment (Haas *et al.*, 2012; Imdahl *et al.*, 2020).

1.9 Bacterial lifestyles

Biofilms are a problem in hospital environments where they can reside on surfaces (Costa *et al.*, 2019) and are commonly found at infection sites (Chhibber *et al.*, 2017; Devanga Ragupathi *et al.*, 2020). Bacteria can exist in both planktonic and biofilm lifestyles although biofilms are thought to be the most common lifestyle in nature (Figure 1.12) (Ghigo, 2001; Hall and Mah, 2017). Biofilms are composed of aggregated cells that are often surface-attached (Hall-Stoodley *et al.*, 2004; Wingender *et al.*, 2016). Conversely, planktonic cells are suspended individually in liquid (Hall-Stoodley *et al.*, 2004; Mikkelsen *et al.*, 2007) and as a result experience mixing in their environment (Stalder and Top, 2016). Planktonic cells are therefore likely to have equal exposure to environmental conditions as their neighbours (Hall and Mah, 2017; Hall-Stoodley *et al.*, 2004) and are unlikely to remain in close proximity to each other, reducing the probability of cell-cell contact (Stalder and Top, 2016).

In contrast, cells in a biofilm produce extracellular polymeric substance (EPS) composed of polysaccharides, DNA, lipids and proteins, which forms a matrix to maintain biofilm structure and provide protection against harmful environmental conditions (Wingender *et al.*, 2016). Biofilms can form on surfaces with a range of prop-

erties, including urinary catheters, teeth, microplastics and plants (Arias-Andres *et al.*, 2018; Donlan, 2002; Karatan and Watnick, 2009; Marsh, 2006; Schroll *et al.*, 2010). The lack of mixing in a biofilm creates gradients of, for example, nutrients and oxygen. As a result, cells at the base of a biofilm are likely to experience nutrient and oxygen depletion whereas surface-exposed cells may have ample oxygen and nutrients available. These gradients, in combination with the variable composition of the matrix, create a heterogeneous environment within the biofilm (Wingender *et al.*, 2016). In addition, cells in a biofilm are in close proximity to each other which may have implications for HGT permitted by cell-cell contact (Stalder and Top, 2016).

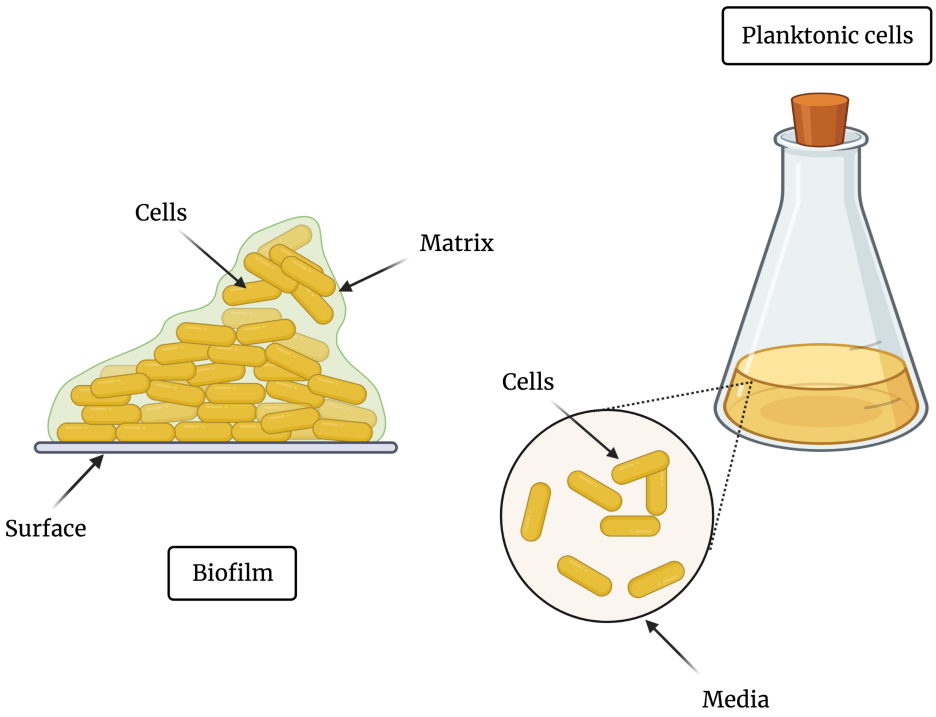

Figure 1.12: Biofilm and planktonic lifestyles. Left: Biofilm cells are in close proximity, surface-attached and encased in a self-produced protective matrix. Right: Planktonic cells, here shown in a flask for illustrative purposes, are free-floating and can be physically distant from each other. Created with BioRender.com.

1.9.1 Biofilm and planktonic populations are distinct

Biofilms provide vastly different conditions to those encountered by planktonic cells (Wingender *et al.*, 2016) and are inherently more drug-tolerant than planktonic cells (Hall and Mah, 2017). Biofilm formation comprises several stages, from initial attachment to a surface to microcolony formation, maturation and dispersal (Hall-Stoodley *et al.*, 2004; Stanley and Lazazzera, 2004). Perhaps due to ease of manipulation, many studies on bacterial cells have been carried out on planktonic populations (Trampari *et al.*, 2021). However, it is essential to study these two lifestyles separately as it is challenging to determine the state of biofilm-embedded cells from that of planktonic cells and vice versa (Wingender *et al.*, 2016). In fact, several studies have demonstrated characteristic transcriptional profiles for cells in the biofilm lifestyle compared to planktonic cells (Guilhen *et al.*, 2016; Lim *et al.*, 2017; Pysz *et al.*, 2004). Guilhen *et al.* (2016) found, when comparing gene expression in *K. pneumoniae* biofilm and planktonic cultures, that transcriptional fingerprints could be determined relating to growth stages in planktonic cultures (exponential phase versus stationary phase) and biofilms (aggregates versus 3D structures and cells dispersed from a biofilm). This demonstrated that gene expression is specifically tailored to the growth stage within each lifestyle. Taken together, it is clear that biofilms are important and unique bacterial lifestyles which require individual study.

1.9.2 A method to study biofilms

Although multiple methods have been used to study biofilms, biofilm is often grown, and its formation measured, in microtitre plates. This is a simple protocol where the planktonic population can be removed by washing, and the adhered population stained with, for example, crystal violet for quantification (using absorbance as a proxy for cell mass) in a microplate reader (Azeredo *et al.*, 2017; O'Toole, 2010). Although this method has been used to quantify biofilm in multiple bacterial species

(O'Toole, 2010), its applications are somewhat limited by the need for staining (crystal violet is anti-bacterial (Maley and Arbiser, 2013), so cells cannot be taken forward for subsequent experiments), and the readout which provides a crude approximation of cell number (Beal *et al.*, 2020). Nonetheless, this remains a broadly-applicable screening tool that can be carried out at low cost (Wilson *et al.*, 2017), and the resulting data can be compared between studies. Crystal violet biofilm assays have been used to investigate several research areas, including evaluating biofilm formation of *K. pneumoniae* clinical isolates (Cusumano *et al.*, 2019) and assessing any impact of plasmid presence on biofilm formation (Gama *et al.*, 2020)).

1.10 Importance

K. pneumoniae is particularly problematic in hospital settings where it contributes to the burden of infections in some of the most vulnerable patients (Wyres *et al.*, 2020a). *K. pneumoniae* is also a carrier of AMR genes, including carbapenem resistance genes, which it can spread horizontally to other bacteria via conjugation (Hendrickx *et al.*, 2020; Wyres and Holt, 2018). There is evidence of intra- (Pedersen *et al.*, 2020) and inter-species (Göttig *et al.*, 2015) transfer of AMR plasmids from *K. pneumoniae* in hospitals, and improved WGS technologies (e.g. long-read sequencing (Pedersen *et al.*, 2020)) are facilitating study of such events.

Alongside drug resistance, *K. pneumoniae* can form biofilms, including at infection sites and on implanted device surfaces (Piperaki *et al.*, 2017; Townsend *et al.*, 2020). These aggregates of cells encased in a matrix are protected by their lifestyle and may be inherently more tolerant to antimicrobials than their planktonic counterparts (Anderl *et al.*, 2000; Wingender *et al.*, 2016). There have been indications that cells in a biofilm may also be more likely to transfer their plasmids horizontally creating a 'hotspot' for HGT, and that this process may be facilitated by the close proximity of biofilm-associated cells (Stalder and Top, 2016). This, in conjunction

with the potential relationship of (conjugative) plasmid carriage and biofilm, where some plasmids have been shown to promote biofilm formation (Gama *et al.*, 2020; Ghigo, 2001) hints at a putative positive feedback loop between biofilm formation, plasmid carriage and plasmid transfer. However, there is no clear consensus on the effect of the biofilm lifestyle on plasmid transfer, or on the effect of plasmid carriage on biofilm formation.

Conjugative plasmids can carry genes encoding resistance to clinically important antibiotics (Chandramohan and Revell, 2012). The conjugative transfer of such plasmids between cells contributes to a large extent to the AMR problem (Carattoli, 2013). There are significant gaps in our knowledge on conjugative plasmid transfer in biofilm settings (Abe *et al.*, 2021; Król *et al.*, 2013; Stalder and Top, 2016).

1.11 Aims, hypotheses and objectives

The aim of this project was to investigate plasmid transfer and prevalence in *K. pneumoniae* planktonic and biofilm lifestyles using clinically-relevant model systems. Based on the existing evidence, the main hypothesis was that there will be higher levels of plasmid transfer in the biofilm lifestyle compared to the planktonic lifestyle.

The objectives of this study were to:

1. Investigate transfer of pKpQIL from a *K. pneumoniae* host in planktonic and biofilm lifestyles using a fluorescence reporter system.
2. Characterise a set of carbapenemase-producing *K. pneumoniae* isolates and their plasmids using whole genome sequencing.
3. Quantify and evaluate plasmid transfer between *K. pneumoniae* clinical isolate donors and a *K. pneumoniae* recipient in planktonic and biofilm lifestyles using classical plating assays.

4. Compare gene expression between a recipient and a transconjugant carrying a carbapenem resistance plasmid in planktonic and biofilm lifestyles using RNA-sequencing.

Chapter 2

Materials and Methods

2.1 Bacterial strains, plasmids and primers

Bacterial strains were originally obtained from -80°C glycerol stocks. Beads in glycerol were used to store strains (Technical Service Consultants Ltd Protect cryobeads). Strains were freshly plated weekly on to Lysogeny Broth agar (LBA) plates from glycerol bead stocks kept at -20°C. These plates were routinely incubated statically at 37°C overnight and kept at 4°C for later use, up to 1 to 2 weeks, unless indicated otherwise. Information on strains (Table 2.1), plasmids (Table 2.2) and antibiotics (Table S1) used in this study is provided. Controls to check for media/diluent contamination were included for each overnight culture and experiment. Media was prepared from ready-to-use powder (Sigma-Aldrich for LBA and Lysogeny Broth (LBB) and VWR Chemicals for Tryptic Soy Broth (TSB)). TSB was supplemented as per Cusumano *et al.* (25 mg/L calcium chloride, 12.5 mg/L magnesium sulphate, and 1.25% total glucose) (Cusumano *et al.*, 2019) and the supplemented media has been abbreviated here as TSBs. Overnight cultures (5-10 mL) prepared using LBB or TSBs were inoculated using single colonies from agar plates and incubated (Innova®44, New Brunswick) with shaking (150 rpm) overnight at

37°C. For optical density (OD) measurements, overnight cultures were diluted 1:10 in LBB, TSBs or phosphate buffered saline (PBS) depending on the experiment. OD measurements were taken at 600 nm (OD_{600}) using a Jenway 6300 spectrophotometer. Unless indicated otherwise, LBB was used for growth and OD adjustment of overnight cultures and three biological replicates were carried out per experiment. Where indicated, technical replicates were included.

Table 2.1: Bacterial strains used in this study

Species	Lab ID	Strain description	Relevant antimicrobial resistance(s) and concentrations (µg/mL) used for selection	Source/reference
Klebsiella pneumoniae	H222	Wild-type (WT) Ecl8 (derivative of human clinical isolate (Forage and Lin, 1982) with *rpoB* mutation (His537Leu) conferring rifampicin resistance	N/A	(Buckner *et al.*, 2018)
Klebsiella pneumoniae	H234	WT Ecl8 carrying an insertion (p*acp*P-*mCherry-aph*) between *putPA* on the chromosome. mCherry production produces red fluorescence. Recipient strain.	Kanamycin, 50	(Buckner *et al.*, 2020)
Klebsiella pneumoniae	H235	WT Ecl8 carrying pKpQIL*gfp*. GFP production produces green fluorescence. Donor strain.	Kanamycin, 50	(Buckner *et al.*, 2020)
Klebsiella pneumoniae	CPE01	Carbapenem-resistant clinical isolate carrying $bla_{\text{NDM-5}}$ and $bla_{\text{OXA-181}}$ originating from a patient's ear	Doripenem, 1	This study
Klebsiella pneumoniae	CPE08	Carbapenem-resistant clinical isolate carrying $bla_{\text{KPC-3}}$ originating from a rectal/faecal swab	Doripenem, 1	This study
Klebsiella pneumoniae	CPE16	Carbapenem-resistant clinical isolate carrying $bla_{\text{NDM-1}}$ originating from a urine sample	Doripenem, 1	This study
Klebsiella pneumoniae	CPE24	Carbapenem-resistant clinical isolate carrying $bla_{\text{OXA-232}}$ originating from a rectal/faecal swab	Doripenem, 1	This study
Klebsiella pneumoniae	CPE25	Carbapenem-resistant clinical isolate carrying $bla_{\text{NDM-5}}$ and $bla_{\text{OXA-181}}$ originating from a urine sample	Doripenem, 1	This study
Klebsiella pneumoniae	KP1	Rifampicin resistant ATCC 43816 (spontaneous mutant)	Ampicillin, 50	(Cano *et al.*, 2015)
Klebsiella pneumoniae	KP21	KP1 containing pACBSCE	Chloramphenicol, 35	Plasmid was a gift from the Antimicrobials Research Group
Klebsiella pneumoniae	KP16	H222 containing pMN402	Hygromycin B, 300	Plasmid originally from (Scholz *et al.*, 2000)
Klebsiella pneumoniae	KP20	KP1 containing chromosomal hygromycin resistance cassette from pSIM18 inserted into bla_{SHV}	Hygromycin B, 300	This study
Klebsiella pneumoniae	KP3	WT Ecl8 carrying pKpQIL-UK	Doripenem, 0.25	(Buckner *et al.*, 2018)
Escherichia coli	EC3	MG1655 carrying pSIM18	Hygromycin B, 150	Gift from the Blair group
Escherichia coli	EC1	alpha-select carrying pACBSCE	Chloramphenicol, 35-100	Gift from the Antimicrobials Research Group
Escherichia coli	EC22	ST131 pMN402	Hygromycin B, 300	Gift from Dr Chris Connor (McNally group)

Table 2.2: Plasmids used in this study

Plasmid name	Relevant antimicrobial resistance(s) and concentrations (µg/mL) used for selection	Relevant information/phenotype	Source/reference
pKpQIL-UK	Doripenem, 0.25	Conjugative F-type plasmid	(Buckner *et al.*, 2018)
pKpQIL*gfp*	Kanamycin, 50	Conjugative F-type plasmid	(Buckner *et al.*, 2018)
pMN402	Hygromycin B, 300	Non-conjugative GFP plasmid	(Scholz *et al.*, 2000) Gift from the McNally group
pACBSCE	Chloramphenicol, 35-100	Recombineering plasmid containing lamda-Red recombinase and I-SceI endonuclease genes. Expression of these genes is controlled by the arabinose-inducible pBAD promoter.	(Lee *et al.*, 2009) Gift from the Antimicrobials Research Group
pSIM18	Hygromycin B, 150	Origin of hygromycin resistance cassette for cloning into KP1	(Chan *et al.*, 2007) Gift from the Blair group
pCPE01_2	Doripenem, 1-4	Conjugative plasmid from CPE01 clinical isolate containing $bla_{\text{NDM-5}}$ conferring carbapenem resistance	This study
pCPE16_3	Doripenem, 1-4	Conjugative plasmid from CPE01 clinical isolate containing $bla_{\text{NDM-1}}$ conferring carbapenem resistance	This study
pCPE25_3	Doripenem, 1-4	Conjugative plasmid from CPE01 clinical isolate containing $bla_{\text{NDM-5}}$ conferring carbapenem resistance	This study

Table 2.3: Primers and colony PCR annealing temperatures (temp.). Colony PCR conditions are described in Table 2.5

Lab ID	Description	Orientation	Sequence (5'-3')	Temp. °C	Designed by
9	Generation of hygromycin resistance cassette from pSIM18. Paired with 10	Forward	ctcgcctttatcggccctcactcaaggatgtattgtggttGATCTGA ATTGCTATGTTTA	N/A	S.J. Element
10	Generation of hygromycin resistance cassette from pSIM18. Paired with 9.	Reverse	AGCGGATACATATTTGAATGccgaataacaaagcagagc gcattgtggtgatttatctg	N/A	S.J. Element
11	Check for location of hygromycin resistance cassette insertion in KP1/ check for recipient chromosome in conjugation assays. Paired with 12.	Forward	GATGACAAATGATGAAGGAA	50	S.J. Element
12	Check for location of hygromycin resistance cassette insertion in KP1/ check for recipient chromosome in conjugation assays. Paired with 11.	Reverse	GGATTTTGGTCATGAGATTA	50	S.J. Element
15	Check for *gam* from pACBSCE to confirm presence of pACBSCE recombineering plasmid Paired with 11.	Forward	CACTAACCCCCTTTCCTGTT	52	S.J. Element
16	Check for *gam* from pACBSCE to confirm presence of pACBSCE recombineering plasmid Paired with 11.	Reverse	GCACCTGTTTGAATCGCTAT	52	S.J. Element
1	Check for $bla_{\text{NDM-5}}$ from pCPE01_2 or pCPE25_3. Paired with 2.	Forward	ATGCCGACACTGAGCACTAC	54	C. Kessler
2	Check for $bla_{\text{NDM-5}}$ from pCPE01_2 or pCPE25_3. Paired with 1.	Reverse	GAATTCGAGCTGCAAACCGC	54	C. Kessler
3	Check for *repA* from pCPE01_2 or pCPE25_3 (designed against pCPE01_2 backbone FII-2 location ∼70,000 bp). Paired with 4.	Forward	TTCACACGACGCTCCACTTC	54	C. Kessler
4	Check for *repA* from pCPE01_2 or pCPE25_3 (designed against pCPE01_2 backbone FII-2 location ∼70,000 bp). Paired with 3.	Reverse	TAAGTCCCGTGGAATAAAACG	54	C. Kessler
17	Check for $bla_{\text{NDM-1}}$ from pCPE16_3. Paired with 18.	Forward	GATAGGGGAAGAATTCGAGC	50	S.J. Element
18	Check for $bla_{\text{NDM-1}}$ from pCPE16_3. Paired with 17.	Reverse	CAATATCACCGTTGGGAT	50	S.J. Element
19	Check for *repA* (FIBK) from pCPE16_3. Paired with 20.	Forward	GACTCATCGGCGGTAAGTTC	50	S.J. Element
20	Check for *repA* (FIBK) from pCPE16_3. Paired with 19.	Reverse	CAGCAGCACCATTGAACTTC	50	S.J. Element
21	Check for *repA* (FIB) from pCPE16_2. Paired with 22.	Forward	GGTCGTATGTTTAGGATAGGA	50	S.J. Element
22	Check for *repA* (FIB) from pCPE16_2. Paired with 21.	Reverse	GCCATACACGGAAATCTGTC	50	S.J. Element
23	Check for *repA* (HIB) from pCPE16_2. Paired with 24.	Forward	GGATGGCAGTGACCCTATGG	50	S.J. Element
24	Check for *repA* (HIB) from pCPE16_2. Paired with 23.	Reverse	GGATCCGTGTCAGTGAGTCG	50	S.J. Element
25	Check for *repA* from pCPE16_4. Paired with 26.	Forward	CGTTCAGTCCGACTGCTGCG	53	S.J. Element
26	Check for *repA* from pCPE16_4. Paired with 25.	Reverse	GGTTCAGTAGAGTTGGCGCT	53	S.J. Element
27	Check for *repA* from pCPE16_5. Paired with 28.	Forward	GAATGGGAGTCTCTTACCGC	50	S.J. Element
28	Check for *repA* from pCPE16_5. Paired with 27.	Reverse	AATACGCAGCAAAGCAATGG	50	S.J. Element
29	Check for pCPE16_3 'region 1' (72,750-72,947). Paired with 30.	Forward	GCTTTATTTCCTGCTGTGTC	50	S.J. Element
30	Check for pCPE16_3 'region 1' (72,750-72,947). Paired with 29.	Reverse	CCTCAGACATCAGACACTAG	50	S.J. Element
31	Check for pCPE16_3 'region 2' (93,043-93,237). Paired with 32.	Forward	CGCTGCATATTTCCTTTATC	50	S.J. Element
32	Check for pCPE16_3 'region 2' (93,043-93,237). Paired with 31.	Reverse	ATTGACCATACAGCCAGGCG	50	S.J. Element
33	Check for pCPE16_3 'region 3' (113,401-113,627). Paired with 34.	Forward	CGGGCGGCAGAAGAACAGCA	50	S.J. Element
34	Check for pCPE16_3 'region 3' (113,401-113,627). Paired with 33.	Reverse	GCCACCTGCTGAATCGCCTC	50	S.J. Element
35	Check for pCPE16_3 'region 4' (15,027-15,203). Paired with 36.	Forward	ATCACACGCACGGAACTCTA	50	S.J. Element
36	Check for pCPE16_3 'region 4' (15,027-15,203). Paired with 35.	Reverse	CGTGCTAACTTGCGTGATAC	50	S.J. Element
37	Check for pCPE16_3 'region 5' (36,129 -36,313). Paired with 38.	Forward	GACGGGGCGGGATTTTTAAG	50	S.J. Element
38	Check for pCPE16_3 'region 5' (36,129 -36,313). Paired with 37.	Reverse	GTCACCCATCCAGCGAAGCA	50	S.J. Element

2.2 Crystal violet biofilm assays

Overnight cultures corrected to an OD_{600} of 0.1 in LBB or TSBs (150 µL) were added to wells of a sterile Cellstar® 96-well polystyrene u-bottom plate (Greiner Bio-one). Plates were covered with a Breathe-Easy® gas-permeable membrane (Diversified Biotech, Sigma-Aldrich) and sterile lid. These were incubated statically at 37°C for 24- 72 h. After incubation, culture was removed from the wells using a multichannel pipette, and the wells were washed once with 150 µL of distilled water. Crystal violet solution (1%) (Sigma-Aldrich) was diluted to 0.1% with distilled water and 150 µL of this solution was added to plate wells and the plate was incubated statically for 15 min at room temperature. The excess stain was removed using a pipette and the wells were washed in distilled water as above. The stain was solubilised in 150 µL ethanol (70%) for 15 min at room temperature with shaking (60 rpm, Orbit LS Labnet International Inc.). Liquid (50 µL) was removed from the wells leaving a final volume of 100 µL. The absorbance 600 nm (A_{600}) of this liquid was measured using a FLUOstar Optima plate reader (BMG Labtech) or a Spark microplate reader (Tecan). For each biological replicate, three technical replicates were included.

2.3 Growth kinetics

Growth kinetics were assessed as previously described (Cottell *et al.*, 2014). Overnight cultures were diluted 1:1000 in LBB or TSBs. This diluted culture (20 µL or 10 µL) was added to 180 µL or 90 µL LBB or TSBs respectively in a Cellstar® 96-well polystyrene u-bottom plate (Greiner Bio-one). A_{600} was recorded over 16 h using a plate reader. Data were analysed by observation of growth curves (absorbance plotted against time) and by calculating maximum growth rate.

Maximum growth rate was determined for each experiment by finding the mean of replicate data (three technical replicates per biological replicate, three biological

replicates per experiment), calculating the growth rate (µ) at each time point and selecting the highest value. Growth rate was calculated as follows where t refers to a given time point and A refers to the A_{600} at that time point:

$$\frac{(ln(At2) - ln(At1))}{(t2 - t1)}$$

2.4 Viable counts

Cultures were serially diluted in PBS and plated by spotting (three technical replicates of 25 µL per biological replicate for each dilution) onto LBA plates containing appropriate antibiotics where required. After static overnight incubation (16 h) at 37°C, colonies were counted and CFU/mL were determined. Three or four biological replicates were carried out (experiment-dependent), each the mean of three technical replicates.

2.5 Fluorescence reporter system for flow cytometry and microscopy

To enable quantification and visualisation of cells and plasmid transmission events, strains carrying fluorescent markers either on the plasmid (*gfp*) or chromosome (*mcherry*) were used (Figure 2.1). Emission spectra of these fluorophores are presented in Figure S1. Construction of the strains, done previously, is described in Buckner *et al.* (2020).

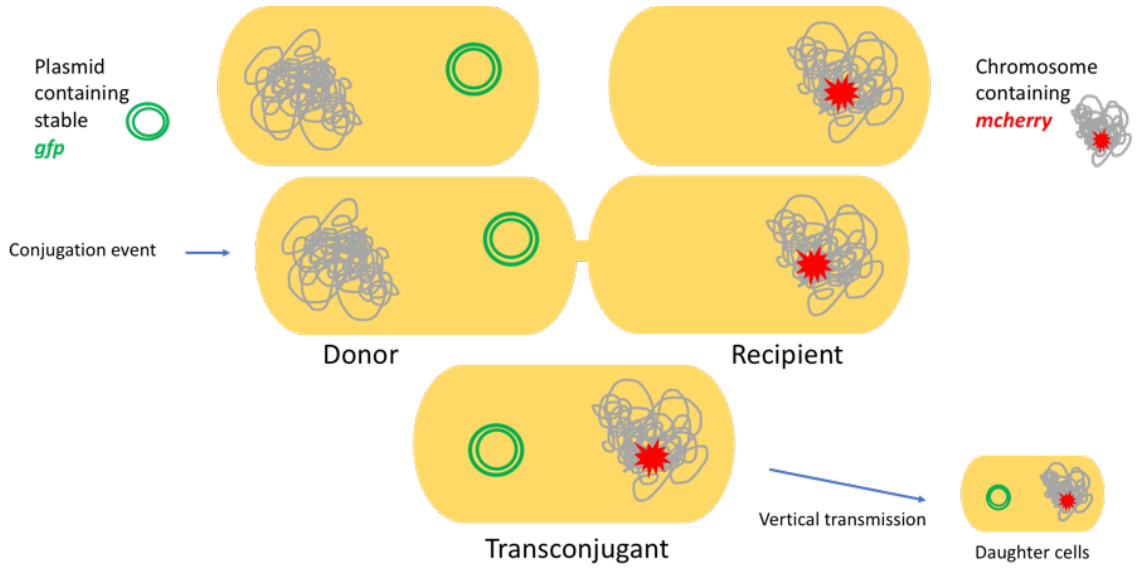

Figure 2.1: Schematic of the fluorescence reporter system used to monitor plasmid transmission/persistence in flow cytometry experiments and for visualisation of cells using microscopy. A *gfp*-containing plasmid (green circles) is transferred via conjugation to a recipient cell labelled with *mcherry* on the chromosome. The resulting transconjugant expresses both mCherry and GFP. Transconjugant daughter cells also have this fluorescence profile.

2.6 Flow cytometry

2.6.1 Preparation of biofilm growth plates in 6-well format for flow cytometry

Overnight cultures corrected to an OD_{600} of 0.1 (2 mL) were added to wells of a sterile CytoOne® 6-well polystyrene plate (Starlab UK). Where strains were mixed for conjugation (plasmid transmission/persistence) experiments, 1 mL of each strain was added for a final volume in the well of 2 mL. Plates were covered with a Breathe-Easy® (Diversified Biotech, Sigma-Aldrich) gas-permeable membrane and a lid and incubated at 37°C statically for 72 h.

2.6.2 Sample preparation for flow cytometry

After 72 h of incubation (see section 2.6.1), the liquid portion from plates was removed using a pipette for later use as the planktonic population. Plates were washed once with 2 mL sterile filtered PBS (Sigma-Aldrich). Next, PBS (1 mL) was added to each well and tissue-culture cell scrapers (catalogue number 83.1830, Sarstedt) were used to remove and disrupt the adhered cells. To do this, the cell scraper was pushed along the base and sides of the wells twice. The PBS containing suspended cells was removed using a pipette for later use as the biofilm population. Each cell suspension (planktonic and biofilm) was mixed by pipetting and further diluted (1:1000 unless indicated otherwise) in PBS and vortexed for 20 s before use on the Attune® NxT Focusing Cytometer (ThermoFisher Scientific).

2.6.3 Experiment settings

Calibration beads (Attune™ Performance Tracking Beads, ThermoFisher Scientific) were used to assess instrument performance before each experiment to ensure consistency between experiment runs. Due to insufficient fluorescent event acquisition for control samples, it was necessary to apply compensation from a single experiment to all experimental data. However, due to limited spectral overlap, the compensation required is minimal (Figure S1). Prepared samples (see section 2.6.2) were run as tube experiments using the Attune® NxT software (Invitrogen). Forward scatter (FSC) and side scatter (SSC) voltages were set at 420 and 380 respectively. Blue (488 nm excitation) laser (BL-1) and yellow (651 nm excitation) laser (YL-2) voltages were both set at 400. The threshold was set at 0.4 x 1000 for FSC and 0.5 x 1000 for SSC. Bandpass filters 530/30 and 620/15 were used. Gating/experiment settings were initially determined by using Spherotech 8-Peak 3 µM Validation Beads (FL-1 - FL3) (BD Biosciences) to locate particles of a similar size to bacterial cells. Gating was carried out firstly to locate fluorescent events using the Attune® NxT

software during sample acquisition. A 'total bacteria' gate (Figure S2) was placed to include these events on FSC-A SSC-A plots. Although non-fluorescent and fluorescent events were mixed, the 'total bacteria' gate was placed to include as many fluorescent events and exclude as many non-fluorescent events as possible. This 'total bacteria' gate was used to set event acquisition (to stop at 10,000 events in the 'total bacteria' gate unless indicated otherwise). BL-1 (excites GFP) and YL-2 (excites mCherry) lasers were selected. Data were further analysed/plotted using FlowJo version 10.5.3 and Graphpad Prism version 8.0.2. Quadrant gating was used to separate populations into non-fluorescent, green fluorescent, red fluorescent and red/green fluorescent.

2.7 Microscopy

Confocal microscopy was carried out to ascertain whether biofilm was formed in the 6-well biofilm assays. Biofilm growth plates were prepared as detailed in section 2.6.1. After 72 h static incubation at 37°C, the liquid portion in the wells was discarded. Plate wells were washed once with 2 mL sterile-filtered PBS. Plate wells were imaged using the Zeiss LSM 710 ConfoCor3 inverted confocal microscope at the University of Birmingham Advanced Light Microscopy facility using 10X and 20X objectives and Ar/ArKr (488 nm) and He/Ne (543 nm) lasers with a pinhole size of 90 µM and a pixel dwell of 1.58 µs. Laser and gain settings were adjusted with the help of the Range Indicator to visualise samples whilst reducing background fluorescence. The plastic wells are not designed for microscopy but were imaged for rapid confirmation of the presence of adhered cells, not for detailed analysis.

To view the biofilm in more detail, biofilm formed in dishes with polymer coverslips at the base (µ-Dish 35 mm, high, ibiTreat polymer cover slip, Ibidi) was imaged after identical treatment to the biofilm in the 6-well plates. Acquisition settings were as above except using a 63X objective under oil with a pinhole size of 99 µM.

In addition, disrupted biofilm from polystyrene 6-well assays (5 µL) was imaged on a glass slide. Acquisition settings were as above except using a 63X objective under oil, with a pixel dwell of 0.64 µs and a pinhole size of 148 µM.

All images were acquired using Zen 2012 (black edition) software. Images were exported using ImageJ version 1.51.

2.8 Construction of KP16 control strain

For flow cytometry experiments, a strain carrying a non-conjugative GFP plasmid (negative control) was required. To obtain this, the parental strain H222 (from which the fluorescent strains H234 and H235 were constructed) was made electrocompetent. To do this, an overnight culture of H222 was sub-cultured (100 µL overnight culture in 100 mL LBB) and grown until mid-exponential phase. The subculture was put on ice, and once cold transferred to pre-cooled centrifuge tubes and centrifuged (15 min, 4°C, 3900 x g). Supernatants were discarded and pellets were washed in 20 mL ice-cold sterile-filtered 10% glycerol twice. Cells were then centrifuged as above, resuspended in 200 µL ice-cold 10% glycerol and kept on ice.

Plasmid pMN402 from EC22 was purified using a QIAprep Spin Miniprep Kit (Qiagen) following the manufacturer's instructions. This was electroporated in to H222 by combining 40 µL of electrocompetent H222 cells with 2, 3, and 4 µL of plasmid. To do this, plasmid DNA was transferred to sterile ice-cold microfuge tubes. Electrocompetent cells were added to these tubes (including a cells-only control) and mixed twice by pipetting. The mixture was transferred to sterile ice-cold 2 mm electroporation cuvettes (Cell Projects) where they were electroporated at 2500 V in a Eporator (Eppendorf). Media (1 mL LBB pre-warmed to 37°C) was added to the cuvette. The cuvette contents was then transferred to a microfuge tube and put at 37°C in a shaking incubator (150 rpm) for 1.5 h for the cells to recover. To select for successful transformants, recovered cells were pelleted (1 min, 12470

x g), the supernatant was discarded and the cells resuspended in LBB were plated out onto hygromycin agar plates (300 µg/mL). GFP fluorescence of this strain was initially checked using a blue light box and then by running on the Attune NxT flow cytometer.

2.9 Conjugation assays

2.9.1 Planktonic conjugation assays (plating method)

This method was developed based on the conjugation protocol by Hardiman *et al.* (2016). Donor and recipient cultures were grown overnight in 5 mL LBB at 37°C shaking (150 rpm). Subcultures were prepared in 5 mL LBB (1% inoculum) and grown to an OD_{600} of approximately 0.5. Cultures (1 mL) were centrifuged (3 min, 4722 x g) and media was replaced with TSBs to correct the OD_{600} to 0.5. The donor and recipient were mixed at a 1:10 ratio and then diluted 1:5 (500 µL total volume) in TSBs in sterile 1.5 mL microfuge tubes. Single strains were diluted 1:5 in TSBs as above. Tubes were incubated statically at 37°C for 20 h. Donor and recipient cells were plated out at 0 h and 20 h to quantify total viable counts. For each biological replicate, three 25 µL technical replicates were spot plated. Serial dilutions were prepared in PBS to achieve countable colonies. At 0 h and 20 h, donors and recipients (single strains) were plated on LBA to assess their individual growth over the incubation period. To determine background growth, at 0 h and 20 h donors were plated onto the antibiotic used to select the recipient (hygromycin 300 µg/mL) and recipients were plated onto the antibiotic used to select the donor (doripenem 4 µg/mL). Mixed donors and recipients were plated onto single antibiotics (doripenem or hygromycin) to select the donor and recipient respectively and determine the proportion of these two strains. At 20 h, mixed strains were also plated on dual antibiotic (doripenem 4 µg/mL and hygromycin 300 µg/mL) to se-

lect putative transconjugants. PBS-only and media-only controls were included. For these, PBS used for serial dilutions was plated on LBA and incubated overnight. For the media-only control, media alone was incubated alongside microfuge tubes containing media and cells. Agar plates were incubated for 16-24 h before colonies were counted. Transconjugant selection plates and plates to determine background were incubated for 24 h, whilst other plates were incubated for 16 h.

Putative transconjugants were restreaked on dual antibiotic (doripenem and hygromycin) to confirm growth. To check for the presence of the plasmid and the recipient chromosome, a selection of single colonies from across the plates/replicates were taken to prepare lysates for colony PCR. The same colonies were replicated onto dual antibiotic. Once the transconjugants were confirmed, these colonies were used to prepare plates for whole genome sequencing and -80°C bead stocks so that transconjugant colonies were saved at the earliest opportunity.

2.9.2 Biofilm conjugation assays (plating method)

Cultures were grown overnight in 5 mL LBB at 37°C shaking (150 rpm). Next, cultures were OD_{600} corrected to 0.1 in TSBs (15 mL). To do this, culture volume to be added for OD correction was removed from 15 mL TSBs and this volume was replaced with overnight culture to achieve OD_{600} 0.1. The donor and recipient were mixed at a 1:10 ratio (from now on called 'mixed cultures') by adding 750 µL of donor culture to 7.5 mL of recipient culture. Single donor and recipient cultures, and mixed cultures (2 mL) were added to wells of a CytoOne® 6-well polystyrene plate (Starlab UK). Plates were covered with a Breathe-Easy® membrane (Diversified Biotech) and a lid and incubated statically at 37°C for 24-72 h.

Donor, recipient and mixed cultures, and PBS and media controls were diluted (where required) and plated on agar as per the planktonic conjugation assay protocol (section 2.9.1) at 0, 24, 48 and 72 h time points. At the 24, 48 and 72 h time points,

adhered cells were harvested by removing liquid culture and washing once with sterile PBS (2 mL). PBS was added to wells (1 mL) and the base and sides of each well were scraped twice using a cell scraper (catalogue number 734-2602, VWR) to disrupt the biofilm for plating. A selection of putative transconjugant colonies were re-streaked on dual antibiotic (doripenem 4 µg/mL and hygromycin 300 µg/mL) to confirm growth.

Conjugation frequencies were calculated as follows using values from assay endpoints

$$\text{Ratio} = \frac{\text{Mean number of donor cells}}{\text{Mean number of recipient cells}}$$

$$\text{Conjugation frequency} = \frac{\text{Mean number of transconjugants}}{\text{Mean number of recipient cells} \times \text{ratio}}$$

This becomes:

$$\frac{\text{Mean CFU/mL transconjugants}}{\text{Mean CFU/mL donors}}$$

2.10 Colony PCR

To prepare lysates, single colonies were added to 50-100 µL of molecular grade water and heated for 10 min at 100°C. Lysates were added to reactions as DNA, or molecular grade water was added in the DNA-free control. Reactions were prepared as per Table 2.4 under the conditions in Table 2.5.

Table 2.4: Reaction components for colony PCR

Component	Volume (µL)
Molecular grade water	7.5
REDtaq® ReadyMix™ 2x (Sigma)	12.5
Forward primer 25 µM	1
Reverse primer 25 µM	1
DNA (or water for control)	3

Table 2.5: Colony PCR conditions. 30 cycles indicated by '*'

Step	Temperature (°C)	Time (s)
Initial denaturation	95	60
Denaturation	95	*15
Annealing	Dependent on experiment (see Table 2.3)	*15
Extension	72	*30
Final extension	72	600
Store	4	hold

2.11 Gel electrophoresis

PCR reactions (7-12 µL) were run on a 1% agarose gel prepared in 1 x TAE for 40-45 min at 100 V using 5 µL HyperLadder™ 1 kb (Bioline) for size determination. SYBR™ Safe stain (Invitrogen) was used as per the manufacturer's instructions for DNA visualisation. Gels were imaged using the Amersham™ Imager 680 (Cytiva).

2.12 Construction of a hygromycin-resistant KP1 recipient strain

2.12.1 Method overview

The following is based on Datsenko and Wanner's method (Datsenko and Wanner, 2000) and includes protocol adaptations made by Dr Jessica Gray. The aim was to insert a hygromycin-resistance cassette from pSIM18 into bla_{SHV} on the chromosome of KP1. Recombineering primers (Table 2.3) were designed to have 40 bp homology to the KP1 chromosome and 20 bp homology to the hygromycin resistance cassette from pSIM18. Sequences corresponding to the bla_{SHV} chromosomal region where the cassette was inserted (Figure S3), to the hygromycin cassette from pSIM18 (Figure S4), and to the predicted final sequence post cassette insertion (Figure S5) are provided. PCR was used to amplify the hygromycin resistance cassette from

pSIM18 using the recombineering primers (Table 2.3).

The pACBSCE recombineering plasmid was used to insert the hygromycin resistance cassette into the KP1 chromosome to interrupt bla_{SHV}. Briefly, electrocompetent cells of KP1 were prepared, pACBSCE was electroporated in to KP1 and successful transformants (KP21) were selected. Next, electrocompetent cells of KP21 (KP1 pACBSCE) were prepared and the hygromycin resistance cassette (DNA donor molecule) was electroporated in. Successful transformant(s) were selected on agar containing hygromycin. To remove the recombineering plasmid, the newly-constructed strain was passaged without antibiotic. PCR and selective plating were used to confirm the presence and location of the resistance cassette, the antimicrobial resistance profile of the new recipient and to check for loss of the recombineering plasmid pACBSCE. Growth and whole genome sequencing checks were carried out by comparison to the ancestral (WT) strain. Further details are provided below.

2.12.2 Method details

Sourcing the lambda Red recombineering plasmid

pACBSCE was extracted from EC1 using a QIAprep$_{®}$ Spin Miniprep Kit (Qiagen) following the manufacturer's instructions.

Preparation of electrocompetent cells of KP1

An overnight culture of KP1 was prepared in LBB and incubated at 37°C with shaking (150 rpm). The next day, this was subcultured (500 µL of culture into 50 mL LBB) and grown up to mid-exponential phase. The culture was put on ice. Once cold, this culture was centrifuged in a sterile ice-cold 50 mL centrifuge tube at 4°C for 10 min (3900 x g), the supernatant removed and the pellet resuspended in 10 mL 10% ice-cold glycerol. A further two washes and resuspensions in 10 mL 10%

glycerol, followed by two washes and resuspensions in 1 mL 10% glycerol (12470 x g, 1 min, 4°C) were carried out. After a final wash, cells were resuspended in 150 µL 10% glycerol and put at -80°C for later use.

Electroporation and strain confirmation

Electrocompetent cells were prepared as in section 2.8, except cells were recovered in SOC media. After recovery, cells were plated out on 35 µg/mL chloramphenicol to select putative transformants. For controls, cells that had been electroporated with no plasmid DNA were plated onto two control plates (chloramphenicol 35 ug/mL and LBA). Agar plates were incubated at 37°C statically overnight. Colonies were checked by re-streaking on 35 µg/mL chloramphenicol and by checking growth on increasing concentrations of chloramphenicol (50 -150 µg/mL) to better distinguish background growth from transformants. For candidate colonies that had strong growth on chloramphenicol versus the WT, extraction using a QIAprep® Spin Miniprep Kit (Qiagen) (following the manufacturer's instructions) and gel electrophoresis was carried out to confirm plasmid presence. A glycerol bead stock prepared from a single colony containing the plasmid was saved at -80°C.

Preparation of donor DNA molecule

EC3 was grown on agar containing 150 µg/mL hygromycin at 30°C overnight. pSIM18 was purified from EC3 using a QIAprep® Spin Miniprep Kit (Qiagen) following the manufacturer's instructions. PCR was used to generate a hygromycin cassette from pSIM18 using the conditions and reactions in Tables 2.6 and 2.7.

Table 2.6: PCR conditions for preparation of DNA donor molecule. 30 cycles indicated by *

Step	Temperature (°C)	Time (s)
Initial denaturation	95	30
Denaturation	95	*30
Annealing	48	*60
Extension	72	*120
Final extension	72	600
Store	4	hold

Table 2.7: Reaction components for preparation of DNA donor molecule. Numbers in brackets refer to lab ID of primers from Table 2.3

Component	Volume (µL)
Molecular grade water	33.5
5 x Phusion HF Reaction Buffer (detergent-free) (NEB)	10
Forward primer (9) 10 µM	2.5
Reverse primer (10) 10 µM	2.5
dNTP mix 100 mM (Meridian Bioscience)	0.5
Plasmid DNA (or water for control)	0.5
Phusion® High-Fidelity DNA polymerase (NEB)	0.5

Gel electrophoresis was used to determine whether the expected product was produced. Gel Loading Dye (GelPilot ® (5X), Qiagen) was used as a marker for running the PCR products. Hyperladder™ 1 kb (Bioline) was used for size determination.

DpnI digestion

To remove the template plasmid whilst leaving the PCR product intact, DpnI was used to remove methylated DNA (Li *et al.*, 2011). Reactions (Table 2.8) were incubated statically at 37°C for 2 h. Reactions (5 µL) were checked using gel electrophoresis and a QIAquick PCR purification kit (Qiagen) was used to purify the digested product following the manufacturer's instructions. Purified product was eluted in 45 µL molecular grade water and stored at -20°C for later use.

Table 2.8: DpnI digestion and control reaction components

Digested reaction (cut)	Undigested reaction (uncut control)
DpnI (NEB) (2 µL)	Molecular-grade water (1 µL)
Cutsmart 10 x (NEB) (5 µL)	Cutsmart 10 x (2.5 µL) (NEB)
PCR product (43 µL)	PCR product (21.5 µL)

Preparation of electrocompetent cells of KP21 for recombineering and electroporation

Overnight cultures of KP21 were prepared (2 x 5 mL in 100 µg/mL chloramphenicol). Two subcultures (OD_{600} corrected to 0.025) in 50 mL LBB supplemented with 0.7 mM EDTA, 0.05% sterile-filtered arabinose and 100 µg/mL chloramphenicol were incubated at 37°C 150 rpm until mid-exponential phase and put on ice. Once cold, cultures were centrifuged for 15 min (3900 x g at 4°C). Supernatants were discarded and pellets were resuspended in 10 mL sterile ice-cold 10% glycerol. This wash step was repeated twice more and the pellet resuspended in 1 mL sterile ice-cold 10% glycerol. This was centrifuged (4722 x g, 3 min at 4°C) and resuspended in 1 mL ice-cold 10% glycerol a further three times. After the final spin, the pellets were resuspended in 150 µL ice-cold 10% glycerol and pooled. Cells were then kept on ice.

Recombineering

pACBSCE contains arabinose-inducible lambda Red machinery and the I-SceI nuclease as well as a chloramphenicol resistance marker (Lee *et al.*, 2009) to facilitate chromosomal integration of the amplified hygromycin cassette DNA and selection respectively. Electroporation of the donor hygromycin cassette DNA molecule and recovery was carried out as described above for electroporation of pACBSCE into KP1 (section 2.12.3). Donor DNA consisted of the purified, digested PCR product from the pSIM18 amplification reaction. Donor DNA (2 µL and 4 µL) was combined

with 40 µL KP21 electrocompetent cells. To assess background, both the digested (cut) and undigested (uncut) donor DNA were included, along with a cells-only (no DNA) control. After recovery, selection for successful transformants was carried out using agar plates containing 150 µg/mL hygromycin. The cells-only control was plated on 150 µg/mL hygromycin and 100 µg/mL chloramphenicol. For each condition, 100 µL of recovered cells were plated out. For all conditions apart from cells-only, an additional 500 µL of recovered cells were centrifuged (60 s, 12470 x g, room temperature) and plated out. The remaining recovered cells were left at room temperature overnight and plated out as above the next day. Agar plates were incubated at 37°C overnight. Candidate colonies were replicated onto LBA plates containing 150 µg/mL hygromycin, 50 µg/mL ampicillin and no antibiotic. Non-selective growth (on LBA) was used to promote pACBSCE loss. Further validation was done by colony PCR, whole genome sequencing and growth assessment.

2.13 Whole Genome Sequencing

Whole genome sequencing was carried out by MicrobesNG (https://microbesng.com). MicrobesNG's instructions for sample preparation were followed. Briefly, strains were grown on agar plates or in liquid culture to achieve sufficiently high cell numbers for DNA extraction as per the provided protocol(s). Cells were washed in PBS and resuspended in media or DNA/RNA Shield (Zymo Research) and delivered to MicrobesNG for whole genome sequencing (Illumina and/or Oxford Nanopore technologies). Sample preparation for Illumina and Oxford Nanopore sequencing and initial data analysis (trimming (Trimmomatic 0.30 (Bolger *et al.*, 2014), assembly (Unicycler 0.4.0 (Wick *et al.*, 2017b)) and annotation (Prokka 1.11 (Seemann, 2014))) were done by MicrobesNG using their in-house scripts. Bandage (Wick *et al.*, 2015) was used for assembly visualisation.

2.14 RNA-sequencing

Four overnight cultures of each strain were prepared in TSBs (10 mL). TSBs and PBS for use in the test conditions was pre-warmed to 37°C. The next day, the overnight cultures were used to set up three test conditions (planktonic exponential, planktonic 24 h and biofilm 24 h) as described below.

TSBs (100 mL) was inoculated with 1 mL of overnight culture and grown at 37°C 150 rpm until mid-exponential phase when 1.8 mL of the culture was harvested by centrifugation (12470 x g for 90 s). Pellets were resuspended in 1.8 mL RNAlater (ThermoFisher) and incubated at room temperature for 30 min. Cells were harvested by centrifugation using the same conditions as above and stored at -80°C. These cells represented the planktonic exponential condition.

Next the planktonic 24 h condition was set up following the same protocol as above but harvesting at 24 h.

For the biofilm 24 h setup, the overnight cultures were OD_{600} corrected to 0.1. Culture (2 mL) was added to 6-well CytoOne® (Starlab UK) polystyrene plates, covered with a Breathe-Easy® (Diversified Biotech) membrane and lid and incubated for 24 h statically at 37°C. After 24 h, all of the culture was removed and wells were washed with 2 mL pre-warmed PBS. RNAlater (1.8 mL) was added to the wells and cells were scraped from the base and sides of the wells twice before the resuspended cells (1.8 mL) were transferred to a microfuge tube. Cells in RNAlater were incubated at room temperature for 30 min before being harvested by centrifugation and transferred to -80°C for later use. These cells represented the biofilm condition.

The conditions being compared in the RNA-Seq experiment are shown in (Figure 2.2).

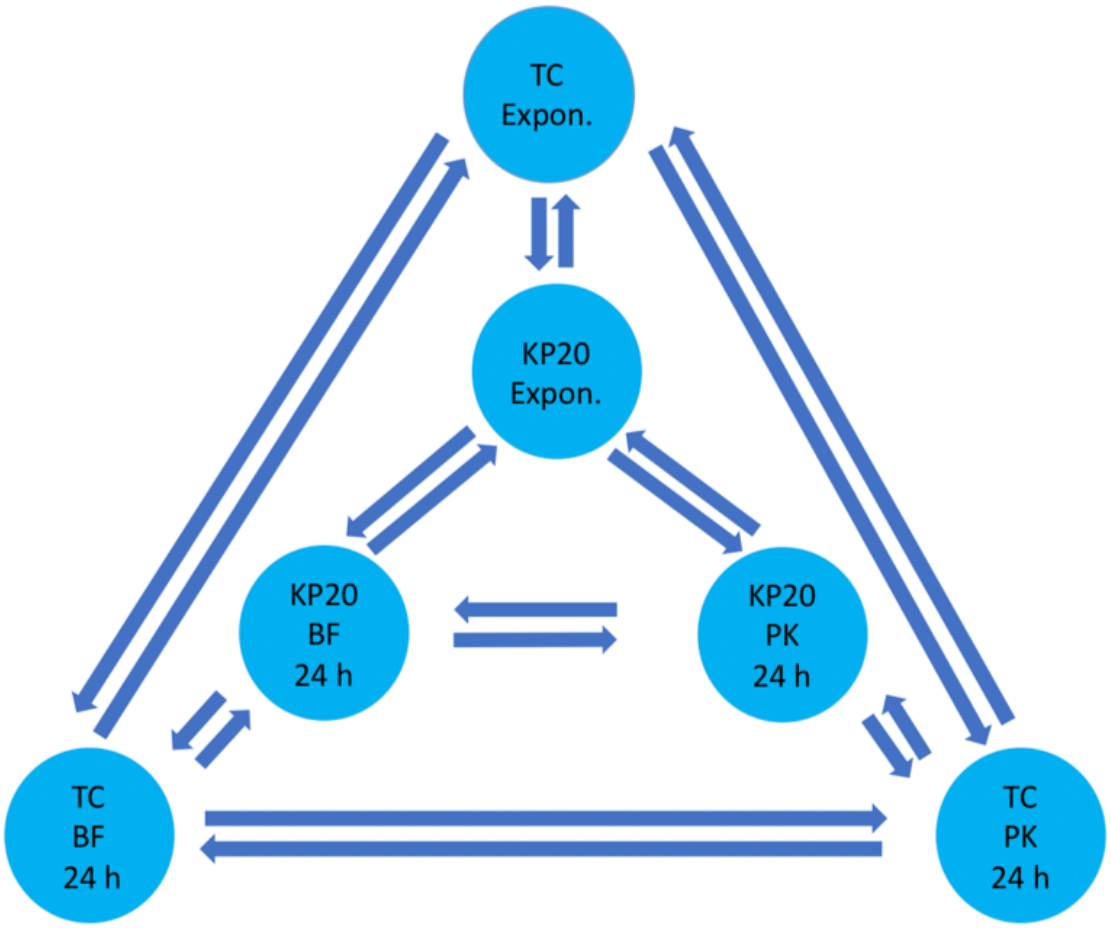

Figure 2.2: Overview of the comparisons for the RNA-Seq experiment. Arrows indicate comparisons. Circles containing text indicate conditions. TC = transconjugant. KP20 = plasmid-free recipient. Expon = exponential. PK = planktonic. BF = biofilm.

2.14.1 Evaluating plasmid persistence

Plasmid persistence for the 24 h planktonic condition and for pooled samples from the biofilm 24 h condition was assessed. Cultures were diluted in PBS and plated on LBA or LBA doripenem 2 µg/mL to distinguish plasmid-containing cells from those lacking the plasmid. Colony counts were converted to CFU/mL and the percentage of cells that maintained the plasmid was calculated.

2.14.2 Processing cell pellets

RNA extraction, sequencing and initial data analysis was performed by GeneWiz UK following their in-house protocols.

2.15 Bioinformatics

Default parameters were used for all tools unless indicated otherwise. Anaconda version (v)4.11.0 (https://www.anaconda.com/) was used, employing Python v3.7.9.

2.15.1 Manual annotation

Annotation was done using BLAST searches against reference sequences on GenBank® (Agarwala *et al.*, 2018) or from the ResFinder database (Zankari *et al.*, 2012). For conjugation module genes, GenBank sequence https://www.ncbi.nlm.nih.gov/nuccore/AP001918.1/ (Frost *et al.*, 1994) was used as a reference where possible as this entry contains annotations for an experimentally-validated conjugation module. Plasmid maps were prepared using Geneious Prime v11.0.6+10 (64 bit).

2.15.2 Characterisation

Multilocus sequence typing (MLST): The PubMLST website (https://pubmlst.org/) (Jolley and Maiden, 2010) and MLST software (Torsten Seemann, https://github.com/tseemann/mlst) were used to type isolates.

PlasmidFinder (Carattoli *et al.*, 2014)/plasmidMLST (Jolley and Maiden, 2010) were used to type putative plasmids and ResFinder (Zankari *et al.*, 2012) to locate acquired AMR genes. PlasmidFinder and ResFinder databases were queried using

ABRicate (Torsten Seeman, https://github.com/tseemann/abricate) or by using the webtools (https://cge.cbs.dtu.dk/services/PlasmidFinder/
and https://cge.cbs.dtu.dk/services/ResFinder/).

2.15.3 Phylogenetic tree

FASTA files for *K. pneumoniae* species complex strains were obtained using accession numbers from Rodrigues *et al.* (2019) with assistance from Dr Axel Janssen. Prokka (v1.14.6) (Seemann, 2014), Roary v3.11.2 (using the -e flag) (Page *et al.*, 2015) and RAxML v8.2.12 (Stamatakis, 2014) were used for annotation, core gene alignment and phylogenetic analysis respectively. RAxML was run using the following: raxmlHPC-PTHREADS-AVX -T 6 -f a -p 13524 -s <core_gene_alignment.aln> -x 12534 -# 100 -m GTRGAMMA -n raxml_phylogeny. FigTree v1.4.4 (A. Rambaut, http://tree.bio.ed.ac.uk/software/figtree/) was used for visualisation.

2.15.4 Strain validation

Genome sequences were compared to published reference genomes for validation. Snippy (https://github.com/tseemann/snippy) was used to identify any SNPs between genomes and reference genomes. Read mapping was carried out using BWA-MEM (Li, 2013) and SAMtools (Li *et al.*, 2009).

2.15.5 RNA-Seq analysis

Hybrid genomes from MicrobesNG were annotated using Prokka (Seemann, 2014), using flags to specify species (–Genus *Klebsiella* –usegenus –species *pneumoniae*), sequencing centre ID (–centre UoB), and force Genbank compliance (–compliant). Kallisto (Bray *et al.*, 2016) was used to pseudo-align reads to references, using the Odd-ends RNAseq_Analysis.txt workflow by Dr Steven Dunn, available at

https://github.com/stevenjdunn/Odd-ends/blob/master/RNAseq_Analysis.txt

Data were visualised and compared using Degust (https://degust.erc.monash.edu/) An adjusted P value (FDR, false discovery rate) of <0.05 and a $\log_2$fold change cut-off of 1 was used to define statistically significant differences between conditions.

2.15.6 Statistical analyses and data analyses

Unpaired t-tests or one-way ANOVA were used to obtain P values, unless indicated otherwise. As standard, data were analysed and plotted using Microscoft® Excel version 16.16.9 and Graphpad Prism version 8.0.2. RNA-Sequencing heatmaps and COG category graphs were prepared using R.app GUI 1.70 (7735 El Capitan build) (R Core Team: R Foundation for Statistical Computing, 2020) employing ggplot2 (Wickham, 2016).

Chapter 3

Monitoring conjugation in planktonic and biofilm populations using a fluorescence reporter system

3.1 Background

Plating assays are often used for measuring conjugation frequencies in bacterial populations (Alderliesten *et al.*, 2020; Dimitriu *et al.*, 2019; Pérez-Mendoza and de la Cruz, 2009; Wang *et al.*, 2003). However, this approach is slow and labour-intensive (Ou *et al.*, 2017), and results can be variable due to the reliance on serial dilution and selective plating to determine colony-forming units (Bethke *et al.*, 2020; Chase and Hoel, 1975; Hazan *et al.*, 2012). Flow cytometry has potential as a more efficient, higher-throughput method for assessing plasmid prevalence with resolution at the single-cell level (Hecht *et al.*, 2016; Wilkinson, 2018) and has been used previously to evaluate conjugation in bacterial systems (del Campo *et al.*, 2012; Sørensen *et al.*, 2003).

A fluorescence reporter system was developed to allow medium throughput screening of conjugation in *K. pneumoniae* planktonic populations using flow cytometry (Buckner *et al.*, 2020). The strains used in this system were *K. pneumoniae* Ecl8 *mcherry* (where *mcherry* was inserted on the chromosome), and Ecl8/pKpQIL*gfp* (where *gfp* was inserted into the pKpQIL plasmid interrupting the bla_{KPC} gene). Both the constructs also contained *aph* conferring kanamycin resistance to facilitate selection of the desired fluorescent strains. This system was designed so that recipients (red), donors (green) and transconjugants (red and green) could be distinguished based on their fluorescence profiles using flow cytometry and microscopy (Buckner *et al.*, 2020). The present study was designed to build on this work, making use of the existing system and adapting it to conjugation monitoring in biofilms.

Biofilms are thought to be the most common bacterial lifestyle (Ghigo, 2001). Despite this, most studies on bacteria are conducted on planktonic cells (Penesyan *et al.*, 2019). As discussed by Stalder and Top in their 2016 review (Stalder and Top, 2016), there is little consensus in the literature on the effect of bacterial lifestyle (planktonic versus biofilm) on conjugative plasmid transfer in bacterial populations despite several studies investigating this (Bradley *et al.*, 1980; Król *et al.*, 2011). It has been reported that the close proximity of cells in a biofilm may act to promote conjugation in this lifestyle (Kostakioti *et al.*, 2013) as conjugation requires cell-cell contact (Koraimann and Wagner, 2014). However, once a biofilm is established, a lack of mixing (Garrett *et al.*, 2008) may reduce donor and recipient encounters and perhaps favour clonal expansion over horizontal transfer. Conversely, cells in a planktonic lifestyle are free to mix (Alderliesten *et al.*, 2020) and rely on chance contact between donors and recipients for conjugation to occur (Abe *et al.*, 2020). To contribute to addressing this knowledge gap, this study aimed to assess the impact of lifestyle on plasmid prevalence in *K. pneumoniae*.

3.1.1 Aims and hypotheses

The aim of this work was to measure and compare plasmid transmission and prevalence between planktonic and biofilm populations. To address this aim, a fluorescence-based biofilm model was developed.

The hypotheses were:

1. Ecl8/pKpQIL*gfp* will form more biofilm than the wild-type and *mcherry* strains.
2. Conjugation in planktonic and biofilm lifestyles can be monitored using flow cytometry.
3. Plasmid transfer will occur more frequently in a biofilm population than in a planktonic population.

3.2 Strain characterisation

Before using flow cytometry to monitor plasmid dynamics in a biofilm, crystal violet assays in LBB in 96-well plates were used to assess the level of biofilm formed by each fluorescent strain compared to the non-fluorescent wild-type (Figure 3.1). The average biofilm formation for the *K. pneumoniae* wild-type strain is similar to that observed for *K. pneumoniae* pKpQIL*gfp* with a mean A_{600} value of 0.92 (unpaired t-test, $P = 0.91$). However, the mean A_{600} for the *K. pneumoniae mcherry* strain is 1.7, approximately double the value of the other two strains (unpaired t-test, $P = 0.026$ between *K. pneumoniae mcherry* and *K. pneumoniae* WT, $P = 0.013$ between *K. pneumoniae mcherry* and *K. pneumoniae*/pKpQIL*gfp*).

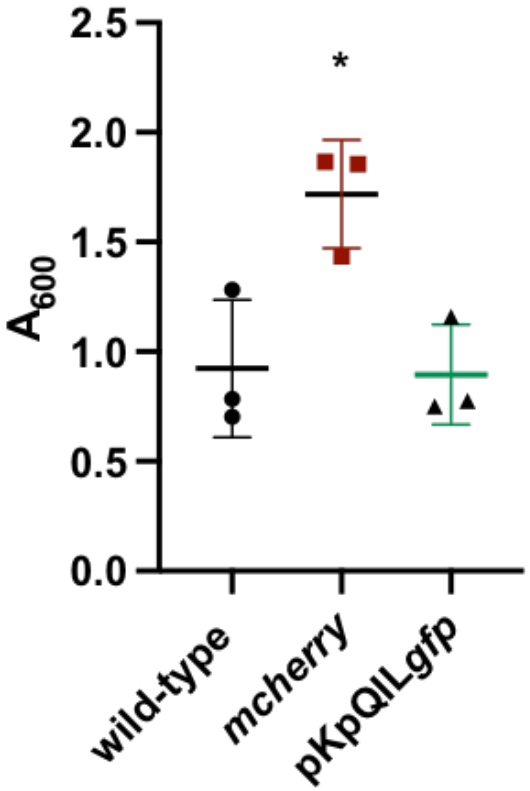

Figure 3.1: Mean biofilm formation at 72 h in LBB quantified by crystal violet for *K. pneumoniae* with either chromosomal *mcherry* or a *gfp* plasmid or neither. Asterisk (*) indicates $P < 0.05$ in an unpaired t-test comparing the *mcherry* strain to the other two strains. Mean A_{600} values from media-only controls have been subtracted to remove background. Data points represent three experimental replicates, each the mean of three biological and three technical replicates. Standard deviation error bars are displayed with means indicated.

It was hypothesised that the difference in biofilm formation may be caused by differential growth profiles. Therefore, planktonic growth was evaluated to determine whether the chromosomal alteration in the *mcherry* strain or the addition of the plasmid in the *gfp*-containing strain impacted this. Planktonic growth kinetics of these strains were determined by reanalysing previously obtained data. Overall the data indicated that the wild-type and *gfp*-containing strains have approximately the same maximum growth rates ($P = 0.87$, unpaired t-test, Figure 3.2A) and growth curve profiles (Figure 3.2B). In contrast, the *mcherry*-containing strain overall displays a lower, although not statistically significantly different, maximum growth rate (unpaired t-test: $P = 0.052$ comparing *mcherry* to WT, $P = 0.054$ comparing

mcherry to pKpQIL*gfp*, (Figure 3.2A)), and longer lag phase (Figure 3.2B) than the other two strains. Therefore, the data demonstrate that the *mcherry* insert may negatively impact growth to a degree, however carriage of the *gfp* plasmid does not.

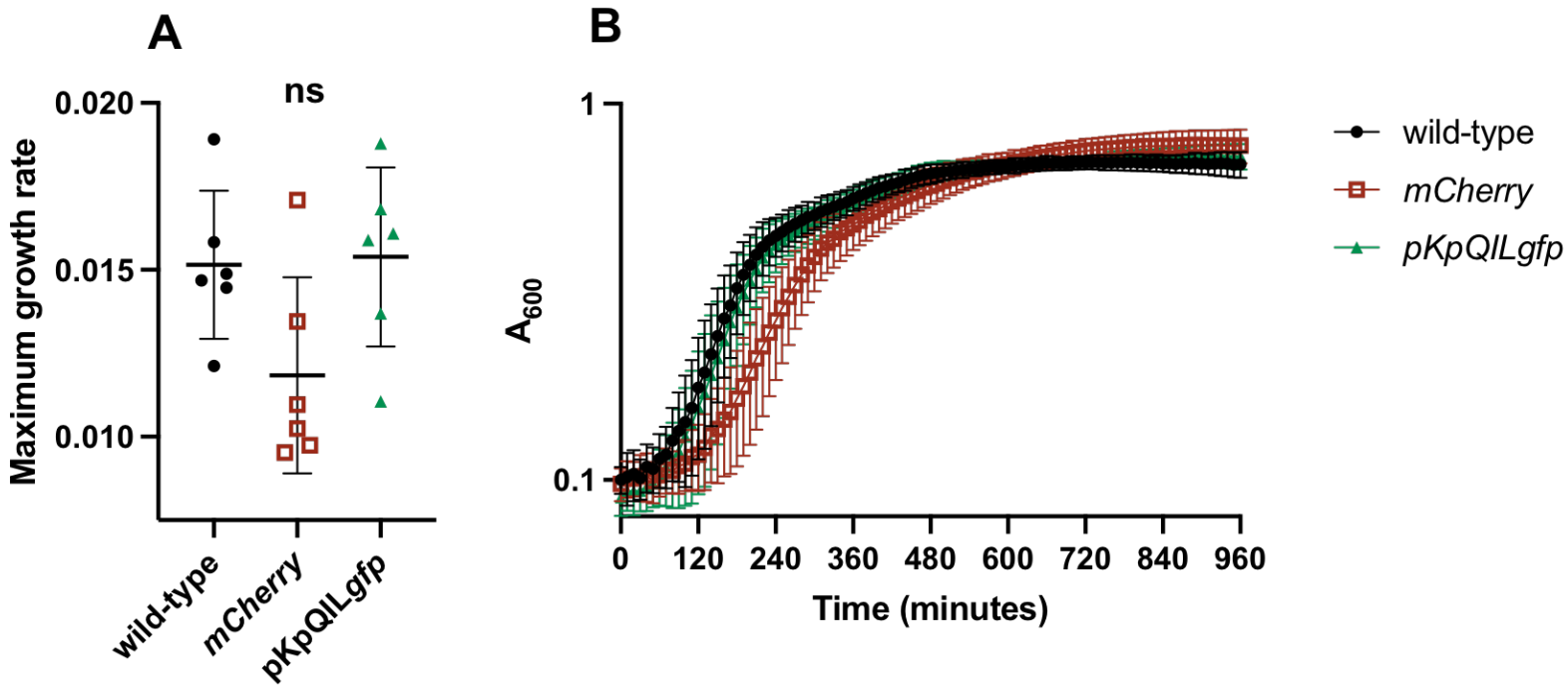

Figure 3.2: Growth kinetics for the *K. pneumoniae* wild-type and fluorescent strains across six experimental replicates, each the mean of three biological and three technical replicates. (A) Maximum growth rate (B) Growth curves for wild-type (black circles), pKpQIL*gfp* (green triangles), *mcherry* (red squares). 'ns' (not significant) indicates $P > 0.05$ in unpaired t-tests. Error bars represent standard deviation from the mean. Data were collected by the Buckner group and reanalysed/reproduced with permission.

The possible planktonic growth defect, in combination with more biofilm formed by the *mcherry* strain compared to the wild-type/*gfp* strains, led to a question about the potential cause of these observations. The *mcherry* strain was constructed by inserting a constitutive promoter p*acpP* upstream of *mcherry*, itself upstream of *aph* (Figure 3.3) (Buckner *et al.*, 2020). It has been suggested that stem loops formed by *mcherry* mRNA (Figure 3.4) can mimic those produced by small RNA regulators of CsrA (Dr Stephan Heeb, personal communication), itself a regulator of biofilm (Müller *et al.*, 2019).

Figure 3.3: Schematic of *mcherry* fragment inserted between *putPA* on the chromosome (Buckner *et al.*, 2020). The blue region represents the p*acpP* promoter sequence

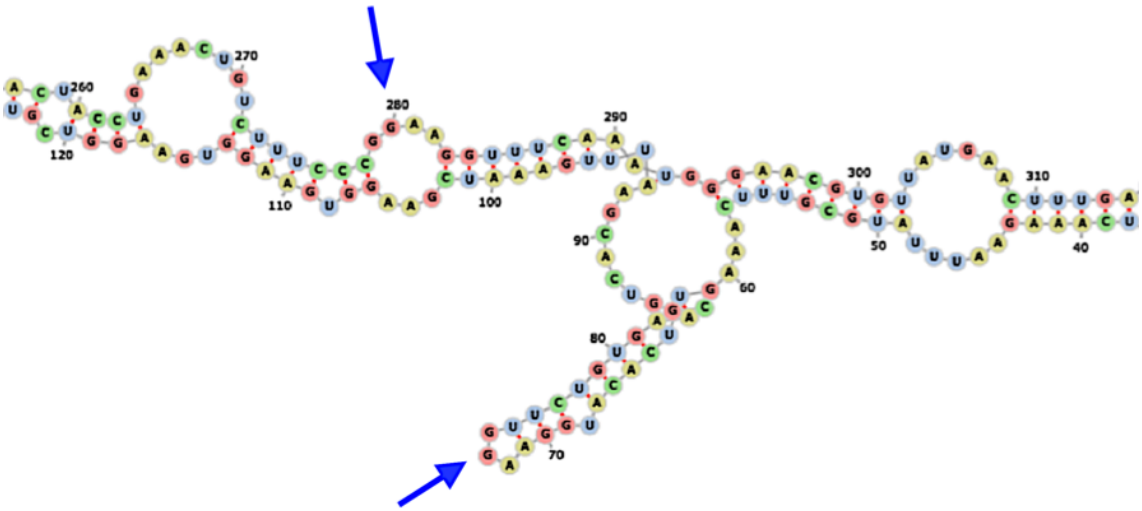

Figure 3.4: Predicted secondary structure of the *mcherry* mRNA produced by the *mcherry* strain. Image created using the ViennaRNA Web Services tool, Theoretical Biochemistry Group (University of Vienna) http://rna.tbi.univie.ac.at/cgi-bin/RNAWebSuite/RNAfold.cgi. Positions of potential CsrA binding sites with putative exposed GGA motifs are indicated (blue arrows).

3.3 Development of a biofilm model

Next, a 6-well format biofilm assay in LBB was developed. This format was designed to allow manual disruption of biofilms with a cell scraper before analysing using flow cytometry. Cell scrapers have been used by others to disrupt biofilm (Rumbo-Feal *et al.*, 2013). The *K. pneumoniae* donor and recipient strains were mixed in a 1:1 ratio after OD_{600} correction to 0.1 for assessment of plasmid transmission/ persistence between cells. As OD approximates cell number (Myers *et al.*, 2013) and more biofilm was apparently formed by the *mcherry* strain than the *gfp* or wild-type strain (Figure 3.1), the number of cells into the experiment from each strain was assessed. To evaluate the true donor:recipient into the biofilm experiments using this method, viable counts were determined from OD_{600} 0.1 cultures of the donor and recipient (Figure 3.5). Viable counts confirmed the mean donor:recipient ratio into the 6-well experiment was approximately 1:1.5. As this ratio was approaching an optimised donor:recipient ratio of 1:2 for maximising transconjugants in this strain setup (as determined by Buckner *et al.* (2020)) and OD correction provided a quick method (Beal *et al.*, 2020) to start biofilm assays, OD correction to 0.1 was chosen as an appropriate starting point for biofilm assays.

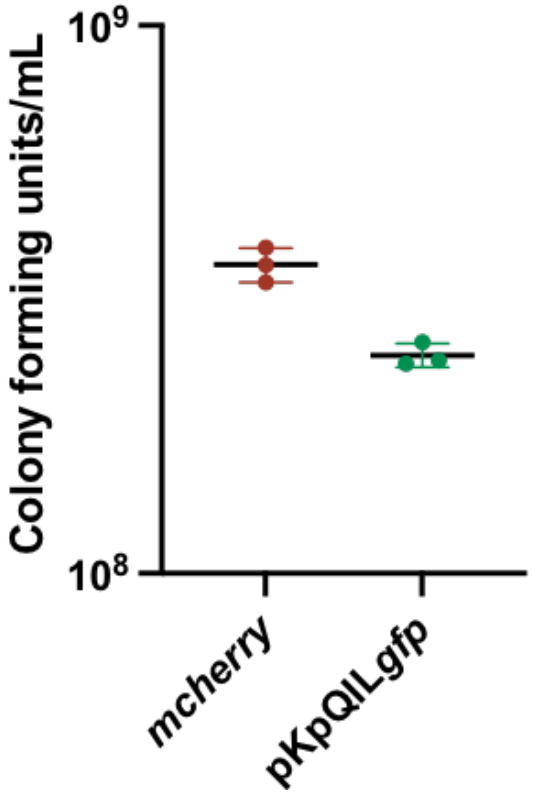

Figure 3.5: Mean viable counts for OD-corrected cultures (OD_{600} 0.1) used to start biofilm assays. *K. pneumoniae mcherry* (red points). *K. pneumoniae*/pKpQIL*gfp* (green points). Three experimental replicates were performed, each the average of three biological replicates. Three technical replicates were averaged per biological replicate. Error bars indicate standard deviation from the mean.

To assess whether the differing cell number input into the biofilm experiments had an impact on biofilm formation, biofilm assays were carried out to correct the 1:1.5 donor:recipient ratio (determined by the viable counts experiments) to the equivalent of a 1:1 ratio (Figure 3.6). Comparing the OD_{600} 0.1 *mcherry* strain to this same strain diluted by 1/3, there was no difference in biofilm formation ($P = 0.26$, unpaired t-test comparing the *mcherry* biofilm to the *mcherry* diluted input). Therefore, it was confirmed that the increased biofilm formed by the *mcherry* strain versus the wild-type and pKpQIL*gfp* strain was a reproducible observation, regardless of cell number input (inoculum).

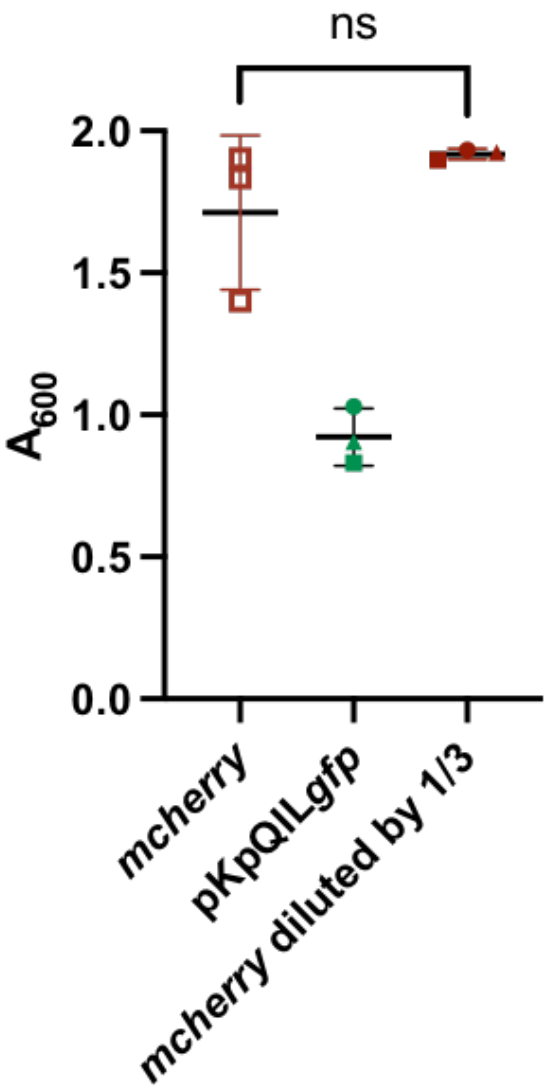

Figure 3.6: Mean biofilm formation in LBB at 72 h quantified by crystal violet for *K. pneumoniae* with chromosomal *mcherry* or pKpQIL*gfp*. 'ns' (not significant) indicates $P > 0.05$ in an unpaired t-test comparing the diluted *mcherry* culture to the undiluted culture. Averaged A_{600} values from media-only controls have been subtracted to remove background. Error bars represent standard deviation from the mean.

Before conducting experiments on the flow cytometer, polystyrene 6-well plates containing cells incubated for 72 h were visualised using confocal microscopy to confirm that biofilm was present in this setup (Figure 3.7A). The image illustrates adhered cells of approximately 50 µM in depth in this setup, which was determined to be suitable for assessment of plasmid transfer. As the polystyrene plates were not specifically designed for use in microscopy, biofilm was also grown on polymer coverslips and imaged (Figure 3.7B). Mature biofilm (≥50 µM depth) (Ma and Bryers, 2013)

was formed on polymer coverslips, similar to what was observed in the polystyrene plate. Imaging on polymer coverslips facilitated a clear view of the biofilm, including areas where donor and recipient cells were mixed (adjacent red and green areas), as well as regions where mixing was not observed. As the cells to be evaluated using flow cytometry originated from biofilms, which are known to aggregate (Wingender *et al.*, 2016), it was important to ensure that the biofilm disruption method for flow cytometry sample preparation was appropriate for achieving single cell suspensions, which are required for this technique (Müller and Nebe-Von-Caron, 2010). The majority of the biofilm cells that were disrupted from the 6-well polystyrene plate were single cells, and it should be possible to use gating strategies to remove large aggregates from the analysis (Figure 3.7C). Therefore, the sample preparation technique was considered to be suitable for flow cytometry.

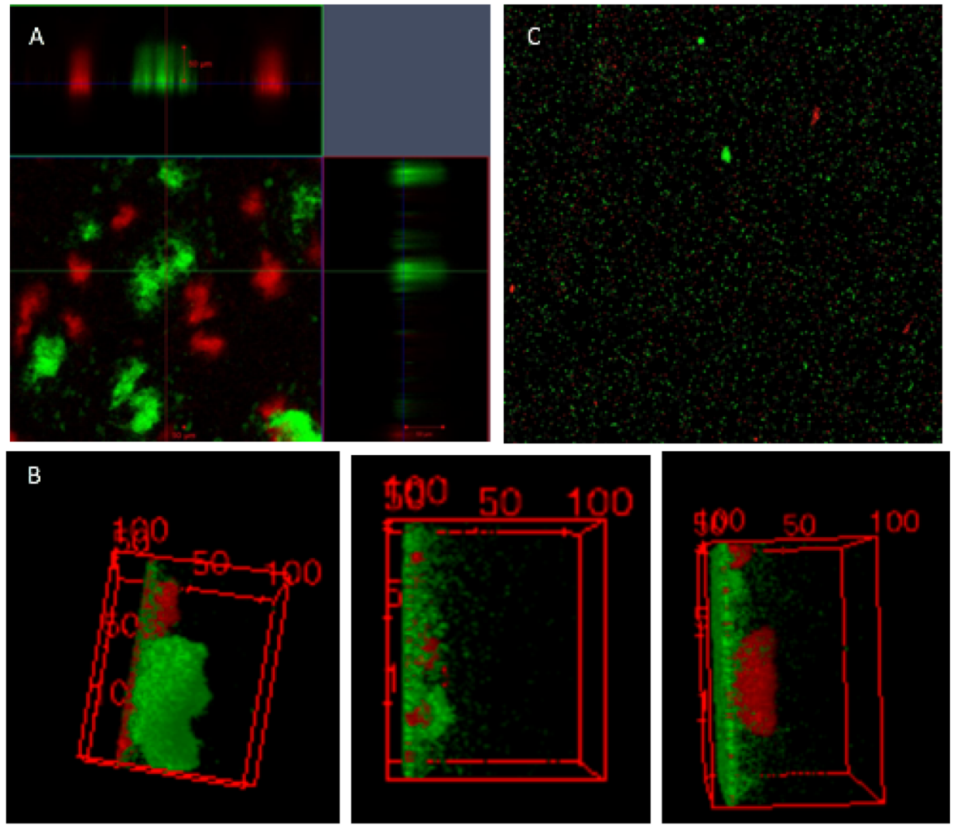

Figure 3.7: Confocal microscopy images of biofilm. (A) Cross section of biofilm formed (single plane) in a polystyrene 6-well cell culture plate after planktonic cells were removed by washing. Scale bar indicates 50 µM. (B) 3D view (Z stacks) of biofilm formed on polymer cover slips viewed using ImageJ 3D viewer in Fiji version 2.0.0-rc-69/1.52p. Images show three views from a single coverslip from a single experiment. Scale (µM) is displayed along the axes. (C) Stitched tile image on a polymer coverslip displaying 25 individual confocal microscopy images of disrupted biofilm on a single coverslip. Before imaging, biofilm was disrupted from 6-well plates using a cell scraper and vortexing as for flow cytometry assays. The donor strain carrying pKpQIL*gfp* (green) and recipient strain containing chromosomal *mcherry* (red) are present.

3.4 Evaluating plasmid transmission in *K. pneumoniae* using flow cytometry

Once it was established that biofilm was formed in the 6-well plates, flow cytometry experiments to assess the presence of transconjugants in planktonic and biofilm *K. pneumoniae* populations were carried out (Figure 3.8). For the flow cytometry experiments, plasmid transmission/persistence between planktonic cells was recorded separately to transmission/persistence in biofilms, although these populations originated from the same biological replicates (the same plate wells). To determine the most appropriate way to analyse data from the 6-well assays and to locate the fluorescent population, different gating strategies were compared. It was not possible to separate cells from background using FCS-A SSC-A plots (Figure 3.8A), therefore fluorescent events were selected for analysis. Gating on the basis of fluorescent events has been used previously (Reardon *et al.*, 2014). Backgating was used to plot fluorescent and non-fluorescent events on SSC-A FSC-A plots to show their positions relative to each other, which confirmed the lack of separation using these parameters and the need to gate based on fluorescent events (Figure 3.8B). For both the planktonic and biofilm populations, it was possible to separate out fluorescent events from the total events using quadrant gating (Figure 3.8C), and to then focus on the dual positive events (mCherry+/GFP+) as potential transconjugant populations. Single positive events (mCherry+ or GFP+) will not be recorded in the dual-positive gate. Plots produced from samples at this dilution (1:1000) appeared to indicate that more transconjugants were produced in the biofilm lifestyle compared to the planktonic lifestyle in this setup. This is reflected by the larger number of points on the mCherry+/GFP+ plots (Figure 3.8D).

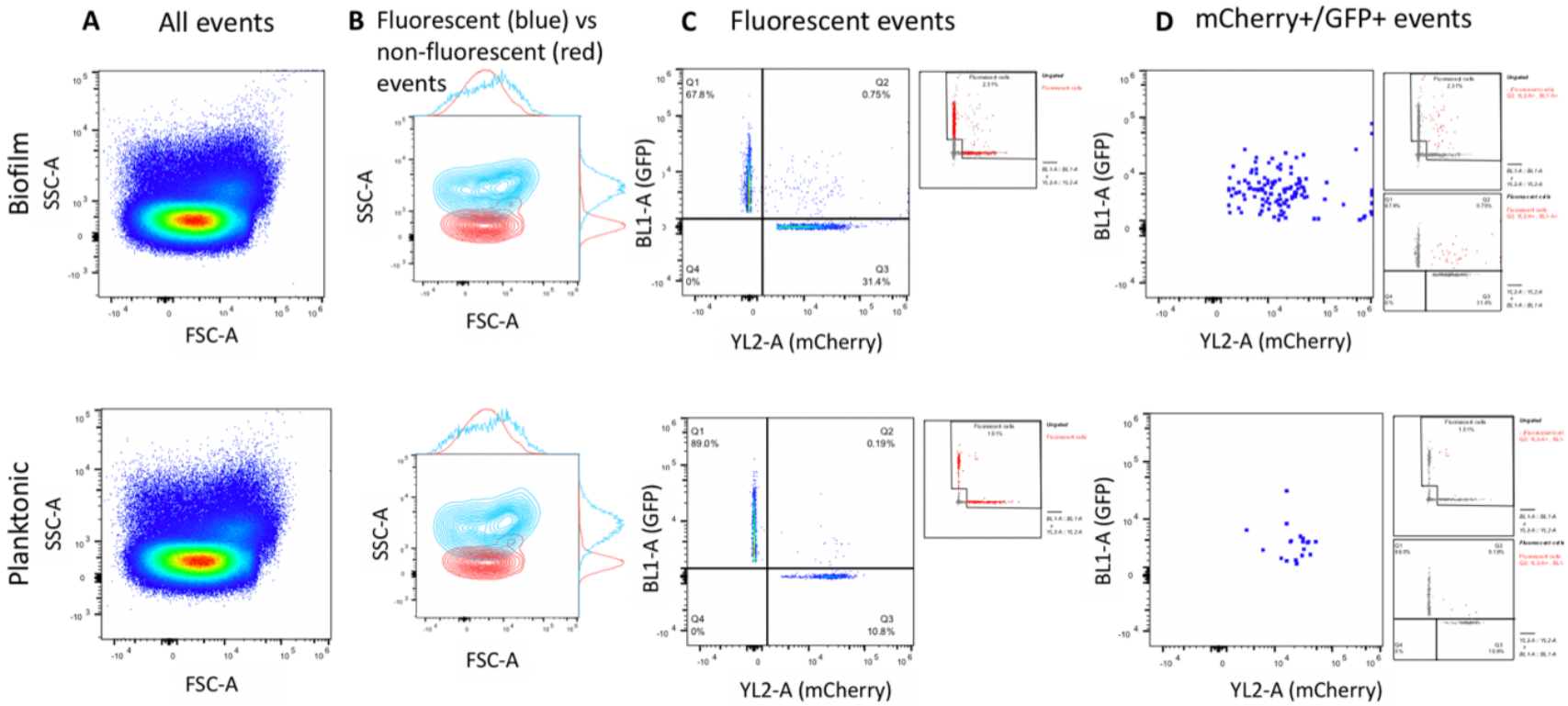

Figure 3.8: Using fluorescence profiles to direct data analysis of planktonic and biofilm populations where donors contain pKpQIL*gfp* and recipients express *mcherry*. Gating strategy for selecting the fluorescent population from the total population (10,000 events in the 'total bacteria' gate) for 6-well assay biofilms (top) and planktonic cells (bottom). Example plots from a single biological replicate diluted 1:1000 in PBS. Backgating is displayed in the small plots to indicate rationale. (A) 'All events' are displayed. (B) 'Fluorescent (blue) and non-fluorescent (red) events' are superimposed. (C) The 'fluorescent events' are selected from the total events. (D) The 'mCherry+/GFP+ events' are selected from the total fluorescent population.

3.4.1 Evaluating the contribution of coincident events

The flow cytometry setup relies on successful and accurate identification of mCherry+/GFP+ (dual positive) events. However, false positives can occur if two cells pass the laser interrogation point concurrently (doublets) (Müller and Nebe-Von-Caron, 2010). For example, if a cell producing mCherry and a cell producing GFP pass through the interrogation point together, the flow cytometer will register this as one event which will falsely appear to correspond to a mCherry+/GFP+ event. To assess whether such events might affect these data, in addition to samples diluted 1:1000 in PBS (Figure 3.8), additional dilutions were run to test for this effect (Figure 3.9). Sample dilution should not affect the proportion of mCherry+/GFP+ events when the machine is set to acquire a set number of events (rather than a set volume), as these should result from single cells expressing both fluorescent proteins. Once the machine has acquired the set number of events, it will stop acquiring regardless of the volume. However, if false positives/doublets are present, increasing sample dilution would result in fewer mCherry+/GFP+ events, as the chance of coincident events decreases as samples become more dilute. Equally, with these same settings, dilution should not cause a change in the proportion of fluorescent events, because again, each event should result from a single cell.

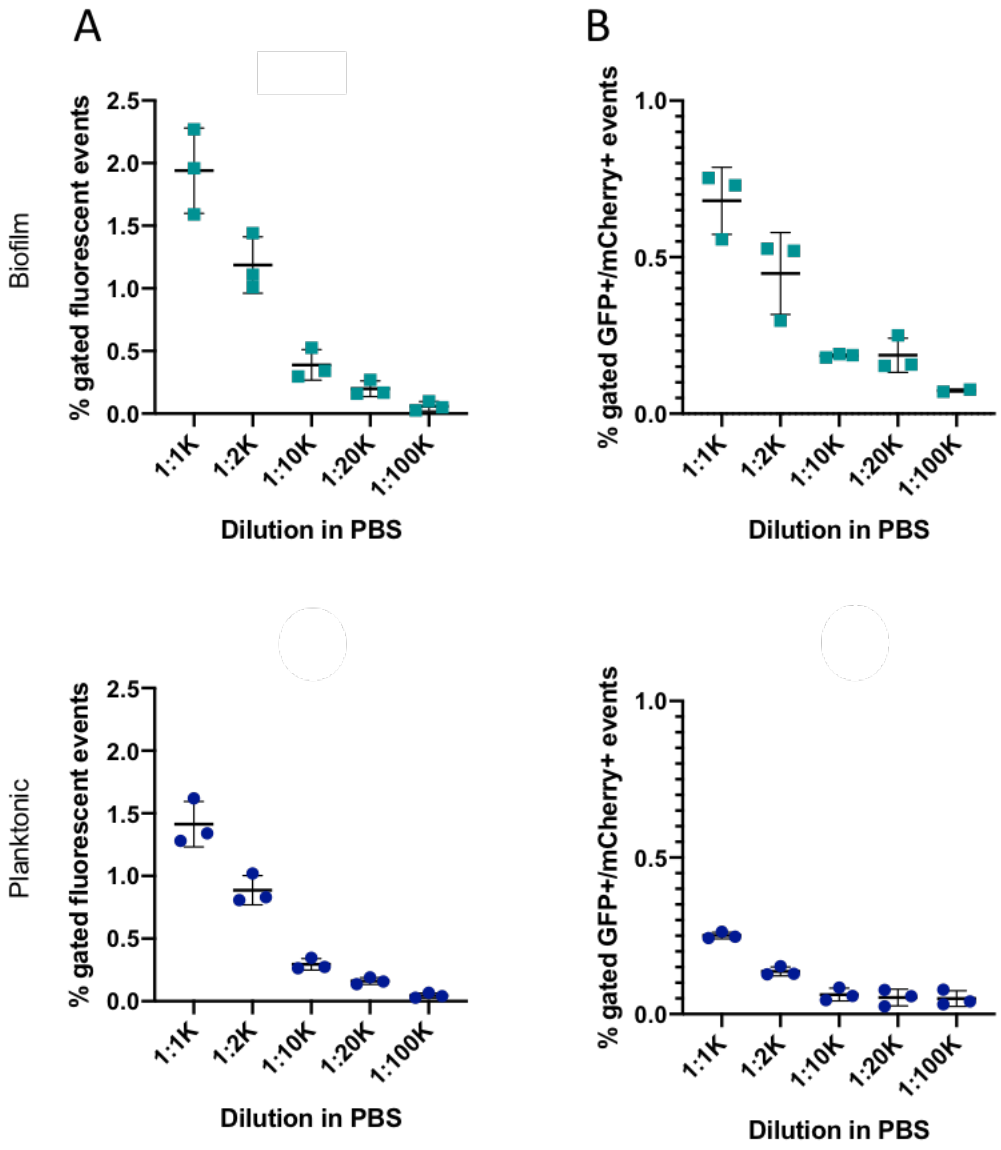

Figure 3.9: The effect of sample dilution on non-fluorescent and fluorescent events (10,000 events in the 'total bacteria' gate) from biofilm and planktonic populations using donors containing pKpQIL*gfp* and *mcherry* recipients. Mean percentage gated events across a dilution series for 6-well assay biofilm (top panel) and planktonic (bottom panel) populations. (A) fluorescent events (proportion of total events), (B) mCherry+/GFP+ fluorescent events as a proportion of total fluorescent events. Three experimental replicates were performed, each the mean of three biological replicates (except for the 1:100K dilution in A for the biofilm population where two experimental replicates were used). 1:1000 dilution data from Figure 3.8 are presented here. Error bars indicate standard deviation from the mean.

For both biofilm and planktonic populations, the proportion of events that are gated as fluorescent and as dual fluorescent over increasing sample dilutions was considered. The more dilute the sample, the lower the proportion of fluorescent events,

until at a 1:100,000 dilution the percentage is close to zero (Figure 3.9A). The non-fluorescent events which increase in proportion as samples are diluted are likely noise. This is because the proportion of non-fluorescent cells/background/debris would not change through sample dilution whereas noise may explain this outcome. A small proportion (0.68% +/- 0.11% standard deviation for the biofilm population and 0.25% +/- 0.011% for the planktonic population) of fluorescent events appear mCherry+/GFP+ in this setup in the most concentrated samples (1:1K). As samples become more dilute, fewer mCherry+/GFP+ events are registered (Figure 3.9B). For the planktonic population, this plateaus at 0.062% at 1:10K, while for biofilm a plateau has not been reached by 1:100K. This indicates that a proportion of the mCherry+/GFP+ events are false positives, with more false positives appearing in more concentrated samples, and more false positives in the biofilm samples compared to the planktonic samples.

Given the presence of false positive events in these experiments and to further assess their contribution, additional control experiments were undertaken comparing outcomes using pKpQIL*gfp* to those using a non-conjugative GFP plasmid pMN402. The rationale behind this is that a non-conjugative plasmid should not transfer to recipient cells, and therefore that no GFP+/mCherry+ events should be detected in this condition. In this planktonic setup, the *mcherry* recipient strain was combined 1:1 with the *gfp* populations. Flow cytometry plots were evaluated and a representative example is presented (Figure 3.10). As for the 6-well assay setup, it was not possible to separate cells from background using FCS-A SSC-A plots (Figure 3.10A). The increased GFP brightness from pMN402 compared to pKpQIL*gfp* could be detected when using quadrant gating to select fluorescent events (Figure 3.10B). Otherwise, the plots for the two strains looked broadly similar. Although pMN402 is non-conjugative, events were present in the mCherry+/GFP+ quadrant (Figure 3.10C). As before, backgating was used to display fluorescent and non-fluorescent events on SSC-A FSC-A plots to determine the degree of separation using these parameters (Figure 3.10D).

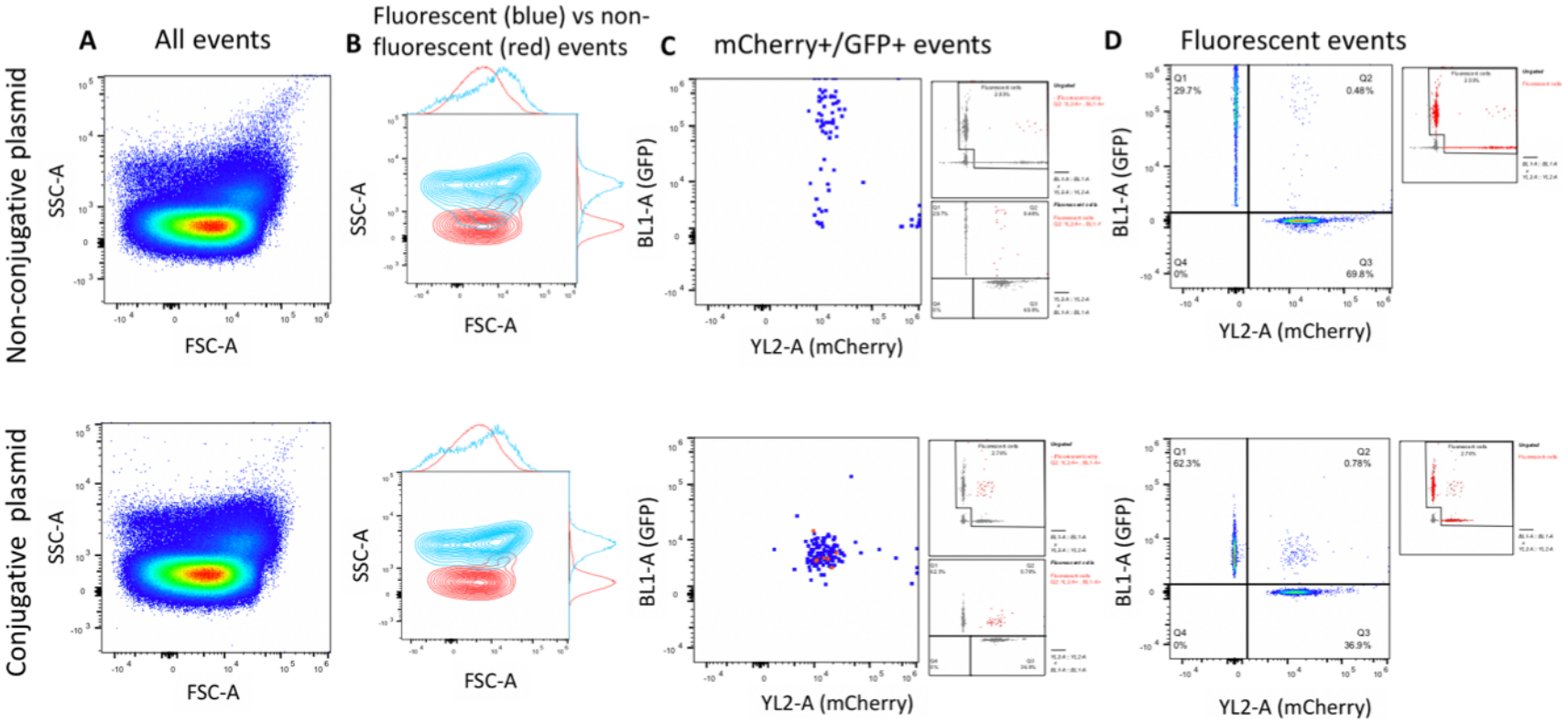

Figure 3.10: Using fluorescence profiles to direct data analysis of populations where donors contain pKpQIL*gfp* (conjugative plasmid) or pMN402 (non-conjugative plasmid) and recipients express *mcherry*. Gating strategy for selecting the fluorescent population from the total population (10,000 events in the 'total bacteria' gate) for the non-conjugative plasmid (pMN402) overnight controls (top) and the conjugative plasmid (pKpQIL*gfp*) overnight controls (bottom). Representative plots from a single biological replicate diluted 1:1000 in PBS. Backgating is displayed in the small plots to indicate rationale. (A) 'All events' are displayed. (B) 'Fluorescent (blue) and non-fluorescent (red) events' are superimposed. (C) The 'fluorescent events' are selected from the total events. (D) The 'mCherry+/GFP+ events' are selected from the total fluorescent population.

Samples were diluted to assess the contribution of false positives in this setup, and to determine the dilution at which these were minimised (Figure 3.11). As with the 6-well setup, increasing dilution decreased the proportion of fluorescent events. A similar proportion of events (<6%) were fluorescent in both conditions (Figure 3.11A). A small proportion of events (<2%) registered as mCherry+/GFP+. The proportion of mCherry+/GFP+ events decreased as sample dilution increased to a similar extent in both the conjugative and non-conjugative setup (Figure 3.11B), and in both cases plateaued at a 1:10K dilution (0.15% +/- 0.10% standard deviation and 0.15% +/- 0.10% for the conjugative and non-conjugative populations respectively at 1:10K). This highlighted that it was not possible to distinguish between the control (non-conjugative plasmid) and test (conjugative plasmid) condition using this setup.

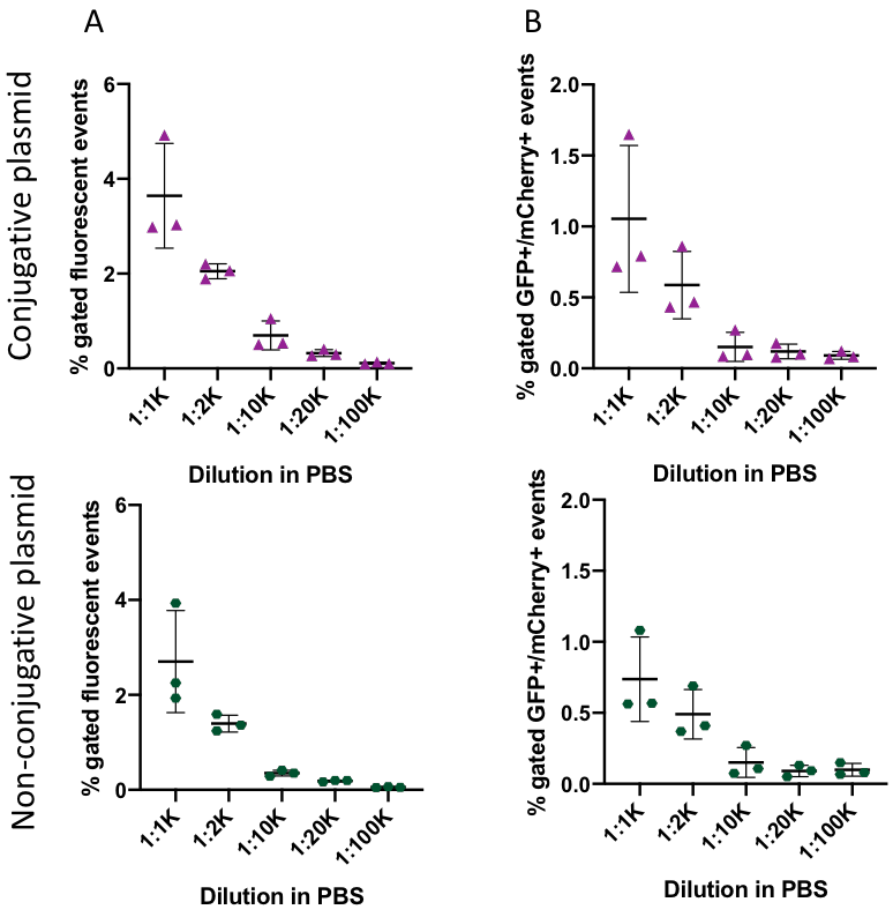

Figure 3.11: The effect of sample dilution on non-fluorescent and fluorescent events (10,000 events in the 'total bacteria' gate) from samples containing a conjugative (pKpQIL*gfp*) versus non-conjugative (pMN402) plasmid. Mean percentage gated events across a dilution series prepared from overnight culture controls. Top panel: *K. pneumoniae*/pKpQIL*gfp* (conjugative plasmid) mixed 1:1 with *K. pneumoniae mcherry*. Bottom panel: *K. pneumoniae*/pMN402 (non-conjugative plasmid) mixed 1:1 with *K. pneumoniae mcherry*. (A) fluorescent events (proportion of total events), (B) mCherry+/GFP+ fluorescent events (proportion of total fluorescent events). Three experimental replicates are displayed, each the mean of three biological replicates. Error bars indicate standard deviation from the mean.

3.4.2 Adjusting the acquisition setup

Given that dilution was required to minimise false positives in these assays, and that increasing dilution leads to a reduction in the proportion of fluorescent events (and an increase in background noise), a change of setup to increase the number of 'true' events through the flow cytometer was attempted. For this, instead of using 10,000 events in the 'total bacteria' gate to determine when acquisition was stopped,

a large sample volume (250 µL) was run at 1:10K and 1:20K, two dilutions where false positives were previously determined to be minimised (Figure 3.12). At these dilutions, registered events would be both 'true' events and background/noise based on previous assessment (Figures 3.9 and 3.11). The rationale was that this larger volume may allow sufficient fluorescent events to be acquired to detect transconjugants whilst reducing false positives.

A representative example of the plots obtained in these experiments is provided (Figure S6). Unsurprisingly, more events were recorded using the larger volume acquisition setup (Figure S6), illustrated by the increased dot plot density for the total events plots. However, this did not lead to a greater proportion of fluorescent events in this setup (0.50% +/- 0.11% standard deviation for 1:10K biofilm and 0.36% +/- 0.09% for 1:10K planktonic) (Figure 3.12) compared to the previous acquisition settings (0.39% +/- 0.12% for 1:10K biofilm and 0.29% +/- 0.046% for 1:10K planktonic) (Figure 3.11). Comparing the 1:10K dilution samples across the two setups (event number versus volume acquisition), an unpaired t-test confirmed no significant differences in the biofilm ($P = 0.30$) or planktonic ($P = 0.33$) samples. Using the adjusted acquisition settings, noise was still responsible for the majority of detected events. In addition, despite using a dilution that minimised false positives, these were still present. This is apparent because increasing dilution reduced the proportion of mCherry+/GFP+ events. This indicates that single GFP+ and mCherry+ cells are still passing the interrogation point concurrently in these samples (Figure 3.12B).

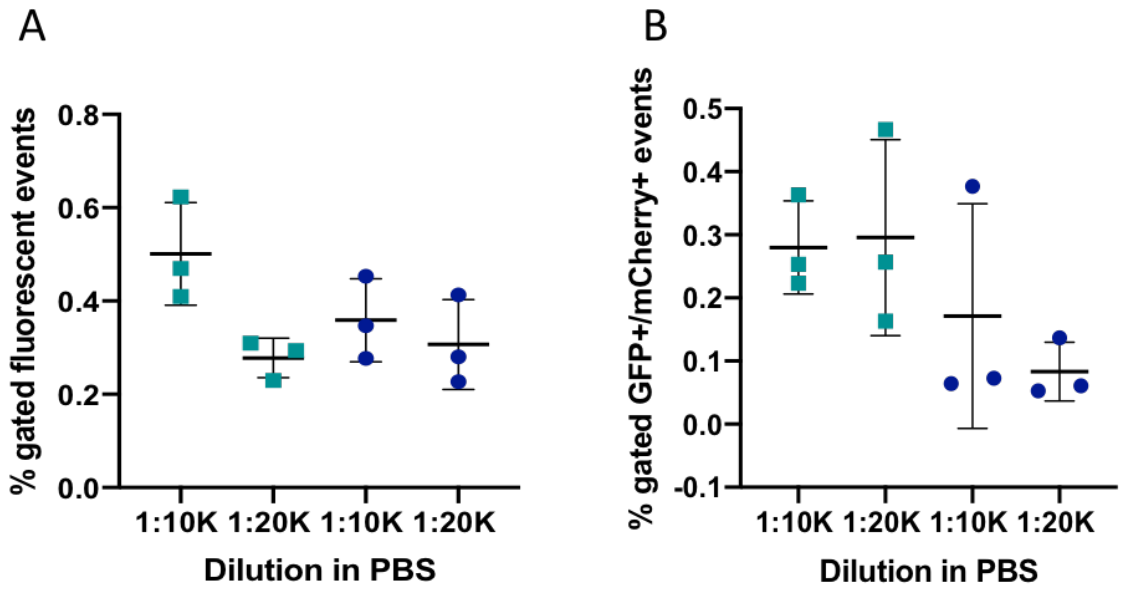

Figure 3.12: Using a volume parameter to increase the total number of events acquired. Mean percentage gated events at two dilutions for 6-well assay (using donors containing pKpQIL*gfp* and recipients expressing *mcherry*) biofilm (green squares) and planktonic (dark blue circles) populations collected from 250 µL sample volumes, rather than on the basis of event number acquired. (A) fluorescent events (proportion of total events), (B) mCherry+/GFP+ fluorescent events (proportion of total fluorescent events). Three experimental replicates are displayed, each the mean of three biological replicates. Error bars indicate standard deviation from the mean.

3.5 Discussion

Although much laboratory work is carried out on planktonic cells, bacteria are predominantly found as biofilms in nature (Ghigo, 2001), and these experience vastly different environmental conditions to their planktonic counterparts (Hall-Stoodley *et al.*, 2004). Some research suggests that the biofilm lifestyle promotes horizontal transfer of plasmids (Bradley *et al.*, 1980; Król *et al.*, 2011; Reisner *et al.*, 2012). Horizontally-transmitted plasmids are major contributors to the spread of AMR genes in Gram-negative bacteria (Carattoli, 2013).

The aim of this work was to measure and compare plasmid dynamics between planktonic and biofilm populations of *K. pneumoniae* Ecl8. To address this aim, a

fluorescence-based biofilm model was developed and flow cytometry was used to compare the transfer of a successful F-type plasmid pKpQIL (Chen *et al.*, 2014) (pKpQIL*gfp* in this setup) in the two lifestyles. Putative transconjugants were identified on the basis of their dual fluorescence profile. However, upon further investigation, the majority of this population was determined to consist of false positive dual fluorescent events rather than single cells expressing both fluorescent proteins. In addition, machine noise impacted fluorescent event acquisition. Therefore, technical limitations mean it was not possible to confidently identify or accurately quantify transconjugants using this system.

Before starting work with the fluorescent *K. pneumoniae* strains, their planktonic and biofilm growth was assessed to evaluate any effect of the fluorescent tags on these phenotypes. For the *mcherry* strain, there was a lack of direct correlation comparing the OD to viable counts data. This highlights the limitations of using OD measurements to approximate cell number and the importance of validating such measurements with colony counting to provide a more robust estimate of the number of viable cells. The OD of solubilised crystal violet is taken as a proxy for biofilm formation in crystal violet assays (O'Toole, 2010). The data indicated that the pKpQIL*gfp* plasmid does not promote or hinder biofilm formation in this experimental model. This result is contrary to some published data showing that the presence of conjugative plasmids can increase biofilm formation in some strains. For example, the pRST98 plasmid promoted biofilm in three Gram-negative bacterial species (Liu *et al.*, 2014). Although carriage of plasmids can impose a fitness cost which may result in a growth defect relative to the wild-type (San Millan and MacLean, 2017), the *gfp* and wild-type strains grew similarly suggesting that carriage of the plasmid does not produce a fitness cost in this host. This is supported by work from Buckner *et al.* which showed that Ecl8 acquisition of the pKpQIL plasmid did not result in fitness defects or compensatory mutations in coding regions. Instead, gene expression changes were sufficient to compensate for cost-of-carriage (Buckner *et al.*, 2018).

Conversely, the *mcherry* strain formed more biofilm than the wild-type and *gfp* strains. Possible explanations for this include that the *mcherry* mRNA may be titrating CsrA away from its usual binding sites (Dr Stephan Heeb, personal communication). CsrA is a regulator of biofilm and is itself regulated by small RNAs that form stem loops (Dubey *et al.*, 2005; Potts *et al.*, 2017). It appears likely that the stem loops predicted in the secondary structure of *mcherry* mRNA mimic those formed by the typical small RNAs that regulate CsrA by sequestration (Dubey *et al.*, 2005). As a result, the overexpressed *mcherry* in the *K. pneumoniae mcherry* strain may be sequestering CsrA to derepress biofilm formation. Two or more binding sites are required for CsrA (Müller *et al.*, 2019)) with 'GGA' reported as a conserved binding motif for this protein (Potts *et al.*, 2017). This binding motif is often present in a hairpin loop at these sites (Dubey *et al.*, 2005), and two potential binding sites are present in the predicted mRNA secondary structure of the *mcherry* used in this work.

As the crystal violet might also bind components of biofilm extracellular polymeric substance (EPS) (Li *et al.*, 2003), it cannot be excluded that higher levels of staining may also relate to higher levels of EPS production in this strain. In addition, it is also feasible that the location of the *mcherry* insertion may have affected physiology. Use of proline as a carbon and nitrogen source is facilitated by the *put* (proline utilisation) operon. Its expression is activated in low nitrogen conditions (Chen and Maloy, 1991). *putP* encodes a proline permease which drives uptake of proline and *putA* encodes a proline oxidase/pyrroline-5-carboxylic acid dehydrogenase which converts proline to glutamate (Bender, 2010; Chen and Maloy, 1991). The intergenic region between *putPA* contains a 25-bp binding site for the Nitrogen Assimilation Control protein (NAC) (Bender, 2010; Goss and Bender, 1995), a transcription factor whose expression is increased in nitrogen limiting conditions. NAC acts to induce expression of sigma 70 controlled operons, (Bender, 2010) including the *put* operon (Chen and Maloy, 1991). It may be that introducing *mcherry* in this location has disrupted NAC binding at this site and increased the pool of available NAC for

binding other regulatory regions whilst preventing the *put* products from providing alternative nutrient sources. This may have an effect on the lifestyle adopted by the *mcherry* strain. In addition, the expression of *yceO* has been associated with biofilm formation. *yceO* is reportedly activated by NAC (Bender, 2010). It might be that a theoretical increased pool of NAC for other promoters, including the *yceO* promoter, has led to the effect on biofilm. Further testing would be required to confirm this.

To further investigate the likely cause for increased biofilm, electrophoretic mobility shift assays (Hellman and Fried, 2007) could be used to evaluate CsrA-*mcherry* mRNA interactions, additional staining could be performed to evaluate biofilm composition (Rooney *et al.*, 2020), and an isogenic strain with an alternative fluorescent protein between *putPA* could be investigated. However, testing these hypotheses was beyond the scope of this work. Growth kinetics data showed a potential growth defect in the *mcherry* strain compared to the wild-type/*gfp* strains. Taken together, these data suggest the insertion has a negative impact on the host cell. Given this, it would be appropriate to consider construction of an alternative recipient strain for any future work with this system. It has been reported previously that the *putPA* intergenic region is a suitable cloning insertion site (Hautefort *et al.*, 2003).

Despite the effect of *mcherry* on the growth of the recipient strain, a 6-well assay was developed for use in flow cytometry as 'proof of principle'. The donor:recipient ratio into the 6-well assays was evaluated using viable counts. These demonstrated that cultures corrected to an OD_{600} of 0.1 gave a donor:recipient ratio of approximately 1:1.5. As this is approaching the ratio shown to be optimal for maximising transconjugants based on work by Buckner *et al.* using an identical strain setup (Buckner *et al.*, 2020), and because OD correction is straightforward and can be consistently achieved, an OD_{600} of 0.1 for each strain was determined to be an appropriate starting point for the assays. Biofilm assays correcting for the larger number of *mcherry* strain cells at OD_{600} 0.1, as indicated by the viable counts data, confirmed no effect

on biofilm from the change in inoculum.

Microscopy was used to confirm biofilm was formed in the polystyrene 6-well plates, set up as for the flow cytometry model. A detailed view of the biofilm revealed likely clonal expansion, shown by large areas of single-colour cells. Other researchers have also observed limited mixing in biofilms using strains that are isogenic apart from single insertions or alterations (Popat *et al.*, 2012). Cell scraper disruption of biofilm was largely effective at obtaining single cell suspensions required for flow cytometry. Therefore, biofilm and planktonic samples were analysed on the flow cytometer to assess the transconjugant population produced over the course of the assays.

Initially the flow cytometry experiments appeared to show a higher percentage of gated mCherry+/GFP+ events in the biofilm population compared to the planktonic population. Doublet discrimination and separation of cells from background can often be achieved using forward and side light scatter information. However, this can be challenging for bacterial populations, primarily due to the small size of bacterial cells, and indeed it was not possible to use these parameters to separate cell populations in this work (Cosma, 2020). Instead, gating based on fluorescence profiles was used to determine donor, recipient and transconjugant populations.

Sample dilution provided a means to assess the contribution of false positives to the setup. Control experiments over a dilution series illustrated that false positives were present due to coincident events and that noise was likely responsible for the majority of the detected events. It is of note that the use of stable *gfp* in the plasmid construct may have impacted the dual positive population, as any dead donor cells would remain fluorescent. The incidence of false positive events was supported by the control experiments using a donor containing a non-conjugative plasmid pMN402 where it should not have been possible for plasmid transfer to occur from donor to recipient cells. However, mCherry+/GFP+ events were observed in these experiments. Next, sample acquisition was determined on the basis of the volume rather than event number in the 'total bacteria' gate to try and increase the likelihood of

fluorescent event acquisition whilst minimising false positives. Unfortunately, this setup did not allow confident or accurate detection of transconjugants. In addition, large volume samples required a long running time (approximately 20 minutes for the most dilute samples). It is conceivable that conjugation may have occurred in this time-frame, thus skewing the results. Despite the adjusted setup, noise remained responsible for the majority of events, with <1% of events registering as fluorescent. Overall, it was not possible to sufficiently optimise this system on the available flow cytometer, nor to confidently distinguish transconjugants from noise.

Access to an alternative machine would likely facilitate continued work with this fluorescence reporter system by reducing the background electrical noise, allowing detection of the small transconjugant population. If it were possible to optimise the flow cytometry assay for detection of transconjugants/transconjugant daughter cells, this would provide a higher-throughput setup for assessment of conjugation in planktonic and biofilm lifestyles where experiments could provide data on thousands of individual bacterial cells (Davey and Kell, 1996). This would avoid the need to rely solely on plating assays, which are time-consuming and approximate donor, recipient and transconjugant populations by scaling up on the basis of plated serial dilutions of culture on selective media (Bethke *et al.*, 2020; Sieuwerts *et al.*, 2008).

Although it has not yet been possible to fully develop this method for use on biofilm samples, confirmation of conjugation between the Ecl8/pKpQIL*gfp* donor strain and a nalidixic acid resistant Ecl8 recipient has been determined previously using liquid matings and classical plating conjugation experiments (Buckner *et al.*, 2020). Work by Buckner *et al.* (2020) determined that transconjugants were produced using this strain combination. Although it was not possible to accurately quantify or confirm detection of transconjugants using flow cytometry, the detection of transconjugants using the nalidixic acid resistant Ecl8 recipient (which differs from Ecl8 *mcherry* only in that it does not contain a *mcherry* cassette and was evolved to resist nalidixic acid) adds support to the likelihood of transconjugants in the 6-well biofilm assay.

A limitation of conjugation assays (either classical assays using plating or flow cytometry conjugation assays) is that they cannot distinguish between a transconjugant population and a population where the plasmid has been horizontally then vertically transmitted. As a result, any putative transconjugant population would contain plasmids transferred both horizontally and then vertically. However, overall plasmid prevalence is of interest because both horizontal and vertical transmission contribute to plasmid spread in a population (Li *et al.*, 2019; Redondo-Salvo *et al.*, 2020). Although it would be interesting to evaluate the individual contribution of each of these factors, and although this has been achieved by others (e.g. Li *et al.* (2019) who monitored plasmid transfer using microfluidics and imaging) this is beyond the scope of this work.

Use of a Fluorescence Activated Cell Sorter (FACS) would permit transconjugant populations to be validated in a similar way as classical plating conjugation experiments, such as using PCR or selective plating, as these machines can allow a population of interest to be selected and isolated for downstream experiments (Liao *et al.*, 2016). This would add further support to conclusions from flow cytometry assays and show that settings and gating strategies were appropriate for transconjugant identification. In addition, transconjugants could be stored for further experiments and cell viability could be verified post sample processing. However, no equipment of this type was available.

Confocal microscopy could also aid validation of conjugation events, and it may be feasible to locate these within a biofilm using this method in conjunction with an analysis tool (Hartmann *et al.*, 2019). This would give information on the spatial localisation of conjugation events and increase the available information on where conjugation is occurring in biofilms (Ma and Bryers, 2013). Currently the 6-well assay used in conjunction with plating or flow cytometry could only reveal whether there was more/less conjugation occurring in one lifestyle versus another (planktonic versus biofilm), not where the conjugation may be happening. Future work should

address this as this information is important to increase our understanding of this process in different lifestyles.

To continue optimisation of this model, it would be of benefit to include a live-dead stain during flow cytometry experiments to more easily discriminate live cell populations from dead cells/background/debris (Tung *et al.*, 2007). However, the commonly-used dyes propidium iodide and SYTO9 (giving red and green fluorescent populations respectively) (Stiefel *et al.*, 2015) are unsuitable for the existing strain setup which has overlapping emission. In addition, there are drawbacks to using DNA staining methods on biofilm populations as extracellular DNA can skew results (Rosenberg *et al.*, 2019). Successful discrimination of doublets/false positives would be another requirement. To do this, it may be possible to use flow cytometry imaging features (Mikami *et al.*, 2020), or to use a DNA stain (Whittle *et al.*, 2019), where a more intense signal may represent coincident events that could be gated out (Reardon *et al.*, 2014). As above, this may be challenging for biofilm populations (Rosenberg *et al.*, 2019), so discrimination on the basis of fluorescence tags may remain a sensible approach for this application. Given the time-frame (as short as 10 minutes) within which conjugation is thought to occur (Król *et al.*, 2013; Nolivos *et al.*, 2019), fixing cells (Lanier and Warner, 1981) before flow cytometery analysis would avoid the possibility of further growth/conjugation occurring during sample acquisition.

Use of a positive control would facilitate visualisation of what a transconjugant/ transconjugant daughter population should look like on flow cytometry plots to aid its identification. It may be that any false positive events have a different profile to a true dual positive event, but it would only be possible to tell using a positive control which was unavailable during this study. In addition, a control where the conjugation machinery on the donor plasmid has been de-repressed may allow detection of transconjugants where this event would otherwise be too rare to detect (Low *et al.*, 2020). Similarly, use of a donor plasmid with reported high conjuga-

tion frequency would also allow assessment of the functionality of the assay, and perhaps a highly conjugative plasmid would render the transconjugant population detectable as a larger proportion of the total population and permit the removal of background false positives. One of the principal challenges with this setup was the rarity of the conjugation events, which is acknowledged as a challenging area in flow cytometry research (Donnenberg and Donnenberg, 2007). As the reported conjugation frequency of pKpQIL is in the region of $1x10^{-5}$ (Buckner *et al.*, 2018), this would mean that a single transconjugant cell is likely to be present in a population of approximately $1x10^{5}$ cells. This is less common than the 0.1% frequency which can be defined as 'rare'. Along with the low frequency of the event, the signal:noise ratio is also regarded as a key factor in rare event detection, as well as the total number of acquired events (Donnenberg and Donnenberg, 2007). Here, this ratio was too low to permit cells to be distinguished from background, but this could be improved using a flow cytometer with a higher signal:noise ratio (Giesecke *et al.*, 2017). Equally, with a higher signal:noise ratio, it may be possible to acquire sufficient 'real' events to detect rare populations, although issues with coincident events would remain.

3.6 Conclusions

A 6-well plate biofilm model was developed and the use of flow cytometry to compare plasmid transmission/persistence in planktonic and biofilm lifestyles was assessed. Success of the flow cytometry assay relies on discrimination between doublets to accurately represent the transconjugant/vertically-transmitted plasmid population. The presence of false positives, combined with the overall small proportion of fluorescent events/events in the mCherry+/GFP+ gates means it was not possible to confidently identify transconjugants in this setup. However, access to a flow cytometer with a higher signal:noise ratio, combined with optimisation of experiment settings and system using a highly conjugative plasmid may facilitate detection of

transconjugants using this fluorescence reporter system. If the encountered technical limitations could be overcome, this system offers a promising method for monitoring plasmids in bacterial populations and comparing their prevalence between bacterial lifestyles.

3.6.1 Key findings

- Fluorescent and wild-type *Klebsiella pneumoniae* Ecl8 strains formed biofilm.
- A biofilm model was adapted for use in flow cytometry experiments. Confocal microscopy was used to evaluate the effectiveness of the biofilm disruption technique for flow cytometry.
- Technical limitations (such as machine noise and false positives) prevented assessment of plasmid prevalence between planktonic and biofilm populations using the Attune NxT.
- Use of an alternative flow cytometer with a higher signal:noise ratio, and/or a donor containing a highly conjugative plasmid may facilitate use of this fluorescence reporter system to study plasmid prevalence in *K. pneumoniae* planktonic and biofilm populations.

Chapter 4

Investigating the plasmid and AMR gene content of five carbapenemase-producing *K. pneumoniae* (CPE) clinical isolates

4.1 Background

Conjugation experiments can be performed using laboratory strains which may have adapted to their artificial growth conditions and be less likely to reflect naturally-occurring strains in human-associated environments (Headd and Bradford, 2020; Knopp and Andersson, 2018; Matsumura *et al.*, 2018). Considering this, and to investigate AMR plasmid transfer in *K. pneumoniae* planktonic and biofilm populations, a set of five carbapenemase-producing *K. pneumoniae* (CPE) clinical isolates from the Queen Elizabeth Hospital (QE) (Birmingham, UK) were selected from a de-duplicated collection for characterisation, comparison to other *K. pneumoniae*

sequences and evaluation as potential donor strains in a new conjugation model (Chapter 5).

The CPE isolates were obtained from patients between March 2018 and March 2019 by staff at the Queen Elizabeth Hospital (Birmingham, UK), either as part of a standard screening procedure, or due to an infection. Collection isolates were sent to the Public Health England Antimicrobial Reference Unit for further characterisation after susceptibility testing on a Vitek 2 (Biomérieux) indicated possible resistance to carbapenems. PCR targeting carbapenem resistance genes was carried out to detect their presence in the isolates. Along with the PCR data, which provided an initial identification of the carbapenem resistance genes, the Vitek 2 antibiogram data were also made available. However, this information alone was not sufficient for selecting suitable donor strains.

For this work, five selected isolates (CPE01, CPE08, CPE16, CPE24 and CPE25) were sent for whole genome sequencing to provide in-depth data on their genetic background, AMR gene content and contexts, plasmid content and likely functionality of any plasmid conjugation modules. These data would also be useful to provide donor reference genomes for transconjugant validation, as well as to facilitate comparison of donor genomes to existing sequences in public databases.

The aim of this work was to characterise five CPE isolates and determine which would be most suitable for conjugation experiments investigating transfer of carbapenem resistance plasmids between *K. pneumoniae*.

The hypotheses were:

1. The CPE isolates will be *K. pneumoniae sensu stricto*.
2. The presence of AMR genes will explain multidrug resistant phenotypes.
3. CPE isolates will contain conjugative plasmids carrying carbapenem resistance genes .

4.2 Core genome phylogenetic analysis

CPE isolates were sent to MicrobesNG for long- and short-read sequencing using Oxford Nanopore and Illumina technologies. Upon receipt of the hybrid assembly data, isolate sequences were typed by MLST. CPE01, CPE08, CPE16, CPE24 and CPE25 were designated as ST147, ST512, ST14, ST395 and ST147 respectively.

All five isolates had been identified as *K. pneumoniae* in clinical laboratory testing. However, standard laboratory tests are unable to reliably designate *Klebsiella* species (Rodrigues *et al.*, 2019). Therefore, using a core-genome phylogeny, the CPE sequences were compared to a set of publicly available *K. pneumoniae* species complex sequences to determine their placement within this group (Figure 4.1).

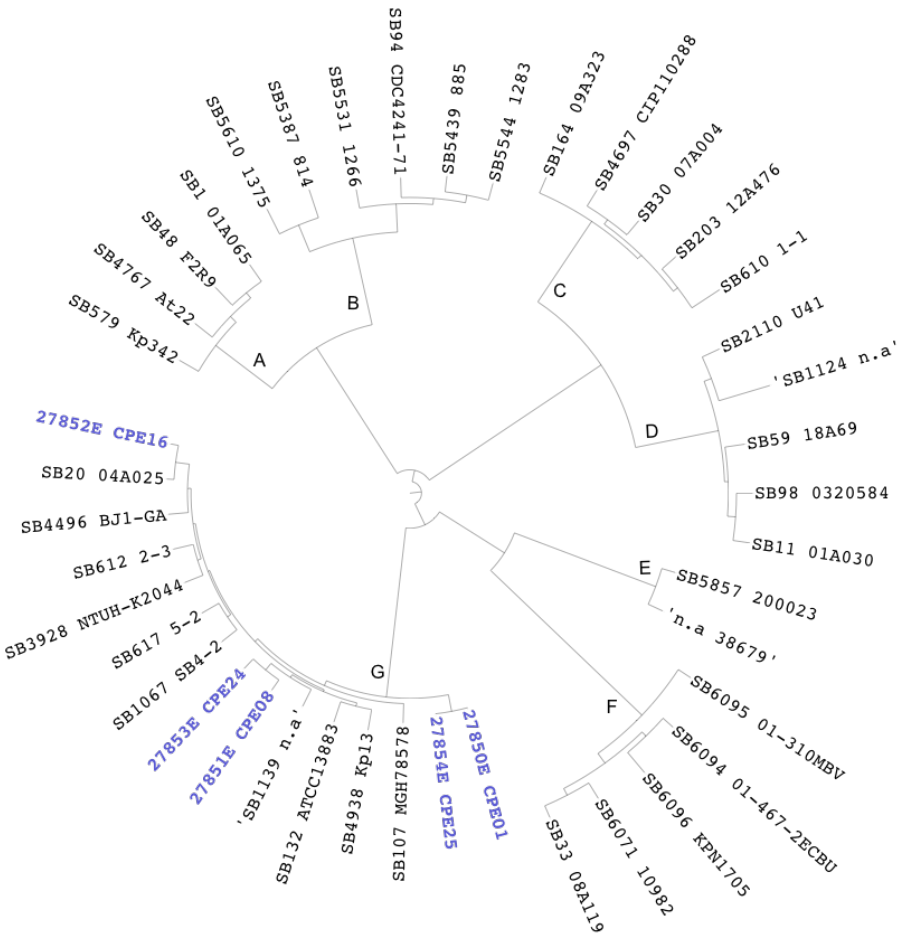

Figure 4.1: Midpoint rooted Maximum Likelihood phylogenetic tree of core genes from *K. pneumoniae* species complex strains (Rodrigues *et al.*, 2019) and CPE isolates visualised on iTOL Version 6.4.2 (Letunic and Bork, 2021). CPE isolates (purple text). Strains clustering as: (A) *K. variicola* subsp. *variicola*, (B) *K. variicola* subsp. *tropicalensis*, (C) *K. quasipneumoniae* subsp. *similipneumoniae*, (D) *K. quasipneumoniae* subsp. *quasipneumoniae*, (E) *K. africanensis*, (F) *K. quasivariicola*, (G) *K. pneumoniae sensu stricto*. Scale bar reflects the number of nucleotide substitutions per site.

The core genome phylogeny demonstrated that the CPE isolates clustered with other members of *K. pneumoniae sensu stricto*. This confirmed that the original species designation was correct. Consistent with their MLST assignment, the short branch length to the common ancestor of CPE01 and CPE25 indicates that these isolates are closely related. On the same basis, CPE08 and CPE24 are more closely related to each other than to CPE01, CPE16 or CPE25. CPE01 and CPE25 form their own tree branch separating them from the rest of the *K. pneumoniae sensu stricto* strains in the tree.

To contextualise the isolates within a curated publicly-available global data set of *K. pneumoniae* genomes, Pathogenwatch (https://pathogen.watch) (and integrated (meta) data, including from Kleborate (Lam *et al.*, 2021) and MLST (Maiden *et al.*, 1998)) was used to visualise the CPE isolates plotted alongside a collection of their respective STs. Maps of these data illustrate the countries of isolation and carbapenem resistance genes present in each of the genomes (Figure 4.2). Core-genome phylogenetic trees highlight structural groupings within each ST (Figure S7).

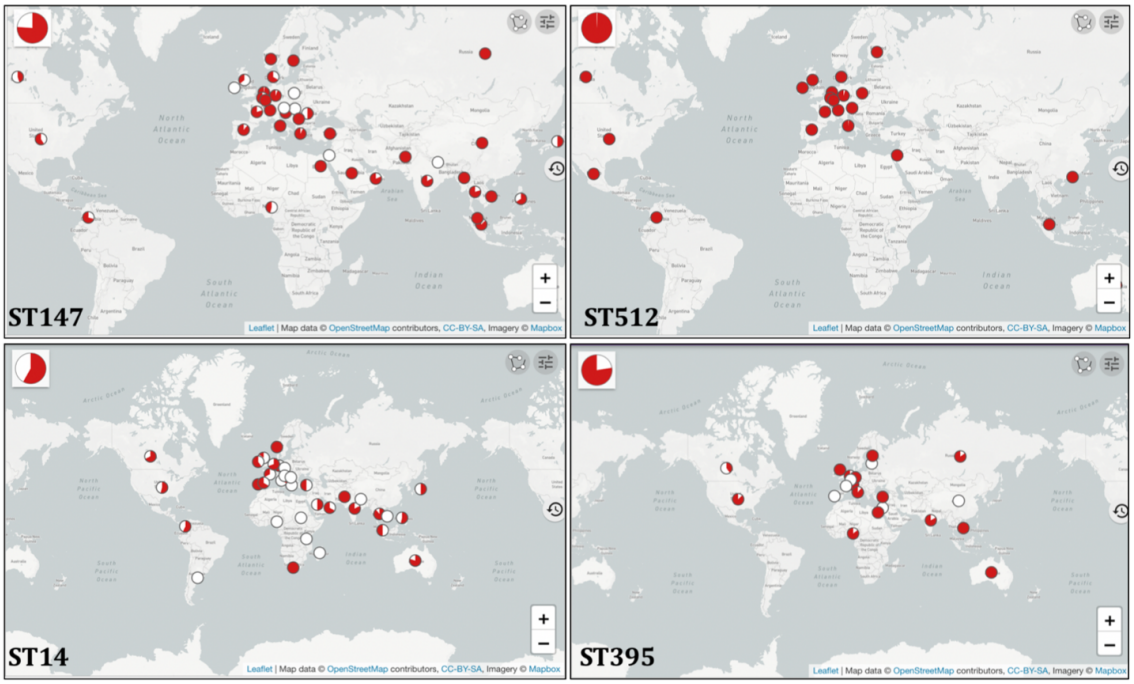

Figure 4.2: World maps (OpenStreetMap) indicating isolation country (where available) of the Pathogenwatch (https://pathogen.watch) publicly available representatives of *K. pneumoniae* (30/11/21 search for all available examples of each ST). Points reflect country of isolation. Red colour indicates carbapenem resistance gene carriage: ST147 (474/623, 76% genomes), ST512 (612/615, 99.5% genomes), ST14 (201/346, 58% genomes) and ST395 (82/106, 77% genomes) (as of 30/11/21). White colour indicates no known carbapenem resistance genes. Point pie charts represent overall carbapenem resistance gene carriage (proportion of red and white) for the sequences originating from each country. The large pie charts indicate overall carbapenem resistance gene carriage for the sequence type data set.

Mapping their countries of isolation (Figure 4.2) indicated that all of the STs are globally distributed and that carbapenem resistance gene carriage is frequently identified within these collections. Although there may be bias in those isolates selected for sequencing, in every case over 50% of isolates representing each sequence type

carry carbapenem resistance genes. For ST512, 99.5% of the sequenced isolates carry carbapenem resistance genes. Overall, the phylogenies indicate that the CPE isolates and the majority of the sequenced isolates of the four STs carry carbapenem resistance gene(s) (Figure S7). The CPE isolates cluster alongside strains from their respective STs as expected.

For a few of the CPE isolates, the phylogenies and metadata highlighted some interesting features which were investigated further. Amongst the ST147 collection sequences, despite overall high levels of carbapenem resistance gene carriage (76% of genomes) (Figure 4.3A), CPE01 and CPE25 are in the minority (32/625 total genomes, 5%) in carrying $bla_{\text{NDM-5}}$ (Figure 4.3B). Instead, the most common carbapenem resistance gene in the ST147 collection sequences is $bla_{\text{NDM-1}}$ (214/623 genomes, 34%). Despite low levels of $bla_{\text{NDM-5}}$ carriage in this set of sequences, strains from the collection carrying this NDM variant have been identified in eight countries (Figure 4.3C).

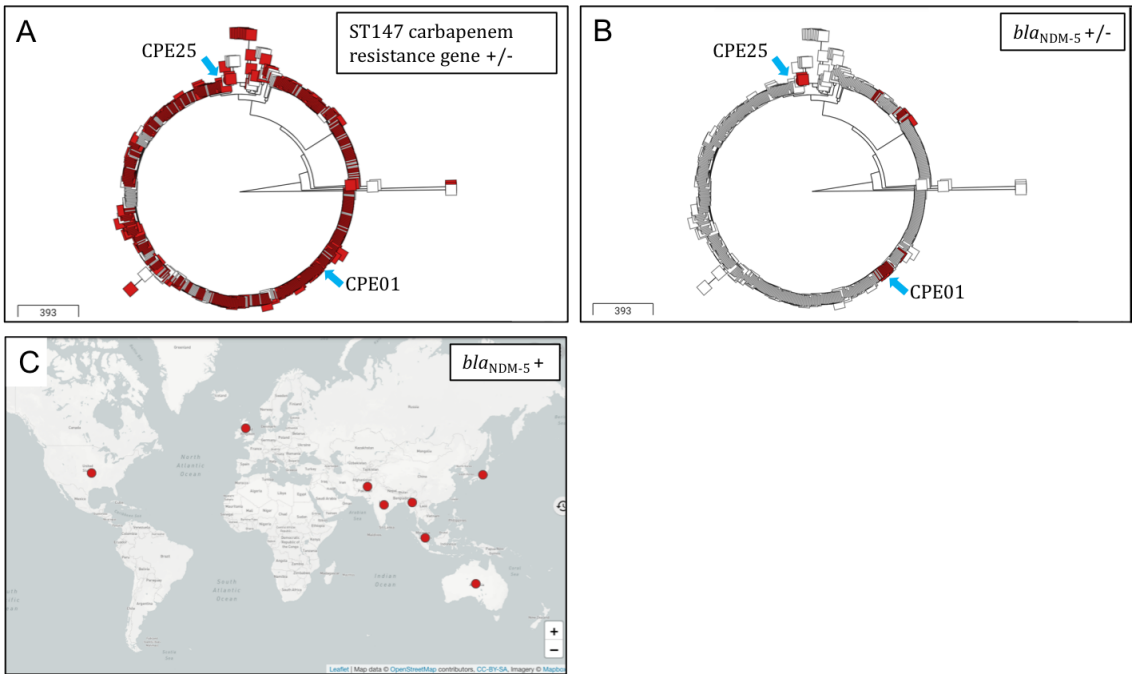

Figure 4.3: CPE01 and CPE25 (blue arrows) alongside ST147 Pathogenwatch collection sequences (30/11/21 search for all available examples of ST147). Core-distance neighbour-joining phylogenies constructed by Pathogenwatch (https://pathogen.watch) using PhyloCanvas (https://www.phylocanvas.gl/) and world map (© OpenStreetMap contributors, https://www.openstreetmap.org/copyright) highlighting carbapenem resistance gene carriage (where data are available). Red colour represents carbapenem resistance gene carriage. White colour in grey outline indicates no detected carbapenem resistance genes. (A) ST147 collection and CPE01 and CPE25 (carbapenem resistance gene presence/absence (+/)), (B) ST147 collection, CPE01 and CPE25 ($bla_{\text{NDM-5}}$ +/-). (C) Geographical distribution (by country) of $bla_{\text{NDM-5}}$ representatives in ST147 collection, including CPE01 and CPE25 (red points). Scales indicate approximate number of substitution mutations.

Isolate CPE16 groups with other ST14 sequences as expected. Interestingly, CPE16 groups with ST14 sequences which form a distinct cluster from the rest of the clade (Figure 4.4). Many of the ST14 collection (200/346 sequences, 58%) carry carbapenem resistance genes (Figure 4.4A), as do most of the strains (14/15, 93%) in the CPE16 sub-group (Figure 4.4B). Although some of the collection sequences (107/346, 31%) carry $bla_{\text{NDM-1}}$ (Figure 4.4C), within the sub-group this is rare, with only CPE16 and one other group member carrying this gene (2/15, 13%) (Figure 4.4D). In the sub-group, $bla_{\text{OXA-232}}$ is present in the majority (13/15, 87%) of sequences, one of which also contains $bla_{\text{NDM-5}}$. CPE16 does not contain $bla_{\text{OXA-232}}$

(Figure 4.4E,F).

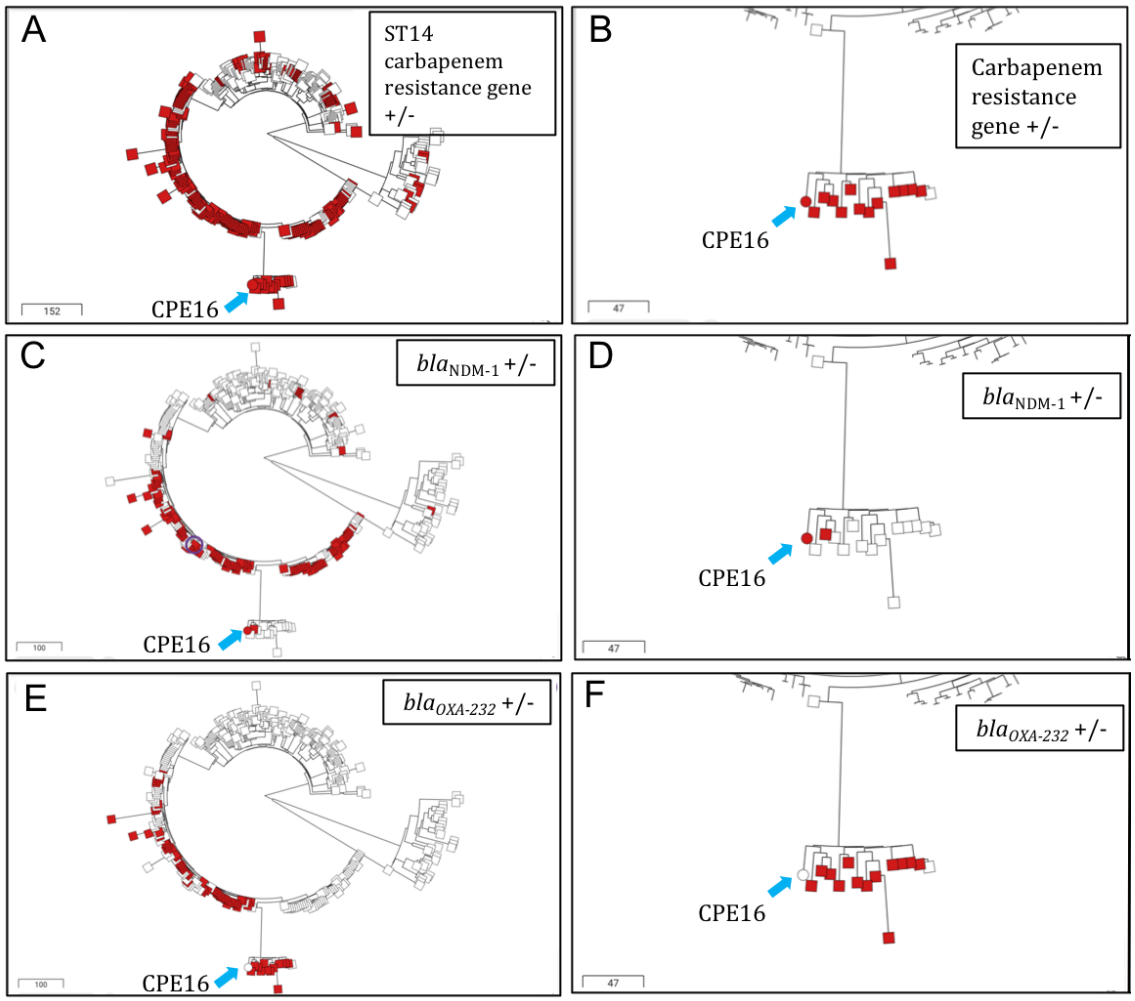

Figure 4.4: CPE16 (circle symbol, blue arrow) alongside ST14 Pathogenwatch collection sequences (30/11/21 search for all available examples of ST14). Core-distance neighbour-joining phylogenies constructed by Pathogenwatch (https://pathogen.watch) using PhyloCanvas (https://www.phylocanvas.gl/) . Red colour represents carbapenem resistance gene carriage. White colour with grey outline indicates no detected carbapenem resistance genes. (A) ST14 collection and CPE16 (carbapenem resistance gene presence/absence (+/-)), (B) Focus on CPE16 clade (carbapenem resistance gene +/-), (C) ST14 collection and CPE16 ($bla_{\text{NDM-1}}$ +/-), (D) Focus on CPE16 clade ($bla_{\text{NDM-1}}$ +/-), (E) ST14 collection and CPE16 ($bla_{\text{OXA-232}}$ +/-). (F) Focus on CPE16 clade ($bla_{\text{OXA-232}}$ +/-). Scales indicate approximate number of substitution mutations.

4.3 Investigating the accessory genome

Next, hybrid whole genome sequences assembled with Unicycer (Wick *et al.*, 2017b) were visualised to assess contig circularisation, and to determine the number of likely plasmids in each isolate (Figure 4.5). For these isolates, most contigs (27/36) were circular (closed), indicating that the assemblies had produced predominantly complete sequences. Each genome contained a closed chromosomal sequence of 5.3-5.5 Mb (large circles) and three to five closed putative plasmid sequences (small circles). However, nodes without edges were present in the CPE01 and CPE24 graphs and the CPE25 graph contained some nodes with uncertain junctions. Based on a pairwise BLASTn search against the chromosomal sequence, the node-without-edges in CPE24 likely originated from the chromosome (99% identity and coverage to the CPE24 chromosomal sequence). This search also suggested that the unresolved assembly was due to a sequencing error from a homopolymer (Figure S8). The CPE01 and CPE25 unresolved assemblies are discussed later in section 4.4.

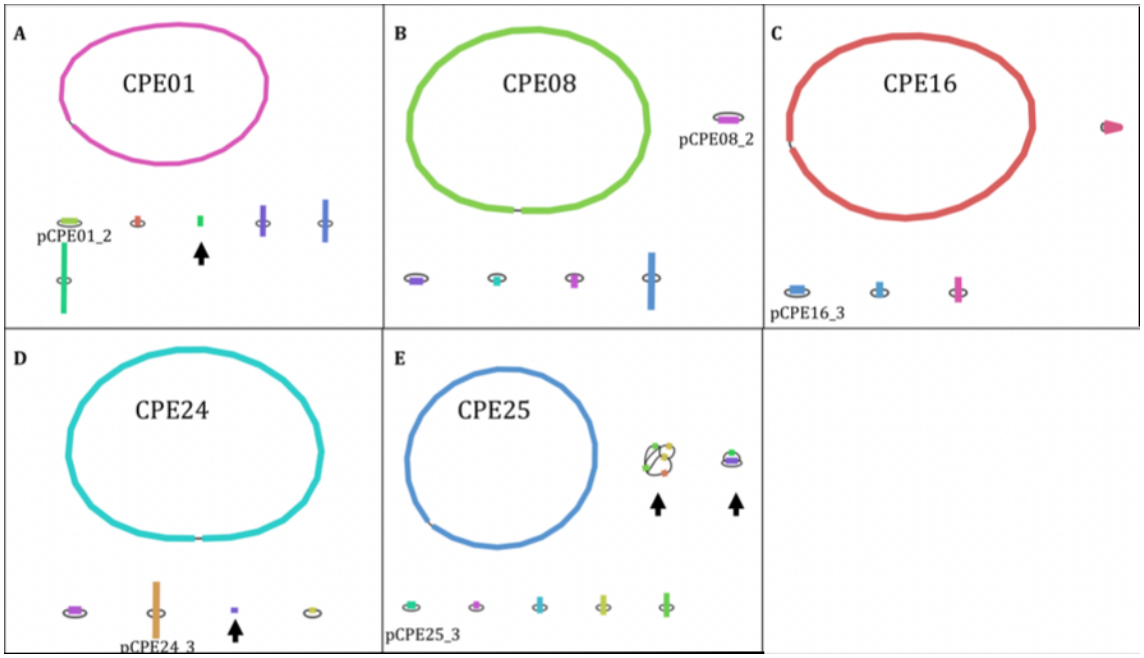

Figure 4.5: Unicycler (Wick *et al.*, 2017b) hybrid assembly graph visualisation using Bandage (Wick *et al.*, 2015). Coloured blocks represent nodes (contigs). Node depth is related to (but not directly proportional to) sequencing depth. Node width is related to (but not directly proportional to) contig length. Black lines (edges) represent links between contigs. A single black line linking a circular contig indicates the sequence has been circularised (closed). There is assembly uncertainty for contigs (nodes) with multiple/ no black lines (black arrows). Carbapenem resistance plasmids are labelled as 'p' followed by the isolate name and contig number below their respective contigs. (A) CPE01. (B) CPE08. (C) CPE16. (D) CPE24. (E) CPE25.

Assemblies were queried with the PlasmidFinder (Carattoli *et al.*, 2014) and ResFinder (Zankari *et al.*, 2012) databases to identify known replicons and AMR genes and to determine their locations (Table 4.1). This revealed that each CPE isolate carries at least one carbapenem resistance gene amongst a large number of other AMR genes (13-24 total). For CPE01 and CPE25, there were two different carbapenem resistance genes identified, with $bla_{\text{OXA-181}}$ on the chromosome and $bla_{\text{NDM-5}}$ in a plasmid. For all other isolates, one type of non-chromosomal carbapenem resistance gene was detected: CPE08, CPE16 and CPE24 contained $bla_{\text{KPC-3}}$, $bla_{\text{NDM-1}}$ and $bla_{\text{OXA-232}}$ respectively. In 4/5 isolates (CPE01, CPE08, CPE16 and CPE25), the carbapenem resistance genes were found in large (∼83-168 kb) plasmids with F-type replicons. However, in CPE24, $bla_{\text{OXA-232}}$ was in a small

(∼6 kb) plasmid with a ColKP3-type replicon. Consistent with their high prevalence in the *Enterobacteriaceae* (Kopotsa *et al.*, 2019), F-type plasmids were present in all of the assemblies, with multi-replicon F-type plasmids found in the complete assemblies of CPE08 and CPE16. For several of the F-type replicons, plasmid sub-typing was possible using plasmidMLST (one sub-type identified for 4/5 isolates). However, the PubMLST database was not able to sub-classify all of the F-type replicons identified by PlasmidFinder. CPE01 and CPE25 contain the same FII replicon type, FII-2. X3 and HI1B replicons were found in CPE08 and CPE16 respectively. All isolates also contained small plasmids with 'Col'-type replicons.

Table 4.1: Information on CPE isolate Unicycler contigs including carbapenem-resistance gene presence (ResFinder), identification of putative plasmid replicons (PlasmidFinder) and plasmid subtyping (PlasmidMLST, exact matches only) (Carattoli *et al.*, 2014; Wick *et al.*, 2017b; Zankari *et al.*, 2012). 'Col' replicons refer to small plasmid replicons identified by PlasmidFinder. CR (carbapenem-resistance) genes. Contigs labelled '1' refer to chromosomes. All other numbers refer to additional sequences where a replicon was identified. Genes in **bold** are predicted to be present and full length on the accessory contig containing the carbapenem resistance gene. Information in line with and to the right-hand side of the contig number relates to a given contig.

Isolate	Total predicted AMR genes (ResFinder)	Contig number	CR gene(s)	Replicon (PlasmidFinder)	plasmidMLST
CPE01	*oqxB, oqxA, catB1, rmtF, ant(3'')-Ii-aac(6')-IId, bla*$_{SHV-11}$, *bla*$_{CTX-M-15}$, *mdf(A), fosA, bla*$_{OXA-181}$, ***qnrB1***, *ant(3'')-Ia,* ***arr-3***, ***sul1***, ***bla***$_{NDM-5}$, ***rmtB***, ***bla***$_{TEM-1B}$, ***dfrA12***	1	*bla*$_{OXA-181}$	Chromosome	
		2	*bla*$_{NDM-5}$	IncFII_1	FII-2
		4		IncFII(pMET)_1_pMET1	
		5		ColRNAI_1	
		6		Col440I_1	
		7		ColpVC_1	
CPE08	*oqxB, oqxA, bla*$_{SHV-182}$, *mdf(A), fosA6, aadA1,* ***bla***$_{OXA-9}$, ***bla***$_{TEM-1A}$, ***bla***$_{KPC-3}$, *bla*$_{SHV-182}$, *aac(6')-Ib, ant(3'')-Ia, bla*$_{TEM-105}$	1		Chromosome	
		2	*bla*$_{KPC-3}$	IncFIB(K)_1_Kpn3 IncFII_1_pKP91	FIIK-1
		3		IncFIB(pKPHS1)_1_pKPHS1 IncFIB(pKPHS1)_1_pKPHS1	
		4		IncX3_1	
		5		ColRNAI_1	
		6		ColRNAI_1	
CPE16	*oqxB, oqxA, aac(6')-Ib-cr, bla*$_{OXA-1}$, *catB3, bla*$_{SHV-106}$, *mdf(A), fosA6, dfrA1, mph(E), msr(E), armA, sul1, aadA2,* dfrA12, *ant(3'')-Ia,* ***bla***$_{NDM-1}$, ***aph(3')-VI***, ***qnrS1***, ***bla***$_{CTX-M-15}$, ***aac(6')-Ib***, *ant(3'')-Ia,* ***bla***$_{OXA-9}$, ***bla***$_{TEM-1B}$	1		Chromosome	
		2		IncFIB(Mar)_1_pNDM-Mar IncHI1B_1_pNDM-MAR	
		3	*bla*$_{NDM-1}$	IncFIB(pQil)_1_pQil IncFII_1_pKP91	FIIK-2
		4		Col440I_1	
CPE24	*oqxB, oqxA, bla*$_{SHV-187}$, *mdf(A), fosA, bla*$_{CTX-M-15}$, *aac(6')-Ib-cr, bla*$_{OXA-1}$, *catB3, qnrB1, bla*$_{SHV-12}$, *bla*$_{TEM-1B}$, *aadA2, dfrA12, ant(3'')-Ia, aac(3)-IId, bla*$_{TEM-1B}$, *qnrS1, catA1,* ***bla***$_{OXA-232}$, *ere(A)*	1		Chromosome	
		2		IncFIB(pQil)_1_pQil	
		3	*bla*$_{OXA-232}$	ColKP3_1	
		5		ColpVC_1	
CPE25	*oqxB, oqxA, catB1, rmtF, ant(3'')-Ii-aac(6')-IId, arr-3, bla*$_{SHV-11}$, *bla*$_{CTX-M-15}$, *mdf(A), bla*$_{OXA-181}$, *fosA, qnrB1, ant(3'')-Ia, dfrA14,* ***bla***$_{NDM-5}$, ***sul1_5***, ***aadA2***, ***dfrA12***, *mph(A), bla*$_{TEM-1B}$, *rmtB, erm(B)*	1	*bla*$_{OXA-181}$	Chromosome	
		2		IncFII(pKPX1)	
		3	*bla*$_{NDM-5}$	IncFII_1	FII-2
		6		ColRNAI_1	
		7		Col440I_1	
		9		ColpVC_1	

As CPE01 and CPE25 appeared closely related, contained the same carbapenem resistance genes and several of the same plasmid replicons, their genomes were com-

pared. Pairwise BLASTn (Altschul *et al.*, 1990) comparisons revealed the nucleotide identity between these genomes to be 100% overall across 98% coverage when inputting CPE01 as the subject and across 97% coverage when CPE25 was the subject. The small ColRNAI, Col440I and ColpVC replicon-containing plasmids in these isolates were found to be identical when compared using BLASTn.

4.4 Carbapenem resistance plasmids

To investigate the carbapenem resistance plasmids, and the likelihood of their transfer by conjugation, their sequences were annotated using a combination of automatic (Prokka (Seemann, 2014)) and manual (reference sequence search) methods. The focus for this was annotation of replicons, AMR genes and conjugation modules (Figure 4.6). For 4/5 isolates (CPE01, 8, 16 and 25), a carbapenem resistance gene was present in a plasmid containing a conjugation module. Unlike for CPE01, CPE16 and CPE25, which had a complete uninterrupted module that spanned approximately 34 kb between *finO* and *traM*, for CPE08 the transfer region was interrupted by a copy of IS*Kpn26* which was found in a remnant of the *traE* gene. The IS*Kpn26* was responsible for a deletion event that removed the *traLAM* genes, which are essential for conjugation in F-type plasmids (Fernandez-Lopez *et al.*, 2016). Replicons are described further in Table 4.1. For these four plasmids, multiple other AMR genes were present in clusters. Conversely, for CPE24, its carbapenem resistance gene was located on a small plasmid with mobilisation genes and there were no other AMR genes present (Figure 4.6D). From these maps, it appears that 3 of 5 of the isolates (CPE01, CPE16 and CPE25) contain putative conjugative carbapenem resistance plasmids. Experimentation will be required to determine if these predictions are accurate.

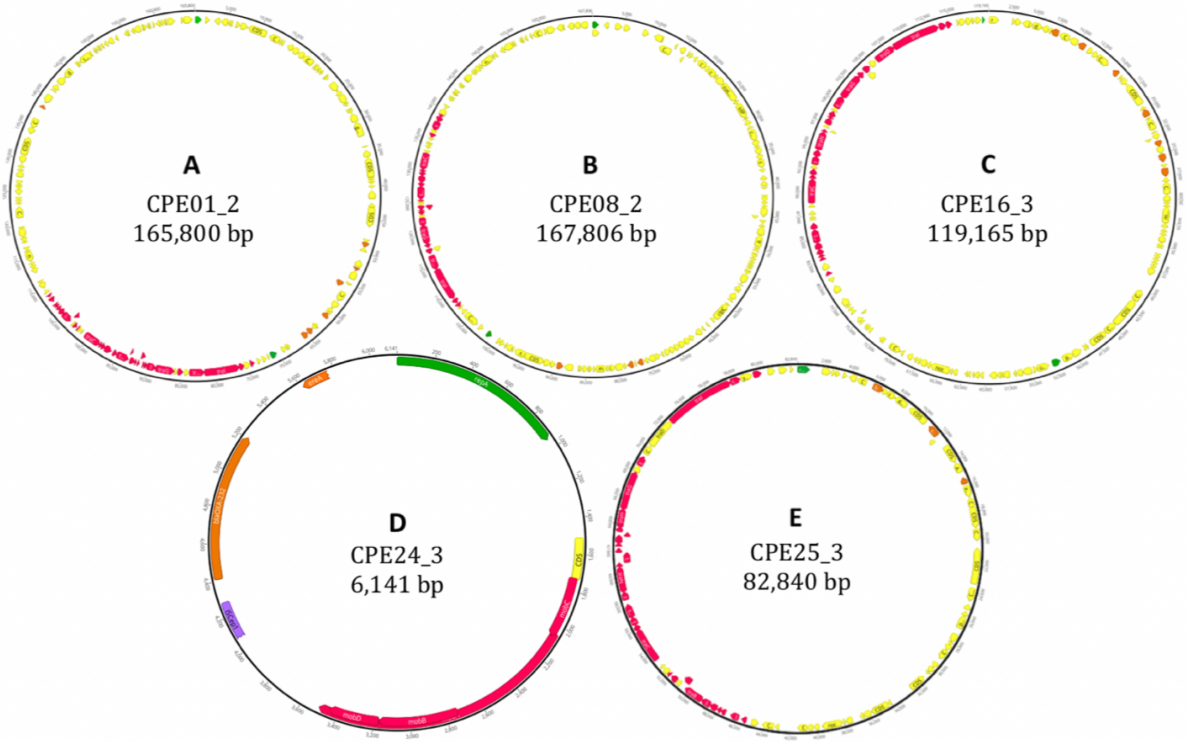

Figure 4.6: Annotated putative carbapenem resistance plasmids from CPE isolates (circular maps). (A) CPE01_2, (B) CPE08_2, (C) CPE16_3, (D) CPE24_3, (E) CPE25_3. Annotations were drawn to scale and transferred from likely coding sequences (CDS) determined via BLASTn and tBLASTn searches (Altschul *et al.*, 1990), where necessary with inferences as to likely start/stop codons and with reference to Prokka annotations (Seemann, 2014). Manual annotations were only included if a start/stop codon could be identified. All putative CDS (except Prokka annotations) were translated to assess premature stop codons (indicated if likely present). Orange arrows (AMR CDS). Green arrows (*repA* CDS). Pink arrows (conjugation module CDS). Yellow arrows (Prokka annotations). For CPE01_2, CPE16_3 and CPE25_3, all 'essential' conjugation genes for similar F- type plasmids (Fernandez-Lopez *et al.*, 2016) were present on the basis of manual annotation versus AP001918 GenBank reference. For CPE08_2, no evidence of the essential conjugation genes *traLAM* was found (Fernandez-Lopez *et al.*, 2016). Maps were prepared using Geneious Prime 2021.1.

As the CPE01 and CPE25 Unicycler (Wick *et al.*, 2017b) hybrid assemblies were not completely circularised, another method of assembly (long-read assembly using Flye (Kolmogorov *et al.*, 2019) followed by short-read polishing using Pilon (Walker *et al.*, 2014) via PorePolish https://github.com/stevenjdunn/porepolish) was used to try and achieve circularised sequences for these isolates. This was done to prepare adequate reference sequences which could be used for future comparison against any transconjugants, such as to determine plasmid content and completeness. Long-read assembly followed by short-read polishing achieved circularised assemblies for both genomes (Figure 4.7). When comparing the polished Flye assemblies to the Illumina-only data using Snippy (https://github.com/tseemann/snippy), for CPE01 there were three SNPs and for CPE25 there were zero SNPs. This result indicated that the polished assemblies were as accurate, or almost as accurate, as the Illumina data. Therefore, these were considered suitable for future use.

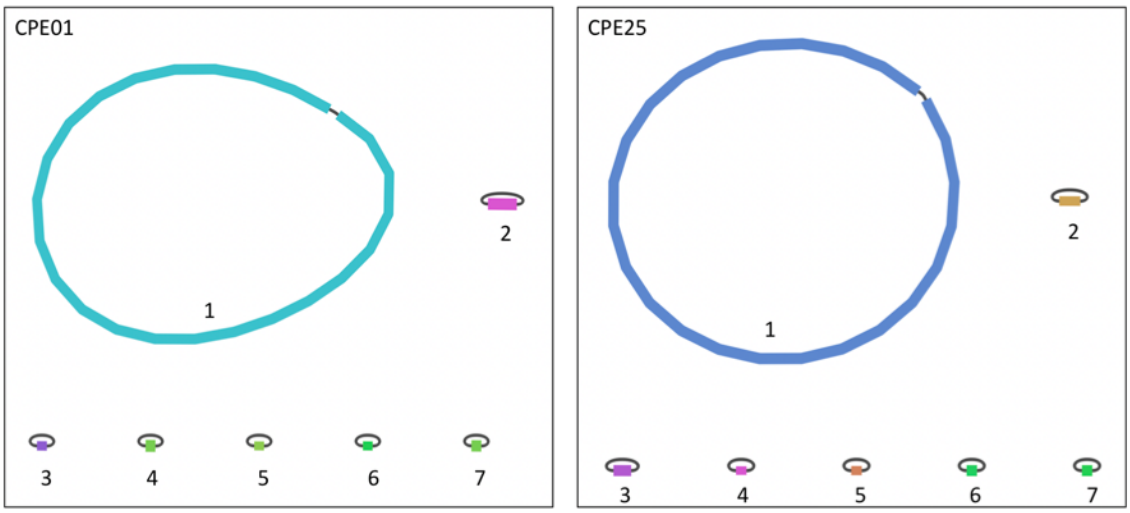

Figure 4.7: Visualisation of CPE01 and CPE25 (unpolished) Flye (Kolmogorov *et al.*, 2019) assembly graphs using Bandage (Wick *et al.*, 2015). Coloured blocks represent nodes (contigs). Black lines (edges) represent links between contigs. A single black line linking a circular contig indicates the sequence has been circularised (closed).

To further evaluate these assemblies, the number of putative plasmids, along with their replicons and AMR genes was assessed (Table 4.2). Replicons were assigned by

PlasmidFinder for 5/6 of the accessory contigs in the CPE01 and CPE25 polished assemblies. These were identical in name to those previously assigned to the original Unicycler assemblies, although they may be associated with a different contig number in the different assemblies. While no replicon was identified by PlasmidFinder for CPE01 contig 4 or CPE25 contig 5, these sequences were identical to each other (100% coverage, 100% identity using CPE01_4 (54404 bp) and CPE25_5 (54402 bp) as the query) and to GenBank accession CP021760.1 (54404 bp) corresponding to a *K. pneumoniae* phage-plasmid.

Table 4.2: Information on CPE isolate polished Flye assembly contigs including carbapenem-resistance gene presence (ResFinder), other AMR gene presence and identification of putative plasmid replicons (PlasmidFinder) (Carattoli *et al.*, 2014; Kolmogorov *et al.*, 2019; Zankari *et al.*, 2012). 'Col' replicons refer to small plasmid replicons identified by PlasmidFinder. CR (carbapenem-resistance) genes. Contigs labelled '1' refer to chromosomes. All other numbers refer to additional sequences where a replicon was identified. Genes in bold are predicted to be present and full length on the accessory contig containing the carbapenem resistance gene. Information in line with and to the right-hand side of the contig number relates to a given contig.

Isolate	Total predicted AMR genes (ResFinder)	Contig no.	CR gene	Replicon (PlasmidFinder)
CPE01	*fosA*, $bla_{OXA-181}$, $bla_{CTX-M-15}$, bla_{SHV-11}, ***arr-3***, *rmtF*, *oqxA*, *oqxB*, ***sul1***, $\mathbf{bla_{NDM-5}}$, ***rmtB***, $\mathbf{bla_{TEM-1B}}$, ***dfrA12***, ***qnrB1***	1	$bla_{OXA-181}$	N/A
		2	bla_{NDM-5}	IncFII_1
		3		IncFII(pMET)_1_pMET1
		5		ColRNAI_1
		6		ColpVC_1
		7		Col440I_1
CPE25	$bla_{OXA-181}$, *oqxB*, *oqxA*, *rmtF*, *arr-3*, bla_{SHV-11}, $bla_{CTX-M-15}$, *fosA*, *dfrA14*, *qnrB1*, ***dfrA12***, *aadA2*, ***sul1***, $\mathbf{bla_{NDM-5}}$, ***rmtB***, $\mathbf{bla_{TEM-1B}}$, ***mph(A)***, ***erm(B)***	1	$bla_{OXA-181}$	N/A
		2		IncFII(pKPX1)
		3	bla_{NDM-5}	IncFII_1
		4		ColRNAI_1
		6		Col440I_1
		7		ColpVC_1

To investigate the genetic context of the carbapenem resistance genes on the putative

plasmid contigs, IS annotations were mapped on to the plasmid sequences (Figure 4.8) and the specific carbapenem resistance gene-flanking sequences were highlighted (Figure 4.9).

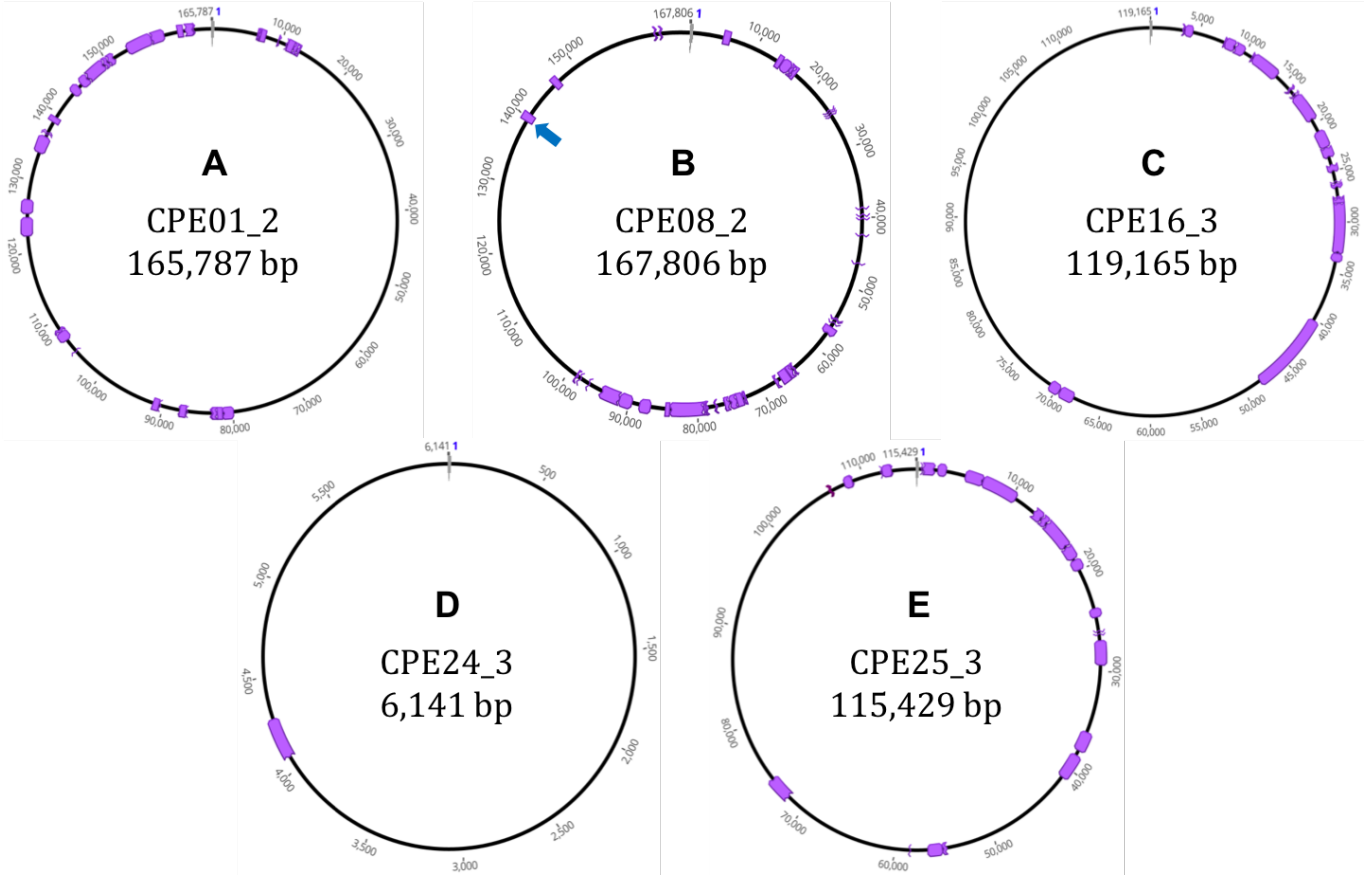

Figure 4.8: Insertion sequences annotated on putative carbapenem resistance plasmids from CPE isolates (circular maps) from Flye or Unicycler assemblies. (A) CPE01_2 (Flye), (B) CPE08_2 (Unicycler), (C) CPE16_3 (Unicycler), (D) CPE24_3 (Unicycler), (E) CPE25_3 (Flye). Annotations (purple boxes) were drawn to scale on the basis of high percentage nucleotide identity to ISfinder database sequences (http://www-is.biotoul.fr, (Siguier *et al.*, 2006)). Conjugation modules were not interrupted by IS elements apart from in CPE08_2 at *traE* where the region was truncated at position 139,212 by IS*Kpn26* (blue arrow). Truncated IS sequences are indicated by a jagged edge.

The IS annotations indicated a large number of putative translocatable genetic element sequences were often clustered together in the carbapenem resistance plasmids. No conjugation module genes were interrupted by these sequences with the exception of CPE08_3 where *traE* has been truncated by IS*Kpn26* at position 139,212, resulting in an incomplete module. All carbapenem resistance genes were found adjacent to IS (Figure 4.9).

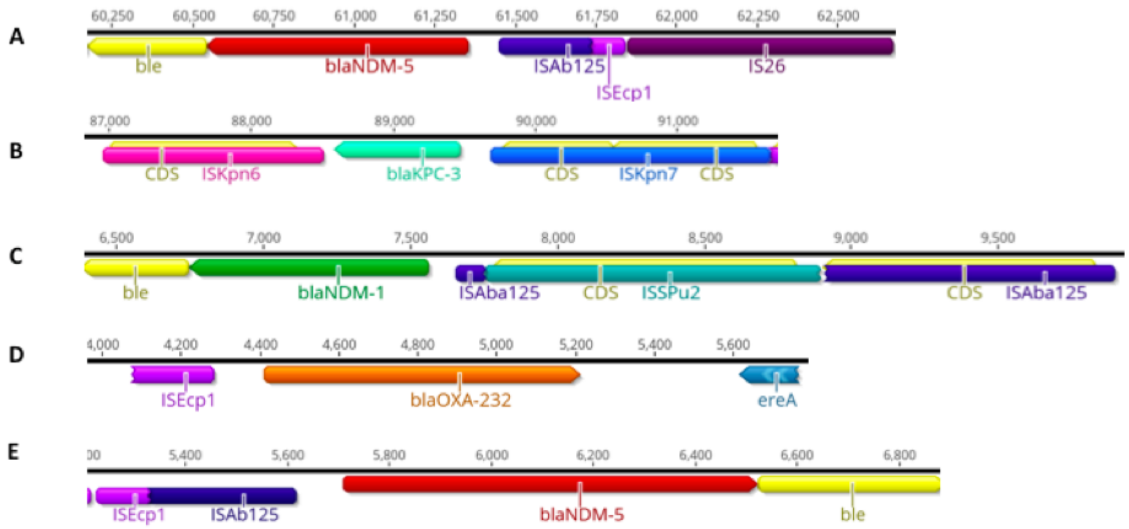

Figure 4.9: Genetic context of the carbapenem resistance genes carried by the CPE isolate plasmids. (A) CPE01_2, (B) CPE08_2, (C) CPE16_3, (D) CPE24_3, (E) CPE25_3. Annotations indicate resistance genes and their flanking regions. Yellow annotations indicate additional Prokka annotations.

Next, BLASTn (Altschul *et al.*, 1990) was used to query the GenBank non-redundant nucleotide database with the carbapenem resistance plasmid sequences from the CPE isolates to determine whether similar plasmids had been sequenced previously. For CPE01 and CPE25, the Flye contigs were used in queries, and for the other isolates the original Unicycler contigs were used (Agarwala *et al.*, 2018; Kolmogorov *et al.*, 2019; Wick *et al.*, 2017b) (Table 4.3). For each of the queried sequences, matches were found in the GenBank database. A ColKP3 plasmid identical to that of CPE24 was found. Using CPE08_2, CPE16_3 and CPE25_3 as queries uncovered high percentage coverage and identity matches (92 to 100%). For CPE01_2, database matches generally corresponded with one half of the query sequence each,

with coverage of approximately 50%. However, the percentage identity of these partial matches was high (99.96-100%). Notably, the second best match for CPE25_3 was CP024840.1 (96185 bp length, 99% coverage, 99.98% identity), which was the closest match to CPE01_2. Based on this observation, it appears likely that the CPE01_2 assembly represents two plasmids.

Table 4.3: Single examples of 'best' coverage and percentage identity matches of putative CPE conjugative carbapenem resistance plasmids on GenBank from BLASTn search (Agarwala *et al.*, 2018; Altschul *et al.*, 1990).

Isolate (query) contig/ length (bp)	E.g. GenBank accessions (subject)/ length (bp)	%coverage	%identity
CPE01_2/ 165,787	CP041957.1/83,648	53 ('left side')	99.96
	CP024840.1/96,185	56 ('right side')	100.00
CPE08_2/167,806	CP022574.1/170,415	92	99.99
CPE16_3/119,165	CP009115.1/118,061	99	100.00
CPE24_3/6,141	LC507653.1/6,141	100	100.00
CPE25_3/96,618	KY130431.1/96549	100	99.97

4.5 Discussion

Whole genome sequencing data were obtained for five *K. pneumoniae* clinical isolates from the Queen Elizabeth Hospital (Birmingham). These data were examined to characterise the isolates, determine how they compare with other global *K. pneumoniae* and to ascertain which may be most suitable for use as donors in a clinically-relevant model to investigate conjugative transfer of carbapenem resistance plasmids.

Although the CPE isolates were determined to be carbapenem-resistant, carbapenemase-producing *K. pneumoniae* based on standard laboratory tests, the species designation was confirmed by placing the isolates amongst a selection of *K. pneumoniae* species complex strains. The isolates were further investigated within the context of a global collection (Pathogenwatch) of strains of the same ST. This illustrated that the CPE isolates group with other strains belonging to the same

ST, but do not always carry the same carbapenem resistance genes as other group members or cluster alongside the majority in geographical distribution or phylogenetic relatedness. A similar pattern of variable carbapenem resistance gene carriage was highlighted in a recent study investigating ST16 *K. pneumoniae* outbreak isolates from Vietnam within a global context (Nguyen *et al.*, 2021). Nguyen *et al.* determined that outbreak and global strains contained a variable complement of AMR genes, including carbapenem resistance genes. This is not unexpected, especially given the accessory nature of many AMR genes (Vrancianu *et al.*, 2020) and the small number of core chromosomal genes used for *K. pneumoniae* MLST classification (Diancourt *et al.*, 2005).

Metadata from Pathogenwatch/OpenStreetMap plotting strain origin by country was visualised to evaluate the overall carbapenem resistance gene carriage levels within ST collection groups. The maps revealed global spread of the STs, alongside a high proportion of carbapenem resistance gene carriage, highlighting the previously reported carbapenem resistance problem in *Enterobacteriaceae* (De Oliveira *et al.*, 2020). For the available ST512 isolates, over 99% of the genomes contained carbapenem resistance genes. Given the association in some regions of ST258 (a close relative of ST512) and bla_{KPC}-mediated carbapenem resistance (Bonnin *et al.*, 2020), this finding is perhaps unsurprising. For all of the STs, the proportion of genomes carrying carbapenem resistance genes was above 50%. Although these percentages are striking, it is important to consider the potential bias in this dataset which may result from preferential sequencing of phenotypically resistant isolates (David *et al.*, 2019). Nonetheless, carbapenem resistance gene carriage in more than half of the available genomes is concerning. The international spread of these STs is evident from these data, and these STs correspond to those previously identified as 'resistance clones' (Lam *et al.*, 2021).

Hybrid genome assemblies were examined to investigate the accessory genomes of CPE isolates, with a focus on characterising the contexts of carbapenem resistance

genes. This revealed that the CPE isolates contained three to six likely plasmid contigs, numbers not uncommon for *K. pneumoniae* (Wyres *et al.*, 2020a). Complete whole genome assemblies of chromosomal and plasmid sequences can be achieved via multiple hybrid methods (De Maio *et al.*, 2019). For example, Unicycler is commonly used to assemble bacterial sequences using short-read data (for accuracy) bridged by long-read data (for structure) (Wick *et al.*, 2017b). This study made use of two hybrid approaches, and highlights through CPE01 and CPE25 assemblies that no method is necessarily able to fully resolve plasmid sequences with absolute certainty. Therefore, although WGS data is undoubtedly informative, assemblies can only provide a guide rather than an authority on the state of any given genome.

To further characterise CPE isolate sequences, PlasmidFinder and ResFinder databases were queried and the AMR gene and plasmid replicon content of the five isolates was predicted. These databases supply curated sequences which can be used as references, facilitating comparison between studies (Carattoli *et al.*, 2014; Zankari *et al.*, 2012). This assessment indicated that the CPE isolates carried multiple plasmid replicons, confirming likely plasmid sequences and indicating that some may be multi-replicon plasmids, which is frequently observed for F-type plasmids (of which there was an example in each isolate) (Villa *et al.*, 2010). Interestingly, but not unexpectedly, most of the putative plasmid sequences carrying carbapenem resistance genes were F-type. In a recent review, approximately 40% of the carbapenem resistance genes found in plasmids in *Enterobacteriaceae* were located in F-type plasmids (Kopotsa *et al.*, 2019). The AMR gene search indicated that multiple AMR genes were present in each isolate. This is also expected, as many *K. pneumoniae* have been reported to carry multiple AMR genes (Wyres and Holt, 2018).

Using the replicon and AMR gene information, combined with reference sequences from an experimentally-characterised conjugation module, putative carbapenem resistance plasmids were annotated and the likelihood of their theoretical transfer by conjugation was assessed by evaluating the completeness of the F-type plasmid con-

jugation module, or through assessment of mobilisation machinery complemented by BLAST searches (Altschul *et al.*, 1990). Overall, for 3/5 isolates, a full conjugation module from *finO* to *traM* (Frost *et al.*, 1994) appeared to be present in the carbapenem resistance plasmids. A lack of annotations for some of the conjugation module genes does not guarantee their absence. Instead, this indicates that the matches against GenBank reference sequences were poor. This might be expected given the variety exhibited by F-type plasmids (Matlock *et al.*, 2021). No IS elements were identified interrupting the complete (*finO-traM*) conjugation modules, increasing the likelihood of the regions being functional. Another consideration is that a full complement of conjugation module genes is not necessarily required for conjugative ability. However, for CPE01_2, CPE16_3 and CPE25_3, the complete set of essential genes (*traABCDEFGHIKLMVW* and *trbC*) (Fernandez-Lopez *et al.*, 2016) was determined to be present by manual annotation versus an experimentally-determined reference sequence. For 1/5 isolates (CPE08), the conjugation module in its carbapenem resistance plasmid was truncated by an IS which interrupted *traE* (a gene described as essential for conjugation (Fernandez-Lopez *et al.*, 2016)) and the remaining module to the 3' end of *traE*. As a result of the deletion event that generated this truncated sequence, three other essential genes (*traLAM*) were missing from the module (Fernandez-Lopez *et al.*, 2016). Therefore, it is unlikely that this plasmid will transfer by conjugation and ultimately (as with all the isolates) assays will be necessary to determine conjugative ability. These experiments are described in Chapter 5.

The carbapenem resistance gene in CPE24 was found in a small plasmid carrying mobilisation (*mob*) genes (Potron *et al.*, 2011). Recently, the role of small plasmids in AMR has been highlighted, including their contribution to carbapenem resistance gene carriage, and several examples of small AMR plasmids have been identified (Barry *et al.*, 2019; Moran and Hall, 2017; Ramirez *et al.*, 2019). Similar to the majority of the (172) small (≤25 kb) *K. pneumoniae* plasmids investigated by Ramirez *et al.* (2016), the carbapenem resistance plasmid in CPE24 contained

a ColE1-type replicon. Several of the small plasmids harboured resistance genes including *blaOXA*$_{-232}$, which was also found in CPE24, and some contained similar features flanking $bla_{\text{OXA-232}}$ (or its close relative $bla_{\text{OXA-181}}$) as those found in this isolate (truncated IS*Ecp1* and *ereA*) (Ramirez *et al.*, 2019). Further investigation of the plasmid content of this isolate may reveal a conjugative plasmid able to mobilise CPE24_3. However, this was beyond the scope of this work.

Carbapenem resistance gene(s) were identified in each isolate as predicted by the previous phenotypic testing at the hospital. Interestingly, two of the isolates (CPE01 and CPE25) appeared to contain multiple chromosomal copies of $bla_{\text{OXA-181}}$ alongside a plasmid-borne copy of $bla_{\text{NDM-5}}$. These isolates both belonged to ST147, and isolate(s) with a similar carbapenem resistance gene profile have been identified in published reports (Rojas *et al.*, 2017; Sherchan *et al.*, 2020). The clinical isolate investigated by Sherchan *et al.* from Nepal (Sherchan *et al.*, 2020) and a clinical isolate from India in the study by Rojas *et al.* (2017) also contained *rmtB* and *rmtF*. These aminoglycoside resistance genes are harboured by CPE01 and CPE25, raising questions about how widespread this resistance profile might be within ST147.

The AMR gene profiles of CPE01 and CPE25, alongside their similar replicon profile and close proximity in the *K. pneumoniae* species complex phylogeny, prompted a comparison of their nucleotide sequences which were found to be 100% identical across the majority of the genome. To fully evaluate the plasmid content of these isolates, an alternative assembly method was employed, using a long-read assembly to ascertain genome structure, followed by polishing using short-read data to achieve better accuracy (De Maio *et al.*, 2019). The assemblies were determined to be almost as accurate as the original Unicycler assemblies on the basis of minimal SNP differences after polishing and circularised contigs were obtained. Based on this circularisation, the genome assembly was considered to be complete and suitable for future use. For subsequent work, the original assemblies were used for CPE08, CPE16 and CPE24 and the Flye assemblies were used for CPE01 and CPE25. The

differences in outcome using the two assembly methods on the same sequencing data highlights that this process is only as good as the technology permits, and remains an approximation of the state of the genome at the time of sequencing. This, combined with the presence of many annotations corresponding to putative mobile genetic elements, indicates that genomes are fluid and can change often. Mobile genetic elements contribute to genome evolution, with IS such as IS*26* often mediating changes in gene repertoire (Hua *et al.*, 2020; Naito and Pawlowska, 2016). Indeed, specific mobile genetic element-AMR gene associations have been identified, including between IS*Aba125* and bla_{NDM} which is illustrated here (Partridge *et al.*, 2018).

Comparison to existing sequences in the GenBank database indicated that carbapenem resistance plasmids similar to those found here have been seen elsewhere. This outcome supports the assemblies and their construction. However, 100% identity and coverage matches were only identified for the small ColKP3 plasmid of CPE24. Otherwise, the carbapenem resistance contigs were novel in not having complete sequence identity to previously sequenced plasmids.

4.6 Limitations and future work

As WGS provides a wealth of information, more (manual) work could be carried out to improve the existing putative annotations for the carbapenem resistance plasmids, such as those identifying IS elements, or to increase the level of confidence in annotations that were not based on experimentally-determined reference sequences. There is also scope to annotate the remaining plasmids in these isolates, or to investigate existing (related) plasmid sequences to evaluate evolutionary trends such as AMR gene carriage, geographical or species distributions. Although these areas remain to be investigated, the work presented here successfully permitted informed decisions regarding subsequent experimental work and model validation.

4.7 Conclusions

Overall, WGS data alongside publicly-available sequence databases and tools have permitted characterisation of the CPE isolates, with a specific focus on their classification within both the *K. pneumoniae* species complex and amongst strains of the same ST. AMR gene content, plasmid replicons and transfer/mobilisation genes were investigated with a specific focus on putative carbapenem resistance plasmids. Taken together, the available data indicate that 3/5 of these plasmids are likely to be conjugative and 1/5 is likely to be mobilisable. This information has suggested that CPE24 should be excluded from future experiments due to its lack of a conjugative carbapenem resistance plasmid. Conversely, the available information suggests inclusion of the remaining four isolates, three of which are likely to conjugate and one of which may be less likely to. These data have been directly useful in supporting decision-making for subsequent experimental approaches and model development which will examine conjugation of carbapenem resistance plasmids in *K. pneumoniae* planktonic and biofilm populations.

4.7.1 Key findings

- The CPE isolates cluster with *K. pneumoniae sensu stricto* and with their respective STs
- Carbapenem resistance gene carriage in the STs evaluated here is internationally distributed
- All CPE isolates contain plasmid-borne carbapenem resistance genes; most of these plasmids contain F-type replicons
- Four of the five carbapenem resistance plasmids examined here appear to encode conjugation machinery; one of the five appears to encode mobilisation machinery

- Publicly-available tools facilitated prediction of all of the required features for informed conjugation model development
- CPE01, CPE16 and CPE25 may be suitable donors for development of clinically-relevant *K. pneumoniae* conjugation model(s).

Chapter 5

Conjugation of carbapenem resistance plasmids in planktonic and biofilm lifestyles

5.1 Background

Five carbapenemase-producing *K. pneumoniae* clinical isolates were sent for whole genome sequencing. This confirmed that the isolates were likely to contain carbapenem resistance genes. As shown in Chapter 4, several of these genes were predicted to be carried on plasmids. In 4/5 isolates (CPE01, CPE08, CPE16 and CPE25), conjugation modules were annotated on the carbapenem resistance plasmids. In 1/5 isolates (CPE24), the carbapenem resistance plasmid was predicted to be mobilisable. Annotation indicated that 1/5 of the carbapenem resistance plasmids (plasmid in CPE08) had a truncation in the conjugation module at *traE*, and would therefore be unlikely to transfer by conjugation as this gene is considered essential for the process (Fernandez-Lopez *et al.*, 2016).

As conjugation is a major route of AMR plasmid transfer (Alderliesten *et al.*, 2020), and gene presence does not guarantee gene expression (Zatyka and Thomas, 1998), it was of interest to determine the transfer rates of these plasmids *in vitro*. The rationale was to determine the transmissibility of the carbapenem resistance plasmids from the donor strains into a single recipient background in both planktonic and biofilm lifestyles, along with assessing whether genotypic data was able to predict conjugation phenotype. Compared to models using laboratory-adapted or environmental plasmids and strains, use of clinical isolate donors facilitates development of assays that are likely more reflective of AMR plasmid transfer in hospital settings (Buckner *et al.*, 2018). This is because the isolates were themselves recently isolated from hospital patients, they carry multiple AMR genes and have not been laboratory-adapted.

With increasing availability of genomic data, and acknowledgement that it is not always reliable as a predictive tool (Lees *et al.*, 2020), it is important to validate predictions with experimental data. There is currently no clear evidence that genomic data alone can predict frequency of plasmid transfer or likelihood for transconjugant production from a particular donor-recipient combination. These aspects are of direct relevance when considering the clinical implications of AMR plasmid transfer by conjugation, and increasing the body of knowledge in this area is important for understanding AMR plasmid spread, developing better predictive models and the use of genomics in clinical diagnostics.

To determine whether the annotated carbapenem resistance plasmids were able to transfer by conjugation, assays using culture plating on selective antibiotics and colony counting were used. Although there are limitations to this approach, as detailed in Chapter 3, the estimation of CFU/mL remains the 'gold-standard' method for quantification of viable bacterial cells (Hazan *et al.*, 2012) which permits determination of conjugation frequency (Suhartono and Savin, 2016). It is also possible to assess transfer in biofilms using plating and CFU/mL determination (Christensen

et al., 1998). Therefore, assessment of plasmid transfer in both planktonic and biofilm lifestyles is possible.

As mentioned previously, there remains a lack of consensus as to the interplay between the biofilm lifestyle and rates of HGT, with some reports that this lifestyle may promote the process and others indicating limited transfer (Stalder and Top, 2016). In addition, some data suggest that the presence of a conjugative plasmid may itself promote biofilm formation due to conjugative pili potentially aiding surface adhesion (Burmølle *et al.*, 2008). However, this effect on biofilm formation is not always observed (Gama *et al.*, 2020).

K. pneumoniae is an important carrier of conjugative AMR plasmids (Hendrickx *et al.*, 2020) and a contributor to the burden of nosocomial infections (Podschun and Ullmann, 1998) as well as to AMR gene/plasmid transfer within hospital environments (Wyres and Holt, 2018). There are limited data available measuring conjugation frequency using *K. pneumoniae* clinical isolates in biofilm models, e.g. Hennequin *et al.* (2012). As biofilms are thought to be the most common bacterial lifestyle (Penesyan *et al.*, 2019), and *K. pneumoniae* biofilms can be present in infection sites (Piperaki *et al.*, 2017) and in environments such as hospital surfaces (Hassan *et al.*, 2019), it is of direct relevance to understand how AMR plasmids may transfer horizontally in *K. pneumoniae* clinical isolate planktonic and biofilm populations. This knowledge could aid in reducing the burden of AMR *K. pneumoniae* infections.

To start addressing the lack of data, this study used *K. pneumoniae* clinical isolates from the QE Hospital Birmingham, and a hygromycin-resistant *K. pneumoniae* recipient strain to quantify transfer of carbapenem resistance plasmids in planktonic and biofilm lifestyles.

5.1.1 Aims and hypotheses

The aims of this work were to determine whether the carbapenem resistance plasmids in the *K. pneumoniae* CPE clinical isolates (annotated in Chapter 4) were able to transfer by conjugation, to quantify their transfer in planktonic and biofilm lifestyles, and to assess whether plasmid acquisition had an effect on the recipient biology. The hypotheses were:

1. *K. pneumoniae* CPE isolates will form biofilm.
2. CPE carbapenem resistance plasmids will conjugate into *K. pneumoniae*.
3. Plasmid acquisition will negatively affect recipient fitness versus the WT.
4. Plasmid acquisition will increase biofilm formation versus the WT.

5.2 Initial characterisation

To evaluate the carbapenem resistance phenotype of the *K. pneumoniae* CPE isolates, an agar MIC was carried out (Table 5.1). This confirmed that the isolates were resistant to meropenem based on the EUCAST breakpoint (>8 mg/L) (The European Committee on Antimicrobial Susceptibility Testing, 2017). However, CPE24 was within one doubling dilution of the breakpoint, which is considered to be within the error of the assay (Brennan-Krohn *et al.*, 2017). This indicates that CPE24 is likely to be less resistant to meropenem than the other CPE isolates.

Along with meropenem, the isolates were tested against several other agents to evaluate the overall resistance profile (where possible) versus the EUCAST breakpoint table (version 11.0) for Enterobacterales (The European Committee on Antimicrobial Susceptibility Testing, 2021). For all of the agents for which breakpoints were

available, the CPE isolates were defined as resistant (Table 5.1). Control strain results were within one doubling dilution of the expected values (Table S2).

Table 5.1: Agar MIC of *K. pneumoniae* CPE isolates against a selection of antibiotics and dyes. Meropenem data are in bold text. Control ATCC 25922 (*E. coli*) MIC was <1 mg/L. The British Society for Antimicrobial Chemotherapy MIC for this reference strain is listed as 0.008 mg/L for meropenem (Andrews, 2001). N/A: Data not available.

Agent	Isolate MIC (mg/L)					EUCAST breakpoint for resistant Enterobacterales (mg/L)
	CPE01	CPE08	CPE16	CPE24	CPE25	
Aztreonam	>32	>32	>32	>32	>32	>4
Benzalkonium Chloride	32	32	64	64	64	N/A
Carbenicillin	>1024	>1024	>1024	>1024	>1024	N/A
Cefotaxime	>256	64	>256	>256	>256	>2
Chloramphenicol	32	64	256	>512	32	>8
Ciprofloxacin	>128	128	128	>128	128	>0.5
Clindamycin hydrochloride	256	256	>256	>256	>256	N/A
Crystal violet	32	64	16	128	64	N/A
Erythromycin	256	128	512	256	1024	N/A
Ethidium bromide	>1024	>1024	>1024	>1024	>1024	N/A
Fusidic acid	1024	1024	512	>1024	1024	N/A
Gentamicin	1024	<1	1024	32	>1024	>2
Meropenem	**64**	**32**	**64**	**16**	**128**	**>8**
Methylene Blue	>1024	>1024	>1024	>1024	>1024	N/A
Moxifloxacin	>32	>32	>32	>32	>32	>0.25
Nalidixic Acid	>1024	>1024	>1024	>1024	>1024	N/A
Novobiocin	256	256	512	>512	512	N/A
Rhodamine 6G	1024	>1024	>1024	>1024	1024	N/A
Rifampicin	>32	32	32	32	>32	N/A
Tetracycline disodium salt	8	4	8	8	4	N/A
Ticarcillin	>1024	>1024	>1024	>1024	>1024	>16

Next, additional phenotypic assessment was carried out to evaluate isolate growth profiles in more detail. Planktonic growth kinetics, including growth curves and maximum growth rates, were evaluated (Figure 5.1). Maximum growth rate was used to compare the planktonic growth profiles of the CPE isolates. A one-way ANOVA indicated no statistically significant differences in the maximum growth rates between the isolates ($P = 0.59$).

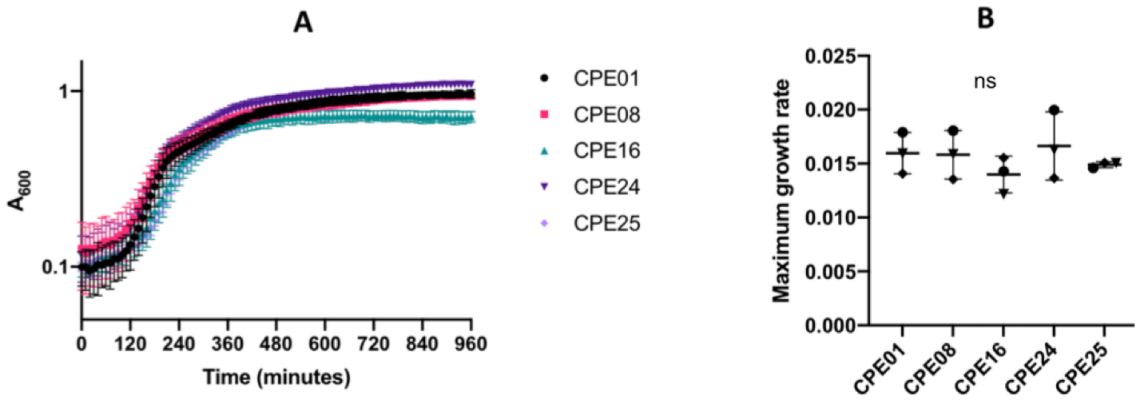

Figure 5.1: *K. pneumoniae* CPE isolate planktonic growth profiles. (A) Growth kinetics and (B) maximum growth rate in LB. 'ns' indicates 'not significant' (one-way ANOVA, $P = 0.59$). Error bars represent standard deviation from the mean. N = three experimental replicates (three biological replicates per experiment, each biological replicate is the mean of three technical replicates).

Next, crystal violet assays were used to determine *K. pneumoniae* CPE isolate biofilm formation (Figure 5.2). Biofilm formation was determined to be variable and isolate-dependent. Cusumano *et al.* (2019) reported that TSBs was optimal for biofilm formation in a set of *K. pneumoniae* clinical isolates (Cusumano *et al.*, 2019). Based on this research, this media was compared to LBB to evaluate whether it facilitated biofilm formation for the CPE isolates.

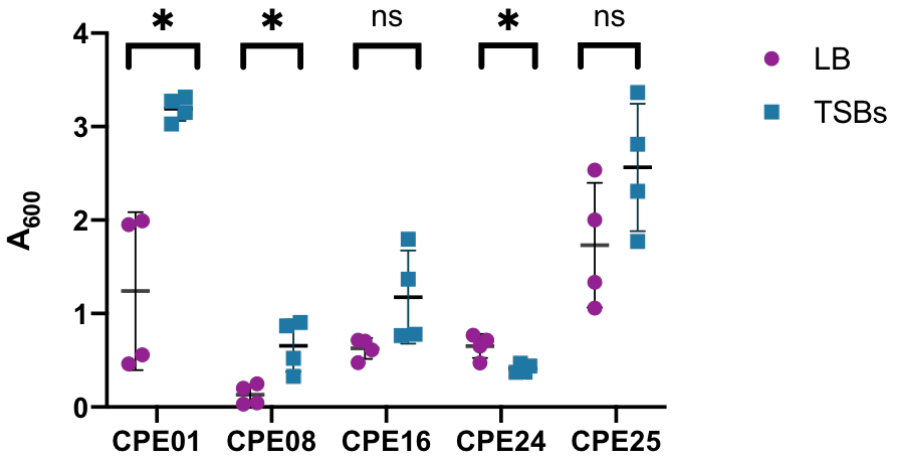

Figure 5.2: Mean biofilm formation (crystal violet staining) of the CPE isolates at 72 h in TSBs and LBB. N = four experimental replicates, each the mean of three biological replicates. Each biological replicate is the mean of three technical replicates. Media-only values have been subtracted. Error bars represent standard deviation from the mean. Asterisks indicate P <0.05 in an unpaired t-test. 'ns' indicates 'not significant'.

Broadly speaking, biofilm formation was greater in TSBs versus in LBB so this media was chosen for use in subsequent experiments to maximise biofilm formed by the CPE isolates. Unpaired t-tests highlighted the media effect between TSBs and LBB (for CPE01 $P = 0.0038$, for CPE08 $P = 0.013$, for CPE16 $P = 0.075$, for CPE24 $P = 0.013$, CPE25 $P = 0.13$). Interestingly, for CPE01 and CPE25, which sequencing data predicted to be closely-related, both isolates showed the highest levels of biofilm production in the conditions tested. CPE24 was the only isolate where biofilm formation was significantly higher in LBB than in TSBs.

Before carrying out conjugation assays, planktonic growth of the isolates was tested in TSBs to better understand growth dynamics in this media (Figure 5.3). Although there was a small but significant difference in the maximum growth rates between strains, the media was considered suitable for use in future experiments. CPE24 was excluded from these and future experiments because its borderline resistance profile (Table 5.1) and the putative mobilisation transfer mechanism of its carbapenem resistance plasmid (Chapter 4) made it unsuitable for the intended conjugation model.

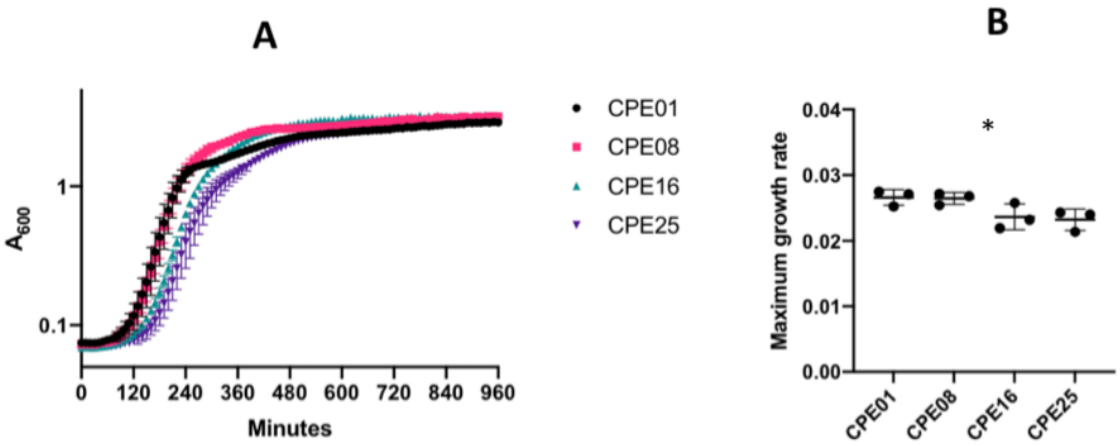

Figure 5.3: Planktonic growth profiles of the CPE isolates in TSBs. (A) Mean 16 h planktonic growth curves and (B) mean maximum growth rates. One-way ANOVA indicated a difference (*) between the maximum growth rates ($P = 0.041$). Error bars represent standard deviation from the mean. N = three experimental replicates (three biological replicates per experiment, each biological replicate is the mean of three technical replicates).

Overall, the CPE isolates were confirmed to be carbapenem-resistant. Their growth profiles were similar in LBB according to the maximum growth rates, but the level of biofilm formed was variable. For 4/5 isolates, TSBs media increased the level of biofilm formed at 72 h compared to LB. As low levels of biofilm were formed for some isolates, including in TSBs, this indicated that some isolates may be unsuitable for future use in biofilm conjugation assays. However, the planktonic growth kinetics data in TSBs showed that the selected isolates (CPE01, CPE08, CPE16 and CPE25) grew sufficiently for use in planktonic conjugation assays.

5.3 Strain construction and validation: KP20

To determine whether the conjugation machinery in the CPE isolates was functional, and to assess whether lifestyle has an impact on conjugation frequency, planktonic and biofilm conjugation experiments using the CPE isolates as donor strains were planned.

Due to the multidrug resistance profile of the isolates, and due to the requirement for a biofilm-forming strain, it was necessary to construct a recipient strain to enable conjugation experiments. For this, a derivative of the well-characterised ATCC 43816 (KP1) strain was selected (Cano *et al.*, 2015; Gomez-Simmonds and Uhlemann, 2017). This relatively antibiotic susceptible strain was originally isolated from a clinical pneumonia sample (Cano *et al.*, 2015; Gomez-Simmonds and Uhlemann, 2017) and is used in mouse models of infection (Fodah *et al.*, 2014; Lavender *et al.*, 2004). It is known to form biofilm (Langstraat *et al.*, 2001) and has been used successfully in the past as a recipient strain (Dorman *et al.*, 2018; Low *et al.*, 2020; Shankar-Sinha *et al.*, 2004)). It is also reported to be amenable to genetic manipulation (Dr Laura Hobley, personal communication). Therefore, to permit selection of this strain in conjugation assays using multidrug resistant donors, recombineering was used to insert a hygromycin resistance cassette from pSIM18 into bla_{SHV} on the

K. pneumoniae KP1 chromosome.

Initially, the PCR-amplified hygromycin cassette from pSIM18 was checked on an agarose gel to confirm it was of the expected size of approximately 1500 bp (Figure S9). The negative control (no DNA) gave no band as expected, and the candidate cassette DNA gave bands of the expected size. Therefore, the DNA fragment was taken forward for use in recombineering. A putative candidate colony (known as KP20) was initially validated by growth/lack of growth on hygromycin and ampicillin antibiotics respectively (Figure S10) and by PCR. The colony was checked using primers flanking the desired cassette insertion to assess whether the hygromycin resistance cassette from pSIM18 had inserted in the correct location (Figure 5.4). As expected, the negative controls, which included KP21 (known to have pACBSCE but no insertion), gave no bands. The KP20 candidate gave bands of the expected size and was taken forward for PCR to check for loss of the recombineering plasmid pACBSCE after non-selective growth. KP21 (known to have pACBSCE) was used as a positive control (Figure 5.5).

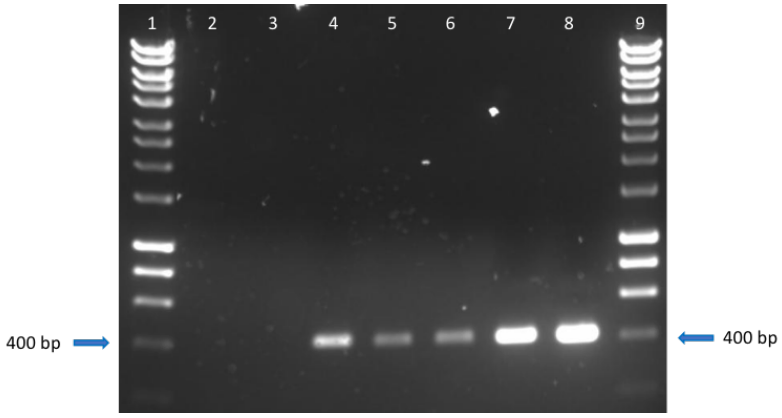

Figure 5.4: Validation of candidate KP20. Agarose gel electrophoresis from a PCR check for the hygromycin resistance cassette insertion in a KP21 colony (now a KP20 candidate) restreaked after recombineering. (1) Ladder (HyperLadder^{TM} 1 kb) (2) Negative control KP21 (no insertion, contains pACBSCE), (3) Negative control (no DNA), (4-8) KP20 candidate, (9) Ladder (Hyperladder^{TM} 1 kb). Expected size is 413 bp. Arrows indicate ladder reference band size.

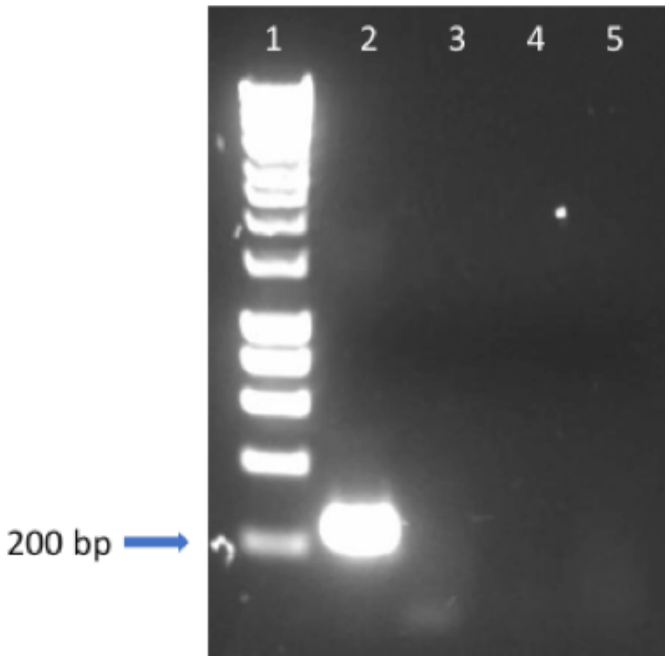

Figure 5.5: Agarose gel electrophoresis of colony PCR check for loss of the recombineering plasmid pACBSCE. Primers designed against *gam* from pACBSCE. (1) Ladder (Hyperladder^{TM} 1 kb). (2) Positive control KP21 (contains pACBSCE) (3) Negative control KP1 (no pACBSCE) (4) Negative control (no DNA) (5) KP20 candidate. Expected band size 222 bp. Arrows indicate ladder reference band size.

KP21 (known to have pACBSCE) gave a band of the expected size, indicating presence of the plasmid in this strain and successful PCR amplification of *gam*. For the KP20 candidate, no band was present. This suggested that the recombineering plasmid had been lost through non-selective growth.

Next, the KP20 candidate was sent for WGS to further validate the strain (Figure 5.6). This confirmed that the cassette was as expected and had inserted in the correct location. The sequence of the insertion matched that of the expected sequence, having the hygromycin cassette inserted into (and interrupting) the existing bla_{SHV} gene on the KP1 chromosome as intended. Apart from the cassette insertion, comparing KP20 to its parental strain there was a single SNP at position 268418 which leads to a non-synonymous change (from threonine to alanine) in the GstB protein. Further work would be required to validate this SNP and to evaluate any impact. WGS also confirmed loss of the recombineering plasmid pACBSCE.

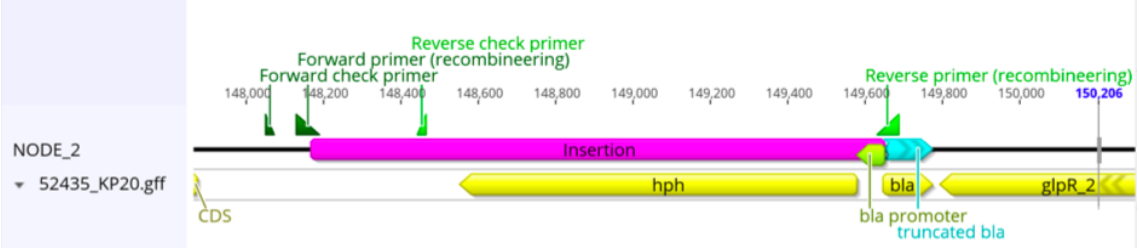

Figure 5.6: Annotated cassette sequence from KP20 whole genome sequence. Screenshot from Geneious Prime software. Purple bar: Full insertion from pSIM18. Dark and medium green arrows: Primer binding locations. Light green arrow: *bla* promoter. Light blue arrow: truncated sequence from chromosomal bla_{SHV} on KP1 chromosome. Yellow arrow '*hph*': hygromycin resistance gene.

5.4 KP20 characterisation

Following confirmation that the insertion in the newly constructed KP20 recipient was as expected, the biofilm and planktonic growth profiles of KP20 versus the ancestral KP1 strain were assessed. This was done to ensure the addition of the hygromycin resistance cassette, and the non-synonymous change in GstB, did not impact fitness and to evaluate KP20 suitability for use in future conjugation experiments. KP1 and KP20 behaved similarly in growth and biofilm assays (Figure 5.7). Their phenotypes were compared using unpaired t-tests. Although media type had an effect on biofilm, with more biofilm formed in LBB versus TSBs for both KP1 and KP20 ($P = 0.0047$ and $P = 0.0087$ respectively), there was no difference in the amount of biofilm formed when comparing the strains to each other ($P = 0.96$ comparing KP1 and KP20 in TSBs, $P = 0.37$ comparing KP1 and KP20 in LB). Equally, when evaluating planktonic growth, there was no difference in the maximum growth rate comparing KP1 to KP20 in TSBs or LBB ($P = 0.47$ in TSBs, $P = 0.39$ in LBB). However, maximum growth rate in TSBs was significantly higher versus LBB in KP20 but not for KP1 ($P = 0.063$ comparing KP1, $P = 0.013$ comparing KP20). Taken together, results from the biofilm and growth kinetics experiments indicated that the insertion had no effect on the measured KP20 phenotypes versus the ancestral KP1 strain.

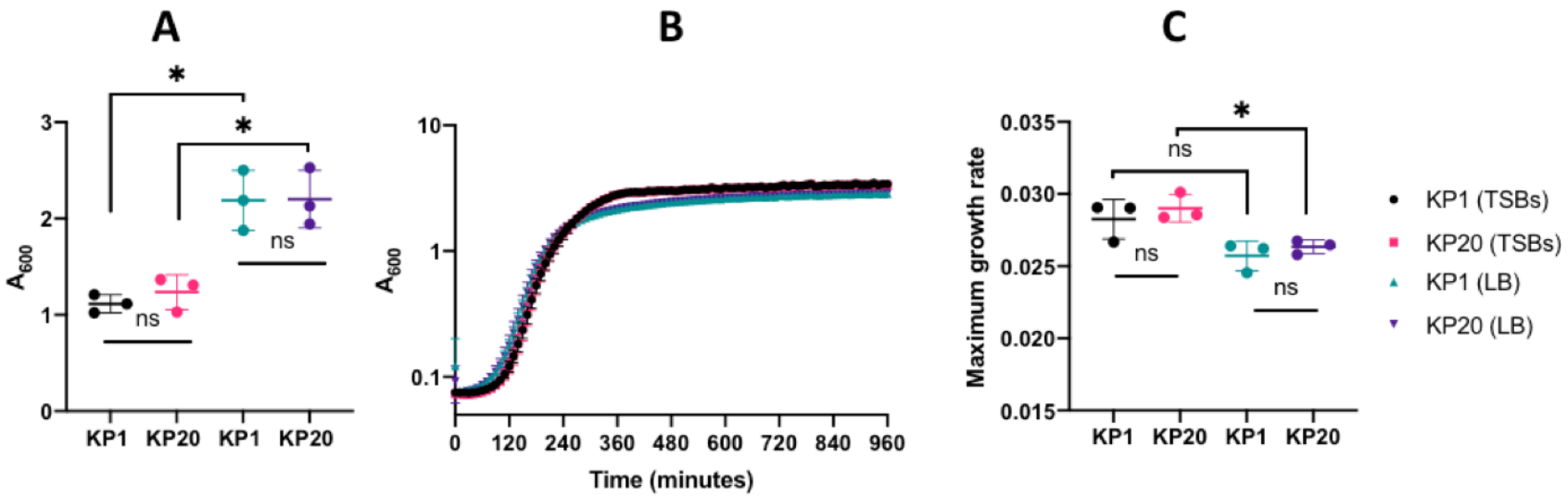

Figure 5.7: Biofilm formation and growth profiles of KP1 and KP20 in TSBs (black and pink points) and LBB (green and purple points). (A) Mean 72 h biofilm formation (crystal violet assay) (B) Mean 16 h planktonic growth curves (C) Mean maximum growth rate. Unpaired t-tests indicated not significant (ns, $P > 0.05$) except for comparisons between KP1 and KP20 biofilm in TSBs versus LBB ($P = 0.0047$ and $P = 0.0087$ respectively) and for KP20 maximum growth rate in TSBs versus LBB ($P = 0.013$). N = three experimental replicates each comprising three biological replicates. Per biological replicate, three technical replicates were included. Error bars indicate standard deviation from the mean.

5.5 Planktonic conjugation assays

As there was no indication of a difference between biofilm formation or planktonic growth of the ancestral strain KP1 compared to KP20, planktonic conjugation experiments using the new recipient strain and the CPE isolates as donors were carried out. As there was no evidence of poor planktonic growth in TSBs (Figure 5.3), and to provide consistency between experiments, this media was used in assays evaluating the conjugative ability of the donor carbapenem resistance plasmids in the planktonic lifestyle (Figure 5.8). As previously indicated, CPE24 was excluded from these experiments.

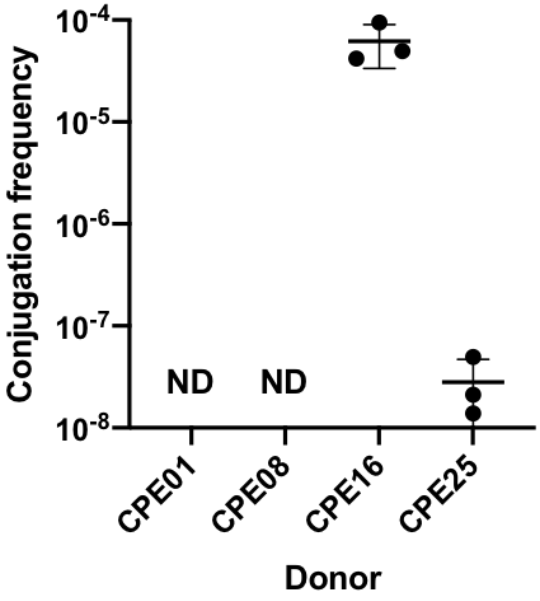

Figure 5.8: Mean conjugation frequencies of carbapenem resistance plasmids from CPE donors into the KP20 recipient in planktonic populations. ND (not detected): No transconjugants were detected in three independent experiments. Four biological replicates were included in each experiment. Error bars show standard deviation from the mean.

Conjugation frequencies (+/− standard deviation) could be calculated for two of the four donors. For CPE01 and CPE08, no transconjugants were detected under the assay conditions tested. For CPE25, the conjugation frequency was low (relative to CPE16) at 2.8 x 10^{-8} (+/−1.9 x 10^{-8}), and near the assay limit of detection. In

contrast, for CPE16 the conjugation frequency was high (relative to CPE25) at 6.2 x 10^{-5} (+/− 2.8 x 10^{-5}).

To evaluate the growth dynamics of the strains from experiments where transconjugants were isolated, the donor:recipient ratios were determined at 0 h and 20 h (Figure 5.9). Over the course of the experiments, the proportion of CPE16 to KP20 cells changed from a mean ratio of approximately 1:10 to a mean ratio of approximately 7:1. In contrast, the ratio remained consistent for experiments using CPE25.

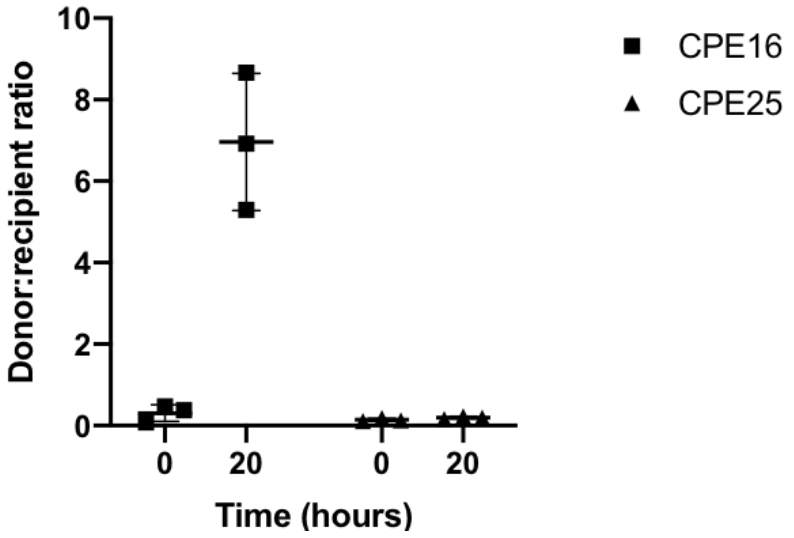

Figure 5.9: Mean donor:recipient ratios at the start (0 h) and end (20 h) of the planktonic conjugation experiments for the donor (plus KP20) strain combinations where transconjugants were produced. N = three experimental replicates, each the mean of four biological replicates. Error bars indicate standard deviation from the mean.

At 0 h, for both strains, the desired ratio was 0.1. Colony counts revealed the mean ratio to be approximately 0.3 for CPE16 and approximately 0.14 for CPE25. At 20 h the mean ratio for CPE16 was around 6.97, indicating a shift such that CPE16 became the dominant population. Conversely, the original ratio was maintained for CPE25, with a mean of 0.19 at 20 h and KP20 as the dominant population.

Next, ten candidate transconjugant colonies were selected for validation using a combination of re-streaking on selective agar, PCR and whole genome sequencing.

Colony PCR checks assessed strain background, the presence of a carbapenem resistance plasmid replicon and carbapenem resistance gene (Figure 5.10). Colonies were named to include the recipient background (KP20) followed by 'pCPE' to represent 'CPE plasmid' and a number to reflect the donor strain. For example, KP20/pCPE16 relates to a KP20 transconjugant containing a plasmid(s) from CPE16. Contig numbers were assigned to indicate individual plasmids. For example, KP20/pCPE25_3 would indicate a KP20 transconjugant containing 'plasmid 3' from CPE25.

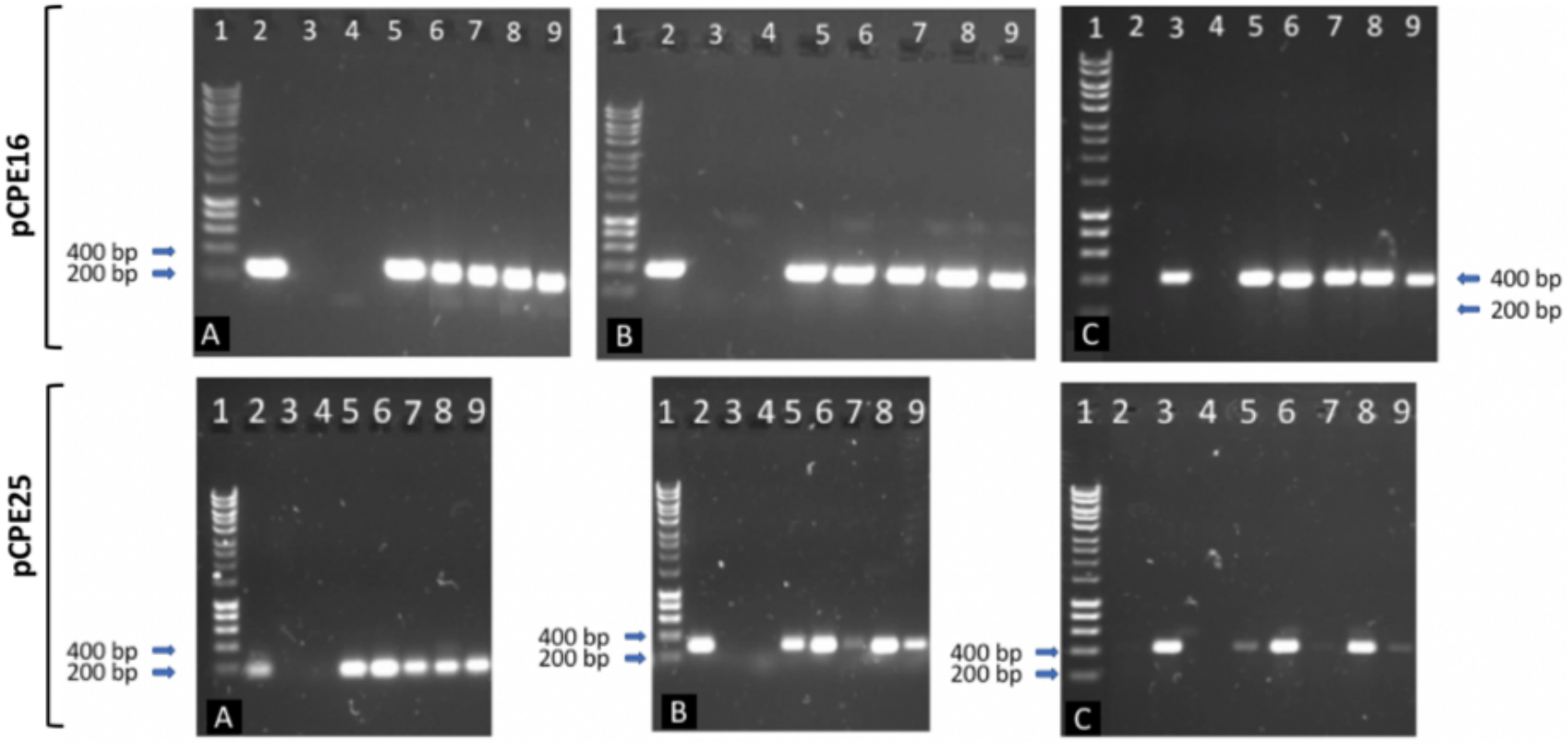

Figure 5.10: Transconjugant colony PCR products. Putative KP20/pCPE16 (top) KP20/pCPE25 (bottom) colonies and controls. (1) Ladder (HyperLadder$_{\text{TM}}$ 1 kb) (2) Donor control (3) Recipient control (4) No DNA control. (5-9) Candidate transconjugants. (A) Primer pair against carbapenem resistance plasmid *repA*. Expected sizes 231 bp and 161 bp for KP20/pCPE16 and KP20/pCPE25 respectively. (B) Primer pair against carbapenem resistance plasmid bla_{NDM}. Expected sizes 392 bp and 290 bp for KP20/pCPE16 and KP20/pCPE25 respectively. (C) Primer pair against KP20 chromosome. Expected size 413 bp. Arrows indicate ladder reference band sizes.

The donor control gave bands of the expected size for primers targeting the plasmid and there were no bands for the recipient control (Figure 5.10A and B). Conversely, the recipient control produced bands of the expected size for primers targeting the recipient chromosome and no bands were present for the donor control (Figure 5.10C). Bands of the expected size were present for each putative transconjugant colony for each primer set. This confirmed that the carbapenem resistance gene and plasmid backbone were present, within the recipient host. Taken together, the data indicate that all tested colonies were transconjugants.

Five PCR-confirmed transconjugants from each set of experiments were sent for whole genome sequencing using short-read Illumina technology. Reads were aligned to donor reference genomes (hybrid assemblies) to validate the PCR data and identify any additional replicons present in the transconjugants (Table 5.2).

Read alignments confirmed that the carbapenem resistance plasmids were present in both KP20/pCPE16 and KP20/pCPE25 transconjugants (pCPE16_3 and pCPE25_3 respectively), thereby supporting the PCR data. For the KP20/pCPE16 transconjugant colonies selected for characterisation, 3 of 5 contained the additional plasmid pCPE16_4 (4173 bp).

Table 5.2: Plasmid contigs present in transconjugants based on read alignment to the donor reference genome*. Number '3' refers to the carbapenem resistance contig. NB: CPE25 donor reference genome was assembled using long-read data and subsequently polished using short-read data. The original Unicycler assembly was used for CPE16 as it was complete.

KP20/**pCPE16** transconjugant colony no.	Plasmid(s) present	KP20/**pCPE25** transconjugant colony no.	Plasmids(s) present
1	pCPE16_3,4	1	pCPE25_3
2	pCPE16_3,4	2	pCPE25_3
3	pCPE16_3,4	3	pCPE25_3
4	pCPE16_3	4	pCPE25_3
5	pCPE16_3	5	pCPE25_3

As many transconjugants were produced in the CPE16 KP20 conjugation experi-

ments, thirteen more KP20/pCPE16 transconjugants were sent for whole genome sequencing in addition to those detailed above to get a better idea of the proportion of colonies containing only the carbapenem resistance plasmid (pCPE16_3) versus those containing multiple replicons. Of 18 transconjugants sequenced in total from the planktonic conjugation experiments, 18/18 (100%) contained the carbapenem resistance plasmid pCPE16_3, 1/18 (5.6%) contained pCPE16_2 and 12/18 (67%) contained pCPE16_4. One colony (1/18, 5.6%) contained all three plasmids (pCPE16_2,3,4).

5.6 Transconjugant characterisation

Next, to determine whether there was any effect on growth as a result of plasmid acquisition, the ten sequenced transconjugants (five generated from each donor) were taken forward for phenotypic characterisation in growth kinetics and biofilm assays (Figure 5.11). Strain designations correspond to those in Table 5.2.

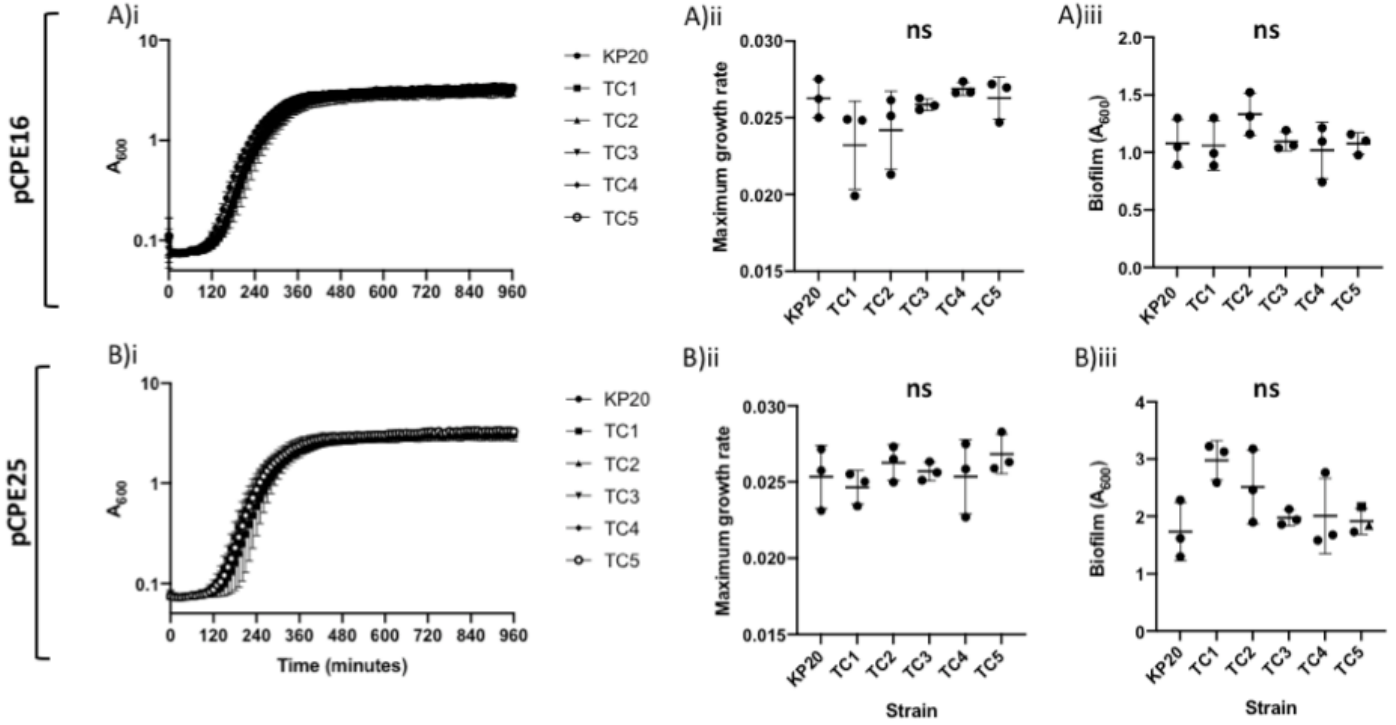

Figure 5.11: Transconjugant growth profiles. (i) Planktonic growth curves, (ii) maximum growth rates and (iii) 72 h crystal violet biofilm assays in TSBs. (A) KP20 and KP20/pCPE16 transconjugants (TC) and (B) KP20 and KP20/pCPE25 transconjugants (TC). One-way ANOVA indicated no difference (not significant, ns) when comparing maximum growth rates of KP20 to any of the transconjugants (P = 0.15 for pCPE16, P = 0.62 for pCPE25) or when evaluating biofilm formation between KP20 and the transconjugants (P = 0.32 for pCPE16, P = 0.052 for pCPE25). Numbers after 'TC' e.g. 'TC1' refer to individual colonies. N = three experimental replicates, each comprising three biological replicates. Each biological replicate is the mean of three technical replicates. Error bars represent standard deviation from the mean.

Considering planktonic growth, there was no clear difference in either the growth curves (i) or the maximum growth rate (ii) when comparing KP20 to any of the transconjugants ($P = 0.15$ for pCPE16, $P = 0.62$ for pCPE25 using a one-way ANOVA). Likewise, for biofilm formation (iii) no clear difference was observed between KP20 and the transconjugants in their ability to form biofilm *(*$P = 0.32$ for pCPE16, $P = 0.05$ for pCPE25 using a one-way ANOVA).

5.7 Biofilm conjugation assays

As most bacteria are thought to exist in biofilms (Ghigo, 2001), and as there are conflicting reports in the literature about the role of this lifestyle in the potential promotion of conjugation (Stalder and Top, 2016), it was of interest to assess conjugation in biofilms. The donor which produced the most transconjugants in the planktonic experiments (CPE16) was selected for these assays. This was done to increase the likelihood of transconjugant detection to give the greatest chance of a measurable conjugation frequency in the new biofilm setup. As biofilms have a lifecycle which broadly comprises attachment, maturation and dispersal (Guilhen *et al.*, 2016), conjugation frequency was assessed over time to see if the biofilm growth stage would affect when conjugation was occurring.

To determine whether 24 h was an appropriate starting point for evaluating conjugation in a biofilm (i.e. whether detectable biofilm was formed by this time point), crystal violet assays in TSBs were carried out for CPE16 and KP20 (Figure 5.12). The 24 h biofilm assays confirmed that biofilm was formed by 24 h and that similar amounts of biofilm were formed by CPE16 and KP20 ($P = 0.056$, unpaired t-test). As a result, biofilm conjugation assays were carried out over a 72 h time period, with plating for transconjugants at 24, 48 and 72 h to capture a maturing biofilm (Singh *et al.*, 2019).

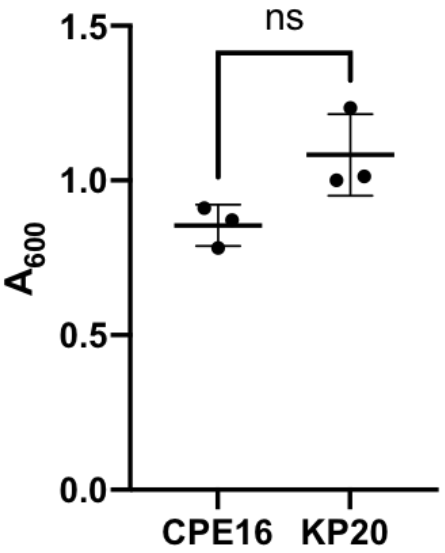

Figure 5.12: Mean biofilm formation of CPE16 and KP20 at 24 h in TSBs. Crystal violet staining was used as a proxy for biofilm formation. Similar amounts of biofilm were formed by CPE16 and KP20 ($P = 0.056$, unpaired t-test). 'ns' indicates 'not significant'. N = three experimental replicates, each the mean of three biological replicates. Three technical replicates were carried out per biological replicate. Media-only values were subtracted to remove background. Error bars show standard deviation from the mean.

A 6-well conjugation assay was developed to facilitate assessment of plasmid transfer in CPE16/KP20 biofilms. The setup made use of the same media and counting procedures used for the planktonic assays. However, cells were incubated in tissue culture plates over longer time-frames and cell scrapers were used to remove adhered cells for plating. As a result, there were necessarily some differences in how the biofilm and planktonic assays were carried out. Conjugation frequencies were determined across three time points (Figure 5.13).

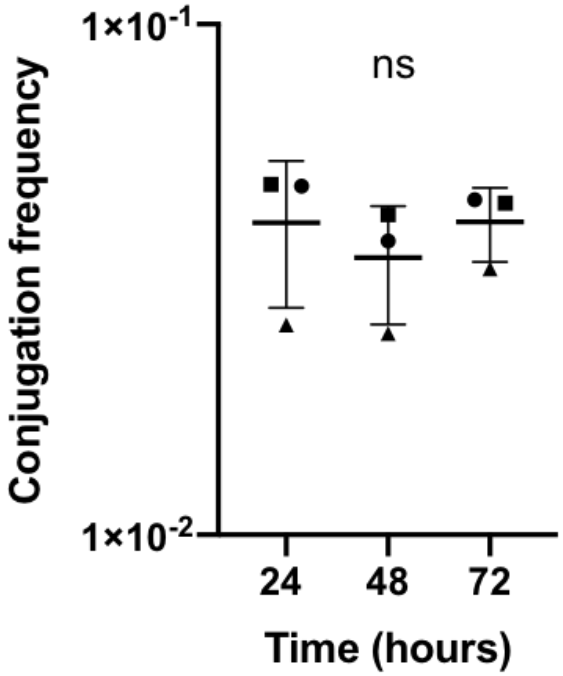

Figure 5.13: Mean conjugation frequencies of pCPE16_3 from the CPE16 donor into the KP20 recipient in a biofilm over time. Different shaped points relate to the experimental replicate. One-way ANOVA indicated no difference ('not significant', 'ns') in the conjugation frequencies across the time-points ($P = 0.71$). N = three experimental replicates, each the mean of four biological replicates. Error bars indicate standard deviation from the mean.

Across the three tested timepoints, mean conjugation frequency of the CPE16 carbapenem resistance plasmid pCPE16_3 was high and consistent (± standard deviation): 4.1 x 10^{-2} (± 1.3 x 10^{-2}) at 24 h, 3.5 x 10^{-2} (± 9.1 x 10^{-3}) at 48 h and 4.1 x 10^{-2} (± 6.8 x 10^{-3}) at 72 h. A one-way ANOVA confirmed no difference between these values ($P = 0.71$).

The frequency of transfer of any plasmids other than pCPE16_3 from this donor strain was not systematically monitored. However, two putative transconjugant colonies from biofilm conjugation experiments were taken forward for validation by colony PCR (Figure S11) and sequencing to determine transferred plasmid(s) as was carried out for the planktonic transconjugants. These assessments revealed that the two colonies were indeed transconjugants, both containing pCPE16_3. In addition, one contained pCPE16_2 and the other contained pCPE16_4.

To further dissect the dynamics in the biofilm setup, and in light of the pattern in the planktonic experiments where CPE16 outcompeted KP20, the donor:recipient ratio over the course of the biofilm conjugation experiments was considered (Figure S12). The initial desired ratio of CPE16:KP20 into these experiments was 0.1. The mean donor:recipient ratio was determined to be approximately 0.18 via colony counts at 0 h. Donor:recipient ratios at 24, 48 and 72 h indicated that CPE16 was outcompeting KP20 across the course of the experiment. By 72 h, the mean donor:recipient ratio had reached approximately 4.3. The growth of CPE16 and KP20 individually over the 72 h corroborated these dynamics, as CPE16 alone produced more CFU/mL than KP20 after the 0 h time point where input cell quantity was determined by OD_{600} correction (Figure S13). At 0 h, after OD correction, CPE16 and KP20 gave similar CFU/mL ($P = 0.13$, unpaired t-test). However, by 24 h, CFU/mL for CPE16 was higher than for KP20 ($P = 0.0009$, unpaired t-test). KP20 reached maximum CFU/mL at 48 h whereas CPE16 reached maximum CFU/mL earlier at 24 h.

Further support for CPE16 outcompeting KP20 was provided by distinct phenotypes. It was possible to distinguish between donors (small, translucent colonies) and colonies with a recipient background (larger, opaque colonies) based on the colony morphologies of the two strains (Figure S14). Observation of phenotypes during the conjugation assays indicated a large proportion of translucent colonies on the mixed population plates containing doripenem (to select for the donor), and a smaller proportion of opaque colonies on the mixed population plates containing hygromycin (to select for the recipient). This highlighted that the majority of colonies plated after the conjugation experiments were likely to be donors, and that the opaque colonies on the hygromycin agar plates represented a mixture of phenotypically indistinguishable KP20 recipients and transconjugants. Based on the large number of transconjugant colonies produced in these experiments, it is likely that few recipients were present on the mixed population hygromycin plates at the experiment endpoint. Another potential explanation for this observation may be ac-

tive killing of the recipient by the donor strain, for example via a Type 6 Secretion System where a toxic product may be delivered by the donor into the recipient cell (Storey *et al.*, 2020).

5.8 Discussion

This work aimed to ascertain whether the putative conjugative carbapenem resistance plasmids in the CPE isolates transfer to a *K. pneumoniae* recipient, and the frequency of this transfer in the planktonic lifestyle. Building on the work from Chapter 3, plasmid transmission was also assessed in biofilms to evaluate the potential for any lifestyle impact on the conjugation frequency. This question was based on the conflicting evidence in the literature where there is no clear consensus on 1) to what extent the biofilm lifestyle impacts conjugation frequency (Stalder and Top, 2016) and 2) whether (conjugative) plasmid carriage indeed promotes biofilm formation, as per the frequently-cited work by Ghigo (Ghigo, 2001). These experiments were also designed to facilitate testing of the sequencing data predictions regarding the likelihood of CPE plasmid conjugative ability from Chapter 4, and evaluate how well genotype was able to predict phenotype.

Phenotypic assays including MIC, growth kinetics and biofilm formation experiments were carried out to characterise the CPE isolates and determine their suitability for the planned planktonic and biofilm conjugation experiments. Although all the isolates were carbapenem resistant on the basis of EUCAST breakpoints, CPE24 resistance to meropenem was within one doubling dilution of the breakpoint, excluding it from future plasmid transfer experiments. All isolates were confirmed to form biofilm, a prerequisite for use in biofilm conjugation experiments, and, in agreement with the evidence presented by Cusumano *et al.* (2019), biofilm formation by CPE isolates was generally promoted in TSBs versus LB.

To facilitate selection in conjugation experiments, a *K. pneumoniae* recipient strain

was constructed by insertion of a hygromycin resistance cassette from pSIM18 into the KP1 chromosome. This was assessed both genotypically and phenotypically and determined to be suitable for use in conjugation experiments. To investigate plasmid transfer from the CPE isolates into the KP20 recipient, planktonic conjugation experiments were designed based on the conjugation protocol from Hardiman *et al.* (2016). This method was selected as it was previously used successfully to quantify transconjugants in the planktonic lifestyle, including for circulating clinically-relevant plasmids into *K. pneumoniae* (Hardiman *et al.*, 2016). Transconjugants were produced in some of the experiments, demonstrating that this method was useful for this application. The conjugation experiments revealed that the carbapenem resistance plasmids were able to transfer to the newly constructed KP20 recipient from two of the four tested donors, CPE16 and CPE25. These assays confirmed that some but not all of the carbapenem resistance plasmids transfer from the CPE isolate donors into *K. pneumoniae*. In the experiments where no transconjugants were detected, it is possible that transconjugants were present below the detection limit. Due to the nucleotide sequence similarity (100% overall across 98% coverage when inputting CPE01 as the subject and across 97% coverage when CPE25 was the subject) between CPE01 and CPE25, and given that transconjugant production using CPE25 was near the limit of detection of the assay, it is conceivable that the conjugation frequency from CPE01 into KP20 is just below the limit of detection. Nonetheless, the results generally correspond to the predictions from the sequencing data but highlight the importance of phenotypic assessment.

For KP20/pCPE25 transconjugant colonies, it was determined that only the carbapenem resistance plasmids selected for in the conjugation experiments had transferred to the recipient. Conversely, for KP20/pCPE16, the majority (61%) of all the sequenced transconjugants contained a plasmid in addition to the carbapenem resistance one that was selected for. This highlights the importance of mobilisable plasmids, especially as these plasmids can be carriers of AMR genes including carbapenem resistance genes (Li *et al.*, 2019). An example of such a plasmid

carrying $bla_{\text{OXA-232}}$ was found in CPE24 in this study. These plasmids may have an under-explored impact on the spread of AMR (Barry *et al.*, 2019).

The conjugation frequency for CPE16 was substantially higher than for CPE25. As both the plasmid(s) and the background differ for these two donors, and both of these elements can have an impact on the conjugation frequency (Dimitriu *et al.*, 2019), it is not straightforward to unpick the factors responsible for the observed conjugation frequencies. However, it is possible to hypothesise as to some of the aspects that may contribute:

- It may be that the eventual donor:recipient ratios had an effect on the frequency, as the 1:10 ratio into the conjugation experiments was maintained over time for CPE25, but for CPE16, many more donors were present versus recipients by the end of the assay on the basis of the observed colony morphologies. The donor:recipient ratio can affect the conjugation frequency, which may explain the outcome (Buckner *et al.*, 2020). Donor background has been shown to affect conjugation frequency when strains carry different plasmids but are otherwise isogenic (Hardiman *et al.*, 2016). On this basis, although the two donors are different in both background and plasmid content, it is conceivable that the donor background alone may be sufficient to account for the observed differences in conjugation frequency.

- Considering the donor plasmids, it may also be relevant that a large proportion of KP20/pCPE16 transconjugants contained plasmids in addition to the carbapenem resistance one that was selected for. It cannot be excluded that co-transfer may have impacted conjugation frequencies. As evidence suggests that plasmid content of the recipient may impact conjugation (Alderliesten *et al.*, 2020), it is conceivable that plasmid content of the donor might also do so.

- The presence of restriction modification systems which act to degrade non-

native DNA may also impact the process, especially if donor and recipient restriction modification systems are of different types such that incoming plasmid DNA has a 'non-self' methylation pattern and is targeted by the host restriction endonuclease (Johnston *et al.*, 2019). A negative impact on conjugation frequency through restriction modification has been previously reported (Roer *et al.*, 2015).

- Capsule production may provide a physical barrier to plasmid transfer (Haudiquet *et al.*, 2021). It may be that CPE16 produces less capsule than CPE25 and therefore has a reduced barrier. However, there is some ambiguity between the effect of the presence and absence of capsule genes and their potential relationship with HGT which is also a consideration (Haudiquet *et al.*, 2021; Rendueles *et al.*, 2018).

To assess whether plasmid carriage had an impact on the recipient, planktonic and biofilm growth profiles of a selection of transconjugants from the planktonic conjugation experiments were evaluated. Plasmid acquisition is often reported to impose a fitness cost on the host, although this is not universally the case (Buckner *et al.*, 2018; Carroll and Wong, 2018). For the KP20 transconjugants, no substantial difference was observed in the planktonic or biofilm growth profiles compared to the recipient alone. Although growth assessment is a relatively crude method of fitness measurement, competition assays alongside calculation of relative fitness, which is considered a more robust approach (Wiser and Lenski, 2015), was not an option in this case due to the transconjugants being able to transfer their plasmid(s) to the recipient when competed directly. The lack of obvious negative growth effect from plasmid acquisition highlights that each strain-plasmid combination merits study, and that it is challenging to generalise across different strains and plasmids. Taken together, the transconjugant planktonic growth and biofilm experiments confirm that plasmid acquisition variably impacts the recipient.

The donor strain that produced the most transconjugants in the planktonic con-

jugation assays (CPE16) was selected for use in biofilm conjugation experiments. This decision was made to increase the chance of transconjugant production in the biofilm setup, given that no alternative positive control was available for the assay. It was of interest to assess conjugation over time as this would allow its monitoring over the biofilm maturation period (Singh *et al.*, 2019). Biofilm of CPE16 and KP20 was quantified at 24 h and at 72 h. The assays confirmed that biofilm was formed at these time points. Therefore, the decision was made to quantify transconjugants at 24, 48 and 72 h to encompass early and late biofilm (Singh *et al.*, 2019). To minimise the presence of any planktonic cells, and to therefore increase confidence that the lifestyle being assessed was a biofilm, only cells that adhered to the plate after washing were considered to be from a biofilm. Methodology that had been used previously for flow cytometry sample preparation formed the basis of the experimental design, as a cell scraper had been previously used successfully to disrupt biofilm to single cells which are also desirable when calculating CFU/mL (Figure 3.7C).

Biofilm conjugation experiments revealed that conjugation frequency (± standard deviation) was consistent from 24-72 h where it was in the range of 3.5×10^{-2} ($\pm 9.1 \times 10^{-3}$) to 4.1×10^{-2} ($\pm 6.8 \times 10^{-3}$). This indicates that most conjugation happened at or before 24 h, which may reflect population saturation by transconjugants by this time point and a low number of remaining recipients, insufficient recipient cells per donor, or conceivably a lack of mixing of donors and recipients by 24 h. This raises the question as to whether most conjugation may be happening before the cells attach to the plate and form biofilm. However, although a direct comparison of conjugation frequency in the planktonic versus biofilm lifestyle cannot be performed (as the assays used are different from each other), it is of relevance that the conjugation frequency in the 6-well biofilm setup at 24 h was 1000-fold higher than in the 20 h planktonic assays. It is unlikely, but cannot be excluded, that the assay setup would be responsible for such a degree of difference. Therefore, this finding provides support that the biofilm lifestyle itself may potentially promote conjugation between

CPE16 and KP20, perhaps due to close cell proximity as proposed in some other studies, e.g. Król *et al.* (2011). Further work would be required to confirm this, using an assay which facilitates direct comparison between planktonic and biofilm lifestyles, and ideally allows precise investigation as to the location of transfer within the biofilm, and the state of the biofilm when transfer is highest. This would permit a more detailed understanding of potential mechanisms.

To further investigate the conjugative ability of the carbapenem resistance plasmids from the CPE isolate donors, additional planktonic conjugation experiments could be conducted. These could include assays making use of a variety of recipient strains, including those from related species to better represent the organisms that may interact in nature (Hibbing *et al.*, 2010). Transfer of conjugative plasmids from *K. pneumoniae* to *E. coli* has been documented for example (Dunn *et al.*, 2021; Goren *et al.*, 2010). It would also be of interest to modify the detection limit to facilitate measurement of rarer conjugation events as CPE01 and CPE08 may conjugate at a very low frequency. To do this it may be feasible to plate more cells (a larger culture volume) on transconjugant selection plates to increase the chance of detection.

For conjugation in biofilms, use of CPE25 as a donor strain in the 6-well setup would allow an indirect comparison of the effect of lifestyle on transfer of its carbapenem resistance plasmid. Based on the effect observed using CPE16 and KP20 (where this suggested a potential facilitation of conjugation in the biofilm lifestyle), it may then be of interest to use the remaining CPE isolates in this setup as this assay may permit detection of conjugation from these donors where the planktonic setup did not. It may also be relevant to use the transconjugants as donor strains to eliminate any difference in donor strain background.

Use of microscopy and staining for biofilm components may reveal more detail as to the biofilm structure formed by both the CPE isolates and the transconjugants. Although crystal violet assays were employed for quick assessment of biofilm formation, these assays have their limitations. For example, they are only able to provide

crude estimates of biofilm formation, especially as the crystal violet stain itself may stain extracellular matrix components as well as cells to give an inflated estimate of biofilm (Merritt *et al.*, 2005). This may be amplified if strains produce different amounts of matrix. Confocal microscopy using stained samples would provide information on biofilm depth, structure and component composition which may reveal as yet undetectable differences in biofilm formed by the different strains. Access to such additional information provided some of the rationale for use of fluorescent strains in Chapter 3, which, as mentioned previously, would facilitate similar investigations without the need for staining. In addition, it would be interesting to see whether there are differences in biofilm formed by transconjugants containing the carbapenem resistance plasmid versus the carbapenem resistance plasmid and others. A comparison of biofilm across transconjugants containing different plasmids may reveal as yet undetected differences in biofilm formed by these strains.

As the CPE16 donor produced many KP20 transconjugants, it may be of benefit to apply this strain combination as a highly conjugative model system. For example, one limitation of the strain setup used in the flow cytometry work in Chapter 3 was the low conjugation frequency reported for the donor plasmid (pKpQIL) (Low *et al.*, 2020). Although it would be best to measure conjugation across the true range of observed frequencies, a model system (which has not been altered to artificially increase conjugation frequency, for example through de-repression of *finO* which may produce a fitness cost (Low *et al.*, 2020)) that is known to produce many transconjugants can serve as a valuable positive control, or allow (differences in) conjugation frequency to be more easily observed and quantified. It may be possible to use fluorescent tagging on such a system, in combination with plating assays for validation, to quantify conjugation using a more suitable flow cytometer, or to use microscopy techniques.

Alternatively, the KP20 recipient alone may be of use in combination with donors of interest, including those carrying multiple AMR genes. Several features of this

strain may make it generally convenient:

- As hygromycin-resistance has rarely been reported in *Enterobacteriaceae* in nature (Rao *et al.*, 1983), it is unlikely that any donor strain belonging to this group will be resistant to this antibiotic.
- *hph* conferring hygromycin resistance (Gritz and Davies, 1983) is KP20's only known functional antimicrobial resistance gene as the chromosomal bla_{SHV} has been inactivated.
- It is a derivative of a widely-used American Type Culture Collection (ATCC) reference strain which has been used in mouse infection models (Broberg *et al.*, 2014; Gomez-Simmonds and Uhlemann, 2017). It therefore retains some activity to approximate an infectious clinical isolate and is therefore useful for studies requiring 'clinical relevance'.
- The whole genome sequence of KP20 is available and has been compared to the WT.
- It has been shown to form biofilm similarly to the WT and has been used in biofilm experiments.
- It has been used successfully as a recipient in conjugation experiments using multiple donors.

5.9 Conclusion

Overall, conjugative transfer of carbapenem resistance plasmids from some of the CPE clinical isolates was observed. The phenotypic data relating to transfer of these plasmids from the CPE isolate donors into KP20 broadly agrees with predictions from the sequencing data. A notable exception to this is CPE01 where no transconjugants were detected in the planktonic conjugation assays where the

sequencing data predicted transfer. Due to the similarity of this isolate to CPE25, and as CPE25 produced only a few transconjugants, it is likely that the carbapenem resistance plasmid from this donor may transfer at a frequency below the assay limit of detection.

Concerning biofilms, evidence from the CPE16 KP20 assays indicates that this lifestyle may promote conjugation when compared to the planktonic setup. The conjugation frequency observed in the biofilm lifestyle was 1000-fold greater than that seen in the planktonic setup, and it is likely that not all of this difference is down to the assay setup alone.

Transconjugant growth profiles were compared to the recipient strain and it was determined that plasmid acquisition did not change how the strains grew planktonically or in a biofilm. Interestingly, when assessing transconjugant plasmid content, for CPE16 KP20 experiments co-transfer of plasmids was observed in the majority of tested cases.

5.9.1 Key findings

- A hygromycin-resistant, biofilm-forming recipient strain was constructed
- The transfer of carbapenem resistance plasmids from CPE isolate donors in planktonic conjugation experiments broadly agreed with predictions from the sequencing data. However, no transconjugants were produced from CPE01 in this assay setup despite an apparent full conjugation module on its carbapenem resistance plasmid.
- The carbapenem resistance plasmid from CPE16 transferred well in both planktonic and biofilm conjugation assays. Indirect comparisons suggest biofilm may facilitate transfer of this plasmid.
- Frequent co-transfer of plasmids was observed from CPE16 to KP20.

- Recipient growth (planktonic and biofilm) phenotypes were not affected by plasmid acquisition. Transconjugants performed no differently to the recipient.

Chapter 6

Investigating the impact of plasmid acquisition and lifestyle on gene expression

6.1 Background

Plasmid carriage may be metabolically costly for a host cell. This may translate to a negative fitness effect when plasmid products provide no benefit in a given environment (San Millan and MacLean, 2017). There is also some evidence that plasmid carriage may promote biofilm formation, due to facilitated adhesion via conjugative pili or through other mechanisms (Gama *et al.*, 2020). However, growth kinetics (as a proxy for fitness) and biofilm assays did not indicate significant differences in planktonic growth or biofilm comparing a set of transconjugants to the plasmid-free KP20 recipient (Chapter 5). To further evaluate any impact of plasmid acquisition on the recipient host, considering that gene expression changes can be sufficient to compensate for any cost of plasmid carriage (Buckner *et al.*, 2018), a transconju-

gant that had recently received the pCPE16_3 carbapenem resistance plasmid was selected alongside the KP20 recipient for an RNA-Sequencing experiment. Three growth conditions across planktonic and biofilm lifestyles were included: planktonic exponential phase, planktonic growth at 24 h and biofilm growth at 24 h. The planktonic exponential phase was selected as a nutrient-rich environment, versus the 24 h conditions as nutrient-poor environments. Three biologically independent cultures grown in TSBs were included for each strain across each condition.

The aims of this work were to determine:

1. The effect of lifestyle on chromosomal gene expression in the recipient and transconjugant
2. The effect of plasmid carriage on chromosomal gene expression in the transconjugant
3. The effect of lifestyle on plasmid gene expression in the transconjugant

The hypotheses were:

1. Lifestyle will have a larger impact than plasmid acquisition on transcriptional profiles.
2. Each lifestyle will produce a distinct transcriptional signature.
3. Conjugation module gene expression will be upregulated in the biofilm lifestyle.

6.2 Selection of a suitable transconjugant

Colony PCR (Figure 6.1) was carried out and combined with the existing whole genome sequencing data (Table 5.2) to confirm plasmid carriage and select a colony

containing only the complete (full-length) carbapenem resistance plasmid of interest. As expected, the donor control gave bands for each tested replicon. No bands were present for the two negative controls (the recipient and the no DNA controls). Colony PCR indicated that in three of the five transconjugants (colonies 1-3), the pCPE16_4 replicon was present. For two of the five transconjugants (colonies 4-5) only the carbapenem resistance plasmid replicon (pCPE16_3) was present. Taken together, these data provide evidence that only pCPE16_3 is present in KP20/pCPE16 colonies 4 and 5, and colony 5 was chosen for use in the RNA-sequencing experiment.

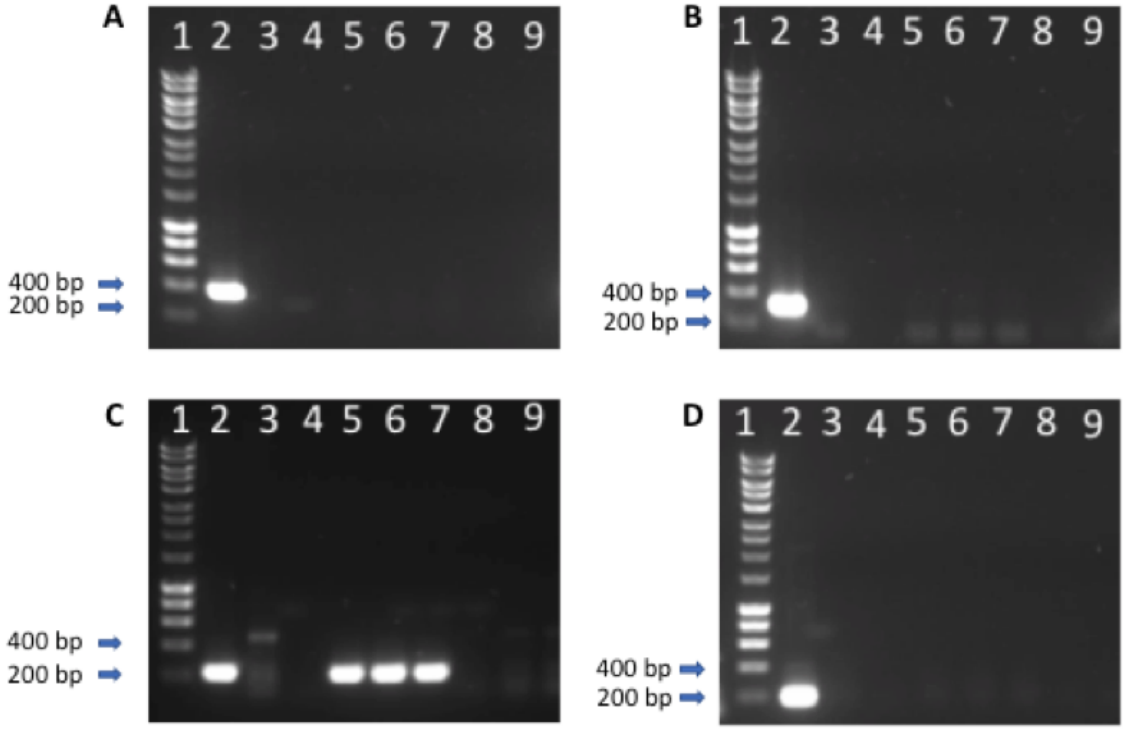

Figure 6.1: KP20/pCPE16 transconjugants replicon check. (1) Ladder (2) Donor control (3) Recipient control (4) Negative control (no DNA) (5-9) KP20/pCPE16 colonies. (A) Primer pair against pCPE16_2 FIB replicon. Expected size 346 bp (B) Primer pair against pCPE16_2 HIB replicon. Expected size 299 bp. (C) Primer pair against pCPE16_4. Expected size 220 bp. (D) Primer pair against pCPE16_5. Expected size 188 bp. Arrows indicate ladder reference band sizes.

To exclude any effect of antibiotic on gene expression, no antibiotic selection was included in the cultures used for RNA isolation. Given the absence of antibiotic, plasmid persistence was measured during the experiment to monitor the proportion

of cells carrying the plasmid at each stage (Table 6.1). This showed that the majority of cells retained the plasmid over the course of the experiment. Therefore, the experiment should be able to test the cells of interest (transconjugant) versus the WT KP20.

Table 6.1: Mean plasmid persistence during the RNA-sequencing experiment (n=1) for three biological replicates. Three technical replicates were averaged per biological replicate, except for the biofilm condition where the liquid in the wells was pooled and plated out as a proxy for maintenance in the biofilm condition.

Condition	pCPE16_3 plasmid persistence (%)
Planktonic 24 h	90
Pooled biofilm liquid 24 h	94

6.3 Lifestyle impact on chromosomal gene expression

To determine the overall effect of lifestyle on chromosomal gene expression, WT and transconjugant samples from the same lifestyle were grouped together for comparison. It is of note that any cells that have lost the plasmid in the transconjugant population may produce some background and act to dilute any plasmid-mediated expression signal. Reads were mapped against the KP20 (plasmid-free) reference genome to exclude plasmid genes from the analysis. To evaluate similarity between samples of the same and different groups, whilst reducing data dimensionality, multidimensional scaling (MDS) plots were used (Urpa and Anders, 2019) alongside percentage variance plots for each MDS dimension. A comparison of samples from the three lifestyle conditions (planktonic exponential, planktonic 24 h and biofilm 24 h) illustrated overall sample clustering by lifestyle, regardless of plasmid presence or absence (Figure 6.2). For the planktonic 24 h condition, samples appear less similar to each other across dimension 2 than those in the exponential phase or biofilm lifestyles. However, the majority of the variance in the plot is encompassed in dimension 1 where samples from this lifestyle are aligned (Figure S15).

To further investigate similarity between samples from the individual lifestyles, each lifestyle was compared to each other one. Considering the planktonic exponential lifestyle samples, these consistently cluster together across both dimensions when comparing to samples from the planktonic 24 h and biofilm 24 h lifestyles (Figure 6.2B and C respectively). For both the planktonic 24 h and biofilm 24 h samples, regardless of lifestyle comparison, these cluster less well in dimension 2 but generally align in dimension 1 (Figure 6.2B, C and D). For the planktonic 24 h samples, these do not appear to cluster based on plasmid presence (Figure 6.2B and C). However, placement of the biofilm samples on these plots is affected by plasmid presence, where transconjugants and plasmid-free biological replicates cluster further apart (Figure 6.2C and D).

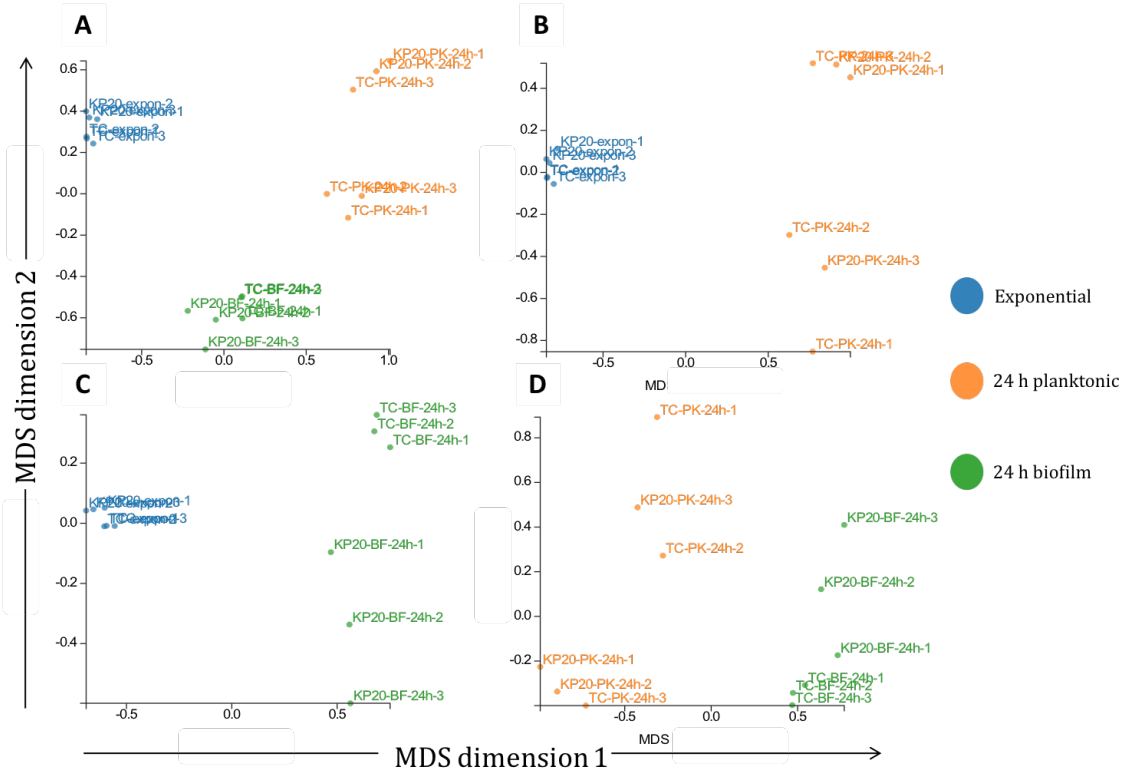

Figure 6.2: Multidimensional scaling (MDS) plots from Degust v4.1.1 (Powell, 2019) of similarity between samples in lifestyle groups compared to the KP20 reference genome. (A) All samples, grouped by lifestyle, are compared to all other samples. (B) Planktonic exponential samples are plotted alongside planktonic 24 h samples. (C) Planktonic exponential samples are plotted alongside biofilm 24 h samples. (D) Planktonic 24 h samples are plotted alongside 24 h biofilm samples. Biological replicates of the WT KP20 and transconjugant (TC) KP20/pCPE16_3 are displayed as individual points for planktonic exponential (blue), planktonic 24 h (orange) and biofilm 24 h (green) groups. Data on percentage variance encompassed by dimensions 1 and 2 are available (Figure S15).

Next, overall chromosomal gene expression patterns between lifestyles were evaluated. To do this, thresholds were applied to the data to minimise the false discovery rate and include only statistically significant and biologically relevant changes in gene expression (adjusted P value set to <0.05 and $\log_2$foldchange set to between >1 and <-1). Heatmaps displaying $\log_2$fold change against the average expression of each gene were used to visualise the inter- and intra-condition variation across the differentially expressed chromosomal genes (Figure 6.3). Comparing individual samples within the planktonic exponential condition, a consistent pattern of expression (up or down-regulation) is apparent for the chromosomal genes across transconju-

gants and WT (plasmid-free) samples. Although more variation in expression is apparent in the planktonic 24 h condition, there are nonetheless regions of consistency within the heatmap. For the planktonic exponential samples, there is no clear differentiation between average expression for the transconjugants or WT samples in the planktonic 24 h condition. Conversely, expression patterns in the biofilm samples cluster based on plasmid presence or absence. Overall, gene expression in biofilm transconjugants is generally upregulated, whereas in plasmid-free samples it is generally downregulated relative to the average. This may indicate a potential role for the plasmid in modulating chromosomal gene expression in the biofilm lifestyle.

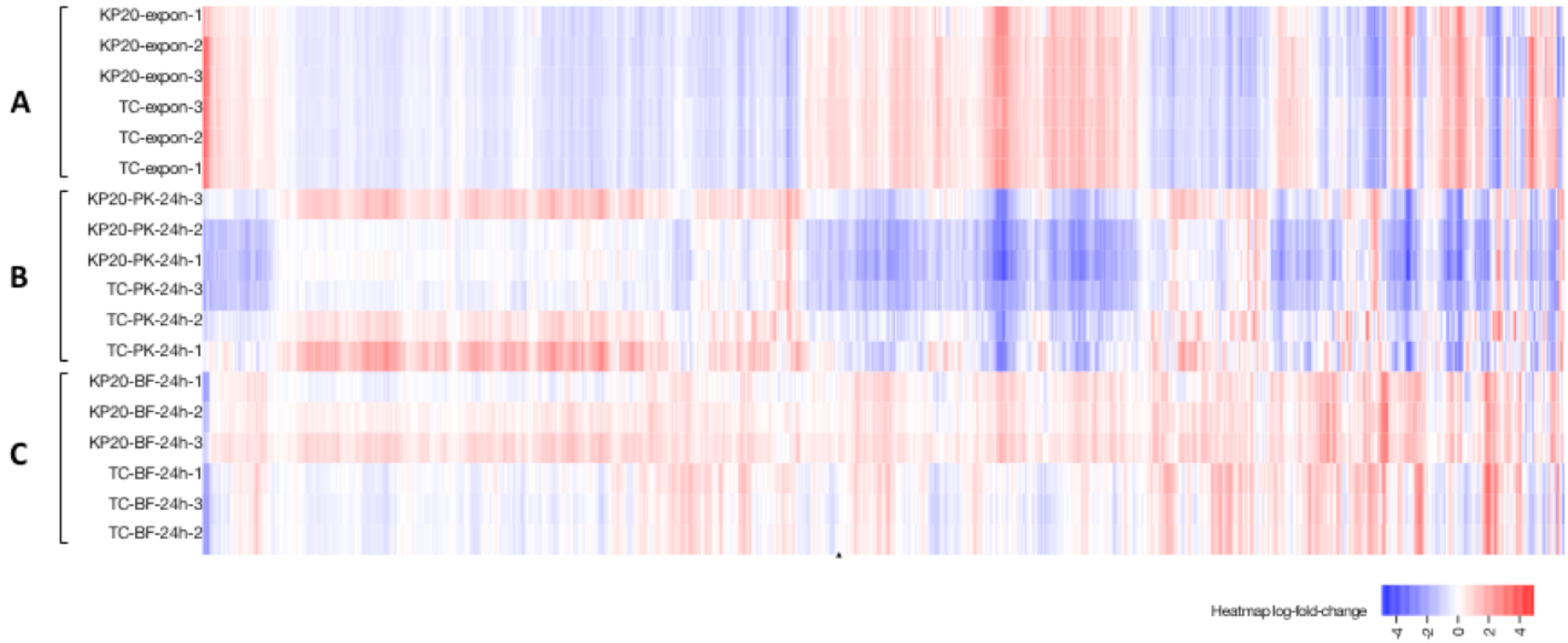

Figure 6.3: Differential expression of chromosomal genes across (A) planktonic exponential (‘−expon−‘), (B) planktonic 24 h (‘−PK-24 h−‘) and (C) 24 h biofilm (‘−BF 24 h−’) conditions relative to the average expression of each gene. Each coloured box in the vertical direction corresponds to a single sample within A, B and C conditions. Each box in the horizontal direction corresponds to an individual gene. Log_2FoldChange against the average expression of each individual gene is displayed and relates to the key on the bottom right. Three biological replicates each of the WT (KP20) and transconjugant (TC) strains were compared for each condition.

6.4 Plasmid impact on chromosomal gene expression

To further evaluate the impact of the plasmid on chromosomal gene expression, MDS plots were used to visualise transconjugant inter- and intra-sample variation across the three lifestyle conditions (Figure 6.4A). Comparing the transconjugants to each other, biological replicates of the planktonic exponential and the biofilm 24 h samples cluster together across dimension 1 and 2, with clear separation by lifestyle particularly across dimension 2. Conversely, the planktonic 24 h samples are more diffuse across both dimensions, which combined include approximately 95% of the total dimensional variance (Figure 6.4B). Nonetheless, the planktonic 24 h samples remain separated from those belonging to the other two lifestyles, forming a dispersed but distinct cluster. Clustering of the transconjugant samples is lifestyle-dependent, as these are isogenic strains and the growth phase was the only variable. This reflects the earlier trend observed using the WT (plasmid-free) and transconjugant strains combined in single lifestyle conditions. It is not possible to separate plasmid or host effects in this comparison, but it is likely that the chromosome is having the largest impact as this trend was also observed without the plasmid.

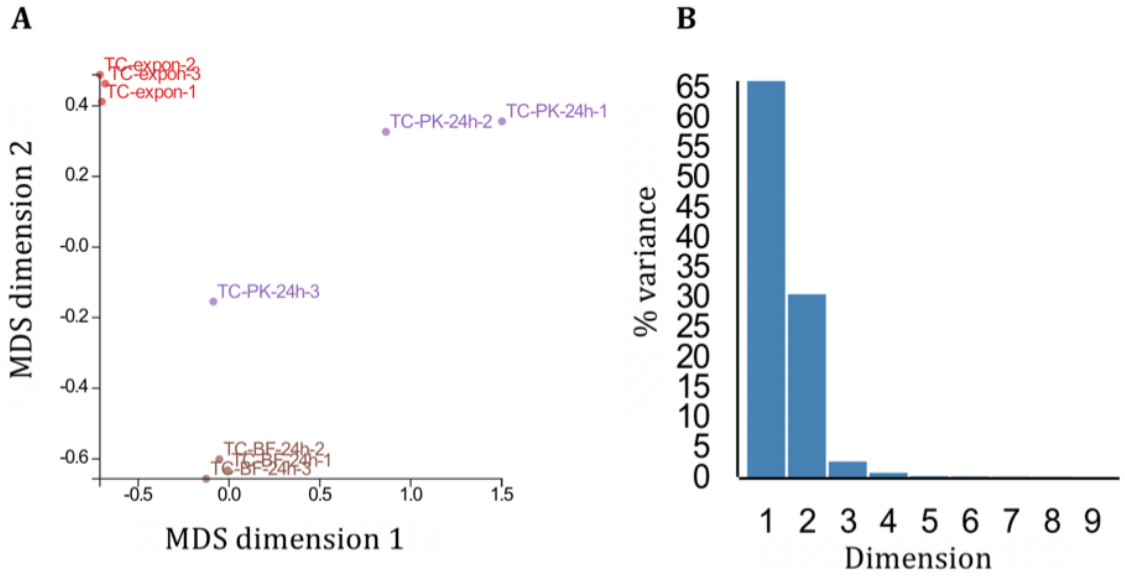

Figure 6.4: Multidimensional scaling (MDS) plots from Degust v4.1.1 (Powell, 2019) compared to the KP20 reference genome. (A) Similarity between transconjugant samples in lifestyle groups. (B) Data on percentage variance encompassed by dimensions 1 and 2. Biological replicates of the transconjugant KP20/pCPE16_3 are displayed as individual points for planktonic exponential (red), planktonic 24 h (purple) and biofilm 24 h (brown) groups.

To determine the impact of plasmid carriage on chromosomal gene expression in the individual lifestyles and establish the plasmid 'signature' in the individual lifestyle conditions, the WT and transconjugant were compared in each condition. For the planktonic exponential condition and the biofilm condition alone, 58 and 523 genes respectively were significantly differentially-expressed in the transconjugant versus the WT samples above the defined thresholds (<0.05 adjusted *P* value, $\log_2$FoldChange set to between >1 and <-1). Therefore, to aid visualisation of general trends in these data, differentially expressed chromosomal genes in the transconjugant versus the KP20 recipient were initially sorted into clusters of orthologous genes (COG) categories (Tatusov *et al.*, 1997) for the biofilm and planktonic exponential conditions respectively. As a single differentially-expressed gene was identified when comparing the WT to the transconjugant in the 24 h planktonic condition, no COG grouping was performed for this condition.

Considering the biofilm 24 h condition, there was a relatively even split between up-

and downregulation of genes in the transconjugant relative to KP20 (Figure 6.5). Although many up- and down-regulated genes had no assigned category, most of the classified upregulated chromosomal genes were found under the 'transcription' group. Conversely, downregulated genes were mostly found within the 'energy production and conversion, amino acid transport and metabolism and inorganic ion transport and metabolism' categories.

For the planktonic exponential condition, the majority of the differentially-expressed genes were upregulated in the transconjugant relative to KP20 (Figure 6.6). Most of the genes were within the 'inorganic ion transport and metabolism' category, followed by the 'secondary metabolites' category. As for the biofilm 24 h condition, several genes involved in transcription were also upregulated in the transconjugant. Again, several genes were in the 'function unknown' or 'no category assigned' groups.

Figure 6.5: Plasmid carriage effect on chromosomal gene expression in the biofilm 24 h condition. The percentage of differentially expressed chromosomal genes that are upregulated (red bars) or downregulated (blue bars) comparing KP20 to the transconjugant categorised by clusters of orthologous genes (COG) category (Tatusov *et al.*, 1997). Where genes were assigned to more than one category, this is indicated separately. Plot prepared using ggplot2 (Wickham, 2016). COG categories assigned using Egg-nog 5.0 (Huerta-Cepas *et al.*, 2019).

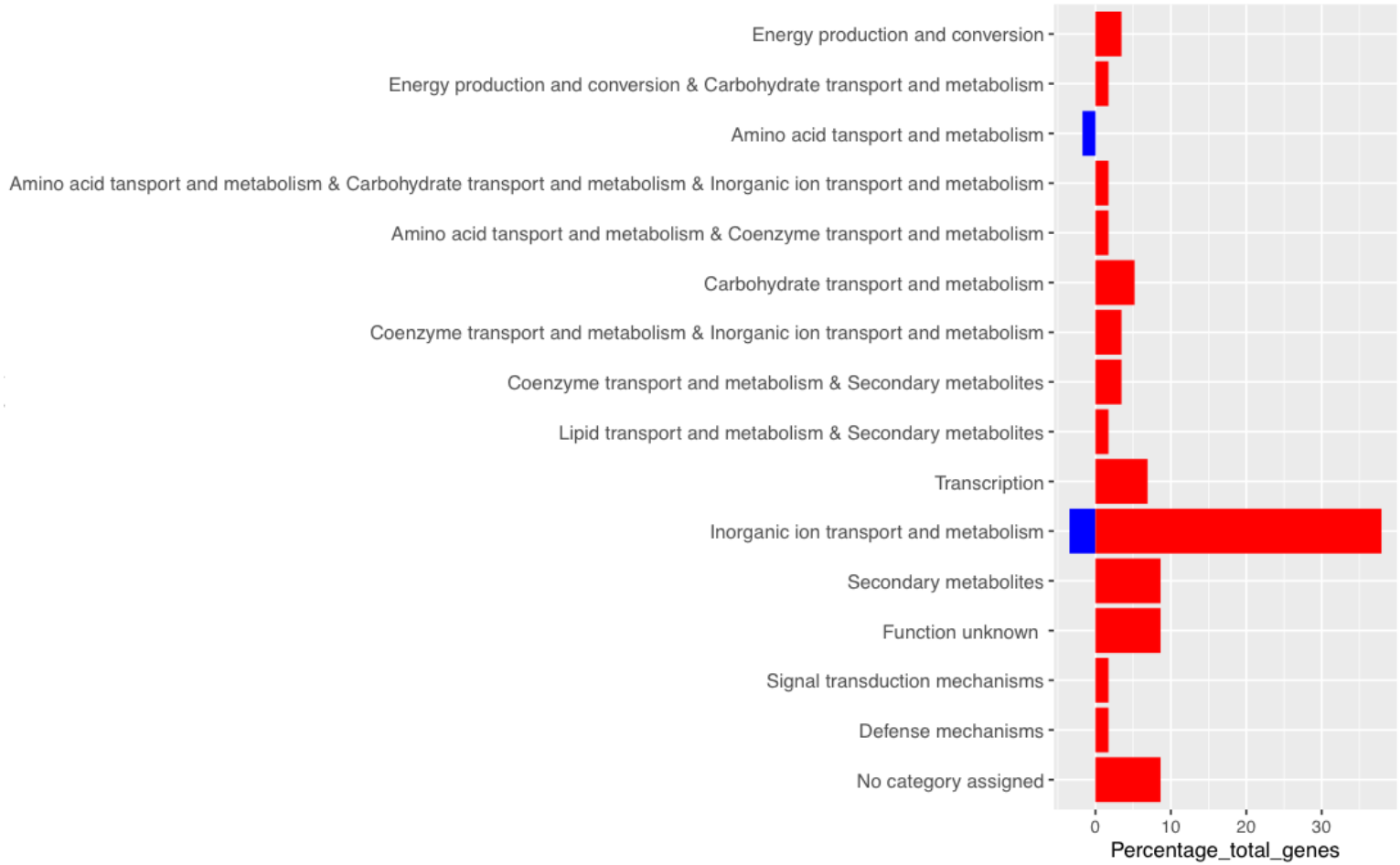

Figure 6.6: Plasmid carriage effect on chromosomal gene expression in the planktonic exponential condition. The percentage of differentially expressed chromosomal genes that are upregulated (red bars) or downregulated (blue bars) comparing KP20 to the transconjugant categorised by clusters of orthologous groups (COG) category (Tatusov *et al.*, 1997). Where genes were assigned to more than one category, this is indicated separately. Plot prepared using ggplot2 (Wickham, 2016). COG categories assigned using Egg-nog 5.0 (Huerta-Cepas *et al.*, 2019).

Next, to visualise the transcriptional response in each condition in more detail, heatmaps were produced displaying differentially expressed chromosomal genes in the transconjugant relative to the KP20 recipient in the planktonic exponential and biofilm 24 h conditions. As a large number of genes were differentially expressed in the biofilm lifestyle, the heatmap includes only those that were the most differentially expressed ($\log_2$ fold change of between ≤ -2 and ≥ 2).

In the biofilm 24 h condition (Figure 6.7), the majority of the most differentially expressed genes were downregulated (50/68 genes, 73.5%). Downregulated genes included those with diverse functions, involved in processes such as translation, management of acid stress and secretion. There was also downregulation of the gene encoding the outer membrane porin A protein. Conversely, the four genes annotated as 'transcriptional regulators' in this subset were upregulated, including *marR* which encodes the 'multiple antibiotic resistance' regulator protein. Additionally, *aaeA*, encoding an efflux pump subunit, was also upregulated.

In the planktonic exponential condition (Figure 6.8), the majority (55/58 genes, 95%) of differentially expressed genes were upregulated in the transconjugant versus KP20. Of these, many genes (24/58, 41%) are predicted to have a role in iron binding, capture, uptake and transport. Three genes annotated as transcriptional regulators are upregulated, alongside a set of genes for manganese transport. The downregulated genes are involved in amino acid metabolism (*avtA*), iron storage (*ftnA*) and manganese efflux (*mntP*).

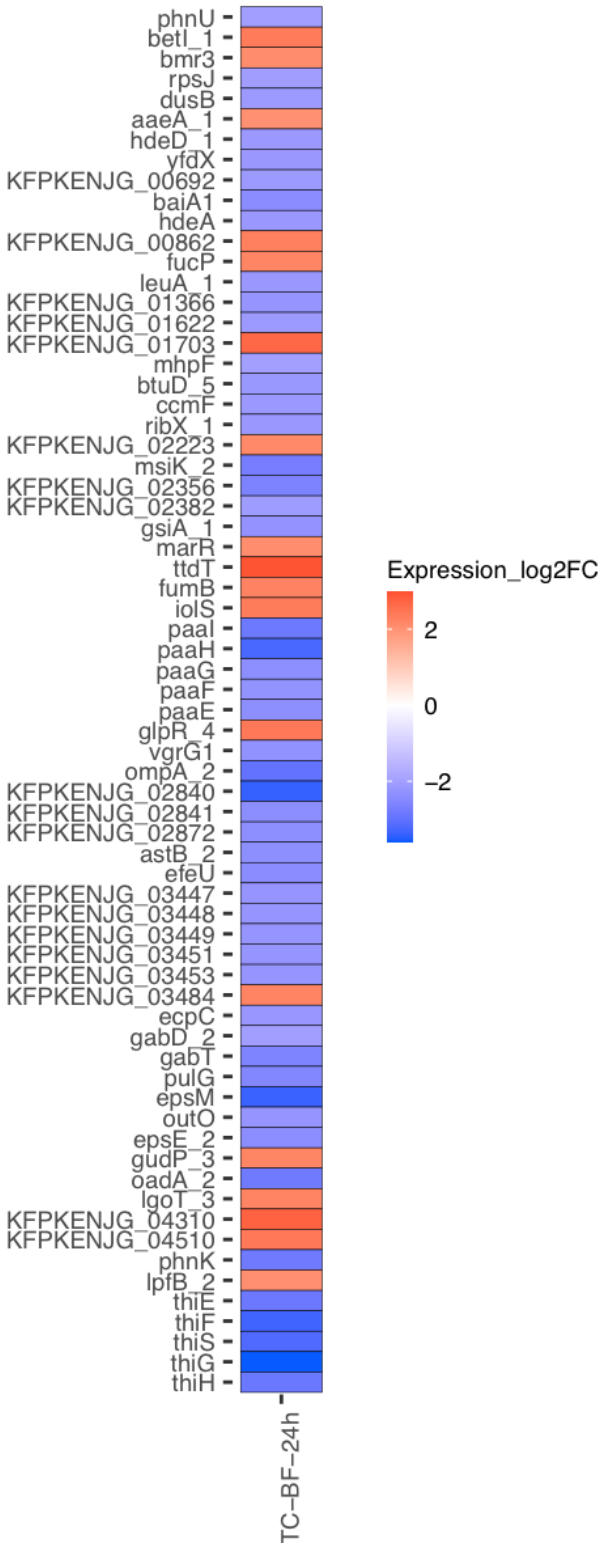

Figure 6.7: Differentially-expressed chromosomal genes in the biofilm 24 h condition comparing KP20 to the transconjugant (TC-BF-24 h) where the adjusted P value = <0.05 and $\log_2$FoldChange mean expression was between $\geq$ 2and ≤ -2. Locus tags represent hypothetical proteins. Plot prepared using ggplot2 (Wickham, 2016).

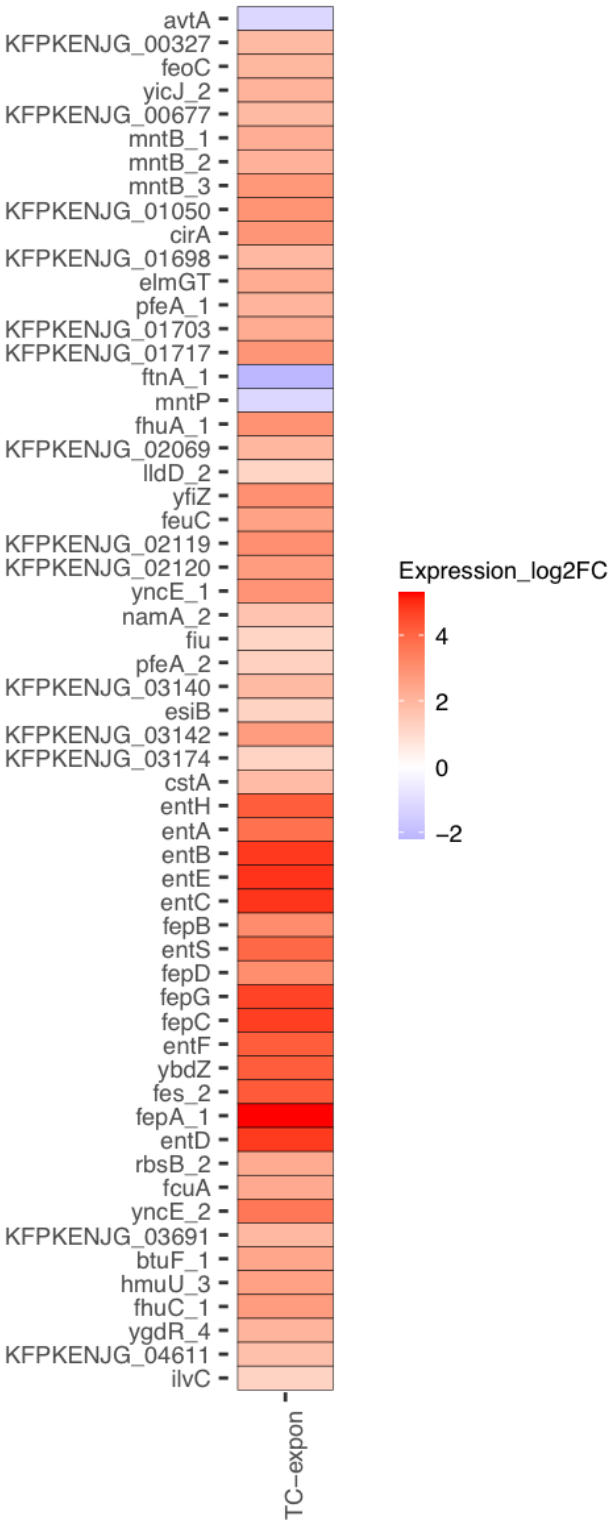

Figure 6.8: Differentially-expressed chromosomal genes in the exponential planktonic condition comparing KP20 to the transconjugant ('TC-expon) where the adjusted P value = <0.05 and $\log_2$FoldChange mean expression was between $\geq$ 1and ≤ -1. Locus tags represent hypothetical proteins. Plot prepared using ggplot2 (Wickham, 2016).

Taken together, for the exponential planktonic and biofilm 24 h, the data indicated a distinct transcriptional response in each condition upon plasmid acquisition. For the planktonic 24 h condition, the data indicated a limited impact on chromosomal gene expression after plasmid acquisition, as a single gene identified as *vapC* was differentially-expressed (upregulated) comparing the transconjugant to KP20. This gene (labelled as the locus tag KFPKENJG_01703) was the only chromosomal gene identified as differentially expressed in transconjugants across all the conditions, and is discussed further below.

6.5 Evaluating a chromosomal plasmid signature

To determine whether plasmid carriage had a lifestyle-independent impact on the expression of chromosomal genes, chromosomal genes that were differentially-expressed in transconjugants versus the WT were identified across the three conditions. Genes that were common to the three conditions were considered to indicate a potential 'plasmid signature' on the chromosome (Figure 6.9). As only a single differentially-expressed gene was identified in the planktonic 24 h WT versus transconjugant samples, common differentially-expressed genes between the biofilm 24 h and planktonic exponential conditions were investigated. Between the planktonic exponential and biofilm 24 h conditions, a set of nine common differentially-expressed chromosomal genes was identified, and these were not universally up or down-regulated. The single differentially-expressed gene in the planktonic 24 h condition was also in this common gene set.

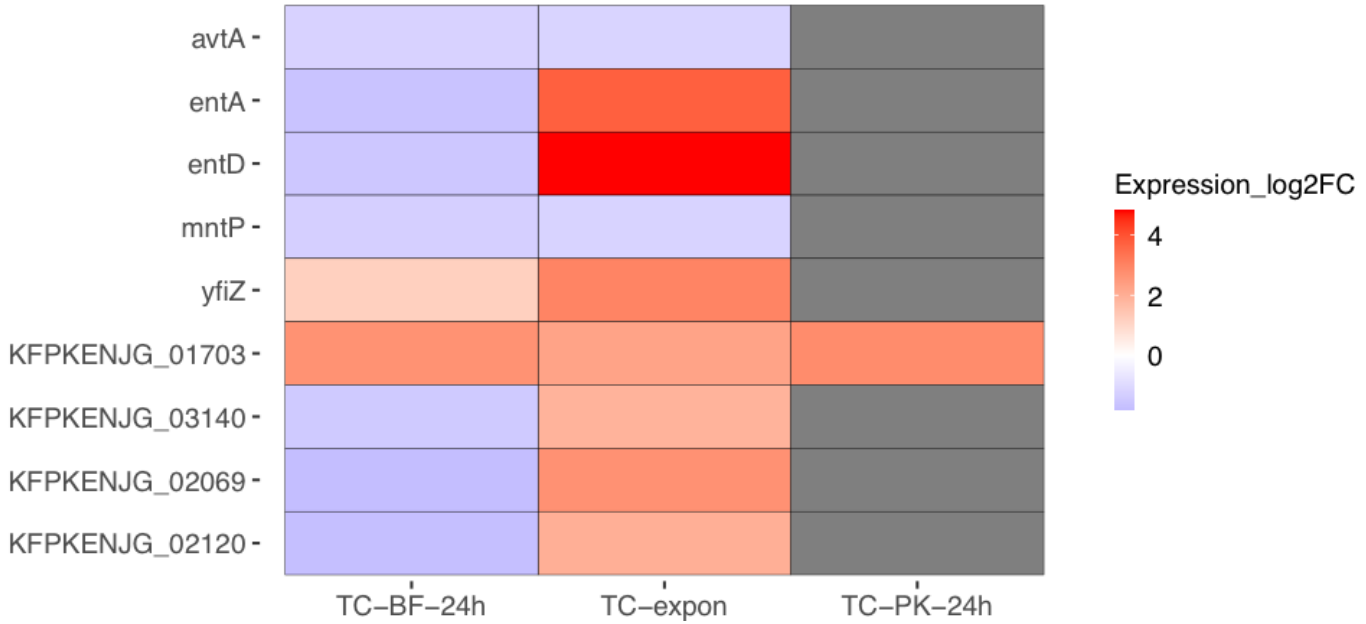

Figure 6.9: Differential gene expression in transconjugants relative to KP20 of chromosomal genes common to the three lifestyle conditions: transconjugant exponential (TC-expon), transconjugant biofilm 24 h (TC-BF-24 h) and transconjugant planktonic 24 h (TC-PK-24 h). Mean $\log_2$FoldChange values of three biological replicates are displayed. Grey filled boxes indicate the gene was not found in a given condition. The following cut-offs were applied: an adjusted P value = <0.05 and $\log_2$FoldChange mean expression was between $\geq$ 1and ≤ -1. Labels with the prefix 'KFPKENJG' relate to locus tags of genes encoding hypothetical proteins. Plot prepared using ggplot2 (Wickham, 2016).

For some of the common differentially-expressed genes, no gene name was available from the Prokka annotation. As such, the locus tags were used as identifiers for these hypothetical proteins. The differentially-expressed gene identified as common to the three lifestyles (locus tag KFPKENJG_01703) was determined to be *vapC*, a copy of which is also present on the plasmid. As a result, it is possible that plasmid reads may have mapped to this chromosomal copy of the gene, representing a false positive. For two of the locus tags (KFPKENJG_02069 and KFPKENJG_02120), searches revealed (putative) general transport or regulatory functions. Considering locus tag KFPKENJG_03140, this remains a 'hypothetical protein'. For the named genes, based on their UniProt Knowledge Base descriptions, several of these (*entA*, *entD* and *yfiZ*) may have a role in iron acquisition (Bateman *et al.*, 2021).

6.6 Lifestyle impact on plasmid gene expression

Since lifestyle had an impact on chromosomal gene expression, and the plasmid affected expression of some chromosomal genes, the potential effect of lifestyle on plasmid gene expression was also considered. MDS plots were used to visualise transconjugant inter- and intra-sample variation across the three lifestyle conditions against the KP20/pCPE16_3 reference genome (Figure 6.10). Regardless of plasmid presence, and consistent with the observed pattern when comparing these samples to the KP20 chromosome alone, lifestyle had an impact on sample clustering. This supports the idea that lifestyle has a greater impact on gene expression than plasmid presence. The trends identified in Figure 6.4 are maintained in this comparison as samples cluster by lifestyle.

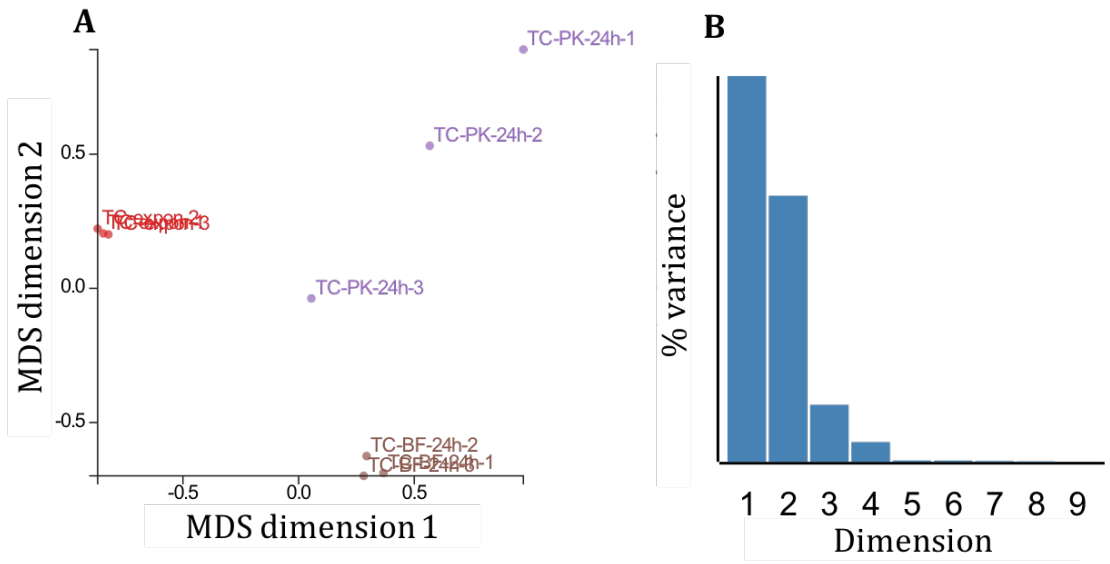

Figure 6.10: Multidimensional scaling (MDS) plots from Degust v4.1.1 (Powell, 2019). (A) Similarity between transconjugant samples in lifestyle groups compared to the transconjugant reference genome. (B) Data on percentage variance encompassed by dimensions 1 and 2. Biological replicates of the transconjugant KP20/pCPE16_3 are displayed as individual points for planktonic exponential (red), planktonic 24 h (purple) and biofilm 24 h (brown) groups.

To evaluate the impact of lifestyle on plasmid gene expression, heatmaps were produced comparing each set of transconjugant samples grown in each condition to the average expression level of a given gene across the three conditions (Figure 6.11). Differentially-expressed plasmid genes (112/134) were identified between the three lifestyle conditions. Plasmid gene expression patterns were generally consistent within conditions but different between conditions, which suggests a lifestyle-dependent plasmid gene expression signature for the transconjugant. Broadly speaking, gene expression was upregulated overall when comparing the biofilm 24 h or the planktonic 24 h lifestyle to the exponential phase samples.

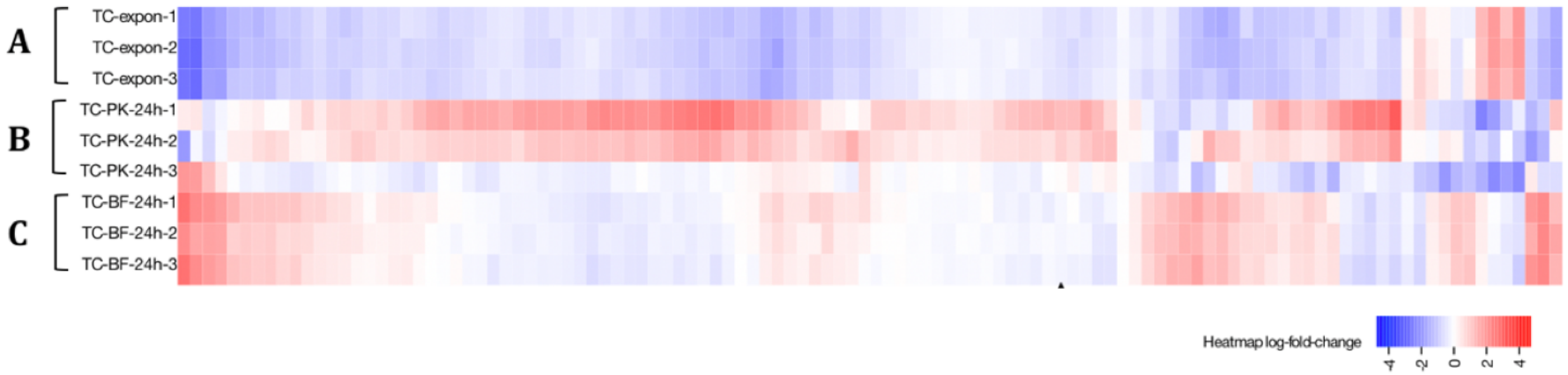

Figure 6.11: Differential expression of 112 plasmid genes across (A) planktonic exponential ('-expon-'), (B) planktonic 24 h ('-PK-24 h-') and (C) 24 h biofilm ('-BF 24 h-') conditions relative to the average expression of each gene. Each coloured box in the vertical direction corresponds to a single sample within A, B and C conditions. Each box in the horizontal direction corresponds to an individual gene. Log_2FoldChange against the average expression of each individual gene is displayed and relates to the key on the bottom right. Three biological replicates each of the WT (KP20) and transconjugant (TC) strains were compared for each condition. Visualisation from Degust v4.1.1 (Powell, 2019).

To investigate the specific plasmid genes that were differentially expressed across the three conditions, differentially expressed genes were assessed relative to the planktonic exponential condition (Figure 6.12). Compared to the planktonic exponential condition, many plasmid genes were upregulated in both the planktonic 24 h and biofilm 24 h samples (57 of 112, 51%). For the lifestyles individually, 92 of 112 genes (82%) were upregulated in the planktonic 24 h condition versus the planktonic exponential, and 68 of 112 genes (61%) were upregulated in the biofilm 24 h versus the planktonic exponential condition. Several genes were annotated as hypothetical proteins (39 of 112, 35%).

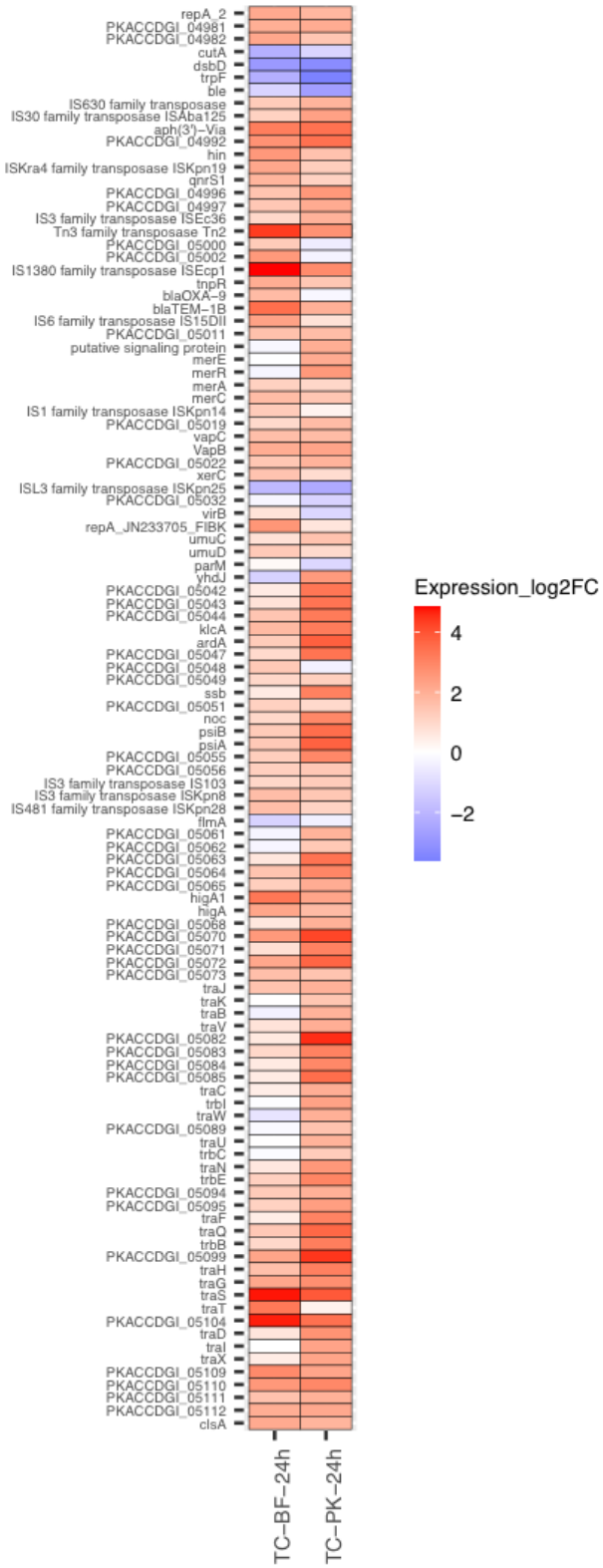

Figure 6.12: Differential expression of plasmid genes in genome order relative to the planktonic exponential condition. Genes, proteins and locus tags were used for annotation. Locus tags represent hypothetical proteins. An annotation is only present if mean differential gene expression was significantly different (adjusted P value = <0.05, $\log_2$ Fold Change of between $\geq 1$and ≤ -1.) between the planktonic exponential phase and at least one of the comparator conditions (biofilm 24 h and planktonic 24 h). Plot prepared using ggplot2 (Wickham, 2016).

Of those with a function assigned (73/112, 65%), several differentially expressed genes (16/73, 22%) encode proteins implicated in mobile element transposition, such as transposases. In most cases (13/16, 81%) these transposition genes were upregulated in both the planktonic 24 h and biofilm 24 h conditions. Of the genes annotated as encoding antimicrobial resistance proteins, 2/4 were upregulated in both the 24 h planktonic and biofilm conditions. Similarly, genes involved in toxin-antitoxin systems and antirestriction were upregulated in these two conditions. Expression of the gene encoding the plasmid segregation protein ParM was either not significantly different (biofilm 24 h) or upregulated (planktonic 24 h) versus the exponential planktonic condition.

Concerning the conjugation module, in the planktonic 24 h condition, all of the differentially-expressed conjugation module genes were upregulated versus the planktonic exponential condition except for *traT*. In the biofilm 24 h condition, transcription of several conjugation module genes was unchanged versus the planktonic exponential condition, including genes involved in pilus assembly, the *traI* helicase, *traN* mating pair stabilisation protein, the *traC* ATP binding protein and the *traD* coupling protein. Several of the upregulated conjugation module genes in the biofilm 24 h condition were identified as hypothetical genes.

6.7 Discussion

For all samples, regardless of plasmid carriage, growth condition had the largest impact on chromosomal gene expression. This was the case when comparing all samples to all other ones, and when comparing samples to each other individually. Corroborating this finding, others have demonstrated the large impact of environmental conditions on the bacterial transcriptome (Harrington *et al.*, 2022), alongside characteristic transcriptional profiles for planktonic and biofilm populations in *K. pneumoniae* and other species (Dötsch *et al.*, 2012; Guilhen *et al.*, 2016; Rumbo-Feal

et al., 2013).

The MDS plots hinted at a plasmid effect on chromosomal gene expression in the biofilm lifestyle. This was confirmed through the separation in profile between the KP20 recipient and the transconjugant in the biofilm condition when compared against the average expression of chromosomal genes across all conditions. Further evaluation of biofilm chromosomal gene expression in the recipient versus the transconjugant revealed differential gene expression of more than 500 chromosomal genes after plasmid acquisition, representing more than 10% of the total (4979) annotated chromosomal genes. This proportion of differentially-expressed chromosomal genes is within the range observed in other studies (Billane *et al.*, 2022; Long *et al.*, 2019).

Genes were assigned COG categories to provide an overall profile of the general functions affected by plasmid carriage (Tatusov *et al.*, 1997). This categorisation system is often used to aid evaluation of gene expression data (Dunn *et al.*, 2021; Guilhen *et al.*, 2016; Shintani *et al.*, 2010). Excluding the 'function unknown' and 'no category assigned' groups to which many genes may be assigned (Guilhen *et al.*, 2016), the majority of the upregulated genes were classified under the 'transcription' category. When considering only the most differentially expressed chromosomal genes in this lifestyle, although most genes were downregulated in the transconjugant compared to the recipient, the most upregulated genes encoded transcriptional regulators including the multiple antibiotic resistance regulator MarR, which forms part of the *mar* (multiple antibiotic resistance) operon. Expression of this operon can affect many downstream processes including efflux, porin production and DNA repair (Sharma *et al.*, 2017). The potential for large expression effects mediated by transcriptional regulators may explain the large number of differentially-regulated genes in this condition (Billane *et al.*, 2022).

Of the downregulated chromosomal genes in the transconjugant in the biofilm condition, most were in 'energy production and conversion' and 'metabolism' COG cat-

egories. Evaluating the most downregulated genes, some of these were implicated in translation, potentially indicating that fewer gene products were synthesised, perhaps to conserve energy (Bervoets and Charlier, 2019). Broad expression effects have been reported upon plasmid acquisition, for example in a *K. pneumoniae* clinical isolate that had received a carbapenem resistance plasmid (Long *et al.*, 2019). However, plasmid acquisition may have variable, and less dramatic effects on host physiology, as was reported for a set of *E. coli* transconjugants that had received a multidrug resistance plasmid from a *K. pneumoniae* donor (Dunn *et al.*, 2021). Indeed host/plasmid differences make predicting the effect of a given plasmid on the transcriptome of a particular host currently infeasible (Billane *et al.*, 2022).

Considering the planktonic exponential condition, chromosomal gene expression patterns were relatively consistent across all samples regardless of plasmid carriage. Differentially-expressed genes were first sorted into COG categories. From this analysis, clear upregulation of gene expression was apparent in transconjugant samples, with the largest proportion of the 58 differentially-expressed genes assigned to the 'inorganic ion transport and metabolism' category. Plasmid carriage in this condition was responsible for differential expression of around 1% of the total (4979) annotated chromosomal genes. This is a similar proportion to that observed evaluating the effect of F-plasmid carriage in *E. coli* harvested in the planktonic exponential condition, where around 4% of chromosomal genes were differentially expressed upon plasmid acquisition (Harr and Schlötterer, 2006).

Focusing next on the specific differentially-expressed genes, the clearest signal for upregulation was for genes involved in iron metabolism. There is precedent for this effect, as carriage of plasmid pCAR1 in *Pseudomonas* resulted in upregulation of chromosomal genes involved in iron metabolism in the exponential growth phase (Shintani *et al.*, 2010). Although this change in expression does not necessarily mean that more iron is required by the transconjugant, a potential explanation for this effect may be increased iron use resulting from plasmid carriage. As

iron is required for growth and DNA replication (which is actively occurring in the exponential phase (Watanabe *et al.*, 2015)) and the transcriptome of *K. pneumoniae* under iron-limiting conditions may be altered to promote scavenging (Muselius *et al.*, 2020), perhaps the presence of additional genetic material, in the form of the plasmid, requiring replication alongside the fast growth rate is sufficient to induce reprogramming for increased transcription of iron acquisition genes. As in the biofilm condition, there was also upregulation of a small number of chromosomal transcriptional regulators in the exponential phase which may have broad effects on gene expression (Billane *et al.*, 2022).

Unlike for the planktonic exponential condition, there was very little effect of plasmid carriage on chromosomal gene expression in the transconjugant in the planktonic 24 h condition. This may be because, in the stationary phase where nutrients are limited, DNA replication is no longer occurring and cells enter a 'non-growth' state where they shift their metabolism and synthesise a fraction of the products that would be made in favourable growth conditions (Navarro Llorens *et al.*, 2010; Rolfe *et al.*, 2012). The only gene that was determined to be significantly differentially expressed in this condition was identified as *vapC*, the toxin component of a toxin-antitoxin system. As this gene is present on both the chromosome and the plasmid, it may be that plasmid reads from the transconjugant were falsely mapping to the homologous chromosomal copy of the gene when the KP20 reference genome was used for the analysis. In that case, it may be that there is no difference in gene expression as a result of plasmid carriage in the 24 h planktonic condition. If the reads are indeed from the chromosomal copy of the gene, this implies that this gene is affected by plasmid carriage itself, as it was the only gene to be consistently upregulated across all conditions. Although every effort was made to check sample naming, inspection of the colour pattern in Figure 6.3 highlights the possibility of a sample exchange within the planktonic 24 h condition. As a result, future work should investigate and validate these results.

Comparing chromosomal gene expression across the planktonic exponential and biofilm conditions, a small set of common genes were identified as differentially expressed in the transconjugant versus KP20. These may represent a potential plasmid signature in the planktonic exponential and biofilm conditions. However, as these were not regulated in the same manner (up or down) across conditions, it is debatable as to whether this is the case. Additionally, the absence of most of these genes in the differentially expressed genes set comparing KP20 to the transconjugant in the planktonic 24 h condition adds further uncertainty. Overall, on the basis of the available data, there is insufficient evidence to state that the plasmid provides a reproducible chromosomal signature on the KP20 recipient. As such, there is no clear evidence for a particular impact of the plasmid on the (lifestyle-independent) chromosomal transcriptional programme. This is in contrast to some reports where a signature of plasmid carriage has been identified. For example, in a *Pseudomonas aeruginosa* model system, a set of metabolic genes was affected by carriage of various plasmids in the exponential growth phase (San Millan *et al.*, 2018). However, it is clear that plasmid carriage has variable effects on host chromosomal gene expression in different growth conditions. Overall, it appears that the plasmid has the largest effect on chromosomal gene expression in the biofilm relative to the planktonic conditions.

Next, the impact of lifestyle on plasmid gene expression was considered. Of the 134 annotated plasmid genes, 112 were significantly differentially-expressed in either or both the planktonic 24 h and biofilm 24 h conditions compared to the planktonic exponential condition. Many of these genes were annotated as involved in mobile element transposition, with most of these genes upregulated versus the planktonic exponential condition. Stress has been demonstrated to increase transposable element transfer (Capy *et al.*, 2000). It has been suggested that this may promote new sequence variation to support host stress adaptation and transposable element proliferation (Fan *et al.*, 2019; Vandecraen *et al.*, 2017). For example, in stationary phase populations of *Pseudomonas putida*, the stationary phase sigma factor RpoS

(transcriptional regulator) has been shown to activate transcription at a transposase promoter (Ilves *et al.*, 2001). Although transcription does not guarantee protein production, transcriptional upregulation of a large number of transposase genes was observed in the cyanobacterium *Microcystis aeruginosa* in certain nutrient-limited conditions versus nutrient-replete conditions (Steffen *et al.*, 2014). Considering applicability to this study, as the 24 h time point conditions for both planktonic and biofilm cultures will be in stationary phase, it is possible that the nutrient limitation is sufficient to upregulate transcription of transposase genes in both of these sample sets.

Concerning the conjugation module, most of the differentially-expressed genes were upregulated in the planktonic 24 h condition versus the exponential planktonic condition. Upregulation might hint at possible DNA transfer in this condition. However, on the basis of the persistence test before the experiment was conducted, the majority of cells in all the tested populations should already contain the plasmid. There is some evidence that growth phase may impact conjugation. For example, in a study into the transfer of an F-type plasmid into an *E. coli* K-12 population, the authors argue that conjugation is likely to occur during transition into a non-growing state (Headd and Bradford, 2020). Although this may provide a plausible explanation for the gene expression profile observed in this work, this was not tested. For the biofilm 24 h condition, the expression of several genes from this module was unchanged compared to the planktonic exponential condition.

Although experiments in Chapter 5 suggested that the conjugation frequency was greater in a biofilm versus the planktonic lifestyle, the gene expression data does not provide an explanation for these findings and indeed deciphering mechanisms behind these data was not an aim of this work. It is important to note that the conjugation experiments were conducted using naïve KP20 recipients mixed with CPE16 donors, and therefore are not comparable to the populations analysed in the gene expression studies where the majority of cells are likely to contain the pCPE16_3 plasmid. It

may be that the physiochemical properties of a biofilm, specifically the packing of cells in a biofilm matrix, are sufficient to facilitate plasmid transfer in this lifestyle.

6.8 Conclusion

Taken together, overall these data indicate that lifestyle had a large effect on chromosomal gene expression, and a greater effect than plasmid carriage. For the planktonic 24 h condition, plasmid carriage did not particularly impact chromosomal gene expression. However, for the planktonic exponential phase and biofilm 24 h conditions, plasmid carriage had variable and principally distinct effects on chromosomal gene expression. For example, a marked effect of plasmid carriage was observed in the planktonic exponential condition where a large number of genes involved in iron acquisition were upregulated. The impact of lifestyle on expression of plasmid genes implicated in mobile element transposition and the variable impact of lifestyle on conjugation module expression was highlighted. As mobile genetic elements frequently carry antimicrobial resistance genes (Rozwandowicz *et al.*, 2018), and conjugation is a major facilitator of plasmid transfer (San Millan and MacLean, 2017), these data suggest that lifestyle may have an effect on both intracellular and intercellular transfer of antimicrobial resistance genes.

6.8.1 Key findings

- Lifestyle has a large impact on chromosomal gene expression, regardless of plasmid carriage
- Plasmid carriage has a distinct impact on chromosomal gene expression in the planktonic exponential and biofilm 24 h conditions
- The plasmid has little to no impact on chromosomal gene expression in the planktonic 24 h condition

- Plasmid gene expression is affected by growth conditions across the majority of annotated genes
- Expression of conjugation module genes is most upregulated in the planktonic 24 h condition
- Lifestyle may impact transfer of antimicrobial resistance genes

Chapter 7

Discussion

This study employed two clinically-relevant models, one making use of a fluorescence-reporter system and the second using plating techniques informed by WGS insights, for assessment of conjugation of carbapenem resistance plasmids in planktonic and biofilm populations. Gene expression of a transconjugant generated in the second model versus the recipient was also assessed across three growth conditions. Overall, this work has contributed to knowledge and understanding in three main aspects of biology, each of which will be discussed below.

7.1 The application of flow cytometry to study conjugation in bacterial populations

Traditional conjugation assays restrict throughput, partly due to the requirement for culturing and colony counting to enable conjugation frequency calculation (Hazan *et al.*, 2012). Flow cytometry and similar techniques may remove the need for these steps and therefore have the potential to reduce the time and resources used for such investigations (Wilkinson, 2018). Although others have reported success using

flow cytometry to monitor conjugation in bacterial populations (e.g. del Campo *et al.* (2012); Sørensen *et al.* (2003)), the evidence provided here indicates that a cautious approach is necessary for data interpretation. Firstly, use of a dual fluorescence reporter system in this work highlighted issues with false positives which were identified through dilution and control samples. Although one could argue that use of a single fluorescent protein (such as in work by Sørensen *et al.* (2003)) would avoid the obvious combined false- and true-positive transconjugant population, this does not mean that such a system avoids coincident events. Instead this suggests that false positives in these systems may require a different detection method (such as DNA stains to aid doublet discrimination by indicating when more DNA is present than would be in expected in a single cell (Reardon *et al.*, 2014)). Secondly, this work highlights the potential challenges of rare event detection which by its nature requires a large number of events to be detected. In practice, depending on equipment specifications, such samples may take considerable time to run which may impact experimental outcomes if using live cells (as transconjugants may be produced during sample analysis). Overall, the importance of careful evaluation of bacterial flow cytometry setups has been emphasised. Potential solutions have been proposed, such as the use of a highly conjugative plasmid in model development and equipment with a high signal:noise ratio.

7.2 Conjugation monitoring in *K. pneumoniae* populations using clinical isolate donors

The ability to evaluate conjugation using naturally-occurring strains and plasmids from hospitals, especially those which contribute to AMR, is essential for understanding how to reduce its impact. Determination of plasmid transfer frequencies from patient isolates was carried out. In the case of the CPE16 donor, particularly high frequencies were revealed which supports existing evidence that conjugation is a

major contributor to the spread of AMR in *K. pneumoniae* (Hendrickx *et al.*, 2020). In addition, concurrent transfer of co-resident plasmids was observed, indicated by WGS data from transconjugant colonies. Alongside provision of frequencies for a selection of isolates, this study produced a *K. pneumoniae* recipient strain which may provide a useful community tool for assessing transfer of AMR plasmids. This may be particularly suitable in cases where donor strains and plasmids prevent use of existing recipient strains due to conflicting resistance profiles. The combination of the CPE16 donor and KP20 recipient may also provide a convenient model, such as in studies where a high conjugation frequency is a useful starting point for comparisons. This work also reinforced some of the benefits and limitations of WGS data which was used here to aid in model development. This study highlighted that, although inferences made from sequencing data about likely conjugative ability of plasmids may be reliable, the conjugation frequency itself cannot (yet) be deciphered from WGS data. For example, it was not possible to predict that pCPE16_3 would transfer at such high frequency, while pCPE25_3 would conjugate at relatively low frequency. In addition, this work provides evidence to corroborate some of the conclusions from previous studies (Hausner and Wuertz, 1999; Król *et al.*, 2011) indicating that conjugation may be facilitated in a biofilm. However, further work is required for direct comparison between planktonic and biofilm lifestyles, and to clarify what the underlying mechanisms may be. For example, could this observation be the result of the biofilm structure promoting cell-cell contact, initial donor-recipient contacts followed by vertical transfer or perhaps another mechanism? These questions remain as yet unanswered.

7.3 The evaluation of plasmid and lifestyle impacts on gene expression

Plasmids may impose a fitness cost on their host, which can manifest as a growth defect (San Millan and MacLean, 2017). Alternatively, there may be little or no growth impact, and gene expression changes may be sufficient for adaptation to plasmid carriage (Buckner *et al.*, 2018). Environmental conditions are likely to impact fitness costs, and artificial laboratory settings may not be reflective of the conditions that would be encountered as a bacterium, for example, infects or colonises a host (Hubbard *et al.*, 2019). However, in the tested conditions, no obvious growth impact was observed upon pCPE16_3 plasmid acquisition by KP20. Therefore, RNA-sequencing was performed to evaluate the effect of the plasmid on host gene expression. The effect of lifestyle on both the host chromosome and the plasmid was also determined, as bacteria are often found as biofilms, including in infection settings (Stalder *et al.*, 2020). Therefore, studying bacteria across different growth conditions is important. Lifestyle (biofilm versus two planktonic conditions) had the greatest impact on gene expression, and the plasmid effect on gene expression was lifestyle-dependent. Growth phase also affected gene expression across most plasmid genes, including several genes implicated in mobile element transposition and conjugation module genes. This work highlighted the importance of studying bacterial populations and their plasmids across different growth conditions, and the benefit of using plasmids from recently obtained clinical isolates to provide more clinically-relevant experimental models. The data suggest that lifestyle may impact gene transfer within cells and via conjugation which could have consequences for the transfer of antimicrobial resistance determinants. However, further work is required to support or refute these tentative hypotheses.

7.4 References

Abe, K., Nomura, N., and Suzuki, S. Biofilms: Hot spots of horizontal gene transfer (HGT) in aquatic environments, with a focus on a new HGT mechanism, may 2021. ISSN 15746941. URL https://academic.oup.com/femsec/article/doi/10.1093/femsec/fiaa031/5766226.

Abe, R., Akeda, Y., Sakamoto, N., Kumwenda, G., Sugawara, Y., Yamamoto, N., Kawahara, R., Tomono, K., Fujino, Y., and Hamada, S. Genomic characterisation of a novel plasmid carrying $bla_{\text{IMP-6}}$ of carbapenem-resistant *Klebsiella pneumoniae* isolated in Osaka, Japan. *Journal of Global Antimicrobial Resistance*, 21: 195–199, jun 2020. ISSN 22137173. doi: 10.1016/j.jgar.2019.10.003. URL https://www.sciencedirect.com/science/article/pii/S2213716519302577.

Agarwala, R., Barrett, T., Beck, J., Benson, D. A., Bollin, C., Bolton, E., Bourexis, D., Brister, J. R., Bryant, S. H., Canese, K., Cavanaugh, M., Charowhas, C., Clark, K., Dondoshansky, I., Feolo, M., Fitzpatrick, L., Funk, K., Geer, L. Y., Gorelenkov, V., Graeff, A., Hlavina, W., Holmes, B., Johnson, M., Kattman, B., Khotomlianski, V., Kimchi, A., Kimelman, M., Kimura, M., Kitts, P., Klimke, W., Kotliarov, A., Krasnov, S., Kuznetsov, A., Landrum, M. J., Landsman, D., Lathrop, S., Lee, J. M., Leubsdorf, C., Lu, Z., Madden, T. L., Marchler-Bauer, A., Malheiro, A., Meric, P., Karsch-Mizrachi, I., Mnev, A., Murphy, T., Orris, R., Ostell, J., O'Sullivan, C., Palanigobu, V., Panchenko, A. R., Phan, L., Pierov, B., Pruitt, K. D., Rodarmer, K., Sayers, E. W., Schneider, V., Schoch, C. L., Schuler, G. D., Sherry, S. T., Siyan, K., Soboleva, A., Soussov, V., Starchenko, G., Tatusova, T. A., Thibaud-Nissen, F., Todorov, K., Trawick, B. W., Vakatov, D., Ward, M., Yaschenko, E., Zasypkin, A., and Zbicz, K. Database resources of the National Center for Biotechnology Information. *Nucleic Acids Research*, 46 (D1):D8–D13, 2018. ISSN 13624962. doi: 10.1093/nar/gkx1095. URL https://www.ncbi.nlm.nih.gov/pmc/articles/PMC5753372/.

Alalam, H., Graf, F. E., Palm, M., Abadikhah, M., Zackrisson, M., Boström, J., Fransson, A., Hadjineophytou, C., Persson, L., Stenberg, S., Mattsson, M., Ghiaci, P., Sunnerhagen, P., Warringer, J., and Farewell, A. A high-throughput method for screening for genes controlling bacterial conjugation of antibiotic resistance. *mSystems*, 5(6), dec 2020. ISSN 2379-5077. doi: 10.1128/mSystems.01226-20. URL http://www.ncbi.nlm.nih.gov/pubmed/33361328http://www.pubmedcentral.nih.gov/articlerender.fcgi?artid=PMC7762799.

Alderliesten, J. B., Duxbury, S. J., Zwart, M. P., De Visser, J. A. G., Stegeman, A., and Fischer, E. A. Effect of donor-recipient relatedness on the plasmid conjugation frequency: A meta-analysis. *BMC Microbiology*, 20(1):135, dec 2020. ISSN 14712180. doi: 10.1186/s12866-020-01825-4. URL https://bmcmicrobiol.biomedcentral.com/articles/10.1186/s12866-020-01825-4.

Alikhan, N. F., Petty, N. K., Ben Zakour, N. L., and Beatson, S. A. BLAST Ring Image Generator (BRIG): Simple prokaryote genome comparisons. *BMC Genomics*, 12(1):402, dec 2011. ISSN 14712164. doi: 10.1186/1471-2164-12-402. URL http://bmcgenomics.biomedcentral.com/articles/10.1186/1471-2164-12-402.

Alonso-del Valle, A., León-Sampedro, R., Rodríguez-Beltrán, J., DelaFuente, J., Hernández-García, M., Ruiz-Garbajosa, P., Cantón, R., Peña-Miller, R., and San Millán, A. Variability of plasmid fitness effects contributes to plasmid persistence in bacterial communities. *Nature Communications*, 12(1):2653, dec 2021. ISSN 20411723. doi: 10.1038/s41467-021-22849-y. URL http://www.nature.com/articles/s41467-021-22849-y.

Altschul, S. F., Gish, W., Miller, W., Myers, E. W., and Lipman, D. J. Basic local alignment search tool. *Journal of Molecular Biology*, 215(3):403–410, oct 1990. ISSN 00222836. doi: 10.1016/S0022-2836(05)80360-2. URL https://www.sciencedirect.com/science/article/pii/S0022283605803602.

Álvarez-Barrientos, A., Arroyo, J., Cantón, R., Nombela, C., and Sánchez-Pérez, M. Applications of flow cytometry to clinical microbiology. *Clinical Microbi-*

ology Reviews, 13(2):167–195, apr 2000. ISSN 0893-8512. doi: 10.1128/cmr.13.2.167. URL http://www.ncbi.nlm.nih.gov/pubmed/10755996http://www.pubmedcentral.nih.gov/articlerender.fcgi?artid=PMC100149.

Álvarez-Rodríguez, I., Arana, L., Ugarte-Uribe, B., Gómez-Rubio, E., Martín-Santamaría, S., Garbisu, C., and Alkorta, I. Type IV coupling proteins as potential targets to control the dissemination of antibiotic resistance, aug 2020. ISSN 2296889X. URL https://www.frontiersin.org/article/10.3389/fmolb.2020.00201/full.

Anderl, J. N., Franklin, M. J., and Stewart, P. S. Role of antibiotic penetration limitation in *Klebsiella pneumoniae* biofilm resistance to ampicillin and ciprofloxacin. *Antimicrobial Agents and Chemotherapy*, 44(7):1818–1824, jul 2000. ISSN 00664804. doi: 10.1128/AAC.44.7.1818-1824.2000. URL http://www.ncbi.nlm.nih.gov/pubmed/10858336http://www.pubmedcentral.nih.gov/articlerender.fcgi?artid=PMC89967.

Andrews, J. M. Determination of minimum inhibitory concentrations. *Journal of Antimicrobial Chemotherapy*, 48(SUPPL. 1):5–16, jul 2001. ISSN 03057453. doi: 10.1093/jac/48.suppl_1.5. URL https://academic.oup.com/jac/article/48/suppl_1/5/2473513.

Anjum, M. F., Zankari, E., and Hasman, H. Molecular methods for detection of antimicrobial resistance. *Microbiology Spectrum*, 5(6), 2017. ISSN 21650497. doi: 10.1128/microbiolspec.arba-0011-2017. URL https://journals.asm.org/doi/10.1128/microbiolspec.ARBA-0011-2017.

Argimón, S., Abudahab, K., Goater, R. J., Fedosejev, A., Bhai, J., Glasner, C., Feil, E. J., Holden, M. T., Yeats, C. A., Grundmann, H., Spratt, B. G., and Aanensen, D. M. Microreact: Visualizing and sharing data for genomic epidemiology and phylogeography. *Microbial genomics*, 2(11):e000093, 2016. ISSN 20575858. doi: 10.1099/mgen.0.

000093. URL http://www.ncbi.nlm.nih.gov/pubmed/28348833http://www.pubmedcentral.nih.gov/articlerender.fcgi?artid=PMC5320705.

Arias-Andres, M., Klümper, U., Rojas-Jimenez, K., and Grossart, H. P. Microplastic pollution increases gene exchange in aquatic ecosystems. *Environmental Pollution*, 237:253–261, jun 2018. ISSN 18736424. doi: 10.1016/j.envpol.2018.02.058. URL https://www.sciencedirect.com/science/article/pii/S0269749117349990.

Arutyunov, D. and Frost, L. S. F conjugation: Back to the beginning, jul 2013. ISSN 0147619X. URL https://www.sciencedirect.com/science/article/pii/S0147619X13000395.

Ayukekbong, J. A., Ntemgwa, M., and Atabe, A. N. The threat of antimicrobial resistance in developing countries: Causes and control strategies, dec 2017. ISSN 20472994. URL http://aricjournal.biomedcentral.com/articles/10.1186/s13756-017-0208-x.

Azeredo, J., Azevedo, N. F., Briandet, R., Cerca, N., Coenye, T., Costa, A. R., Desvaux, M., Di Bonaventura, G., Hébraud, M., Jaglic, Z., Kačániová, M., Knøchel, S., Lourenço, A., Mergulhão, F., Meyer, R. L., Nychas, G., Simões, M., Tresse, O., and Sternberg, C. Critical review on biofilm methods, may 2017. ISSN 15497828. URL https://www.tandfonline.com/doi/full/10.1080/1040841X.2016.1208146.

Baric, R. S., Crosson, S., Damania, B., Miller, S. I., and Rubin, E. J. Next-generation high-throughput functional annotation of microbial genomes. *mBio*, 7(5), nov 2016. ISSN 21507511. doi: 10.1128/mBio.01245-16. URL http://www.ncbi.nlm.nih.gov/pubmed/27703071http://www.pubmedcentral.nih.gov/articlerender.fcgi?artid=PMC5050336.

Barry, K. E., Wailan, A. M., Sheppard, A. E., Crook, D., Vegesana, K., Stoesser, N., Parikh, H. I., Sebra, R., and Mathers, A. J. Don't overlook the little guy: An

evaluation of the frequency of small plasmids co-conjugating with larger carbapenemase gene containing plasmids. *Plasmid*, 103:1–8, may 2019. ISSN 10959890. doi: 10.1016/j.plasmid.2019.03.005. URL https://www.sciencedirect.com/science/article/pii/S0147619X18301550?via%3Dihub.

Bassetti, M., Peghin, M., Vena, A., and Giacobbe, D. R. Treatment of infections due to MDR Gram-negative bacteria, apr 2019. ISSN 2296858X. URL https://www.frontiersin.org/article/10.3389/fmed.2019.00074/full.

Bateman, A., Martin, M. J., Orchard, S., Magrane, M., Agivetova, R., Ahmad, S., Alpi, E., Bowler-Barnett, E. H., Britto, R., Bursteinas, B., Bye-A-Jee, H., Coetzee, R., Cukura, A., Silva, A. D., Denny, P., Dogan, T., Ebenezer, T. G., Fan, J., Castro, L. G., Garmiri, P., Georghiou, G., Gonzales, L., Hatton-Ellis, E., Hussein, A., Ignatchenko, A., Insana, G., Ishtiaq, R., Jokinen, P., Joshi, V., Jyothi, D., Lock, A., Lopez, R., Luciani, A., Luo, J., Lussi, Y., MacDougall, A., Madeira, F., Mahmoudy, M., Menchi, M., Mishra, A., Moulang, K., Nightingale, A., Oliveira, C. S., Pundir, S., Qi, G., Raj, S., Rice, D., Lopez, M. R., Saidi, R., Sampson, J., Sawford, T., Speretta, E., Turner, E., Tyagi, N., Vasudev, P., Volynkin, V., Warner, K., Watkins, X., Zaru, R., Zellner, H., Bridge, A., Poux, S., Redaschi, N., Aimo, L., Argoud-Puy, G., Auchincloss, A., Axelsen, K., Bansal, P., Baratin, D., Blatter, M. C., Bolleman, J., Boutet, E., Breuza, L., Casals-Casas, C., de Castro, E., Echioukh, K. C., Coudert, E., Cuche, B., Doche, M., Dornevil, D., Estreicher, A., Famiglietti, M. L., Feuermann, M., Gasteiger, E., Gehant, S., Gerritsen, V., Gos, A., Gruaz-Gumowski, N., Hinz, U., Hulo, C., Hyka-Nouspikel, N., Jungo, F., Keller, G., Kerhornou, A., Lara, V., Le Mercier, P., Lieberherr, D., Lombardot, T., Martin, X., Masson, P., Morgat, A., Neto, T. B., Paesano, S., Pedruzzi, I., Pilbout, S., Pourcel, L., Pozzato, M., Pruess, M., Rivoire, C., Sigrist, C., Sonesson, K., Stutz, A., Sundaram, S., Tognolli, M., Verbregue, L., Wu, C. H., Arighi, C. N., Arminski, L., Chen, C., Chen, Y., Garavelli, J. S., Huang, H., Laiho, K., McGarvey, P., Natale, D. A., Ross, K., Vinayaka, C. R., Wang, Q., Wang, Y., Yeh, L. S., and Zhang, J. UniProt:

The universal protein knowledgebase in 2021. *Nucleic Acids Research*, 49(D1): D480–D489, jan 2021. ISSN 13624962. doi: 10.1093/nar/gkaa1100. URL https://academic.oup.com/nar/article/49/D1/D480/6006196.

Baxter, J. C. and Funnell, B. E. Plasmid partition mechanisms. *Microbiology Spectrum*, 2(6), nov 2014. ISSN 21650497. doi: 10.1128/microbiolspec.plas-0023-2014. URL https://journals.asm.org/doi/10.1128/microbiolspec.PLAS-0023-2014.

Beal, J., Farny, N. G., Haddock-Angelli, T., Selvarajah, V., Baldwin, G. S., Buckley-Taylor, R., Gershater, M., Kiga, D., Marken, J., Sanchania, V., Sison, A., and Workman, C. T. Robust estimation of bacterial cell count from optical density. *Communications Biology*, 3(1):512, dec 2020. ISSN 2399-3642. doi: 10.1038/s42003-020-01127-5. URL http://www.nature.com/articles/s42003-020-01127-5.

Bell, G. and MacLean, C. The search for 'evolution-proof' antibiotics, jun 2018. ISSN 18784380. URL https://www.sciencedirect.com/science/article/pii/S0966842X17302548?via%3Dihub.

Bender, R. A. A NAC for regulating metabolism: The nitrogen assimilation control protein (NAC) from Klebsiella pneumoniae, oct 2010. ISSN 00219193. URL http://www.ncbi.nlm.nih.gov/pubmed/20675498http://www.pubmedcentral.nih.gov/articlerender.fcgi?artid=PMC2944532.

Bengtsson-Palme, J., Kristiansson, E., and Larsson, D. G. Environmental factors influencing the development and spread of antibiotic resistance, jan 2018. ISSN 15746976. URL https://academic.oup.com/femsre/article/doi/10.1093/femsre/fux053/4563583.

Bervoets, I. and Charlier, D. Diversity, versatility and complexity of bacterial gene regulation mechanisms: Opportunities and drawbacks for applications in synthetic biology. *FEMS Microbiology Reviews*, 43(3):304–339, may 2019. ISSN 1574-

6976. doi: 10.1093/femsre/fuz001. URL https://academic.oup.com/femsre/article/43/3/304/5306444.

Bethke, J. H., Davidovich, A., Cheng, L., Lopatkin, A. J., Song, W., Thaden, J. T., Fowler, V. G., Xiao, M., and You, L. Environmental and genetic determinants of plasmid mobility in pathogenic *Escherichia coli*. *Science Advances*, 6(4):eaax3173, jan 2020. ISSN 23752548. doi: 10.1126/sciadv.aax3173. URL https://advances.sciencemag.org/lookup/doi/10.1126/sciadv.aax3173.

Bialek-Davenet, S., Criscuolo, A., Ailloud, F., Passet, V., Jones, L., Delannoy-Vieillard, A. S., Garin, B., Hello, S. L., Arlet, G., Nicolas-Chanoine, M. H., Decré, D., and Brisse, S. Genomic definition of hypervirulent and multidrug-resistant *Klebsiella pneumoniae* clonal groups. *Emerging Infectious Diseases*, 20(11):1812–1820, nov 2014. ISSN 10806059. doi: 10.3201/eid2011.140206. URL http://www.ncbi.nlm.nih.gov/pubmed/25341126http://www.pubmedcentral.nih.gov/articlerender.fcgi?artid=PMC4214299http://wwwnc.cdc.gov/eid/article/20/11/14-0206_article.htm.

Billane, K., Harrison, E., Cameron, D., and Brockhurst, M. A. Why do plasmids manipulate the expression of bacterial phenotypes? *Philosophical Transactions of the Royal Society B: Biological Sciences*, 377(1842), jan 2022. ISSN 14712970. doi: 10.1098/rstb.2020.0461. URL https://royalsocietypublishing.org/doi/10.1098/rstb.2020.0461.

Bingle, L. E. and Thomas, C. M. Regulatory circuits for plasmid survival, 2001. ISSN 13695274. URL https://pdf.sciencedirectassets.com/272017/1-s2.0-S1369527400X00112/1-s2.0-S1369527400001880/main.pdf?x-amz-security-token=AgoJb3JpZ2luX2VjEAYaCXVzLWVhc3QtMSJGMEQCIEE%2BjaA75Wce7gOFPke6%2FdRyoljg0XTPBw6gnbITGcg2AiBctD6pvDCgpLYDFvSlEibpPSQoy9bNk8zKjUqEWZmS.

Blair, J., Richmond, G. E., and Piddock, L. J. Multidrug efflux pumps in Gram-

negative bacteria and their role in antibiotic resistance. *Future Microbiol*, 9(10): 1165–1177, 2014. ISSN 1746-0913. doi: 10.2217/FMB.14.66.

Blair, J. M., Webber, M. A., Baylay, A. J., Ogbolu, D. O., and Piddock, L. J. Molecular mechanisms of antibiotic resistance. *Nature Reviews Microbiology*, 47(14):4055–4061, jan 2011. ISSN 1364-548X. doi: 10.1039/c0cc05111j. URL http://www.nature.com/articles/nrmicro3380http://dx.doi.org/10.1038/nrmicro3380.

Blair, J. M., Webber, M. A., Baylay, A. J., Ogbolu, D. O., and Piddock, L. J. Molecular mechanisms of antibiotic resistance, jan 2015. ISSN 17401534. URL http://www.nature.com/articles/nrmicro3380.

Bolger, A. M., Lohse, M., and Usadel, B. Trimmomatic: A flexible trimmer for Illumina sequence data. *Bioinformatics*, 30(15):2114–2120, aug 2014. ISSN 14602059. doi: 10.1093/bioinformatics/btu170. URL https://academic.oup.com/bioinformatics/article-lookup/doi/10.1093/bioinformatics/btu170.

Bonnin, R. A., Jousset, A. B., Chiarelli, A., Emeraud, C., Glaser, P., Naas, T., and Dortet, L. Emergence of new non-clonal group 258 high-risk clones among *Klebsiella pneumoniae* carbapenemase-producing *K. pneumoniae* isolates, France. *Emerging Infectious Diseases*, 26(6):1212–1220, jun 2020. ISSN 10806059. doi: 10.3201/EID2606.191517. URL http://wwwnc.cdc.gov/eid/article/26/6/19-1517_article.htm.

Bortolaia, V., Kaas, R. S., Ruppe, E., Roberts, M. C., Schwarz, S., Cattoir, V., Philippon, A., Allesoe, R. L., Rebelo, A. R., Florensa, A. F., Fagelhauer, L., Chakraborty, T., Neumann, B., Werner, G., Bender, J. K., Stingl, K., Nguyen, M., Coppens, J., Xavier, B. B., Malhotra-Kumar, S., Westh, H., Pinholt, M., Anjum, M. F., Duggett, N. A., Kempf, I., Nykäsenoja, S., Olkkola, S., Wieczorek, K., Amaro, A., Clemente, L., Mossong, J., Losch, S., Ragimbeau, C., Lund, O., and Aarestrup, F. M. ResFinder 4.0 for predictions of phenotypes from

genotypes. *Journal of Antimicrobial Chemotherapy*, 75(12):3491–3500, aug 2020. ISSN 14602091. doi: 10.1093/jac/dkaa345. URL https://academic.oup.com/jac/advance-article/doi/10.1093/jac/dkaa345/5890997.

Bradley, D. E., Taylor, D. E., and Cohen, D. R. Specification of surface mating systems among conjugative drug resistance plasmids in *Escherichia coli* K-12. *Journal of Bacteriology*, 143(3):1466–1470, sep 1980. ISSN 00219193. doi: 10.1128/jb.143.3.1466-1470.1980. URL http://www.ncbi.nlm.nih.gov/pubmed/6106013http://www.pubmedcentral.nih.gov/articlerender.fcgi?artid=PMC294536.

Bray, N. L., Pimentel, H., Melsted, P., and Pachter, L. Near-optimal probabilistic RNA-seq quantification. *Nature Biotechnology*, 34(5):525–527, may 2016. ISSN 15461696. doi: 10.1038/nbt.3519. URL http://www.nature.com/articles/nbt.3519.

Brennan-Krohn, T., Smith, K. P., and Kirby, J. E. The poisoned well: Enhancing the predictive value of antimicrobial susceptibility testing in the era of multidrug resistance, 2017. ISSN 1098660X. URL http://www.ncbi.nlm.nih.gov/pubmed/28468856http://www.pubmedcentral.nih.gov/articlerender.fcgi?artid=PMC5527407.

Broberg, C. A., Wu, W., Cavalcoli, J. D., Miller, V. L., and Bachman, M. A. Complete genome sequence of *Klebsiella pneumoniae* strain ATCC 43816 KPPR1, a rifampin-resistant mutant commonly used in animal, genetic, and molecular biology studies. *Genome announcements*, 2(5), sep 2014. ISSN 2169-8287. doi: 10.1128/genomeA.00924-14. URL http://www.ncbi.nlm.nih.gov/pubmed/25291761http://www.pubmedcentral.nih.gov/articlerender.fcgi?artid=PMC4175196.

Buckner, M. M., Laura Ciusa, M., Meek, R. W., Moorey, A. R., McCallum, G. E., Prentice, E. L., Reid, J. P., Alderwick, L. J., Di Maio, A., and Piddock, L. J. HIV

drugs inhibit transfer of plasmids carrying extended-spectrum β-lactamase and carbapenemase genes. *mBio*, 11(1), 2020. ISSN 21507511. doi: 10.1128/mBio.03355-19. URL https://doi.org/10.1128/mBio.03355-19.

Buckner, M. M. C., Ciusa, M. L., and Piddock, L. J. V. Strategies to combat antimicrobial resistance: Anti-plasmid and plasmid curing. *FEMS microbiology reviews*, In Press(Accepted), jul 2018. ISSN 1574-6976. doi: 10.1093/femsre/fuy031. URL https://academic.oup.com/femsre/advance-article/doi/10.1093/femsre/fuy031/5061628.

Burmølle, M., Bahl, M. I., Jensen, L. B., Sørensen, S. J., and Hansen, L. H. Type 3 fimbriae, encoded by the conjugative plasmid pOLA52, enhance biofilm formation and transfer frequencies in *Enterobacteriaceae* strains. *Microbiology*, 154(1):187–195, jan 2008. ISSN 13500872. doi: 10.1099/mic.0.2007/010454-0. URL https://www.microbiologyresearch.org/content/journal/micro/10.1099/mic.0.2007/010454-0.

Burrus, V., Pavlovic, G., Decaris, B., and Guédon, G. Conjugative transposons: The tip of the iceberg, nov 2002. ISSN 0950382X. URL http://www.ncbi.nlm.nih.gov/pubmed/12410819.

Bush, K. and Bradford, P. A. β-lactams and β-lactamase inhibitors: An overview. *Cold Spring Harbor Perspectives in Medicine*, 6(8):a025247, aug 2016. ISSN 21571422. doi: 10.1101/cshperspect.a025247. URL http://www.ncbi.nlm.nih.gov/pubmed/27329032http://www.pubmedcentral.nih.gov/articlerender.fcgi?artid=PMC4968164.

Bush, K. and Bradford, P. A. Interplay between β-lactamases and new β-lactamase inhibitors, may 2019. ISSN 17401534. URL http://www.nature.com/articles/s41579-019-0159-8.

Bush, K. and Jacoby, G. A. Updated functional classification of β-lactamases, mar 2010. ISSN 00664804. URL http://www.ncbi.nlm.nih.gov/pubmed/

19995920http://www.pubmedcentral.nih.gov/articlerender.fcgi?artid=PMC2825993.

Cabezón, E., Ripoll-Rozada, J., Peña, A., de la Cruz, F., and Arechaga, I. Towards an integrated model of bacterial conjugation, sep 2015. ISSN 15746976. URL https://academic.oup.com/femsre/article-lookup/doi/10.1111/1574-6976.12085.

Cano, V., March, C., Insua, J. L., Aguiló, N., Llobet, E., Moranta, D., Regueiro, V., Brennan, G. P., Millán-Lou, M. I., Martín, C., Garmendia, J., and Bengoechea, J. A. *Klebsiella pneumoniae* survives within macrophages by avoiding delivery to lysosomes. *Cellular Microbiology*, 17(11):1537–1560, nov 2015. ISSN 14625822. doi: 10.1111/cmi.12466. URL http://doi.wiley.com/10.1111/cmi.12466.

Capy, P., Gasperi, G., Biémont, C., and Bazin, C. Stress and transposable elements: Co-evolution or useful parasites?, aug 2000. ISSN 0018067X. URL http://www.nature.com/doifinder/10.1046/j.1365-2540.2000.00751.x.

Carabarin-Lima, A., León-Izurieta, L., del Carmen Rocha-Gracia, R., Castañeda-Lucio, M., Torres, C., Gutiérrez-Cazarez, Z., González-Posos, S., Martínez de la Peña, C. F., Martinez-Laguna, Y., and Lozano-Zarain, P. First evidence of polar flagella in *Klebsiella pneumoniae* isolated from a patient with neonatal sepsis. *Journal of Medical Microbiology*, 65(8):729–737, aug 2016. ISSN 00222615. doi: 10.1099/jmm.0.000291. URL https://www.microbiologyresearch.org/content/journal/jmm/10.1099/jmm.0.000291.

Carattoli, A. Plasmids and the spread of resistance, aug 2013. ISSN 14384221. URL https://www.sciencedirect.com/science/article/pii/S1438422113000167.

Carattoli, A., Zankari, E., Garciá-Fernández, A., Larsen, M. V., Lund, O., Villa, L., Aarestrup, F. M., and Hasman, H. *In silico* detection and typing of plasmids using plasmidfinder and plasmid multilocus sequence typing. *Antimicrobial Agents*

and Chemotherapy, 58(7):3895–3903, jul 2014. ISSN 10986596. doi: 10.1128/AAC.02412-14. URL http://www.ncbi.nlm.nih.gov/pubmed/24777092http://www.pubmedcentral.nih.gov/articlerender.fcgi?artid=PMC4068535.

Carranza, G., Menguiano, T., Valenzuela-Gómez, F., García-Cazorla, Y., Cabezón, E., and Arechaga, I. Monitoring bacterial conjugation by optical microscopy. *Frontiers in Microbiology*, 12:2982, oct 2021. ISSN 1664302X. doi: 10.3389/fmicb.2021.750200. URL https://www.frontiersin.org/articles/10.3389/fmicb.2021.750200/full.

Carroll, A. C. and Wong, A. Plasmid persistence: Costs, benefits and the plasmid paradox. *Canadian Journal of Microbiology*, 64(5):293–304, may 2018. ISSN 0008-4166. doi: 10.1139/cjm-2017-0609. URL http://www.nrcresearchpress.com/doi/10.1139/cjm-2017-0609.

CDC. National action plan for combating antibiotic-resistant bacteria 2020-2025. Number October. 2020. URL https://aspe.hhs.gov/sites/default/files/migrated_legacy_files//196436/CARB-National-Action-Plan-2020-2025.pdf.

Chan, W., Costantino, N., Li, R., Lee, S. C., Su, Q., Melvin, D., Court, D. L., and Liu, P. A recombineering based approach for high-throughput conditional knockout targeting vector construction. *Nucleic Acids Research*, 35(8):e64, 2007. ISSN 03051048. doi: 10.1093/nar/gkm163. URL https://www.ncbi.nlm.nih.gov/pmc/articles/PMC1885671/.

Chandramohan, L. and Revell, P. A. Prevalence and molecular characterization of extended-spectrum-β-lactamase-producing *Enterobacteriaceae* in a pediatric patient population. *Antimicrobial Agents and Chemotherapy*, 56(9):4765–4770, sep 2012. ISSN 0066-4804. doi: 10.1128/aac.00666-12. URL http://www.ncbi.nlm.nih.gov/pubmed/22733062http://www.pubmedcentral.nih.gov/articlerender.fcgi?artid=PMC3421901.

Chase, G. R. and Hoel, D. G. Serial dilutions: Error effects and optimal designs. *Biometrika*, 62(2):329–334, 1975. ISSN 00063444. doi: 10.1093/biomet/62.2.329. URL https://academic.oup.com/biomet/article/62/2/329/337083.

Chen, L., Chavda, K. D., Melano, R. G., Jacobs, M. R., Koll, B., Hong, T., Rojtman, A. D., Levi, M. H., Bonomo, R. A., and Kreiswirth, B. N. Comparative genomic analysis of KPC-encoding pKpQIL-like plasmids and their distribution in New Jersey and New York Hospitals. *Antimicrobial Agents and Chemotherapy*, 58(5):2871–7, may 2014. ISSN 1098-6596. doi: 10.1128/AAC.00120-14. URL http://www.ncbi.nlm.nih.gov/pubmed/24614371http://www.pubmedcentral.nih.gov/articlerender.fcgi?artid=PMC3993205.

Chen, L. M. and Maloy, S. Regulation of proline utilization in enteric bacteria: cloning and characterization of the Klebsiella put control region. *Journal of bacteriology*, 173(2):783–90, jan 1991. ISSN 0021-9193. doi: 10.1128/jb.173.2.783-790.1991. URL http://www.ncbi.nlm.nih.gov/pubmed/1987164http://www.pubmedcentral.nih.gov/articlerender.fcgi?artid=PMC207072.

Chhibber, S., Gondil, V. S., Sharma, S., Kumar, M., Wangoo, N., and Sharma, R. K. A novel approach for combating *Klebsiella pneumoniae* biofilm using histidine functionalized silver nanoparticles. *Frontiers in Microbiology*, 8(JUN):1104, jun 2017. ISSN 1664302X. doi: 10.3389/fmicb.2017.01104. URL http://journal.frontiersin.org/article/10.3389/fmicb.2017.01104/full.

Choby, J. E., Howard-Anderson, J., and Weiss, D. S. Hypervirulent *Klebsiella pneumoniae* – Clinical and molecular perspectives, mar 2020. ISSN 13652796. URL https://onlinelibrary.wiley.com/doi/10.1111/joim.13007.

Christensen, B. B., Sternberg, C., Andersen, J. B., Eberl, L., Møller, S., Givskov, M., and Molin, S. Establishment of new genetic traits in a microbial biofilm community. *Applied and Environmental Microbiology*, 64(6):2247–2255, jun 1998. ISSN 00992240. doi: 10.1128/aem.64.6.2247-2255.1998. URL https://journals.asm.org/doi/10.1128/AEM.64.6.2247-2255.1998.

Clarke, M., Maddera, L., Harris, R. L., and Silverman, P. M. F-pili dynamics by live-cell imaging. *Proceedings of the National Academy of Sciences of the United States of America*, 105(46):17978–17981, nov 2008. ISSN 00278424. doi: 10.1073/pnas.0806786105. URL http://www.ncbi.nlm.nih.gov/pubmed/19004777http://www.pubmedcentral.nih.gov/articlerender.fcgi?artid=PMC2582581.

Clegg, S. and Murphy, C. N. Epidemiology and Virulence of *Klebsiella pneumoniae*. *Microbiology Spectrum*, 4(1), 2016. ISSN 21650497. doi: 10.1128/microbiolspec.uti-0005-2012. URL https://journals.asm.org/doi/10.1128/microbiolspec.UTI-0005-2012.

Consuegra, J., Gaffé, J., Lenski, R. E., Hindré, T., Barrick, J. E., Tenaillon, O., and Schneider, D. Insertion-sequence-mediated mutations both promote and constrain evolvability during a long-term experiment with bacteria. *Nature Communications*, 12(1):980, dec 2021. ISSN 20411723. doi: 10.1038/s41467-021-21210-7. URL http://www.nature.com/articles/s41467-021-21210-7.

Cosma, A. The nightmare of a single cell: Being a doublet, aug 2020. ISSN 15524930. URL https://onlinelibrary.wiley.com/doi/10.1002/cyto.a.23929.

Costa, D. M., Johani, K., Melo, D. S., Lopes, L. K., Lopes Lima, L. K., Tipple, A. F., Hu, H., and Vickery, K. Biofilm contamination of high-touched surfaces in intensive care units: Epidemiology and potential impacts. *Letters in Applied Microbiology*, 68(4):269–276, apr 2019. ISSN 1472765X. doi: 10.1111/lam.13127. URL https://onlinelibrary.wiley.com/doi/10.1111/lam.13127.

Cottell, J. L., Saw, H. T., Webber, M. A., and Piddock, L. J. Functional genomics to identify the factors contributing to successful persistence and global spread of an antibiotic resistance plasmid. *BMC Microbiology*, 14(1):168, jun 2014. ISSN 14712180. doi: 10.1186/1471-2180-14-168. URL http://bmcmicrobiol.biomedcentral.com/articles/10.1186/1471-2180-14-168.

Cui, X., Zhang, H., and Du, H. Carbapenemases in *Enterobacteriaceae*: De-

tection and antimicrobial therapy, aug 2019. ISSN 1664302X. URL https://www.frontiersin.org/article/10.3389/fmicb.2019.01823/full.

Currie, C. J., Berni, E., Jenkins-Jones, S., Poole, C. D., Ouwens, M., Driessen, S., De Voogd, H., Butler, C. C., and Morgan, C. L. Antibiotic treatment failure in four common infections in UK primary care 1991-2012: Longitudinal analysis. *BMJ (Online)*, 349:g5493, sep 2014. ISSN 17561833. doi: 10.1136/bmj.g5493. URL http://www.ncbi.nlm.nih.gov/pubmed/25249162.

Cusumano, J. A., Caffrey, A. R., Daffinee, K. E., Luther, M. K., Lopes, V., and LaPlante, K. L. Weak biofilm formation among carbapenem-resistant *Klebsiella pneumoniae*. *Diagnostic Microbiology and Infectious Disease*, 95(4):114877, dec 2019. ISSN 18790070. doi: 10.1016/j.diagmicrobio.2019.114877. URL https://www.sciencedirect.com/science/article/pii/S0732889319302391.

Dadgostar, P. Antimicrobial resistance: Implications and costs, 2019. ISSN 11786973. URL http://www.ncbi.nlm.nih.gov/pubmed/31908502http://www.pubmedcentral.nih.gov/articlerender.fcgi?artid=PMC6929930.

Darphorn, T. S., Bel, K., Koenders-van Sint Anneland, B. B., Brul, S., and Ter Kuile, B. H. Antibiotic resistance plasmid composition and architecture in *Escherichia coli* isolates from meat. *Scientific Reports*, 11(1):2136, dec 2021. ISSN 2045-2322. doi: 10.1038/s41598-021-81683-w. URL http://www.nature.com/articles/s41598-021-81683-w.

Datsenko, K. A. and Wanner, B. L. One-step inactivation of chromosomal genes in *Escherichia coli* K-12 using PCR products. *Proceedings of the National Academy of Sciences of the United States of America*, 97(12):6640–6645, 2000. ISSN 00278424. doi: 10.1073/pnas.120163297. URL www.pnas.orgcgidoi10.1073pnas.120163297.

Davey, H. M. and Kell, D. B. Flow cytometry and cell sorting of heterogeneous microbial populations: The importance of single-cell analyses.

Microbiological reviews, 60(4):641–96, 1996. ISSN 0146-0749. URL http://mmbr.asm.org/http://www.ncbi.nlm.nih.gov/pubmed/8987359%0Ahttp://www.pubmedcentral.nih.gov/articlerender.fcgi?artid=PMC239459.

David, S., Reuter, S., Harris, S. R., Glasner, C., Feltwell, T., Argimon, S., Abudahab, K., Goater, R., Giani, T., Errico, G., Aspbury, M., Sjunnebo, S., Koraqi, A., Lacej, D., Apfalter, P., Hartl, R., Glupczynski, Y., Huang, T. D., Strateva, T., Marteva-Proevska, Y., Andrasevic, A. T., Butic, I., Pieridou-Bagatzouni, D., Maikanti-Charalampous, P., Hrabak, J., Zemlickova, H., Hammerum, A., Jakobsen, L., Ivanova, M., Pavelkovich, A., Jalava, J., Österblad, M., Dortet, L., Vaux, S., Kaase, M., Gatermann, S. G., Vatopoulos, A., Tryfinopoulou, K., Tóth, Á., Jánvári, L., Boo, T. W., McGrath, E., Carmeli, Y., Adler, A., Pantosti, A., Monaco, M., Raka, L., Kurti, A., Balode, A., Saule, M., Miciuleviciene, J., Mierauskaite, A., Perrin-Weniger, M., Reichert, P., Nestorova, N., Debattista, S., Mijovic, G., Lopicic, M., Samuelsen, Ø., Haldorsen, B., Zabicka, D., Literacka, E., Caniça, M., Manageiro, V., Kaftandzieva, A., Trajkovska-Dokic, E., Damian, M., Lixandru, B., Jelesic, Z., Trudic, A., Niks, M., Schreterova, E., Pirs, M., Cerar, T., Oteo, J., Aracil, B., Giske, C., Sjöström, K., Gür, D., Cakar, A., Woodford, N., Hopkins, K., Wiuff, C., Brown, D. J., Feil, E. J., Rossolini, G. M., Aanensen, D. M., and Grundmann, H. Epidemic of carbapenem-resistant *Klebsiella pneumoniae* in Europe is driven by nosocomial spread. *Nature Microbiology*, 4(11): 1919–1929, nov 2019. ISSN 20585276. doi: 10.1038/s41564-019-0492-8. URL http://www.nature.com/articles/s41564-019-0492-8.

David, S., Cohen, V., Reuter, S., Sheppard, A. E., Giani, T., Parkhill, J., Rossolini, G. M., Feil, E. J., Grundmann, H., and Aanensen, D. M. Integrated chromosomal and plasmid sequence analyses reveal diverse modes of carbapenemase gene spread among *Klebsiella pneumoniae*. *Proceedings of the National Academy of Sciences of the United States of America*, 117(40):25043–25054, sep 2020. ISSN 10916490. doi: 10.1073/pnas.2003407117. URL http://www.ncbi.nlm.nih.gov/pubmed/32968015.

Davies, J. and Davies, D. Origins and evolution of antibiotic resistance. *Microbiology and Molecular Biology Reviews*, 74(3):417–433, sep 2010. ISSN 1092-2172. doi: 10.1128/MMBR.00016-10. URL http://www.ncbi.nlm.nih.gov/pubmed/20805405http://www.pubmedcentral.nih.gov/articlerender.fcgi?artid=PMC2937522http://mmbr.asm.org/cgi/doi/10.1128/MMBR.00016-10.

De La Cruz, F., Frost, L. S., Meyer, R. J., and Zechner, E. L. Conjugative DNA metabolism in Gram-negative bacteria, jan 2010. ISSN 01686445. URL https://academic.oup.com/femsre/article-lookup/doi/10.1111/j.1574-6976.2009.00195.x.

De Maio, N., Shaw, L. P., Hubbard, A., George, S., Sanderson, N. D., Swann, J., Wick, R., Oun, M. A., Stubberfield, E., Hoosdally, S. J., Crook, D. W., Peto, T. E., Sheppard, A. E., Bailey, M. J., Read, D. S., Anjum, M. F., Sarah Walker, A., and Stoesser, N. Comparison of long-read sequencing technologies in the hybrid assembly of complex bacterial genomes. *Microbial Genomics*, 5(9), sep 2019. ISSN 20575858. doi: 10.1099/mgen.0.000294. URL http://www.ncbi.nlm.nih.gov/pubmed/31483244http://www.pubmedcentral.nih.gov/articlerender.fcgi?artid=PMC6807382https://www.microbiologyresearch.org/content/journal/mgen/10.1099/mgen.0.000294.

De Oliveira, D. M., Forde, B. M., Kidd, T. J., Harris, P. N., Schembri, M. A., Beatson, S. A., Paterson, D. L., and Walker, M. J. Antimicrobial resistance in ESKAPE pathogens. *Clinical Microbiology Reviews*, 33(3), jun 2020. ISSN 10986618. doi: 10.1128/CMR.00181-19. URL https://journals.asm.org/doi/10.1128/CMR.00181-19.

de Sales, R. O., Migliorini, L. B., Puga, R., Kocsis, B., and Severino, P. A core genome multilocus sequence typing scheme for *Pseudomonas aeruginosa*. *Frontiers in Microbiology*, 11:1049, may 2020. ISSN 1664302X. doi:

10.3389/fmicb.2020.01049. URL https://www.frontiersin.org/article/10.3389/fmicb.2020.01049/full.

del Campo, I., Ruiz, R., Cuevas, A., Revilla, C., Vielva, L., and De la Cruz, F. Determination of conjugation rates on solid surfaces. *Plasmid*, 67(2):174–182, mar 2012. ISSN 0147619X. doi: 10.1016/j.plasmid.2012.01.008. URL https://www.sciencedirect.com/science/article/pii/S0147619X12000121?via%3Dihub.

Department of Health and Social Care. Projects supported by DHSC through the Global AMR Innovation Fund. 1(May):1–13, 2020. URL https://assets.publishing.service.gov.uk/government/uploads/system/uploads/attachment_data/file/886146/projects-funded-by-GAMRIF.pdf.

Devanga Ragupathi, N. K., Muthuirulandi Sethuvel, D. P., Triplicane Dwarakanathan, H., Murugan, D., Umashankar, Y., Monk, P. N., Karunakaran, E., and Veeraraghavan, B. The influence of biofilms on carbapenem susceptibility and patient outcome in device associated *K. pneumoniae* infections: Insights into phenotype vs genome-wide analysis and correlation. *Frontiers in Microbiology*, 11: 3220, dec 2020. ISSN 1664302X. doi: 10.3389/fmicb.2020.591679. URL https://www.frontiersin.org/articles/10.3389/fmicb.2020.591679/full.

Diancourt, L., Passet, V., Verhoef, J., Grimont, P. A., and Brisse, S. Multilocus sequence typing of *Klebsiella pneumoniae* nosocomial isolates. *Journal of Clinical Microbiology*, 43(8):4178–4182, aug 2005. ISSN 00951137. doi: 10.1128/JCM.43.8.4178-4182.2005. URL http://www.ncbi.nlm.nih.gov/pubmed/16081970http://www.pubmedcentral.nih.gov/articlerender.fcgi?artid=PMC1233940.

Dimitriu, T., Marchant, L., Buckling, A., and Raymond, B. Bacteria from natural populations transfer plasmids mostly towards their kin. *Proceedings of the Royal Society B: Biological Sciences*, 286(1905):20191110, jun 2019. ISSN 14712954. doi: 10.1098/rspb.2019.1110. URL https://royalsocietypublishing.org/doi/10.1098/rspb.2019.1110.

Dimitriu, T., Matthews, A. C., and Buckling, A. Increased copy number couples the evolution of plasmid horizontal transmission and plasmid-encoded antibiotic resistance. *Proceedings of the National Academy of Sciences of the United States of America*, 118(31), aug 2021. ISSN 10916490. doi: 10.1073/pnas.2107818118. URL http://www.ncbi.nlm.nih.gov/pubmed/34326267http://www.pubmedcentral.nih.gov/articlerender.fcgi?artid=PMC8346908.

Donlan, R. M. Biofilms: Microbial life on surfaces. *Emerging infectious diseases*, 8(9):881–90, sep 2002. ISSN 1080-6040. doi: 10.3201/eid0809.020063. URL http://www.ncbi.nlm.nih.gov/pubmed/12194761http://www.pubmedcentral.nih.gov/articlerender.fcgi?artid=PMC2732559.

Donnenberg, A. D. and Donnenberg, V. S. Rare-event analysis in flow cytometry, sep 2007. ISSN 02722712. URL http://www.ncbi.nlm.nih.gov/pubmed/17658410.

Dookie, N., Sturm, A. W., and Moodley, P. Mechanisms of first-line antimicrobial resistance in multi-drug and extensively drug resistant strains of *Mycobacterium tuberculosis* in KwaZulu-Natal, South Africa. *BMC Infectious Diseases*, 16(1):609, oct 2016. ISSN 14712334. doi: 10.1186/s12879-016-1906-3. URL http://www.ncbi.nlm.nih.gov/pubmed/27784282http://www.pubmedcentral.nih.gov/articlerender.fcgi?artid=PMC5080726.

Dorado-Morales, P., Pilar Garcillán-Barcia, M., Lasa, I., and Solano, C. Fitness cost evolution of natural plasmids of *Staphylococcus aureus*. *mBio*, 12(1):1–18, feb 2021. ISSN 21507511. doi: 10.1128/mBio.03094-20. URL https://journals.asm.org/doi/10.1128/mBio.03094-20.

Dorman, M. J., Feltwell, T., Goulding, D. A., Parkhill, J., and Short, F. L. The capsule regulatory network of *Klebsiella pneumoniae* defined by density-traDISort. *mBio*, 9(6), 2018. ISSN 21507511. doi: 10.1128/mBio.01863-18. URL https://www.ncbi.nlm.nih.gov/pmc/articles/PMC6247091/#textS1.

Doron, S. and Davidson, L. E. Antimicrobial stewardship. In *Mayo Clinic Proceed-*

ings, volume 86, pages 1113–1123. Mayo Foundation, nov 2011. doi: 10.4065/mcp.2011.0358. URL http://www.ncbi.nlm.nih.gov/pubmed/22033257http://www.pubmedcentral.nih.gov/articlerender.fcgi?artid=PMC3203003.

Dostál, L., Shao, S., and Schildbach, J. F. Tracking F plasmid TraI relaxase processing reactions provides insight into F plasmid transfer. *Nucleic Acids Research*, 39(7):2658–2670, apr 2011. ISSN 03051048. doi: 10.1093/nar/gkq1137. URL http://www.ncbi.nlm.nih.gov/pubmed/21109533http://www.pubmedcentral.nih.gov/articlerender.fcgi?artid=PMC3074121.

Dötsch, A., Eckweiler, D., Schniederjans, M., Zimmermann, A., Jensen, V., Scharfe, M., Geffers, R., and Häussler, S. The *Pseudomonas aeruginosa* transcriptome in planktonic cultures and static biofilms using RNA Sequencing. *PLoS ONE*, 7 (2):e31092, feb 2012. ISSN 1932-6203. doi: 10.1371/journal.pone.0031092. URL https://dx.plos.org/10.1371/journal.pone.0031092.

Doumith, M., Findlay, J., Hirani, H., Hopkins, K. L., Livermore, D. M., Dodgson, A., and Woodford, N. Major role of pKpQIL-like plasmids in the early dissemination of KPC-type carbapenemases in the UK. *Journal of Antimicrobial Chemotherapy*, 72(8):2241–2248, aug 2017. ISSN 14602091. doi: 10.1093/jac/dkx141. URL https://pdf.sciencedirectassets.com/272017/1-s2.0-S1369527400X00112/1-s2.0-S1369527400001880/main.pdf?x-amz-security-token=AgoJb3JpZ2luX2VjEAYaCXVzLWVhc3QtMSJGMEQCIEE%2BjaA75Wce7gOFPke6%2FdRyoljg0XTPBw6gnbITGcg2AiBctD6pvDCgpLYDFvSlEibpPSQoy9bNk8zKj\UqEWZmS.

Dubey, A. K., Baker, C. S., Romeo, T., and Babitzke, P. RNA sequence and secondary structure participate in high-affinity CsrA-RNA interaction. *RNA*, 11(10):1579–1587, oct 2005. ISSN 13558382. doi: 10.1261/rna.2990205. URL http://www.ncbi.nlm.nih.gov/pubmed/16131593http://www.pubmedcentral.nih.gov/articlerender.fcgi?artid=PMC1370842.

Dunn, S., Carrilero, L., Brockhurst, M., and McNally, A. Limited and strain-specific transcriptional and growth responses to acquisition of a multidrug resistance plasmid in genetically diverse *Escherichia coli* lineages. *mSystems*, 6 (2), apr 2021. ISSN 2379-5077. doi: 10.1128/msystems.00083-21. URL https://journals.asm.org/doi/10.1128/mSystems.00083-21.

Fair, R. J. and Tor, Y. Antibiotics and bacterial resistance in the 21st century. *Perspectives in Medicinal Chemistry*, 6(6):25–64, 2014. ISSN 1177391X. doi: 10.4137/PMC.S14459. URL http://www.ncbi.nlm.nih.gov/pubmed/25232278http://www.pubmedcentral.nih.gov/articlerender.fcgi?artid=PMC4159373.

Fan, C., Wu, Y. H., Decker, C. M., Rohani, R., Gesell Salazar, M., Ye, H., Cui, Z., Schmidt, F., and Huang, W. E. Defensive function of transposable elements in bacteria. *ACS Synthetic Biology*, 8(9):2141–2151, sep 2019. ISSN 21615063. doi: 10.1021/acssynbio.9b00218. URL https://pubs.acs.org/doi/10.1021/acssynbio.9b00218.

Fernandez-Lopez, R., de Toro, M., Moncalian, G., Garcillan-Barcia, M. P., and de la Cruz, F. Comparative genomics of the conjugation region of F-like plasmids: Five shades of F. *Frontiers in Molecular Biosciences*, 3(NOV), 2016. ISSN 2296889X. doi: 10.3389/fmolb.2016.00071. URL https://www.ncbi.nlm.nih.gov/pmc/articles/PMC5102898/.

Ferreira, C., Bikkarolla, S. K., Frykholm, K., Pohjanen, S., Brito, M., Lameiras, C., Nunes, O. C., Westerlund, F., and Manaia, C. M. Polyphasic characterization of carbapenemresistant *Klebsiella pneumoniae* clinical isolates suggests vertical transmission of the $bla_{\text{KPC-3 gene}}$. *PLoS ONE*, 16 (2 Febuary):e0247058, 2021. ISSN 19326203. doi: 10.1371/journal.pone.0247058. URL http://www.ncbi.nlm.nih.gov/pubmed/33635888http://www.pubmedcentral.nih.gov/articlerender.fcgi?artid=PMC7909683.

Flores-Mireles, A. L., Walker, J. N., Caparon, M., and Hultgren, S. J. Urinary tract

infections: Epidemiology, mechanisms of infection and treatment options, may 2015. ISSN 17401534. URL http://www.nature.com/articles/nrmicro3432.

Fodah, R. A., Scott, J. B., Tam, H. H., Yan, P., Pfeffer, T. L., Bundschuh, R., and Warawa, J. M. Correlation of *Klebsiella pneumoniae* comparative genetic analyses with virulence profiles in a murine respiratory disease model. *PLoS ONE*, 9(9), 2014. ISSN 19326203. doi: 10.1371/journal.pone.0107394. URL https://www.ncbi.nlm.nih.gov/pmc/articles/PMC4159340/.

Forage, R. G. and Lin, E. C. *dha* System mediating aerobic and anaerobic dissimilation of glycerol in *Klebsiella pneumoniae* NCIB 418. *Journal of Bacteriology*, 151(2):591–599, 1982. ISSN 00219193. URL https://www.ncbi.nlm.nih.gov/pmc/articles/PMC220299/pdf/jbacter00255-0073.pdf.

Frost, L. S., Ippen-Ihler, K., and Skurray, R. A. Analysis of the sequence and gene products of the transfer region of the F sex factor, 1994. ISSN 01460749. URL http://mmbr.asm.org/.

Gabrielaite, M. and Marvig, R. L. GenAPI: A tool for gene absence-presence identification in fragmented bacterial genome sequences. *BMC Bioinformatics*, 21(1):320, dec 2020. ISSN 14712105. doi: 10.1186/s12859-020-03657-5. URL https://bmcbioinformatics.biomedcentral.com/articles/10.1186/s12859-020-03657-5.

Gama, J. A., Fredheim, E. G., Cléon, F., Reis, A. M., Zilhão, R., and Dionisio, F. Dominance between plasmids determines the extent of biofilm formation. *Frontiers in Microbiology*, 11:2070, aug 2020. ISSN 1664302X. doi: 10.3389/fmicb.2020.02070. URL https://www.frontiersin.org/article/10.3389/fmicb.2020.02070/full.

Garrett, T. R., Bhakoo, M., and Zhang, Z. Bacterial adhesion and biofilms on surfaces, sep 2008. ISSN 10020071. URL https://www.sciencedirect.com/science/article/pii/S1002007108002049.

George, S., Pankhurst, L., Hubbard, A., Votintseva, A., Stoesser, N., Sheppard, A. E., Mathers, A., Norris, R., Navickaite, I., Eaton, C., Iqbal, Z., Crook, D. W., and Phan, H. T. Resolving plasmid structures in *Enterobacteriaceae* using the MinION nanopore sequencer: Assessment of MinION and MinION/illumina hybrid data assembly approaches. *Microbial Genomics*, 3(8), 2017. ISSN 20575858. doi: 10.1099/mgen.0.000118. URL https://www.ncbi.nlm.nih.gov/pmc/articles/PMC5610714/.

Ghigo, J. M. Natural conjugative plasmids induce bacterial biofilm development. *Nature*, 412(6845):442–445, jul 2001. ISSN 00280836. doi: 10.1038/35086581. URL http://www.nature.com/articles/35086581.

Giesecke, C., Feher, K., von Volkmann, K., Kirsch, J., Radbruch, A., and Kaiser, T. Determination of background, signal-to-noise, and dynamic range of a flow cytometer: A novel practical method for instrument characterization and standardization. *Cytometry Part A*, 91(11):1104–1114, nov 2017. ISSN 15524930. doi: 10.1002/cyto.a.23250. URL https://onlinelibrary.wiley.com/doi/10.1002/cyto.a.23250.

Gollan, B., Grabe, G., Michaux, C., and Helaine, S. Bacterial persisters and infection: Past, present, and progressing, sep 2019. ISSN 15453251. URL https://www.annualreviews.org/doi/10.1146/annurev-micro-020518-115650.

Gomes, A. É. I., Pacheco, T., dos Santos, C. d. S., Pereira, J. A., Ribeiro, M. L., Darrieux, M., and Ferraz, L. F. C. Functional insights from KpfR, a new transcriptional regulator of fimbrial expression that is crucial for *Klebsiella pneumoniae* pathogenicity. *Frontiers in Microbiology*, 11, 2021. ISSN 1664302X. doi: 10.3389/fmicb.2020.601921. URL https://doi.org/10.1101/2020.08.31.276717.

Gomez-Simmonds, A. and Uhlemann, A. C. Clinical implications of genomic adaptation and evolution of carbapenem-resistant *Klebsiella pneumoniae*. *Journal of Infectious Diseases*, 215(Suppl 1):S18–S27, 2017. ISSN 15376613. doi:

10.1093/infdis/jiw378. URL https://www.ncbi.nlm.nih.gov/pmc/articles/PMC5853309/.

Goren, M. G., Carmeli, Y., Schwaber, M. J., Chmelnitsky, I., Schechner, V., and Navon-Venezia, S. Transfer of carbapenem-resistant plasmid from *Klebsiella pneumoniae* ST258 to *Escherichia coli* in patient. *Emerging Infectious Diseases*, 16(6):1014–1017, jun 2010. ISSN 10806040. doi: 10.3201/eid1606.091671. URL http://www.ncbi.nlm.nih.gov/pubmed/20507761http://www.pubmedcentral.nih.gov/articlerender.fcgi?artid=PMC3086234.

Goss, T. J. and Bender, R. A. The nitrogen assimilation control protein, NAC, is a DNA binding transcription activator in Klebsiella aerogenes. *Journal of bacteriology*, 177(12):3546–55, jun 1995. ISSN 0021-9193. doi: 10.1128/jb.177.12.3546-3555.1995. URL http://www.ncbi.nlm.nih.gov/pubmed/7768865http://www.pubmedcentral.nih.gov/articlerender.fcgi?artid=PMC177061.

Göttig, S., Gruber, T. M., Stecher, B., Wichelhaus, T. A., and Kempf, V. A. *In vivo* horizontal gene transfer of the carbapenemase OXA-48 during a nosocomial outbreak. *Clinical Infectious Diseases*, 60(12):1808–1815, jun 2015. ISSN 15376591. doi: 10.1093/cid/civ191. URL https://academic.oup.com/cid/article-lookup/doi/10.1093/cid/civ191.

Graf, F. E., Palm, M., Warringer, J., and Farewell, A. Inhibiting conjugation as a tool in the fight against antibiotic resistance, feb 2019. ISSN 10982299. URL http://doi.wiley.com/10.1002/ddr.21457.

Gritz, L. and Davies, J. Plasmid-encoded hygromycin B resistance: The sequence of hygromycin B phosphotransferase gene and its expression in *Escherichia coli* and *Saccharomyces cerevisiae*. *Gene*, 25(2-3):179–188, nov 1983. ISSN 03781119. doi: 10.1016/0378-1119(83)90223-8. URL https://www.sciencedirect.com/science/article/pii/0378111983902238?via=ihub.

Gruber, C. J., Lang, S., Rajendra, V. K., Nuk, M., Raffl, S., Schildbach, J. F.,

and Zechner, E. L. Conjugative DNA transfer is enhanced by plasmid R1 partitioning proteins. *Frontiers in Molecular Biosciences*, 3(JUL):32, jul 2016. ISSN 2296889X. doi: 10.3389/fmolb.2016.00032. URL http://journal.frontiersin.org/Article/10.3389/fmolb.2016.00032/abstract.

Gu, D., Dong, N., Zheng, Z., Lin, D., Huang, M., Wang, L., Chan, E. W. C., Shu, L., Yu, J., Zhang, R., and Chen, S. A fatal outbreak of ST11 carbapenem-resistant hypervirulent *Klebsiella pneumoniae* in a Chinese hospital: A molecular epidemiological study. *The Lancet Infectious Diseases*, 18(1):37–46, 2018. ISSN 14744457. doi: 10.1016/S1473-3099(17)30489-9. URL http://www.ncbi.nlm.nih.gov/pubmed/28864030.

Guilhen, C., Charbonnel, N., Parisot, N., Gueguen, N., Iltis, A., Forestier, C., and Balestrino, D. Transcriptional profiling of *Klebsiella pneumoniae* defines signatures for planktonic, sessile and biofilm-dispersed cells. *BMC Genomics*, 17(1):237, dec 2016. ISSN 14712164. doi: 10.1186/s12864-016-2557-x. URL http://www.biomedcentral.com/1471-2164/17/237.

Guiney, D. G., Hasegawa, P., and Davis, C. E. Plasmid transfer from *Escherichia coli* to *Bacteroides fragilis*: Differential expression of antibiotic resistance phenotypes. *Proceedings of the National Academy of Sciences of the United States of America*, 81(22 I):7203–7206, 1984. ISSN 00278424. doi: 10.1073/pnas.81.22.7203. URL https://www.pnas.org/content/pnas/81/22/7203.full.pdf.

Guo, Y., Cen, Z., Zou, Y., Fang, X., Li, T., Wang, J., Chang, D., Su, L., Liu, Y., Chen, Y., Yang, R., and Liu, C. Whole-genome sequence of *Klebsiella pneumoniae* strain LCT-KP214, jun 2012. ISSN 00219193. URL https://journals.asm.org/doi/10.1128/JB.00531-12.

Haas, B. J., Chin, M., Nusbaum, C., Birren, B. W., and Livny, J. How deep is deep enough for RNA-Seq profiling of bacterial transcriptomes? *BMC Genomics*, 13 (1):734, dec 2012. ISSN 14712164. doi: 10.1186/1471-2164-13-734. URL https://bmcgenomics.biomedcentral.com/articles/10.1186/1471-2164-13-734.

Hall, C. W. and Mah, T. F. Molecular mechanisms of biofilm-based antibiotic resistance and tolerance in pathogenic bacteria, may 2017. ISSN 15746976. URL https://academic.oup.com/femsre/article-lookup/doi/10.1093/femsre/fux010.

Hall, J. P., Wright, R. C., Harrison, E., Muddiman, K. J., Wood, A. J., Paterson, S., and Brockhurst, M. A. Plasmid fitness costs are caused by specific genetic conflicts enabling resolution by compensatory mutation. *PLoS Biology*, 19(10): e3001225, oct 2021. ISSN 15457885. doi: 10.1371/journal.pbio.3001225. URL https://dx.plos.org/10.1371/journal.pbio.3001225.

Hall, R. J., Whelan, F. J., McInerney, J. O., Ou, Y., and Domingo-Sananes, M. R. Horizontal gene transfer as a source of conflict and cooperation in prokaryotes. *Frontiers in Microbiology*, 11:1569, jul 2020. ISSN 1664302X. doi: 10.3389/fmicb.2020.01569. URL https://www.frontiersin.org/article/10.3389/fmicb.2020.01569/full.

Hall-Stoodley, L., Costerton, J. W., and Stoodley, P. Bacterial biofilms: From the natural environment to infectious diseases, feb 2004. ISSN 17401526. URL http://www.nature.com/articles/nrmicro821.

Hardiman, C. A., Weingarten, R. A., Conlan, S., Khil, P., Dekker, J. P., Mathers, A. J., Sheppard, A. E., Segre, J. A., and Frank, K. M. Horizontal transfer of carbapenemase-encoding plasmids and comparison with hospital epidemiology data. *Antimicrobial Agents and Chemotherapy*, 60(8):4910–4919, aug 2016. ISSN 10986596. doi: 10.1128/AAC.00014-16. URL http://www.ncbi.nlm.nih.gov/pubmed/27270289http://www.pubmedcentral.nih.gov/articlerender.fcgi?artid=PMC4958172.

Harmer, C. J., Moran, R. A., and Hall, R. M. Movement of IS*26*-Associated antibiotic resistance genes occurs via a translocatable unit that includes a single IS*26* and preferentially inserts adjacent to another IS*26*. *mBio*, 5(5), oct 2014. ISSN

21507511. doi: 10.1128/mBio.01801-14. URL https://journals.asm.org/doi/10.1128/mBio.01801-14.

Harr, B. and Schlötterer, C. Gene expression analysis indicates extensive genotype-specific crosstalk between the conjugative F-plasmid and the *E. coli* chromosome. *BMC Microbiology*, 6:80, sep 2006. ISSN 14712180. doi: 10.1186/1471-2180-6-80. URL http://www.ncbi.nlm.nih.gov/pubmed/16981998http://www.pubmedcentral.nih.gov/articlerender.fcgi?artid=PMC1590023.

Harrington, N. E., Littler, J. L., and Harrison, F. Transcriptome analysis of *Pseudomonas aeruginosa* biofilm infection in an *ex vivo* pig model of the cystic fibrosis lung. *Applied and Environmental Microbiology*, 88(3), feb 2022. ISSN 0099-2240. doi: 10.1128/aem.01789-21. URL https://journals.asm.org/doi/10.1128/aem.01789-21.

Harrison, E. and Brockhurst, M. A. Plasmid-mediated horizontal gene transfer is a co-evolutionary process, jun 2012. ISSN 0966842X. URL http://www.ncbi.nlm.nih.gov/pubmed/22564249.

Hartmann, R., Jeckel, H., Jelli, E., Singh, P. K., Vaidya, S., Bayer, M., Vidakovic, L., Díaz-Pascual, F., Fong, J. C., Dragoš, A., Besharova, O., Nadell, C. D., Sourjik, V., Kovács, Á. T., Yildiz, F. H., and Drescher, K. BiofilmQ, a software tool for quantitative image analysis of microbial biofilm communities. *bioRxiv*, page 735423, aug 2019. doi: 10.1101/735423. URL https://www.biorxiv.org/content/10.1101/735423v1.fullhttps://www.biorxiv.org/content/10.1101/735423v1.

Hassan, M. Z., Sturm-Ramirez, K., Rahman, M. Z., Hossain, K., Aleem, M. A., Bhuiyan, M. U., Islam, M. M., Rahman, M., and Gurley, E. S. Contamination of hospital surfaces with respiratory pathogens in Bangladesh. *PLoS ONE*, 14(10):e0224065, 2019. ISSN 19326203. doi: 10.1371/journal.pone.0224065. URL http://www.ncbi.nlm.nih.gov/pubmed/31658279http://www.pubmedcentral.nih.gov/articlerender.fcgi?artid=PMC6816543.

Haudiquet, M., Buffet, A., Rendueles, O., and Rocha, E. P. Interplay between the cell envelope and mobile genetic elements shapes gene flow in populations of the nosocomial pathogen *Klebsiella pneumoniae*. *PLoS Biology*, 19(7):e3001276, jul 2021. ISSN 15457885. doi: 10.1371/journal.pbio.3001276. URL `https://dx.plos.org/10.1371/journal.pbio.3001276`.

Hausner, M. and Wuertz, S. High rates of conjugation in bacterial biofilms as determined by quantitative *in situ* analysis. *Applied and Environmental Microbiology*, 65(8):3710–3713, 1999. ISSN 00992240. doi: 10.1128/aem.65.8.3710-3713.1999. URL `http://aem.asm.org/`.

Hautefort, I., Proença, M. J., and Hinton, J. C. Single-copy green fluorescent protein gene fusions allow accurate measurement of *Salmonella* gene expression *in vitro* and during infection of mammalian cells. *Applied and Environmental Microbiology*, 69(12):7480–7491, dec 2003. ISSN 00992240. doi: 10.1128/AEM.69.12.7480-7491.2003. URL `http://www.ncbi.nlm.nih.gov/pubmed/14660401http://www.pubmedcentral.nih.gov/articlerender.fcgi?artid=PMC310007`.

Hawkey, P. M. and Livermore, D. M. Carbapenem antibiotics for serious infections. *BMJ (Online)*, 344(7863):e3236, may 2012. ISSN 17561833. doi: 10.1136/bmj.e3236. URL `http://www.ncbi.nlm.nih.gov/pubmed/22654063`.

Hawkey, P. M., Warren, R. E., Livermore, D. M., McNulty, C. A., Enoch, D. A., Otter, J. A., and Wilson, A. P. R.

Hazan, R., Que, Y. A., Maura, D., and Rahme, L. G. A method for high throughput determination of viable bacteria cell counts in 96-well plates. *BMC Microbiology*, 12:259, nov 2012. ISSN 14712180. doi: 10.1186/1471-2180-12-259. URL `http://www.ncbi.nlm.nih.gov/pubmed/23148795http://www.pubmedcentral.nih.gov/articlerender.fcgi?artid=PMC3534621`.

Headd, B. and Bradford, S. A. The conjugation window in an *Escherichia coli* K-12 strain with an IncFII plasmid. *Applied and Environmental Microbiology*,

86(17), jun 2020. ISSN 10985336. doi: 10.1128/AEM.00948-20. URL https://aem.asm.org/content/early/2020/06/23/AEM.00948-20.long.

Hecht, A., Endy, D., Salit, M., and Munson, M. S. When wavelengths collide: Bias in cell abundance measurements due to expressed fluorescent proteins. *ACS Synthetic Biology*, 5(9):1024–1027, sep 2016. ISSN 21615063. doi: 10.1021/acssynbio.6b00072. URL https://pubs.acs.org/doi/10.1021/acssynbio.6b00072.

Hellman, L. M. and Fried, M. G. Electrophoretic mobility shift assay (EMSA) for detecting protein-nucleic acid interactions. *Nature Protocols*, 2(8):1849–1861, 2007. ISSN 17542189. doi: 10.1038/nprot.2007.249. URL http://www.ncbi.nlm.nih.gov/pubmed/17703195http://www.pubmedcentral.nih.gov/articlerender.fcgi?artid=PMC2757439.

Hendrickx, A. P., Landman, F., de Haan, A., Borst, D., Witteveen, S., van Santen-Verheuvel, M. G., van der Heide, H. G., Schouls, L. M., Halaby, T., Steingrover, R., Cohen Stuart, J. W., Melles, D. C., van Dijk, K., Spijkerman, I. J., Notermans, D. W., Oudbier, J. H., van Ogtrop, M. L., van Dam, A., den Reijer, M., Kluytmans, J. A., van der Linden, M. P., Mattsson, E. E., van der Vusse, M., de Jong, E., Maijer-Reuwer, A., van Trijp, M., van Griethuysen, A. J., Ott, A., Bathoorn, E., Sinnige, J. C., Heikens, E., de Brauwer, E. I., Stals, F. S., Silvis, W., Dorigo-Zetsma, J. W., Waar, K., van Mens, S. P., Roescher, N., Voss, A., Wertheim, H., Slingerland, B. C., Frenay, H. M., Schulin, T., Diederen, B. M., Bode, L., van Rijn, M., Dinant, S., Damen, M., de Man, P., Leversteijn-van Hall, M. A., van Elzakker, E. P., Muller, A. E., Schneeberger, P., van Dam, D. W., Buiting, A. G., Vlek, A. L., Stam, A., Troelstra, A., Overdevest, I. T., Bosboom, R. W., Trienekens, T. A., Wolfhagen, M. J., and Paltansing, S. Plasmid diversity among genetically related *Klebsiella pneumoniae* $bla_{\text{KPC-2}}$ and $bla_{\text{KPC-3}}$ isolates collected in the Dutch national surveillance. *Scientific Reports*, 10(1):16778, dec 2020. ISSN 20452322. doi: 10.1038/s41598-020-73440-2. URL https://www.nature.com/articles/s41598-020-73440-2.

Hennequin, C., Aumeran, C., Robin, F., Traore, O., and Forestier, C. Antibiotic resistance and plasmid transfer capacity in biofilm formed with a CTX-M-15-producing *Klebsiella pneumoniae* isolate. *Journal of Antimicrobial Chemotherapy*, 67(9):2123–2130, sep 2012. ISSN 03057453. doi: 10.1093/jac/dks169. URL `https://academic.oup.com/jac/article-lookup/doi/10.1093/jac/dks169`.

Heuer, H., Abdo, Z., and Smalla, K. Patchy distribution of flexible genetic elements in bacterial populations mediates robustness to environmental uncertainty, sep 2008. ISSN 01686496. URL `https://academic.oup.com/femsec/article-lookup/doi/10.1111/j.1574-6941.2008.00539.x`.

Hibbing, M. E., Fuqua, C., Parsek, M. R., and Peterson, S. B. Bacterial competition: Surviving and thriving in the microbial jungle, 2010. ISSN 17401526.

Holmes, A. H., Moore, L. S., Sundsfjord, A., Steinbakk, M., Regmi, S., Karkey, A., Guerin, P. J., and Piddock, L. J. Understanding the mechanisms and drivers of antimicrobial resistance, 2016. ISSN 1474547X.

Holt, K. E., Wertheim, H., Zadoks, R. N., Baker, S., Whitehouse, C. A., Dance, D., Jenney, A., Connor, T. R., Hsu, L. Y., Severin, J., Brisse, S., Cao, H., Wilksch, J., Gorrie, C., Schultz, M. B., Edwards, D. J., Van Nguyen, K., Nguyen, T. V., Dao, T. T., Mensink, M., Le Minh, V., Nhu, N. T. K., Schultsz, C., Kuntaman, K., Newton, P. N., Moore, C. E., Strugnell, R. A., and Thomson, N. R. Genomic analysis of diversity, population structure, virulence, and antimicrobial resistance in *Klebsiella pneumoniae*, an urgent threat to public health. *Proceedings of the National Academy of Sciences of the United States of America*, 112(27):E3574–E3581, jul 2015. ISSN 10916490. doi: 10.1073/pnas.1501049112. URL `http://www.ncbi.nlm.nih.gov/pubmed/26100894http://www.pubmedcentral.nih.gov/articlerender.fcgi?artid=PMC4500264`.

Hsieh, P.-F., Lin, T.-L., Yang, F.-L., Wu, M.-C., Pan, Y.-J., Wu, S.-H., and Wang, J.-T. Lipopolysaccharide O1 antigen contributes to the

virulence in *Klebsiella pneumoniae* causing pyogenic liver abscess. *PloS one*, 7(3):e33155, 2012. ISSN 1932-6203. doi: 10.1371/journal.pone.0033155. URL http://www.ncbi.nlm.nih.gov/pubmed/22427976http://www.pubmedcentral.nih.gov/articlerender.fcgi?artid=PMC3299736.

Hu, B., Khara, P., and Christie, P. J. Structural bases for F plasmid conjugation and F pilus biogenesis in *Escherichia coli*. *Proceedings of the National Academy of Sciences of the United States of America*, 116(28):14222–14227, jul 2019. ISSN 10916490. doi: 10.1073/pnas.1904428116. URL http://www.ncbi.nlm.nih.gov/pubmed/31239340http://www.pubmedcentral.nih.gov/articlerender.fcgi?artid=PMC6628675.

Hua, X., Zhang, L., Moran, R. A., Xu, Q., Sun, L., van Schaik, W., and Yu, Y. Cointegration as a mechanism for the evolution of a KPC-producing multidrug resistance plasmid in *Proteus mirabilis*. *Emerging Microbes and Infections*, 9(1):1206–1218, jan 2020. ISSN 22221751. doi: 10.1080/22221751.2020.1773322. URL https://www.tandfonline.com/doi/full/10.1080/22221751.2020.1773322.

Hubbard, A. T., Jafari, N. V., Feasey, N., Rohn, J. L., and Roberts, A. P. Effect of environment on the evolutionary trajectories and growth characteristics of antibiotic-resistant escherichia coli mutants. *Frontiers in Microbiology*, 10 (AUG):2001, aug 2019. ISSN 1664302X. doi: 10.3389/fmicb.2019.02001. URL https://www.frontiersin.org/article/10.3389/fmicb.2019.02001/full.

Huerta-Cepas, J., Szklarczyk, D., Heller, D., Hernández-Plaza, A., Forslund, S. K., Cook, H., Mende, D. R., Letunic, I., Rattei, T., Jensen, L. J., Von Mering, C., and Bork, P. EggNOG 5.0: A hierarchical, functionally and phylogenetically annotated orthology resource based on 5090 organisms and 2502 viruses. *Nucleic Acids Research*, 47(D1):D309–D314, jan 2019. ISSN 13624962. doi: 10.1093/nar/gky1085. URL https://academic.oup.com/nar/article/47/D1/D309/5173662.

Ilangovan, A., Kay, C. W., Roier, S., El Mkami, H., Salvadori, E., Zechner, E. L., Zanetti, G., and Waksman, G. Cryo-EM Structure of a relax-

ase reveals the molecular basis of DNA unwinding during bacterial conjugation. *Cell*, 169(4):708–721.e12, 2017. ISSN 10974172. doi: 10.1016/j.cell.2017.04.010. URL http://www.ncbi.nlm.nih.gov/pubmed/28457609http://www.pubmedcentral.nih.gov/articlerender.fcgi?artid=PMC5422253.

Ilves, H., Hõrak, R., and Kivisaar, M. Involvement of σS in starvation-induced transposition of *Pseudomonas putida* transposon Tn4652. *Journal of Bacteriology*, 183(18):5445–5448, sep 2001. ISSN 00219193. doi: 10.1128/JB.183.18.5445-5448.2001. URL http://www.ncbi.nlm.nih.gov/pubmed/11514532http://www.pubmedcentral.nih.gov/articlerender.fcgi?artid=PMC95431.

Imdahl, F., Vafadarnejad, E., Homberger, C., Saliba, A. E., and Vogel, J. Single-cell RNA-sequencing reports growth-condition-specific global transcriptomes of individual bacteria. *Nature Microbiology*, 5(10):1202–1206, oct 2020. ISSN 20585276. doi: 10.1038/s41564-020-0774-1. URL https://www.nature.com/articles/s41564-020-0774-1.

Jackson, R. W., Vinatzer, B., Arnold, D. L., Dorus, S., and Murillo, J. The influence of the accessory genome on bacterial pathogen evolution. *Mobile Genetic Elements*, 1(1):55–65, may 2011. ISSN 2159-2543. doi: 10.4161/mge.1.1.16432. URL http://www.ncbi.nlm.nih.gov/pubmed/22016845http://www.pubmedcentral.nih.gov/articlerender.fcgi?artid=PMC3190274.

Johnston, C. D., Cotton, S. L., Rittling, S. R., Starr, J. R., Borisy, G. G., Dewhirst, F. E., and Lemon, K. P. Systematic evasion of the restriction-modification barrier in bacteria. *Proceedings of the National Academy of Sciences of the United States of America*, 166(23):11454–11459, jun 2019. ISSN 10916490. doi: 10.1073/pnas.1820256116. URL http://www.ncbi.nlm.nih.gov/pubmed/31097593http://www.pubmedcentral.nih.gov/articlerender.fcgi?artid=PMC6561282.

Jolley, K. A. and Maiden, M. C. BIGSdb: Scalable analysis of bacterial genome variation at the population level. *BMC Bioinformatics*, 11(1):595, dec 2010. ISSN

14712105. doi: 10.1186/1471-2105-11-595. URL https://bmcbioinformatics.biomedcentral.com/articles/10.1186/1471-2105-11-595.

Karatan, E. and Watnick, P. Signals, Regulatory Networks, and Materials That Build and Break Bacterial Biofilms. *Microbiology and Molecular Biology Reviews*, 73(2):310–347, jun 2009. ISSN 1092-2172. doi: 10.1128/mmbr.00041-08. URL http://www.ncbi.nlm.nih.gov/pubmed/19487730http://www.pubmedcentral.nih.gov/articlerender.fcgi?artid=PMC2698413.

Kazmierczak, K. M., Biedenbach, D. J., Hackel, M., Rabine, S., de Jonge, B. L. M., Bouchillon, S. K., Sahm, D. F., and Bradford, P. A. Global dissemination of bla_{KPC} into bacterial species beyond *Klebsiella pneumoniae* and *in vitro* susceptibility to ceftazidime-avibactam and aztreonam-avibactam. *Antimicrobial agents and chemotherapy*, 60(8):4490–500, 2016. ISSN 1098-6596. doi: 10.1128/AAC.00107-16. URL http://www.ncbi.nlm.nih.gov/pubmed/27161636http://www.pubmedcentral.nih.gov/articlerender.fcgi?artid=PMC4958145.

Kelly, R., Zoubiane, G., Walsh, D., Ward, R., and Goossens, H. Public funding for research on antibacterial resistance in the JPIAMR countries, the European Commission, and related European Union agencies: A systematic observational analysis. *The Lancet Infectious Diseases*, 16 (4):431–440, apr 2016. ISSN 14744457. doi: 10.1016/S1473-3099(15)00350-3. URL http://www.ncbi.nlm.nih.gov/pubmed/26708524http://www.pubmedcentral.nih.gov/articlerender.fcgi?artid=PMC4802226.

Kmietowicz, Z. Few novel antibiotics in the pipeline, WHO warns, sep 2017. ISSN 17561833. URL https://www.bmj.com/content/358/bmj.j4339.

Knopp, M. and Andersson, D. I. Predictable phenotypes of antibiotic resistance mutations. *mBio*, 9(3), 2018. ISSN 2150-7511. doi: 10.1128/mBio.00770-18. URL http://www.ncbi.nlm.nih.gov/pubmed/29764951http://www.pubmedcentral.nih.gov/articlerender.fcgi?artid=PMC5954217.

Kolmogorov, M., Yuan, J., Lin, Y., and Pevzner, P. A. Assembly of long, error-prone reads using repeat graphs. *Nature Biotechnology*, 37(5):540–546, may 2019. ISSN 1087-0156. doi: 10.1038/s41587-019-0072-8. URL http://www.nature.com/articles/s41587-019-0072-8.

Kopotsa, K., Osei Sekyere, J., and Mbelle, N. M. Plasmid evolution in carbapenemase-producing *Enterobacteriaceae*: A review, dec 2019. ISSN 17496632. URL https://onlinelibrary.wiley.com/doi/abs/10.1111/nyas.14223.

Koraimann, G. Spread and persistence of virulence and antibiotic resistance genes: A Ride on the F plasmid conjugation module. *EcoSal Plus*, 8(1), 2018. ISSN 2324-6200. doi: 10.1128/ecosalplus.esp-0003-2018. URL www.asmscience.org.

Koraimann, G. and Wagner, M. A. Social behavior and decision making in bacterial conjugation. *Frontiers in Cellular and Infection Microbiology*, 4:54, 2014. ISSN 2235-2988. doi: 10.3389/fcimb.2014.00054. URL http://www.ncbi.nlm.nih.gov/pubmed/24809026http://www.pubmedcentral.nih.gov/articlerender.fcgi?artid=PMC4010749.

Kostakioti, M., Hadjifrangiskou, M., and Hultgren, S. J. Bacterial biofilms: Development, dispersal, and therapeutic strategies in the dawn of the postantibiotic era. *Cold Spring Harbor Perspectives in Medicine*, 3(4):a010306, apr 2013. ISSN 21571422. doi: 10.1101/cshperspect.a010306. URL http://www.ncbi.nlm.nih.gov/pubmed/23545571http://www.pubmedcentral.nih.gov/articlerender.fcgi?artid=PMC3683961.

Kottara, A., Hall, J. P., Harrison, E., and Brockhurst, M. A. Variable plasmid fitness effects and mobile genetic element dynamics across *Pseudomonas* species. *FEMS Microbiology Ecology*, 94(1), 2018. ISSN 15746941. doi: 10.1093/femsec/fix172. URL https://www.ncbi.nlm.nih.gov/pmc/articles/PMC5812508/.

Król, J. E., Nguyen, H. D., Rogers, L. M., Beyenal, H., Krone, S. M., and Top,

E. M. Increased transfer of a multidrug resistance plasmid in *Escherichia coli* biofilms at the air-liquid interface. *Applied and Environmental Microbiology*, 77 (15):5079–5088, aug 2011. ISSN 00992240. doi: 10.1128/AEM.00090-11. URL https://aem.asm.org/content/77/15/5079.

Król, J. E., Wojtowicz, A. J., Rogers, L. M., Heuer, H., Smalla, K., Krone, S. M., and Top, E. M. Invasion of *E. coli* biofilms by antibiotic resistance plasmids. *Plasmid*, 70(1):110–119, jul 2013. ISSN 0147619X. doi: 10.1016/j.plasmid.2013.03.003. URL https://www.sciencedirect.com/science/article/pii/S0147619X13000310?via%3Dihub.

Kroll, J., Klinter, S., Schneider, C., Voß, I., and Steinbüchel, A. Plasmid addiction systems: Perspectives and applications in biotechnology, nov 2010. ISSN 17517907. URL http://www.ncbi.nlm.nih.gov/pubmed/21255361http://www.pubmedcentral.nih.gov/articlerender.fcgi?artid=PMC3815339.

Lam, M. M., Wick, R. R., Watts, S. C., Cerdeira, L. T., Wyres, K. L., and Holt, K. E. A genomic surveillance framework and genotyping tool for *Klebsiella pneumoniae* and its related species complex. *Nature Communications*, 12(1):4188, dec 2021. ISSN 20411723. doi: 10.1038/s41467-021-24448-3. URL http://www.nature.com/articles/s41467-021-24448-3.

Land, M., Hauser, L., Jun, S. R., Nookaew, I., Leuze, M. R., Ahn, T. H., Karpinets, T., Lund, O., Kora, G., Wassenaar, T., Poudel, S., and Ussery, D. W. Insights from 20 years of bacterial genome sequencing, mar 2015. ISSN 14387948. URL http://www.ncbi.nlm.nih.gov/pubmed/25722247http://www.pubmedcentral.nih.gov/articlerender.fcgi?artid=PMC4361730.

Langstraat, J., Bohse, M., and Clegg, S. Type 3 fimbrial shaft (MrkA) of *Klebsiella pneumoniae*, but not the fimbrial adhesin (MrkD), facilitates biofilm formation. *Infection and Immunity*, 69(9):5805–5812, sep 2001. ISSN 00199567. doi: 10.1128/IAI.69.9.5805-5812.2001. URL http:

//www.ncbi.nlm.nih.gov/pubmed/11500458http://www.pubmedcentral.nih.gov/articlerender.fcgi?artid=PMC98698.

Lanier, L. L. and Warner, N. L. Paraformaldehyde fixation of hematopoietic cells for quantitative flow cytometry (FACS) analysis. *Journal of Immunological Methods*, 47(1):25–30, nov 1981. ISSN 00221759. doi: 10.1016/0022-1759(81)90253-2. URL https://www.sciencedirect.com/science/article/abs/pii/0022175981902532?via%3Dihub.

Lavender, H. F., Jagnow, J. R., and Clegg, S. Biofilm formation *in vitro* and virulence *in vivo* of mutants of *Klebsiella pneumoniae*. *Infection and Immunity*, 72(8):4888–4890, aug 2004. ISSN 00199567. doi: 10.1128/IAI.72.8.4888-4890.2004. URL http://www.ncbi.nlm.nih.gov/pubmed/15271955http://www.pubmedcentral.nih.gov/articlerender.fcgi?artid=PMC470696.

Leavitt, A., Chmelnitsky, I., Carmeli, Y., and Navon-Venezia, S. Complete nucleotide sequence of KPC-3-encoding plasmid pKpQIL in the epidemic *Klebsiella pneumoniae* sequence type 258. *Antimicrobial Agents and Chemotherapy*, 54(10):4493–4496, oct 2010. ISSN 00664804. doi: 10.1128/AAC.00175-10. URL http://www.ncbi.nlm.nih.gov/pubmed/20696875http://www.pubmedcentral.nih.gov/articlerender.fcgi?artid=PMC2944570.

Lederberg, J. and Tatum, E. L. Gene recombination in *Escherichia coli*, oct 1946. ISSN 00280836. URL https://www.nature.com/articles/158558a0.

Lee, D. J., Bingle, L. E., Heurlier, K., Pallen, M. J., Penn, C. W., Busby, S. J., and Hobman, J. L. Gene doctoring: A method for recombineering in laboratory and pathogenic *Escherichia coli* strains. *BMC Microbiology*, 9:252, dec 2009. ISSN 14712180. doi: 10.1186/1471-2180-9-252. URL http://www.ncbi.nlm.nih.gov/pubmed/20003185http://www.pubmedcentral.nih.gov/articlerender.fcgi?artid=PMC2796669.

Lees, J. A., Mai, T. T., Galardini, M., Wheeler, N. E., Horsfield, S. T., Parkhill,

J., and Corander, J. Improved prediction of bacterial genotype-phenotype associations using interpretable pangenome-spanning regressions. *mBio*, 11(4):1–22, aug 2020. ISSN 21507511. doi: 10.1128/mBio.01344-20. URL https://journals.asm.org/doi/10.1128/mBio.01344-20.

Letunic, I. and Bork, P. Interactive tree of life (iTOL) v5: An online tool for phylogenetic tree display and annotation. *Nucleic Acids Research*, 49(W1):W293–W296, jul 2021. ISSN 13624962. doi: 10.1093/nar/gkab301. URL https://academic.oup.com/nar/article/49/W1/W293/6246398.

Li, C., Wen, A., Shen, B., Lu, J., Huang, Y., and Chang, Y. FastCloning: A highly simplified, purification-free, sequence- and ligation-independent PCR cloning method. *BMC Biotechnology*, 11(1):92, dec 2011. ISSN 14726750. doi: 10.1186/1472-6750-11-92. URL https://bmcbiotechnol.biomedcentral.com/articles/10.1186/1472-6750-11-92.

Li, H. Aligning sequence reads, clone sequences and assembly contigs with BWA-MEM. mar 2013. URL http://arxiv.org/abs/1303.3997.

Li, H., Handsaker, B., Wysoker, A., Fennell, T., Ruan, J., Homer, N., Marth, G., Abecasis, G., and Durbin, R. The Sequence Alignment/Map format and SAMtools. *Bioinformatics*, 25(16):2078–2079, aug 2009. ISSN 13674803. doi: 10.1093/bioinformatics/btp352. URL https://academic.oup.com/bioinformatics/article-lookup/doi/10.1093/bioinformatics/btp352.

Li, X., Yan, Z., and Xu, J. Quantitative variation of biofilms among strains in natural populations of *Candida albicans*, feb 2003. ISSN 13500872. URL http://mic.microbiologyresearch.org/content/journal/micro/10.1099/mic.0.25932-0.

Li, X., Ma, W., Qin, Q., Liu, S., Ye, L., Yang, J., and Li, B. Nosocomial spread of OXA-232-producing *Klebsiella pneumoniae* ST15 in a teaching hospital, Shanghai, China. *BMC Microbiology*, 19(1):235, dec 2019. ISSN 1471-2180. doi:

10.1186/s12866-019-1609-1. URL https://bmcmicrobiol.biomedcentral.com/articles/10.1186/s12866-019-1609-1.

Liao, X., Makris, M., and Luo, X. M. Fluorescence-activated cell sorting for purification of plasmacytoid dendritic cells from the mouse bone marrow. *Journal of Visualized Experiments*, 2016(117), 2016. ISSN 1940087X. doi: 10.3791/54641. URL http://www.ncbi.nlm.nih.gov/pubmed/27842369http://www.pubmedcentral.nih.gov/articlerender.fcgi?artid=PMC5226086.

Lim, S. Y., Teh, C. S. J., and Thong, K. L. Biofilm-related diseases and omics: Global transcriptional profiling of *Enterococcus faecium* reveals different gene expression patterns in the biofilm and planktonic cells. *OMICS A Journal of Integrative Biology*, 21(10):592–602, oct 2017. ISSN 15578100. doi: 10.1089/omi.2017.0119. URL http://www.liebertpub.com/doi/10.1089/omi.2017.0119.

Lisa, M. N., Palacios, A. R., Aitha, M., González, M. M., Moreno, D. M., Crowder, M. W., Bonomo, R. A., Spencer, J., Tierney, D. L., Llarrull, L. I., and Vila, A. J. A general reaction mechanism for carbapenem hydrolysis by mononuclear and binuclear metallo-β-lactamases. *Nature Communications*, 8(1):538, dec 2017. ISSN 20411723. doi: 10.1038/s41467-017-00601-9. URL http://www.nature.com/articles/s41467-017-00601-9.

Liu, H., Moran, R. A., Chen, Y., Doughty, E. L., Hua, X., Jiang, Y., Xu, Q., Zhang, L., Blair, J. M., McNally, A., Van Schaik, W., and Yu, Y. Transferable *Acinetobacter baumannii* plasmid pDETAB2 encodes OXA-58 and NDM-1 and represents a new class of antibiotic resistance plasmids. *Journal of Antimicrobial Chemotherapy*, 76(5):1130–1134, apr 2021. ISSN 14602091. doi: 10.1093/jac/dkab005. URL https://academic.oup.com/jac/article/76/5/1130/6121227.

Liu, Z., Que, F., Liao, L., Zhou, M., You, L., Zhao, Q., Li, Y., Niu, H., Wu, S., and Huang, R. Study on the promotion of bacterial biofilm formation by a *Salmonella* conjugative plasmid and the underlying mechanism. *PLoS ONE*, 9

(10):e109808, oct 2014. ISSN 19326203. doi: 10.1371/journal.pone.0109808. URL http://dx.plos.org/10.1371/journal.pone.0109808.

Livermore, D. M. Has the era of untreatable infections arrived? *Journal of Antimicrobial Chemotherapy*, 64(SUPPL.1):i29–i36, sep 2009. ISSN 03057453. doi: 10.1093/jac/dkp255. URL https://academic.oup.com/jac/article-lookup/doi/10.1093/jac/dkp255.

Long, D., Zhu, L. L., Du, F. L., Xiang, T. X., Wan, L. G., Wei, D. D., Zhang, W., and Liu, Y. Phenotypical profile and global transcriptomic profile of hypervirulent *Klebsiella pneumoniae* due to carbapenemase-encoding plasmid acquisition. *BMC Genomics*, 20(1):480, dec 2019. ISSN 14712164. doi: 10.1186/s12864-019-5705-2. URL https://bmcgenomics.biomedcentral.com/articles/10.1186/s12864-019-5705-2.

Lorenzo-Díaz, F., Fernández-López, C., Lurz, R., Bravo, A., and Espinosa, M. Crosstalk between vertical and horizontal gene transfer: Plasmid replication control by a conjugative relaxase. *Nucleic Acids Research*, 45(13):7774–7785, jul 2017. ISSN 13624962. doi: 10.1093/nar/gkx450. URL http://academic.oup.com/nar/article/45/13/7774/3835314.

Low, W. W., Wong, J. L., Peña, A., Seddon, C., Costa, T. R., Beis, K., and Frankel, G. OmpK36 and TraN facilitate conjugal transfer of the *Klebsiella pneumoniae* carbapenem resistance plasmid pKpQIL. 2020. doi: 10.1101/2020.07.01.180638. URL https://doi.org/10.1101/2020.07.01.180638.

Lu, J., Peng, Y., Wan, S., Frost, L. S., Raivio, T., and Mark Glover, J. N. Cooperative function of TraJ and ArcA in regulating the F plasmid *tra* operon. *Journal of Bacteriology*, 201(1), jan 2019. ISSN 10985530. doi: 10.1128/JB.00448-18. URL http://www.ncbi.nlm.nih.gov/pubmed/30322855http://www.pubmedcentral.nih.gov/articlerender.fcgi?artid=PMC6287455.

Ma, H. and Bryers, J. D. Non-invasive determination of conjugative transfer of

plasmids bearing antibiotic-resistance genes in biofilm-bound bacteria: Effects of substrate loading and antibiotic selection. *Applied Microbiology and Biotechnology*, 97(1):317–328, jan 2013. ISSN 01757598. doi: 10.1007/s00253-012-4179-9. URL http://www.ncbi.nlm.nih.gov/pubmed/22669634http://www.pubmedcentral.nih.gov/articlerender.fcgi?artid=PMC3465625http://link.springer.com/10.1007/s00253-012-4179-9.

Madsen, J. S., Riber, L., Kot, W., Basfeld, A., Burmølle, M., Hansen, L. H., and Sørensen, S. J. Type 3 fimbriae encoded on plasmids are expressed from a unique promoter without affecting host motility, facilitating an exceptional phenotype that enhances conjugal plasmid transfer. *PLoS ONE*, 11(9):e0162390, sep 2016. ISSN 19326203. doi: 10.1371/journal.pone.0162390. URL https://dx.plos.org/10.1371/journal.pone.0162390.

Mahillon, J. and Chandler, M. Insertion sequences. *Microbiology and Molecular Biology Reviews*, 62(3):725–774, sep 1998. ISSN 1092-2172. doi: 10.1128/mmbr.62.3.725-774.1998. URL https://mmbr.asm.org/content/62/3/725.

Maiden, M. C., Bygraves, J. A., Feil, E., Morelli, G., Russell, J. E., Urwin, R., Zhang, Q., Zhou, J., Zurth, K., Caugant, D. A., Feavers, I. M., Achtman, M., and Spratt, B. G. Multilocus sequence typing: A portable approach to the identification of clones within populations of pathogenic microorganisms. *Proceedings of the National Academy of Sciences of the United States of America*, 95(6):3140–3145, mar 1998. ISSN 00278424. doi: 10.1073/pnas.95.6.3140. URL http://www.ncbi.nlm.nih.gov/pubmed/9501229http://www.pubmedcentral.nih.gov/articlerender.fcgi?artid=PMC19708.

Maley, A. M. and Arbiser, J. L. Gentian violet: A 19th century drug re-emerges in the 21st century, dec 2013. ISSN 09066705. URL http://www.ncbi.nlm.nih.gov/pubmed/24118276http://www.pubmedcentral.nih.gov/articlerender.fcgi?artid=PMC4396813.

Marco-Puche, G., Lois, S., Benítez, J., and Trivino, J. C. RNA-Seq perspectives

to improve clinical diagnosis, nov 2019. ISSN 16648021. URL https://www.frontiersin.org/article/10.3389/fgene.2019.01152/full.

Marsh, P. D. Dental plaque as a biofilm and a microbial community - Implications for health and disease. In *BMC Oral Health*, volume 6, page S14. BioMed Central, jun 2006. doi: 10.1186/1472-6831-6-S1-S14. URL http://www.ncbi.nlm.nih.gov/pubmed/16934115http://www.pubmedcentral.nih.gov/articlerender.fcgi?artid=PMC2147593.

Martin, M. J., Corey, B. W., Sannio, F., Hall, L. R., MacDonald, U., Jones, B. T., Mills, E. G., Harless, C., Stam, J., Maybank, R., Kwak, Y., Schaufler, K., Becker, K., Hübner, N. O., Cresti, S., Tordini, G., Valassina, M., Cusi, M. G., Bennett, J. W., Russo, T. A., McGann, P. T., Lebreton, F., and Docquier, J. D. Anatomy of an extensively drug-resistant *Klebsiella pneumoniae* outbreak in Tuscany, Italy. *Proceedings of the National Academy of Sciences of the United States of America*, 118(48), nov 2021. ISSN 10916490. doi: 10.1073/pnas.2110227118. URL http://www.ncbi.nlm.nih.gov/pubmed/34819373.

Martin, R. M. and Bachman, M. A. Colonization, infection, and the accessory genome of *Klebsiella pneumoniae*, 2018. ISSN 22352988. URL https://www.ncbi.nlm.nih.gov/pmc/articles/PMC5786545/.

Matlock, W., Chau, K. K., AbuOun, M., Stubberfield, E., Barker, L., Kavanagh, J., Pickford, H., Gilson, D., Smith, R. P., Gweon, H. S., Hoosdally, S. J., Swann, J., Sebra, R., Bailey, M. J., Peto, T. E., Crook, D. W., Anjum, M. F., Read, D. S., Walker, A. S., Stoesser, N., Shaw, L. P., AbuOun, M., Anjum, M. F., Bailey, M. J., Brett, H., Bowes, M. J., Chau, K. K., de Maio, N., Duggett, N., Wilson, D. J., Gilson, D., Gweon, H. S., Hubbard, A., Hoosdally, S. J., Matlock, W., Kavanagh, J., Jones, H., Peto, T. E., Read, D. S., Sebra, R., Shaw, L. P., Sheppard, A. E., Smith, R. P., Stubberfield, E., Stoesser, N., Swann, J., Walker, A. S., and Woodford, N. Genomic network analysis of environmental and livestock F-type plasmid populations. *ISME Journal*, 15(8):2322–2335, aug 2021. ISSN

17517370. doi: 10.1038/s41396-021-00926-w. URL http://www.nature.com/articles/s41396-021-00926-w.

Matsumura, Y., Peirano, G., and Pitout, J. D. Complete genome sequence of *Escherichia coli* J53, an azide-resistant laboratory strain used for conjugation experiments. *Genome Announcements*, 6(21), 2018. ISSN 21698287. doi: 10.1128/genomeA.00433-18. URL https://www.ncbi.nlm.nih.gov/pmc/articles/PMC5968721/.

Meletis, G. Carbapenem resistance: overview of the problem and future perspectives. *Therapeutic Advances in Infectious Disease*, 3(1): 15–21, feb 2016. ISSN 2049-9361. doi: 10.1177/2049936115621709. URL http://www.ncbi.nlm.nih.gov/pubmed/26862399http://www.pubmedcentral.nih.gov/articlerender.fcgi?artid=PMC4735501.

Merritt, J. H., Kadouri, D. E., and O'Toole, G. A. Growing and analyzing static biofilms. In *Current Protocols in Microbiology*, volume Chapter 1, page Unit 1B.1. NIH Public Access, jul 2005. doi: 10.1002/9780471729259.mc01b01s00. URL http://www.ncbi.nlm.nih.gov/pubmed/18770545http://www.pubmedcentral.nih.gov/articlerender.fcgi?artid=PMC4568995.

Mikami, H., Kawaguchi, M., Huang, C. J., Matsumura, H., Sugimura, T., Huang, K., Lei, C., Ueno, S., Miura, T., Ito, T., Nagasawa, K., Maeno, T., Watarai, H., Yamagishi, M., Uemura, S., Ohnuki, S., Ohya, Y., Kurokawa, H., Matsusaka, S., Sun, C. W., Ozeki, Y., and Goda, K. Virtual-freezing fluorescence imaging flow cytometry. *Nature Communications*, 11(1):1162, dec 2020. ISSN 20411723. doi: 10.1038/s41467-020-14929-2. URL http://www.nature.com/articles/s41467-020-14929-2.

Mikkelsen, H., Duck, Z., Lilley, K. S., and Welch, M. Interrelationships between colonies, biofilms, and planktonic cells of *Pseudomonas aeruginosa*. *Journal of Bacteriology*, 189(6):2411–2416, mar 2007. ISSN 00219193. doi: 10.1128/JB.

01687-06. URL http://www.ncbi.nlm.nih.gov/pubmed/17220232http://www.pubmedcentral.nih.gov/articlerender.fcgi?artid=PMC1899361.

Miyakoshi, M., Nishida, H., Shintani, M., Yamane, H., and Nojiri, H. High-resolution mapping of plasmid transcriptomes in different host bacteria. *BMC Genomics*, 10:12, jan 2009. ISSN 14712164. doi: 10.1186/1471-2164-10-12. URL http://www.ncbi.nlm.nih.gov/pubmed/19134166http://www.pubmedcentral.nih.gov/articlerender.fcgi?artid=PMC2642839.

Mol, O. and Oudega, B. Molecular and structural aspects of fimbriae biosynthesis and assembly in *Escherichia coli*. *FEMS Microbiology Reviews*, 19(1): 25–52, oct 1996. ISSN 1574-6976. doi: 10.1111/j.1574-6976.1996.tb00252.x. URL https://academic.oup.com/femsre/article-lookup/doi/10.1111/j.1574-6976.1996.tb00252.x.

Moran, R. A. and Hall, R. M. Analysis of pCERC7, a small antibiotic resistance plasmid from a commensal ST131 *Escherichia coli*, defines a diverse group of plasmids that include various segments adjacent to a multimer resolution site and encode the same NikA relaxase accessory protein. *Plasmid*, 89:42–48, jan 2017. ISSN 10959890. doi: 10.1016/j.plasmid.2016.11.001. URL https://www.sciencedirect.com/science/article/pii/S0147619X16300592?via%3Dihub.

Müller, P., Gimpel, M., Wildenhain, T., and Brantl, S. A new role for CsrA: promotion of complex formation between an sRNA and its mRNA target in *Bacillus subtilis*. *RNA Biology*, 16(7):972–987, jul 2019. ISSN 15558584. doi: 10.1080/15476286.2019.1605811. URL https://www.tandfonline.com/doi/full/10.1080/15476286.2019.1605811.

Müller, S. and Nebe-Von-Caron, G. Functional single-cell analyses: Flow cytometry and cell sorting of microbial populations and communities, jul 2010. ISSN 01686445. URL https://academic.oup.com/femsre/article-lookup/doi/10.1111/j.1574-6976.2010.00214.x.

Munita, J. M. and Arias, C. A. Mechanisms of antibiotic resistance. *Microbiology Spectrum*, 2016. doi: 10.1128/MICROBIOLSPEC.VMBF-0016-2015. URL https://journals.asm.org/doi/10.1128/microbiolspec.VMBF-0016-2015.

Muselius, B., Sukumaran, A., Yeung, J., and Geddes-McAlister, J. Iron limitation in *Klebsiella pneumoniae* defines new roles for Lon protease in homeostasis and degradation by quantitative proteomics. *Frontiers in Microbiology*, 11:546, apr 2020. ISSN 1664302X. doi: 10.3389/fmicb.2020.00546. URL https://www.frontiersin.org/article/10.3389/fmicb.2020.00546/full.

Myers, J. A., Curtis, B. S., and Curtis, W. R. Improving accuracy of cell and chromophore concentration measurements using optical density. *BMC Biophysics*, 6(1):4, apr 2013. ISSN 2046-1682. doi: 10.1186/2046-1682-6-4. URL http://bmcbiophys.biomedcentral.com/articles/10.1186/2046-1682-6-4.

Naito, M. and Pawlowska, T. E. The role of mobile genetic elements in evolutionary longevity of heritable endobacteria. *Mobile Genetic Elements*, 6(1):e1136375, 2016. doi: 10.1080/2159256x.2015.1136375. URL https://www.ncbi.nlm.nih.gov/pmc/articles/PMC4802751/.

Navarro Llorens, J. M., Tormo, A., and Martínez-García, E. Stationary phase in Gram-negative bacteria, jul 2010. ISSN 15746976. URL https://academic.oup.com/femsre/article-lookup/doi/10.1111/j.1574-6976.2010.00213.x.

Navon-Venezia, S., Kondratyeva, K., and Carattoli, A. *Klebsiella pneumoniae*: A major worldwide source and shuttle for antibiotic resistance, may 2017. ISSN 15746976. URL https://academic.oup.com/femsre/article-lookup/doi/10.1093/femsre/fux013.

Nguyen, T. N. T., Nguyen, P. L. N., Le, N. T. Q., Nguyen, L. P. H., Duong, T. B., Ho, N. D. T., Nguyen, Q. P. N., Pham, T. D., Tran, A. T., The, H. C., Nguyen, H. H., Nguyen, C. V. V., Thwaites, G. E., Rabaa, M. A., and Pham, D. T. Emerging carbapenem-resistant *Klebsiella pneumoniae* se-

quence type 16 causing multiple outbreaks in a tertiary hospital in southern Vietnam. *Microbial Genomics*, 7(3):000519, mar 2021. ISSN 20575858. doi: 10.1099/mgen.0.000519. URL https://www.microbiologyresearch.org/content/journal/mgen/10.1099/mgen.0.000519.

Ni, S., Li, B., Tang, K., Yao, J., Wood, T. K., Wang, P., and Wang, X. Conjugative plasmid-encoded toxin-antitoxin system PrpT/PrpA directly controls plasmid copy number. *Proceedings of the National Academy of Sciences of the United States of America*, 118(4), jan 2021. ISSN 1091-6490. doi: 10.1073/pnas.2011577118. URL http://www.ncbi.nlm.nih.gov/pubmed/33483419http://www.pubmedcentral.nih.gov/articlerender.fcgi?artid=PMC7848731.

Nolivos, S., Cayron, J., Dedieu, A., Page, A., Delolme, F., and Lesterlin, C. Role of AcrAB-TolC multidrug efflux pump in drug-resistance acquisition by plasmid transfer. *Science (New York, N.Y.)*, 364(6442):778–782, may 2019. ISSN 10959203. doi: 10.1126/science.aav6390. URL http://www.ncbi.nlm.nih.gov/pubmed/31123134.

Nordmann, P., Naas, T., and Poirel, L. Global spread of carbapenemase producing *Enterobacteriaceae*. *Emerging Infectious Diseases*, 17(10):1791–1798, oct 2011. ISSN 10806059. doi: 10.3201/eid1710.110655. URL http://wwwnc.cdc.gov/eid/article/17/10/11-0655_article.htm.

Norman, A., Hansen, L. H., and Sørensen, S. J. Conjugative plasmids: Vessels of the communal gene pool, aug 2009. ISSN 14712970. URL http://www.ncbi.nlm.nih.gov/pubmed/19571247http://www.pubmedcentral.nih.gov/articlerender.fcgi?artid=PMC2873005.

O'Neill, J. Tackling drug-resistant infections globally : Final report and recommendations. (May), 2016. ISSN 0042-9686. doi: 10.1016/j.jpha.2015.11.005. URL https://amr-review.org/sites/default/files/160525_Finalpaper_withcover.pdf.

Orlek, A., Stoesser, N., Anjum, M. F., Doumith, M., Ellington, M. J., Peto, T., Crook, D., Woodford, N., Sarah Walker, A., Phan, H., and Sheppard, A. E. Plasmid classification in an era of whole-genome sequencing: Application in studies of antibiotic resistance epidemiology, feb 2017. ISSN 1664302X. URL http://journal.frontiersin.org/article/10.3389/fmicb.2017.00182/full.

Orr, H. A. Fitness and its role in evolutionary genetics, aug 2009. ISSN 14710056. URL http://www.nature.com/articles/nrg2603.

O'Toole, G. A. Microtiter dish biofilm formation assay. *Journal of Visualized Experiments*, (47), jan 2010. ISSN 1940087X. doi: 10.3791/2437. URL http://www.ncbi.nlm.nih.gov/pubmed/21307833http://www.pubmedcentral.nih.gov/articlerender.fcgi?artid=PMC3182663.

Ou, F., McGoverin, C., Swift, S., and Vanholsbeeck, F. Absolute bacterial cell enumeration using flow cytometry. *Journal of Applied Microbiology*, 123(2):464–477, aug 2017. ISSN 13652672. doi: 10.1111/jam.13508. URL http://doi.wiley.com/10.1111/jam.13508.

Paczosa, M. K. and Mecsas, J. *Klebsiella pneumoniae*: Going on the Offense with a Strong Defense. *Microbiology and Molecular Biology Reviews*, 80(3):629–661, 2016. ISSN 1092-2172. doi: 10.1128/mmbr.00078-15. URL http://mmbr.asm.org/.

Page, A. J., Cummins, C. A., Hunt, M., Wong, V. K., Reuter, S., Holden, M. T., Fookes, M., Falush, D., Keane, J. A., and Parkhill, J. Roary: Rapid large-scale prokaryote pan genome analysis. *Bioinformatics*, 31(22):3691–3693, nov 2015. ISSN 14602059. doi: 10.1093/bioinformatics/btv421. URL https://academic.oup.com/bioinformatics/article-lookup/doi/10.1093/bioinformatics/btv421.

Papp-Wallace, K. M., Endimiani, A., Taracila, M. A., and Bonomo, R. A. Carbapenems: Past, present, and future, nov 2011. ISSN

00664804. URL http://www.ncbi.nlm.nih.gov/pubmed/21859938http://www.pubmedcentral.nih.gov/articlerender.fcgi?artid=PMC3195018.

Partridge, S. R., Kwong, S. M., Firth, N., and Jensen, S. O. Mobile genetic elements associated with antimicrobial resistance, oct 2018. ISSN 10986618. URL https://cmr.asm.org/content/31/4/e00088-17.

Patel, G., Huprikar, S., Factor, S. H., Jenkins, S. G., and Calfee, D. P. Outcomes of carbapenem-resistant *Klebsiella pneumoniae* infection and the impact of antimicrobial and adjunctive therapies. *Infection Control Hospital Epidemiology*, 29(12):1099–1106, dec 2008. ISSN 0899-823X. doi: 10.1086/592412. URL http://www.ncbi.nlm.nih.gov/pubmed/18973455.

Paterson, D. L. and Bonomo, R. A. Extended-spectrum β-lactamases: A clinical update, oct 2005. ISSN 08938512. URL http://www.ncbi.nlm.nih.gov/pubmed/16223952http://www.pubmedcentral.nih.gov/articlerender.fcgi?artid=PMC1265908.

Pearson, W. R. An introduction to sequence similarity ("homology") searching. *Current Protocols in Bioinformatics*, Chapter 3(SUPPL.42): Unit3.1, jun 2013. ISSN 19343396. doi: 10.1002/0471250953.bi0301s42. URL http://www.ncbi.nlm.nih.gov/pubmed/23749753http://www.pubmedcentral.nih.gov/articlerender.fcgi?artid=PMC3820096.

Pedersen, T., Tellevik, M. G., Kommedal, Ø., Lindemann, P. C., Moyo, S. J., Janice, J., Blomberg, B., Samuelsen, Ø., and Langeland, N. Horizontal plasmid transfer among *Klebsiella pneumoniae* isolates is the key factor for dissemination of extended-spectrum β-lactamases among children in Tanzania. *mSphere*, 5(4), aug 2020. ISSN 2379-5042. doi: 10.1128/msphere.00428-20. URL https://journals.asm.org/doi/10.1128/mSphere.00428-20.

Penesyan, A., Nagy, S. S., Kjelleberg, S., Gillings, M. R., and Paulsen, I. T. Rapid microevolution of biofilm cells in response to antibiotics. *npj Biofilms and Micro-*

biomes, 5(1):34, dec 2019. ISSN 20555008. doi: 10.1038/s41522-019-0108-3. URL http://www.nature.com/articles/s41522-019-0108-3.

Pérez-Mendoza, D. and de la Cruz, F. *Escherichia coli* genes affecting recipient ability in plasmid conjugation: Are there any? *BMC Genomics*, 10(1):71, feb 2009. ISSN 14712164. doi: 10.1186/1471-2164-10-71. URL http://bmcgenomics.biomedcentral.com/articles/10.1186/1471-2164-10-71.

Piperaki, E. T., Syrogiannopoulos, G. A., Tzouvelekis, L. S., and Daikos, G. L. *Klebsiella pneumoniae*: Virulence, biofilm and antimicrobial resistance. *Pediatric Infectious Disease Journal*, 36(10):1002–1005, 2017. ISSN 15320987. doi: 10.1097/INF.0000000000001675. URL http://www.ncbi.nlm.nih.gov/pubmed/28914748.

Podschun, R. and Ullmann, U. *Klebsiella* spp. as nosocomial pathogens: Epidemiology, taxonomy, typing methods, and pathogenicity factors, oct 1998. ISSN 08938512. URL http://www.ncbi.nlm.nih.gov/pubmed/9767057http://www.pubmedcentral.nih.gov/articlerender.fcgi?artid=PMC88898.

Popat, R., Crusz, S. A., Messina, M., Williams, P., West, S. A., and Diggle, S. P. Quorum-sensing and cheating in bacterial biofilms. *Proceedings of the Royal Society B: Biological Sciences*, 279(1748):4765–4771, dec 2012. ISSN 14712954. doi: 10.1098/rspb.2012.1976. URL http://www.ncbi.nlm.nih.gov/pubmed/23034707http://www.pubmedcentral.nih.gov/articlerender.fcgi?artid=PMC3497100.

Pope, J. L., Yang, Y., Newsome, R. C., Sun, W., Sun, X., Ukhanova, M., Neu, J., Issa, J. P., Mai, V., and Jobin, C. Microbial colonization coordinates the pathogenesis of a *Klebsiella pneumoniae* infant isolate. *Scientific Reports*, 9(1):3380, dec 2019. ISSN 20452322. doi: 10.1038/s41598-019-39887-8. URL http://www.nature.com/articles/s41598-019-39887-8.

Pornsukarom, S. and Thakur, S. Horizontal dissemination of antimicrobial resistance

determinants in multiple *Salmonella* serotypes following isolation from the commercial swine operation environment after manure application. *Applied and Environmental Microbiology*, 83(20):e01503–17, oct 2017. ISSN 0099-2240. doi: 10.1128/aem.01503-17. URL https://aem.asm.org/content/83/20/e01503-17.

Potron, A., Nordmann, P., Lafeuille, E., Al Maskari, Z., Al Rashdi, F., and Poirel, L. Characterization of OXA-181, a carbapenem-hydrolyzing class D β-lactamase from *Klebsiella pneumoniae*. *Antimicrobial Agents and Chemotherapy*, 55(10): 4896–4899, oct 2011. ISSN 00664804. doi: 10.1128/AAC.00481-11. URL https://aac.asm.org/content/55/10/4896.

Potter, R. F., D'Souza, A. W., and Dantas, G. The rapid spread of carbapenem-resistant *Enterobacteriaceae*, nov 2016. ISSN 15322084. URL https://www.sciencedirect.com/science/article/abs/pii/S1368764616300449?via%3Dihub.

Potts, A. H., Vakulskas, C. A., Pannuri, A., Yakhnin, H., Babitzke, P., and Romeo, T. Global role of the bacterial post-transcriptional regulator CsrA revealed by integrated transcriptomics. *Nature Communications*, 8(1):1596, dec 2017. ISSN 20411723. doi: 10.1038/s41467-017-01613-1. URL http://www.nature.com/articles/s41467-017-01613-1.

Powell, D. drpowell/degust 4.1.1, oct 2019. URL https://zenodo.org/record/3501067#.YfFRey2cagR.

Prensky, H., Gomez-Simmonds, A., Uhlemann, A., and Lopatkin, A. J. Conjugation dynamics depend on both the plasmid acquisition cost and the fitness cost. *Molecular Systems Biology*, 17(3):e9913, mar 2021. ISSN 1744-4292. doi: 10.15252/msb.20209913. URL https://onlinelibrary.wiley.com/doi/10.15252/msb.20209913.

Prestinaci, F., Pezzotti, P., and Pantosti, A. Antimicrobial resistance: A global multifaceted phenomenon, 2015. ISSN 20477732. URL http:

//www.ncbi.nlm.nih.gov/pubmed/26343252http://www.pubmedcentral.nih.gov/articlerender.fcgi?artid=PMC4768623.

Pysz, M. A., Conners, S. B., Montero, C. I., Shockley, K. R., Johnson, M. R., Ward, D. E., and Kelly, R. M. Transcriptional analysis of biofilm formation processes in the anaerobic, hyperthermophilic bacterium *Thermotoga maritima*. *Applied and Environmental Microbiology*, 70(10):6098–6112, oct 2004. ISSN 00992240. doi: 10.1128/AEM.70.10.6098-6112.2004. URL https://aem.asm.org/content/70/10/6098.

Queenan, A. M. and Bush, K. Carbapenemases: The versatile β-lactamases, jul 2007. ISSN 08938512. URL http://www.ncbi.nlm.nih.gov/pubmed/17630334http://www.pubmedcentral.nih.gov/articlerender.fcgi?artid=PMC1932750.

R Core Team: R Foundation for Statistical Computing. R: A language and environment for statistical computing, 2020. URL https://www.r-project.org/.

Ramirez, M. S., Iriarte, A., Reyes-Lamothe, R., Sherratt, D. J., and Tolmasky, M. E. Small *Klebsiella pneumoniae* plasmids: Neglected contributors to antibiotic resistance. *Frontiers in Microbiology*, 10:2182, sep 2019. ISSN 1664302X. doi: 10.3389/fmicb.2019.02182. URL https://www.frontiersin.org/article/10.3389/fmicb.2019.02182/full.

Ramsay, J. P. and Firth, N. Diverse mobilization strategies facilitate transfer of non-conjugative mobile genetic elements, aug 2017. ISSN 18790364. URL https://www.sciencedirect.com/science/article/pii/S1369527416301680?via%3Dihub.

Rao, R. N., Allen, N. E., Hobbs, J. N., Alborn, W. E., Kirst, H. A., and Paschal, J. W. Genetic and enzymatic basis of hygromycin B resistance in *Escherichia coli*. *Antimicrobial Agents and Chemotherapy*, 24(5):689–695, 1983.

ISSN 00664804. doi: 10.1128/AAC.24.5.689. URL https://www.ncbi.nlm.nih.gov/pmc/articles/PMC185926/.

Razavi, M., Kristiansson, E., Flach, C.-F., and Larsson, D. G. J. The association between insertion sequences and antibiotic resistance genes. *mSphere*, 5(5), oct 2020. ISSN 23795042. doi: 10.1128/msphere.00418-20. URL https://journals.asm.org/doi/10.1128/mSphere.00418-20.

Reardon, A. J., Elliott, J. A., and McGann, L. E. Fluorescence as an alternative to light-scatter gating strategies to identify frozen-thawed cells with flow cytometry. *Cryobiology*, 69(1):91–99, aug 2014. ISSN 10902392. doi: 10.1016/j.cryobiol.2014.05.009. URL https://www.sciencedirect.com/science/article/pii/S0011224014001205.

Redondo-Salvo, S., Fernández-López, R., Ruiz, R., Vielva, L., de Toro, M., Rocha, E. P., Garcillán-Barcia, M. P., and de la Cruz, F. Pathways for horizontal gene transfer in bacteria revealed by a global map of their plasmids. *Nature Communications*, 11(1):3602, dec 2020. ISSN 20411723. doi: 10.1038/s41467-020-17278-2. URL http://www.nature.com/articles/s41467-020-17278-2.

Reisner, A., Wolinski, H., and Zechner, E. L. *In situ* monitoring of IncF plasmid transfer on semi-solid agar surfaces reveals a limited invasion of plasmids in recipient colonies. *Plasmid*, 67(2):155–161, mar 2012. ISSN 0147619X. doi: 10.1016/j.plasmid.2012.01.001. URL http://www.ncbi.nlm.nih.gov/pubmed/22248925http://www.pubmedcentral.nih.gov/articlerender.fcgi?artid=PMC3338210https://linkinghub.elsevier.com/retrieve/pii/S0147619X12000054.

Rendueles, O., de Sousa, J. A., Bernheim, A., Touchon, M., and Rocha, E. P. Genetic exchanges are more frequent in bacteria encoding capsules. *PLoS Genetics*, 14(12):e1007862, dec 2018. ISSN 15537404. doi: 10.1371/journal.pgen.1007862. URL https://dx.plos.org/10.1371/journal.pgen.1007862.

Reyes-Lamothe, R. and Sherratt, D. J. The bacterial cell cycle, chromosome inheritance and cell growth. *Nature Reviews Microbiology*, 17(8):467–478, aug 2019. ISSN 1740-1526. doi: 10.1038/s41579-019-0212-7. URL http://www.nature.com/articles/s41579-019-0212-7.

Richardson, E. J. and Watson, M. The automatic annotation of bacterial genomes. *Briefings in Bioinformatics*, 14(1):1–12, jan 2013. ISSN 14675463. doi: 10.1093/bib/bbs007. URL http://www.ncbi.nlm.nih.gov/pubmed/22408191http://www.pubmedcentral.nih.gov/articlerender.fcgi?artid=PMC3548604.

Rodrigues, C., Passet, V., Rakotondrasoa, A., Diallo, T. A., Criscuolo, A., and Brisse, S. Description of *Klebsiella africanensis* sp. nov., *Klebsiella variicola* subsp. *tropicalensis* subsp. nov. and *Klebsiella variicola* subsp. *variicola* subsp. nov. *Research in Microbiology*, 170(3):165–170, apr 2019. ISSN 17697123. doi: 10.1016/j.resmic.2019.02.003. URL https://www.sciencedirect.com/science/article/pii/S0923250819300191?via%3Dihub#fig1.

Rodríguez-Baño, J., Gutiérrez-Gutiérrez, B., Machuca, I., and Pascual, A. Treatment of infections caused by extended-spectrum-beta-lactamase-, *ampC*-, and carbapenemase-producing *Enterobacteriaceae*, apr 2018. ISSN 10986618. URL http://www.ncbi.nlm.nih.gov/pubmed/29444952http://www.pubmedcentral.nih.gov/articlerender.fcgi?artid=PMC5967687.

Rodríguez-Beltrán, J., DelaFuente, J., León-Sampedro, R., MacLean, R. C., and San Millán, Á. Beyond horizontal gene transfer: the role of plasmids in bacterial evolution. *Nature Reviews Microbiology*, 19(6):347–359, jun 2021. ISSN 1740-1526. doi: 10.1038/s41579-020-00497-1. URL http://www.nature.com/articles/s41579-020-00497-1.

Roer, L., Aarestrup, F. M., and Hasman, H. The EcoKI type I restriction-modification system in *Escherichia coli* affects but is not an absolute barrier for conjugation. *Journal of Bacteriology*, 197(2):337–342,

jan 2015. ISSN 10985530. doi: 10.1128/JB.02418-14. URL http://www.ncbi.nlm.nih.gov/pubmed/25384481http://www.pubmedcentral.nih.gov/articlerender.fcgi?artid=PMC4272590.

Rojas, L. J., Hujer, A. M., Rudin, S. D., Wright, M. S., Domitrovic, T. N., Marshall, S. H., Hujer, K. M., Richter, S. S., Cober, E., Perez, F., Adams, M. D., van Duin, D., and Bonomo, R. A. NDM-5 and OXA-181 beta-Lactamases, a significant threat continues to spread in the Americas. *Antimicrobial Agents and Chemotherapy*, 61(7), 2017. doi: 10.1128/AAC.00454-17. URL https://www.ncbi.nlm.nih.gov/pmc/articles/PMC5487671/.

Rolfe, M. D., Rice, C. J., Lucchini, S., Pin, C., Thompson, A., Cameron, A. D. S., Alston, M., Stringer, M. F., Betts, R. P., Baranyi, J., Peck, M. W., and Hinton, J. C. D. Lag phase is a distinct growth phase that prepares bacteria for exponential growth and involves transient metal accumulation. *Journal of bacteriology*, 194(3):686–701, feb 2012. ISSN 1098-5530. doi: 10.1128/JB.06112-11. URL http://www.ncbi.nlm.nih.gov/pubmed/22139505http://www.pubmedcentral.nih.gov/articlerender.fcgi?artid=PMC3264077.

Rooney, L. M., Amos, W. B., Hoskisson, P. A., and McConnell, G. Intra-colony channels in *E. coli* function as a nutrient uptake system. *ISME Journal*, 14(10):2461–2473, jun 2020. ISSN 17517370. doi: 10.1038/s41396-020-0700-9. URL http://www.nature.com/articles/s41396-020-0700-9.

Rosenberg, M., Azevedo, N. F., and Ivask, A. Propidium iodide staining underestimates viability of adherent bacterial cells. *Scientific Reports*, 9(1):6483, dec 2019. ISSN 2045-2322. doi: 10.1038/s41598-019-42906-3. URL http://www.nature.com/articles/s41598-019-42906-3.

Rothfield, L. I. and Justice, S. S. Bacterial cell division: The cycle of the ring, mar 1997. ISSN 00928674. URL http://www.ncbi.nlm.nih.gov/pubmed/9054497.

Rozwandowicz, M., Brouwer, M. S., Fischer, J., Wagenaar, J. A., Gonzalez-Zorn,

B., Guerra, B., Mevius, D. J., and Hordijk, J. Plasmids carrying antimicrobial resistance genes in *Enterobacteriaceae*. *Journal of Antimicrobial Chemotherapy*, 73(5):1121–1137, 2018. ISSN 14602091. doi: 10.1093/jac/dkx488. URL https://academic.oup.com/jac/article-abstract/73/5/1121/4822282.

Rumbo-Feal, S., Gómez, M. J., Gayoso, C., Álvarez-Fraga, L., Cabral, M. P., Aransay, A. M., Rodríguez-Ezpeleta, N., Fullaondo, A., Valle, J., Tomás, M., Bou, G., and Poza, M. Whole transcriptome analysis of *Acinetobacter baumannii* assessed by RNA-sequencing reveals different mRNA expression profiles in biofilm compared to planktonic cells. *PLoS ONE*, 8(8):e72968, aug 2013. ISSN 1932-6203. doi: 10.1371/journal.pone.0072968. URL https://dx.plos.org/10.1371/journal.pone.0072968.

Russo, T. A., Olson, R., Fang, C. T., Stoesser, N., Miller, M., MacDonald, U., Hutson, A., Barker, J. H., La Hoz, R. M., Johnson, J. R., Backer, M., Bajwa, R., Catanzaro, A. T., Crook, D., De Almeida, K., Fierer, J., Greenberg, D. E., Klevay, M., Patel, P., Ratner, A., Wang, J. T., and Zola, J. Identification of biomarkers for differentiation of hypervirulent *Klebsiella pneumoniae* from classical *K. pneumoniae*. *Journal of Clinical Microbiology*, 56(9), 2018. ISSN 1098660X. doi: 10.1128/JCM.00776-18. URL https://doi.org/10.1128/JCM.00776-18.

San Millan, A. and MacLean, R. C. Fitness costs of plasmids: a limit to plasmid transmission. *Microbiology Spectrum*, 5(5), 2017. ISSN 2165-0497. doi: 10.1128/microbiolspec.mtbp-0016-2017. URL www.asmscience.org.

San Millan, A., Toll-Riera, M., Qi, Q., Betts, A., Hopkinson, R. J., McCullagh, J., and MacLean, R. C. Integrative analysis of fitness and metabolic effects of plasmids in *Pseudomonas aeruginosa* PAO1. *The ISME Journal*, 12(12):3014–3024, dec 2018. ISSN 1751-7362. doi: 10.1038/s41396-018-0224-8. URL http://www.nature.com/articles/s41396-018-0224-8.

Scholz, O., Thiel, A., Hillen, W., and Niederweis, M. Quantitative analysis of gene expression with an improved green fluorescent protein. *European Journal*

of Biochemistry, 267(6):1565–1570, mar 2000. ISSN 00142956. doi: 10.1046/j.1432-1327.2000.01170.x. URL http://doi.wiley.com/10.1046/j.1432-1327.2000.01170.x.

Schröder, G. and Lanka, E. The mating pair formation system of conjugative plasmids - A versatile secretion machinery for transfer of proteins and DNA, jul 2005. ISSN 0147619X. URL https://www.sciencedirect.com/science/article/pii/S0147619X05000168?via%3Dihub.

Schroll, C., Barken, K. B., Krogfelt, K. A., and Struve, C. Role of type 1 and type 3 fimbriae in *Klebsiella pneumoniae* biofilm formation. *BMC Microbiology*, 10 (1):179, jun 2010. ISSN 14712180. doi: 10.1186/1471-2180-10-179. URL http://bmcmicrobiol.biomedcentral.com/articles/10.1186/1471-2180-10-179.

Seemann, T. Prokka: Rapid prokaryotic genome annotation. *Bioinformatics*, 30(14):2068–2069, jul 2014. ISSN 14602059. doi: 10.1093/bioinformatics/btu153. URL https://academic.oup.com/bioinformatics/article-lookup\/doi/10.1093/bioinformatics/btu153.

Shankar, C., Vasudevan, K., Jacob, J., Baker, S., Isaac, B. J., Neeravi, A. R., Prabaa, D., Sethuvel, M., George, B., and Veeraraghavan, B. Mosaic antimicrobial resistance/virulence plasmid in hypervirulent ST2096 *Klebsiella pneumoniae* in India: The rise of a new superbug? *bioRxiv*, page 2020.12.11.422261, dec 2020. doi: 10.1101/2020.12.11.422261. URL https://www.biorxiv.org/content/10.1101/2020.12.11.422261v1.fullhttps://www.biorxiv.org/content/10.1101/2020.12.11.422261v1%0Ahttps://www.biorxiv.org/content/10.1101/2020.12.11.422261v1.abstract.

Shankar-Sinha, S., Valencia, G. A., Janes, B. K., Rosenberg, J. K., Whitfield, C., Bender, R. A., Standiford, T. J., and Younger, J. G. The *Klebsiella pneumoniae* O antigen contributes to bacteremia and lethality during murine pneumonia. *Infection and Immunity*, 72(3):1423–1430, mar 2004. ISSN 00199567. doi: 10.1128/IAI.72.3.1423-1430.

2004. URL http://www.ncbi.nlm.nih.gov/pubmed/14977947http://www.pubmedcentral.nih.gov/articlerender.fcgi?artid=PMC355988.

Sharma, P., Haycocks, J. R., Middlemiss, A. D., Kettles, R. A., Sellars, L. E., Ricci, V., Piddock, L. J., and Grainger, D. C. The multiple antibiotic resistance operon of enteric bacteria controls DNA repair and outer membrane integrity. *Nature Communications*, 8(1):1444, dec 2017. ISSN 20411723. doi: 10.1038/s41467-017-01405-7. URL http://www.nature.com/articles/s41467-017-01405-7.

Shen, Z., Zhang, H., Gao, Q., Qin, J., Zhang, C., Zhu, J., and Li, M. Increased plasmid copy number contributes to the elevated carbapenem resistance in OXA-232-producing *Klebsiella pneumoniae*. *Microbial Drug Resistance*, 26(6):561–568, jun 2020. ISSN 19318448. doi: 10.1089/mdr.2018.0407. URL http://www.ncbi.nlm.nih.gov/pubmed/31895640.

Sherchan, J. B., Tada, T., Shrestha, S., Uchida, H., Hishinuma, T., Morioka, S., Shahi, R. K., Bhandari, S., Twi, R. T., Kirikae, T., and Sherchand, J. B. Emergence of clinical isolates of highly carbapenem-resistant *Klebsiella pneumoniae* co-harboring $bla_{\text{NDM-5}}$ and $bla_{\text{OXA-181}}$ or $_{\text{-232}}$ in Nepal. *International Journal of Infectious Diseases*, 92:247–252, mar 2020. ISSN 18783511. doi: 10.1016/j.ijid.2020.01.040. URL https://www.sciencedirect.com/science/article/pii/S1201971220300424.

Sheu, C. C., Chang, Y. T., Lin, S. Y., Chen, Y. H., and Hsueh, P. R. Infections caused by carbapenem-resistant *Enterobacteriaceae*: An update on therapeutic options, jan 2019. ISSN 1664302X. URL https://www.frontiersin.org/article/10.3389/fmicb.2019.00080/full.

Shintani, M., Takahashi, Y., Tokumaru, H., Kadota, K., Hara, H., Miyakoshi, M., Naito, K., Yamane, H., Nishida, H., and Nojiri, H. Response of the *Pseudomonas* host chromosomal transcriptome to carriage of the IncP-7 plasmid

pCAR1. *Environmental Microbiology*, 12(6):1413–1426, dec 2010. ISSN 14622912. doi: 10.1111/j.1462-2920.2009.02110.x. URL https://onlinelibrary.wiley.com/doi/10.1111/j.1462-2920.2009.02110.x.

Sieuwerts, S., De Bok, F. A., Mols, E., De Vos, W. M., and Van Hylckama Vlieg, J. E. A simple and fast method for determining colony forming units. *Letters in Applied Microbiology*, 47(4):275–278, oct 2008. ISSN 02668254. doi: 10.1111/j.1472-765X.2008.02417.x. URL http://doi.wiley.com/10.1111/j.1472-765X.2008.02417.x.

Siguier, P., Perochon, J., Lestrade, L., Mahillon, J., and Chandler, M. ISfinder: The reference centre for bacterial insertion sequences. *Nucleic acids research*, 34(Database issue):D32–D36, jan 2006. ISSN 13624962. doi: 10.1093/nar/gkj014. URL https://academic.oup.com/nar/article-lookup/doi/10.1093/nar/gkj014.

Siguier, P., Gourbeyre, E., and Chandler, M. Bacterial insertion sequences: Their genomic impact and diversity. *FEMS Microbiology Reviews*, 38(5):865–891, sep 2014. ISSN 15746976. doi: 10.1111/1574-6976.12067. URL https://academic.oup.com/femsre/article-lookup/doi/10.1111/1574-6976.12067.

Singh, A. K., Yadav, S., Chauhan, B. S., Nandy, N., Singh, R., Neogi, K., Roy, J. K., Srikrishna, S., Singh, R. K., and Prakash, P. Classification of clinical isolates of *Klebsiella pneumoniae* based on their *in vitro* biofilm forming capabilities and elucidation of the biofilm matrix chemistry with special reference to the protein content. *Frontiers in Microbiology*, 10(APR):669, apr 2019. ISSN 1664302X. doi: 10.3389/fmicb.2019.00669. URL https://www.frontiersin.org/article/10.3389/fmicb.2019.00669/full.

Smith, R. A., M'ikanatha, N. M., and Read, A. F. Antibiotic resistance: A primer and call to action. *Health Communication*, 30 (3):309–314, 2015. ISSN 15327027. doi: 10.1080/10410236.2014.

943634. URL http://www.ncbi.nlm.nih.gov/pubmed/\25121990http://www.pubmedcentral.nih.gov/articlerender.fcgi?artid=PMC4275377.

Sørensen, S. J., Sørensen, A. H., Hansen, L. H., Oregaard, G., and Veal, D. Direct detection and quantification of horizontal gene transfer by using flow cytometry and gfp as a reporter gene. *Current Microbiology*, 47(2):129–133, aug 2003. ISSN 03438651. doi: 10.1007/s00284-002-3978-0. URL http://link.springer.com/10.1007/s00284-002-3978-0.

Stalder, T. and Top, E. Plasmid transfer in biofilms: A perspective on limitations and opportunities, nov 2016. ISSN 20555008. URL http://www.nature.com/articles/npjbiofilms201622.

Stalder, T., Cornwell, B., Lacroix, J., Kohler, B., Dixon, S., Yano, H., Kerr, B., Forney, L. J., and Top, E. M. Evolving populations in biofilms contain more persistent plasmids. *Molecular Biology and Evolution*, 37(6):1563–1576, jun 2020. ISSN 15371719. doi: 10.1093/molbev/msaa024. URL https://academic.oup.com/mbe/article/37/6/1563/5728644.

Stamatakis, A. RAxML version 8: A tool for phylogenetic analysis and post-analysis of large phylogenies. *Bioinformatics*, 30(9):1312–1313, may 2014. ISSN 14602059. doi: 10.1093/bioinformatics/btu033. URL https://academic.oup.com/bioinformatics/article-lookup/doi/10.1093/bioinformatics/btu033.

Stanley, N. R. and Lazazzera, B. A. Environmental signals and regulatory pathways that influence biofilm formation, apr 2004. ISSN 0950382X. URL http://doi.wiley.com/10.1111/j.1365-2958.2004.04036.x.

Stanton, T. B. A call for antibiotic alternatives research, mar 2013. ISSN 0966842X. URL https://www.sciencedirect.com/science/article/pii/S0966842X12001990.

Steffen, M. M., Dearth, S. P., Dill, B. D., Li, Z., Larsen, K. M., Campagna, S. R., and Wilhelm, S. W. Nutrients drive transcriptional changes that maintain metabolic

homeostasis but alter genome architecture in *Microcystis*. *ISME Journal*, 8(10): 2080–2092, oct 2014. ISSN 17517370. doi: 10.1038/ismej.2014.78. URL http://www.nature.com/articles/ismej201478.

Stiefel, P., Schmidt-Emrich, S., Maniura-Weber, K., and Ren, Q. Critical aspects of using bacterial cell viability assays with the fluorophores SYTO9 and propidium iodide. *BMC Microbiology*, 15(1):36, feb 2015. ISSN 14712180. doi: 10.1186/s12866-015-0376-x. URL http://www.biomedcentral.com/1471-2180/15/36.

Stoesser, N., Sheppard, A. E., Peirano, G., Anson, L. W., Pankhurst, L., Sebra, R., Phan, H. T., Kasarskis, A., Mathers, A. J., Peto, T. E., Bradford, P., Motyl, M. R., Walker, A. S., Crook, D. W., and Pitout, J. D. Genomic epidemiology of global *Klebsiella pneumoniae* carbapenemase (KPC)-producing Escherichia coli. *Scientific Reports*, 7(1):5917, dec 2017. ISSN 20452322. doi: 10.1038/s41598-017-06256-2. URL http://www.nature.com/articles/s41598-017-06256-2.

Storey, D., McNally, A., Åstrand, M., sa-Pessoa Graca Santos, J., Rodriguez-Escudero, I., Elmore, B., Palacios, L., Marshall, H., Hobley, L., Molina, M., Cid, V. J., Salminen, T. A., and Bengoechea, J. A. Klebsiella pneumoniae type VI secretion system-mediated microbial competition is PhoPQ controlled and reactive oxygen species dependent. *PLOS Pathogens*, 16(3):e1007969, mar 2020. ISSN 1553-7374. doi: 10.1371/journal.ppat.1007969. URL https://dx.plos.org/10.1371/journal.ppat.1007969.

Struve, C. and Krogfelt, K. A. Role of capsule in *Klebsiella pneumoniae* virulence: Lack of correlation between *in vitro* and *in vivo* studies. *FEMS Microbiology Letters*, 218(1):149–154, jan 2003. ISSN 03781097. doi: 10.1111/j.1574-6968.2003.tb11511.x. URL https://academic.oup.com/femsle/article-lookup/doi/10.1111/\j.1574-6968.2003.tb11511.x.

Struve, C., Bojer, M., and Krogfelt, K. A. Identification of a conserved chromosomal region encoding *Klebsiella pneumoniae* type 1 and type 3 fimbriae

and assessment of the role of fimbriae in pathogenicity. *Infection and Immunity*, 77(11):5016–5024, nov 2009. ISSN 00199567. doi: 10.1128/IAI.00585-09. URL http://www.ncbi.nlm.nih.gov/pubmed/19703972http://www.pubmedcentral.nih.gov/articlerender.fcgi?artid=PMC2772557.

Suhartono, S. and Savin, M. Conjugative transmission of antibiotic-resistance from stream water *Escherichia coli* as related to number of sulfamethoxazole but not class 1 and 2 integrase genes. *Mobile Genetic Elements*, 6(6):e1256851, nov 2016. ISSN 2159-256X. doi: 10.1080/2159256X.2016.1256851. URL https://www.tandfonline.com/doi/full/10.1080/2159256X.2016.1256851.

Tacconelli, E., Carrara, E., Savoldi, A., Kattula, D., and Burkert, F. Global priority list of antibiotic-resistant bacteria to guide research, discovery, and development of new antibiotics, 2017. URL http://www.cdc.gov/drugresistance/threat-report-2013/.

Tatusov, R. L., Koonin, E. V., and Lipman, D. J. A genomic perspective on protein families. *Science*, 278(5338):631–637, oct 1997. ISSN 00368075. doi: 10.1126/science.278.5338.631. URL http://www.ncbi.nlm.nih.gov/pubmed/9381173.

Tazzyman, S. J. and Bonhoeffer, S. Why there are no essential genes on plasmids. *Molecular Biology and Evolution*, 32(12):3079–3088, dec 2015. ISSN 15371719. doi: 10.1093/molbev/msu293. URL https://academic.oup.com/mbe/article-lookup/doi/10.1093/molbev/msu293.

The European Committee on Antimicrobial Susceptibility Testing. Breakpoint tables for interpretation of MICs and zone diameters, version 7.0, 2017. Technical report, 2017. URL http://www.eucast.org/fileadmin/src/media/PDFs/EUCAST_files/Breakpoint_tables/v_5.0_Breakpoint_Table_01.pdf.

The European Committee on Antimicrobial Susceptibility Testing. Breakpoint tables for interpretation of MICs and zone diameters. Version 11.0. Technical report, 2021. URL http://www.eucast.org.

Thomas, C. M. and Nielsen, K. M. Mechanisms of, and barriers to, horizontal gene transfer between bacteria, sep 2005. ISSN 17401526. URL http://www.nature.com/articles/nrmicro1234.

Townsend, E. M., Moat, J., and Jameson, E. CAUTI's next top model – Model dependent *Klebsiella* biofilm inhibition by bacteriophages and antimicrobials. *Biofilm*, 2:100038, dec 2020. ISSN 25902075. doi: 10.1016/j.bioflm.2020.100038. URL https://www.sciencedirect.com/science/article/pii/S2590207520300216.

Trampari, E., Holden, E. R., Wickham, G. J., Ravi, A., Martins, L. d. O., Savva, G. M., and Webber, M. A. Exposure of *Salmonella* biofilms to antibiotic concentrations rapidly selects resistance with collateral tradeoffs. *npj Biofilms and Microbiomes*, 7(1):3, dec 2021. ISSN 20555008. doi: 10.1038/s41522-020-00178-0. URL http://www.nature.com/articles/s41522-020-00178-0.

Tran, F. and Boedicker, J. Q. Plasmid characteristics modulate the propensity of gene exchange in bacterial vesicles. *Journal of Bacteriology*, 201(7):e00430–18, apr 2019. ISSN 0021-9193. doi: 10.1128/jb.00430-18. URL http://www.ncbi.nlm.nih.gov/pubmed/30670543.

Tung, J. W., Heydari, K., Tirouvanziam, R., Sahaf, B., Parks, D. R., Herzenberg, L. A., and Herzenberg, L. A. Modern flow cytometry: A practical approach, sep 2007. ISSN 02722712. URL http://www.ncbi.nlm.nih.gov/pubmed/17658402http://www.pubmedcentral.nih.gov/articlerender.fcgi?\artid=PMC1994577.

Uelze, L., Grützke, J., Borowiak, M., Hammerl, J. A., Juraschek, K., Deneke, C., Tausch, S. H., and Malorny, B. Typing methods based on whole genome sequencing data. *One Health Outlook*, 2(1):3, dec 2020. ISSN 2524-4655. doi: 10.1186/s42522-020-0010-1. URL https://onehealthoutlook.biomedcentral.com/articles/10.1186/s42522-020-0010-1.

Ur Rahman, S., Ali, T., Ali, I., Khan, N. A., Han, B., and Gao, J. The growing genetic and functional diversity of extended spectrum beta-lactamases, mar 2018. ISSN 23146141. URL https://www.hindawi.com/journals/bmri/2018/9519718/.

Urpa, L. M. and Anders, S. Focused multidimensional scaling: Interactive visualization for exploration of high-dimensional data. *BMC Bioinformatics*, 20(1):221, dec 2019. ISSN 14712105. doi: 10.1186/s12859-019-2780-y. URL https://bmcbioinformatics.biomedcentral.com/articles/10.1186/s12859-019-2780-y.

Vandecraen, J., Chandler, M., Aertsen, A., and Van Houdt, R. The impact of insertion sequences on bacterial genome plasticity and adaptability, nov 2017. ISSN 15497828. URL https://www.tandfonline.com/doi/full/10.1080/1040841X.2017.1303661.

Ventola, C. L. The antibiotic resistance crisis: Part 1: causes and threats. *P T : a peer-reviewed journal for formulary management*, 40(4):277–83, apr 2015. ISSN 1052-1372. URL http://www.ncbi.nlm.nih.gov/pubmed/25859123http://www.pubmedcentral.nih.gov/articlerender.fcgi?artid=PMC4378521.

Villa, L., García-Fernández, A., Fortini, D., and Carattoli, A. Replicon sequence typing of IncF plasmids carrying virulence and resistance determinants. *Journal of Antimicrobial Chemotherapy*, 65(12):2518–2529, dec 2010. ISSN 03057453. doi: 10.1093/jac/dkq347. URL https://academic.oup.com/jac/article-lookup/doi/10.1093/jac/dkq347.

Vogan, A. A. and Higgs, P. G. The advantages and disadvantages of horizontal gene transfer and the emergence of the first species. *Biology Direct*, 6 (1):1, jan 2011. ISSN 17456150. doi: 10.1186/1745-6150-6-1. URL http://biologydirect.biomedcentral.com/articles/10.1186/1745-6150-6-1.

Vrancianu, C. O., Popa, L. I., Bleotu, C., and Chifiriuc, M. C. Targeting plas-

mids to limit acquisition and transmission of antimicrobial resistance. *Frontiers in Microbiology*, 11:761, 2020. ISSN 1664302X. doi: 10.3389/fmicb.2020.00761. URL http://www.ncbi.nlm.nih.gov/pubmed/32435238\http://www.pubmedcentral.nih.gov/articlerender.fcgi?artid=PMC7219019.

Waksman, G. From conjugation to T4S systems in Gram-negative bacteria: A mechanistic biology perspective. *EMBO reports*, 20(2):e47012, feb 2019. ISSN 1469-221X. doi: 10.15252/embr.201847012. URL http://www.ncbi.nlm.nih.gov/pubmed/30602585\http://www.pubmedcentral.nih.gov/articlerender.fcgi?artid=PMC6362355.

Walker, B. J., Abeel, T., Shea, T., Priest, M., Abouelliel, A., Sakthikumar, S., Cuomo, C. A., Zeng, Q., Wortman, J., Young, S. K., and Earl, A. M. Pilon: An integrated tool for comprehensive microbial variant detection and genome assembly improvement. *PLoS ONE*, 9(11):e112963, nov 2014. ISSN 19326203. doi: 10.1371/journal.pone.0112963. URL https://dx.plos.org/10.1371/journal.pone.0112963.

Wang, M., Tran, J. H., Jacoby, G. A., Zhang, Y., Wang, F., and Hooper, D. C. Plasmid-mediated quinolone resistance in clinical isolates of *Escherichia coli* from Shanghai, China. *Antimicrobial Agents and Chemotherapy*, 47(7):2242–2248, jul 2003. ISSN 00664804. doi: 10.1128/AAC.47.7.2242-2248.2003. URL http://www.ncbi.nlm.nih.gov/pubmed/12821475http://www.pubmedcentral.nih.gov/articlerender.fcgi?artid=PMC161834.

Wang, Z., Gerstein, M., and Snyder, M. RNA-Seq: A revolutionary tool for transcriptomics, jan 2009. ISSN 14710056. URL http://www.ncbi.nlm.nih.gov/pubmed/19015660http://www.pubmedcentral.nih.gov/articlerender.fcgi?artid=PMC2949280.

Watanabe, S., Ohbayashi, R., Kanesaki, Y., Saito, N., Chibazakura, T., Soga, T., and Yoshikawa, H. Intensive DNA replication and metabolism

during the lag phase in *Cyanobacteria*. *PLoS ONE*, 10(9):e0136800, 2015. ISSN 19326203. doi: 10.1371/journal.pone.0136800. URL http://www.ncbi.nlm.nih.gov/pubmed/26331851http://www.pubmedcentral.nih.gov/articlerender.fcgi?artid=PMC4558043.

Wein, T., Wang, Y., Barz, M., Stu cker, F. T., Hammerschmt, K., and Dagan, T. Essential gene acquisition destabilizes plasmid inheritance. *PLoS Genetics*, 17(7): e1009656, jul 2021. ISSN 15537404. doi: 10.1371/journal.pgen.1009656. URL https://dx.plos.org/10.1371/journal.pgen.1009656.

Whittle, E. E., Legood, S. W., Alav, I., Dulyayangkul, P., Overton, T. W., and Blair, J. M. Flow cytometric analysis of efflux by dye accumulation. *Frontiers in Microbiology*, 10:2319, 2019. ISSN 1664302X. doi: 10.3389/fmicb.2019.02319. URL http://www.ncbi.nlm.nih.gov/pubmed/31636625\http://www.pubmedcentral.nih.gov/articlerender.fcgi?artid=PMC6787898.

Wick, R. R., Schultz, M. B., Zobel, J., and Holt, K. E. Bandage: Interactive visualization of *de novo* genome assemblies. *Bioinformatics*, 31(20): 3350–3352, oct 2015. ISSN 14602059. doi: 10.1093/bioinformatics/btv383. URL https://academic.oup.com/bioinformatics/article-lookup/doi/10.1093/bioinformatics/btv383.

Wick, R. R., Judd, L. M., Gorrie, C. L., and Holt, K. E. Completing bacterial genome assemblies with multiplex MinION sequencing. *Microbial Genomics*, 3 (10), 2017a. ISSN 20575858. doi: 10.1099/mgen.0.000132. URL https://github.com/rrwick/Bacterial-genome-assem-.

Wick, R. R., Judd, L. M., Gorrie, C. L., and Holt, K. E. Unicycler: Resolving bacterial genome assemblies from short and long sequencing reads. *PLoS Computational Biology*, 13(6):e1005595, jun 2017b. ISSN 15537358. doi: 10.1371/journal.pcbi.1005595. URL https://dx.plos.org/10.1371/journal.pcbi.1005595.

Wickham, H. *ggplot2: Elegant graphics for data analysis*. Springer, 2016. ISBN

9780387981413. doi: 10.18637/jss.v035.b01. URL https://ggplot2.tidyverse.org.

Wilkinson, M. G. Flow cytometry as a potential method of measuring bacterial viability in probiotic products: A review, 2018. ISSN 09242244. URL https://doi.org/10.1016/j.tifs.2018.05.006.

Wilson, C., Lukowicz, R., Merchant, S., Valquier-Flynn, H., Caballero, J., Sandoval, J., Okuom, M., Huber, C., Brooks, T. D., Wilson, E., Clement, B., Wentworth, C. D., and Holmes, A. E. Quantitative and qualitative assessment methods for biofilm growth: A mini-review. *Research reviews. Journal of engineering and technology*, 6(4), dec 2017. ISSN 2319-9873. URL http://www.ncbi.nlm.nih.gov/pubmed/30214915\http://www.pubmedcentral.nih.gov/articlerender.fcgi?artid=PMC6133255\http://www.ncbi.nlm.nih.gov/pubmed/30214915%0Ahttp://www.pubmedcentral.nih.gov/articlerender.fcgi?artid=PMC6133255.

Wingender, J., Szewzyk, U., Steinberg, P., Rice, S. A., Flemming, H.-C., and Kjelleberg, S. Biofilms: An emergent form of bacterial life. *Nature Reviews Microbiology*, 14(9):563–575, sep 2016. ISSN 1740-1526. doi: 10.1038/nrmicro.2016.94. URL http://www.nature.com/articles/nrmicro.2016.94.

Wiser, M. J. and Lenski, R. E. A comparison of methods to measure fitness in *Escherichia coli*. *PLoS ONE*, 10(5):e0126210, 2015. ISSN 19326203. doi: 10.1371/journal.pone.0126210. URL http://www.ncbi.nlm.nih.gov/pubmed/25961572http://www.pubmedcentral.nih.gov/articlerender.fcgi?artid=PMC4427439.

Woods, L. C., Gorrell, R. J., Taylor, F., Connallon, T., Kwok, T., and McDonald, M. J. Horizontal gene transfer potentiates adaptation by reducing selective constraints on the spread of genetic variation. *Proceedings of the National Academy of Sciences of the United States of America*, 117(43):26868–26875, oct 2020. ISSN 10916490. doi: 10.1073/pnas.

2005331117. URL http://www.ncbi.nlm.nih.gov/pubmed/33055207\http://www.pubmedcentral.nih.gov/articlerender.fcgi?artid=PMC7604491.

World Health Organization. *Global action plan on antimicrobial resistance*. World Health Organization, Geneva PP - Geneva, 2015. ISBN 9789241509763. URL https://apps.who.int/iris/handle/10665/193736.

Wyres, K. and Holt, K. Regional differences in carbapenem-resistant *Klebsiella pneumoniae*. *The Lancet Infectious Diseases*, 22(3):309–310, mar 2022. ISSN 14733099. doi: 10.1016/s1473-3099(21)00425-4. URL https://www.sciencedirect.com/science/article/abs/pii/S1473309921004254.

Wyres, K. L. and Holt, K. E. *Klebsiella pneumoniae* as a key trafficker of drug resistance genes from environmental to clinically important bacteria, oct 2018. ISSN 18790364. URL https://www.sciencedirect.com/science/\article/pii/S1369527418300225.

Wyres, K. L., Wick, R. R., Judd, L. M., Froumine, R., Tokolyi, A., Gorrie, C. L., Lam, M. M., Duchêne, S., Jenney, A., and Holt, K. E. Distinct evolutionary dynamics of horizontal gene transfer in drug resistant and virulent clones of *Klebsiella pneumoniae*. *PLoS Genetics*, 15(4):e1008114, apr 2019. ISSN 15537404. doi: 10.1371/journal.pgen.1008114. URL http://dx.plos.org/10.1371/journal.pgen.1008114.

Wyres, K. L., Lam, M. M., and Holt, K. E. Population genomics of *Klebsiella pneumoniae*, feb 2020a. ISSN 17401534. URL http://www.nature.com/articles/s41579-019-0315-1.

Wyres, K. L., Nguyen, T. N., Lam, M. M., Judd, L. M., Van Vinh Chau, N., Dance, D. A., Ip, M., Karkey, A., Ling, C. L., Miliya, T., Newton, P. N., Lan, N. P. H., Sengduangphachanh, A., Turner, P., Veeraraghavan, B., Vinh, P. V., Vongsouvath, M., Thomson, N. R., Baker, S., and Holt, K. E. Genomic surveillance for hypervirulence and multi-drug resistance in invasive *Klebsiella pneumoniae*

from South and Southeast Asia. *Genome Medicine*, 12(1):11, dec 2020b. ISSN 1756994X. doi: 10.1186/s13073-019-0706-y. URL https://genomemedicine.biomedcentral.com/articles/10.1186/s13073-019-0706-y.

Xu, L., Sun, X., and Ma, X. Systematic review and meta-analysis of mortality of patients infected with carbapenem-resistant *Klebsiella pneumoniae*. *Annals of Clinical Microbiology and Antimicrobials*, 16 (1):18, mar 2017. ISSN 14760711. doi: 10.1186/s12941-017-0191-3. URL http://www.ncbi.nlm.nih.gov/pubmed/28356109\http://www.pubmedcentral.nih.gov/articlerender.fcgi?artid=PMC5371217.

Xu, M., Fu, Y., Fang, Y., Xu, H., Kong, H., Liu, Y., Chen, Y., and Li, L. High prevalence of KPC-2-producing hypervirulent *Klebsiella pneumoniae* causing meningitis in Eastern China. *Infection and Drug Resistance*, 12:641–653, 2019. ISSN 11786973. doi: 10.2147/IDR.S191892. URL http://www.ncbi.nlm.nih.gov/pubmed/30936727\http://www.pubmedcentral.nih.gov/articlerender.fcgi?artid=PMC6430001.

Yang, F., Deng, B., Liao, W., Wang, P., Chen, P., and Wei, J. High rate of multiresistant *Klebsiella pneumoniae* from human and animal origin. *Infection and Drug Resistance*, 12:2729–2737, 2019. ISSN 11786973. doi: 10.2147/IDR.S219155. URL http://www.ncbi.nlm.nih.gov/pubmed/31564923\http://www.pubmedcentral.nih.gov/articlerender.fcgi?artid=PMC6731983.

Yang, F., Tian, X., Han, B., Zhao, R., Li, J., and Zhang, K. Tracking high-risk β-lactamase gene (*bla* gene) transfers in two Chinese intensive dairy farms. *Environmental Pollution*, 274:116593, apr 2021. ISSN 18736424. doi: 10.1016/j.envpol.2021.116593. URL https://www.sciencedirect.com/science/article/abs/pii/\S0269749121001718?dgcid=rss_sd_all.

Yigit, H., Queenan, A. M., Anderson, G. J., Domenech-Sanchez, A., Biddle, J. W., Steward, C. D., Alberti, S., Bush, K., and Tenover, F. C. Novel

carbapenem-hydrolyzing β-lactamase, KPC-1, from a carbapenem-resistant strain of *Klebsiella pneumoniae*. *Antimicrobial Agents and Chemotherapy*, 45(4): 1151–1161, apr 2001. ISSN 00664804. doi: 10.1128/AAC.45.4.1151-1161.2001. URL http://www.ncbi.nlm.nih.gov/pubmed/11257029http://www.pubmedcentral.nih.gov/articlerender.fcgi?artid=PMC90438.

Yong, D., Toleman, M. A., Giske, C. G., Cho, H. S., Sundman, K., Lee, K., and Walsh, T. R. Characterization of a new metallo-β-lactamase gene, $bla_{\text{NDM-1}}$, and a novel erythromycin esterase gene carried on a unique genetic structure in *Klebsiella pneumoniae* sequence type 14 from India. *Antimicrobial Agents and Chemotherapy*, 53(12):5046–5054, dec 2009. ISSN 00664804. doi: 10.1128/AAC.00774-09. URL https://journals.asm.org/doi/10.1128/AAC.00774-09.

Yoshioka, Y., Ohtsubo, H., and Ohtsubo, E. Repressor gene *finO* in plasmids R100 and F: Constitutive transfer of plasmid F is caused by insertion of IS*3* into F *finO*. *Journal of Bacteriology*, 169(2): 619–623, feb 1987. ISSN 00219193. doi: 10.1128/jb.169.2.619-623.1987. URL http://www.ncbi.nlm.nih.gov/pubmed/3027040\http://www.pubmedcentral.nih.gov/articlerender.fcgi?artid=PMC211823.

Zankari, E., Hasman, H., Cosentino, S., Vestergaard, M., Rasmussen, S., Lund, O., Aarestrup, F. M., and Larsen, M. V. Identification of acquired antimicrobial resistance genes. *Journal of Antimicrobial Chemotherapy*, 67(11):2640–2644, nov 2012. ISSN 03057453. doi: 10.1093/jac/dks261. URL http://www.ncbi.nlm.nih.gov/pubmed/22782487\http://www.pubmedcentral.nih.gov/articlerender.fcgi?artid=PMC3468078.

Zatyka, M. and Thomas, C. M. Control of genes for conjugative transfer of plasmids and other mobile elements. *FEMS Microbiology Reviews*, 21(4): 291–319, feb 1998. ISSN 1574-6976. doi: 10.1111/j.1574-6976.1998.tb00355.x. URL https://academic.oup.com/femsre/article-lookup/doi/10.1111/j.1574-6976.1998.tb00355.x.

Zeng, X. and Lin, J. Beta-lactamase induction and cell wall metabolism in Gram-negative bacteria. *Frontiers in Microbiology*, 4(MAY):128, 2013. ISSN 1664302X. doi: 10.3389/fmicb.2013.00128. URL `http://www.ncbi.nlm.nih.gov/pubmed/23734147\http://www.pubmedcentral.nih.gov/articlerender.fcgi?artid=PMC3660660`.

Chapter 8

Appendices

8.1 Appendix 1 - Chapter 2

Table S1: Antibiotic stock preparation

Compound	Solvent	Stock concentration (µg/mL)
Ampicillin (sodium salt)	Sterile distilled water (SDW)	10,000
Chloramphenicol	Ethanol	100,000
Doripenem hydrate (powder)	SDW	5000
Hygromycin B	SDW	50,000
Kanamycin disulfate	SDW	10,000

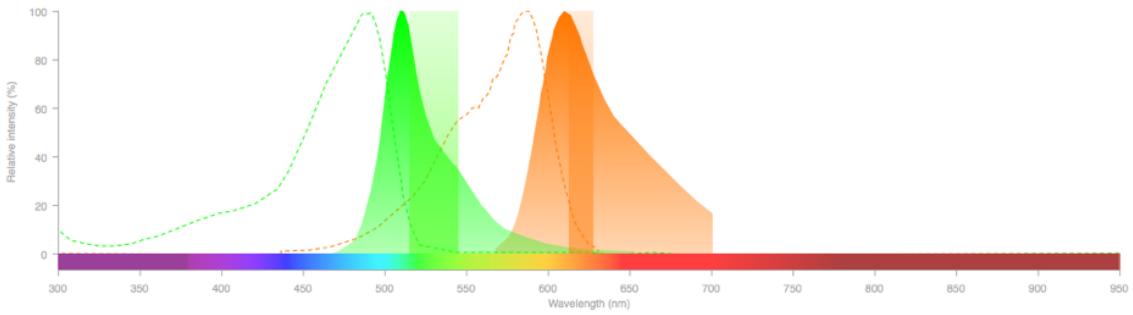

Figure S1: ThermoFisher Fluorescence SpectraViewer image of (excitation and) emission spectra for GFP and mCherry fluorophores shows limited overlap. Dotted and filled curves represent excitation and emission wavelengths respectively. Band-pass filter settings are displayed as filled boxes overlaying the curves.

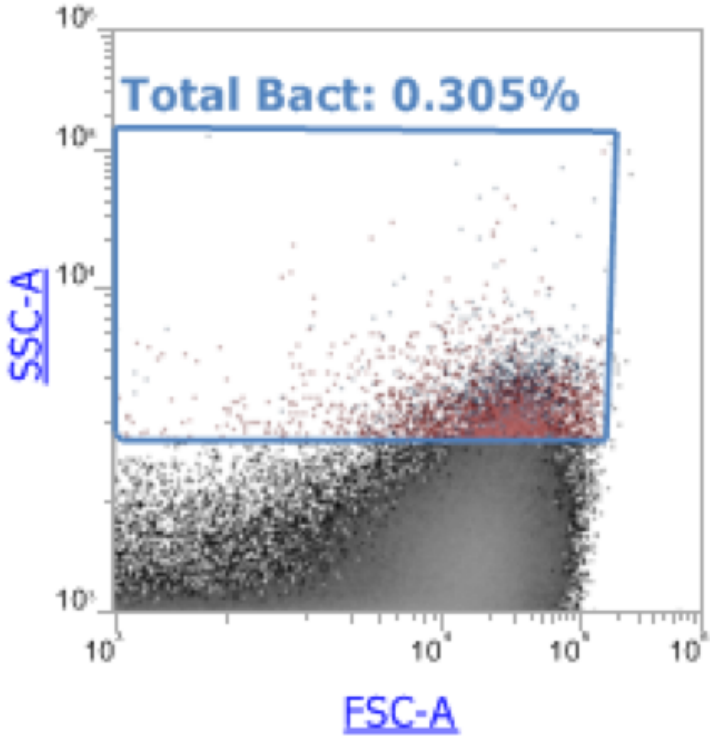

Figure S2: Placement of the 'total bacteria' gate for acquisition of events on the Attune NxT Flow cytometer. Example screenshot taken from Attune NxT software.

Figure S3: bla_{SHV} from KP1 chromosomal sequence (pink highlight) plus 400 bp upstream and downstream sequence. Portions of forward and reverse recombineering primers with homology to this region are in bold-underlined and italic-underlined text respectively. The forward check primer for the hygromycin cassette insertion is in bold purple text.

GATCTGAATTGCTATGTTTAGTGAGTTGTATCTATTTATTTTTCAATAAATACAATTGGTTATGT
GTTTTGGGGGCGATCGTGAGGCAAAGAAAACCCGGCGCTGAGGCCGGGTTAAGAGTTGGTAGCTC
TTGATCCGGCAAACAAACCACCGCTGGTAGCGGTGGTTTTTTTGTTTGCAAGCAGCAGATTACGC
GCAGAAAAAAAGGATCTCAAGAAGATCCTTTGATCTTTTCTACGGGGTCTGACGCTCAGTGGAAC
GAAAACTCACGTTAAG**GGATTTTGGTCATGAGATTA**TCAAAAAGGATCTTCACCTAGATCCTTTT
AAATTAAAAATGAAGTTTTAAATCAATCTAAAGTATATATGAGTAAACTTGGTCTGACAGCTATT
CCTTTGCCCTCGGACGAGTGCTGGGGCGTCGGTTTCCACTATCGGCGAGTACTTCTACACAGCCA
TCGGTCCAGACGGCCGCGCTTCTGCGGGCGATTTGTGTACGCCCGACAGTCCCGGCTCCGGATCG
GACGATTGCGTCGCATCGACCCTGCGCCCAAGCTGCATCATCGAAATTGCCGTCAACCAAGCTCT
GATAGAGTTGGTCAAGACCAATGCGGAGCATATACGCCCGGAGCCGCGGCGATCCTGCAAGCTCC
GGATGCCTCCGCTCGAAGTAGCGCGTCTGCTGCTCCATACAAGCCAACCACGGCCTCCAGAAGAA
GATGTTGGCGACCTCGTATTGGGAATCCCCGAACATCGCCTCGCTCCAGTCAATGACCGCTGTTA
TGCGGCCATTGTCCGTCAGGACATTGTTGGAGCCGAAATCCGCGTGCACGAGGTGCCGGACTTCG
GGGCAGTCCTCGGCCCAAAGCATCAGCTCATCGAGAGCCTGCGCGACGGACGCACTGACGGTGTC
GTCCATCACAGTTTGCCAGTGATACACATGGGGATCAGCAATCGCGCATATGAAATCACGCCATG
TAGTGTATTGACCGATTCCTTGCGGTCCGAATGGGCCGAACCCGCTCGTCTGGCTAAGATCGGCC
GCAGCGATCGCATCCATGGCCTCCGCGACCGGCTGCAGAACAGCGGGCAGTTCGGTTTCAGGCAG
GTCTTGCAACGTGACACCCTGTGCACGGCGGGAGATGCAATAGGTCAGGCTCTCGCTGAATTCCC
CAATGTCAAGCACTTCCGGAATCGGGAGCGCGGCCGATGCAAAGTGCCGATAAACATAACGATCT
TTGTAGAAACCATCGGCGCAGCTATTTACCCGCAGGACATATCCACGCCCTCCTACATCGAAGCT
GAAAGCACGAGATTCTTCGCCCTCCGAGAGCTGCATCAGGTCGGAGACGCTGTCGAACTTTTCGA
TCAGAAACTTCTCGACAGACGTCGCGGTGAGTTCAGGCTTTTTCAT**ACTCTTCCTTTTTCAATAT**
TATTGAAGCATTTATCAGGGTTATTGTCTCATGAGCGGATACATATTTGAATG

Figure S4: Hygromycin resistance cassette (1483 bp) produced by PCR amplification of the pSIM18 sequence. The forward (green highlight) and reverse (blue highlight) portions of the recombineering primers with homology to the hygromycin cassette are displayed. The *bla* promoter from pSIM18 is indicated (bold sequence in black text). The hygromycin resistance gene from pSIM18 (blue text) is indicated with stop and start codons underlined. The reverse check primer for insertion of the cassette is shown (purple bold text).

Figure S5: Predicted final sequence after recombineering where *bla*$_{\text{SHV}}$ has been interrupted by insertion of the hygromycin cassette from pSIM18. Sequence (400 bp) upstream and downstream of original *bla* gene is included Forward (purple bold lowercase text) and reverse (purple bold uppercase text) check primers for the cassette are shown. Forward and reverse recombineering primers are indicated, with the portions homologous to the cassette highlighted in green (forward orientation) and blue (reverse orientation) respectively, and the regions homologous to the chromosome indicated in adjacent bold black text. Pink highlighted text corresponds to the remaining *bla*$_{\text{SHV}}$ chromosomal sequence. The size of the inserted cassette is predicted to be 1562 bp (including primer sequences which are retained).

8.2 Appendix 2 - Chapter 3

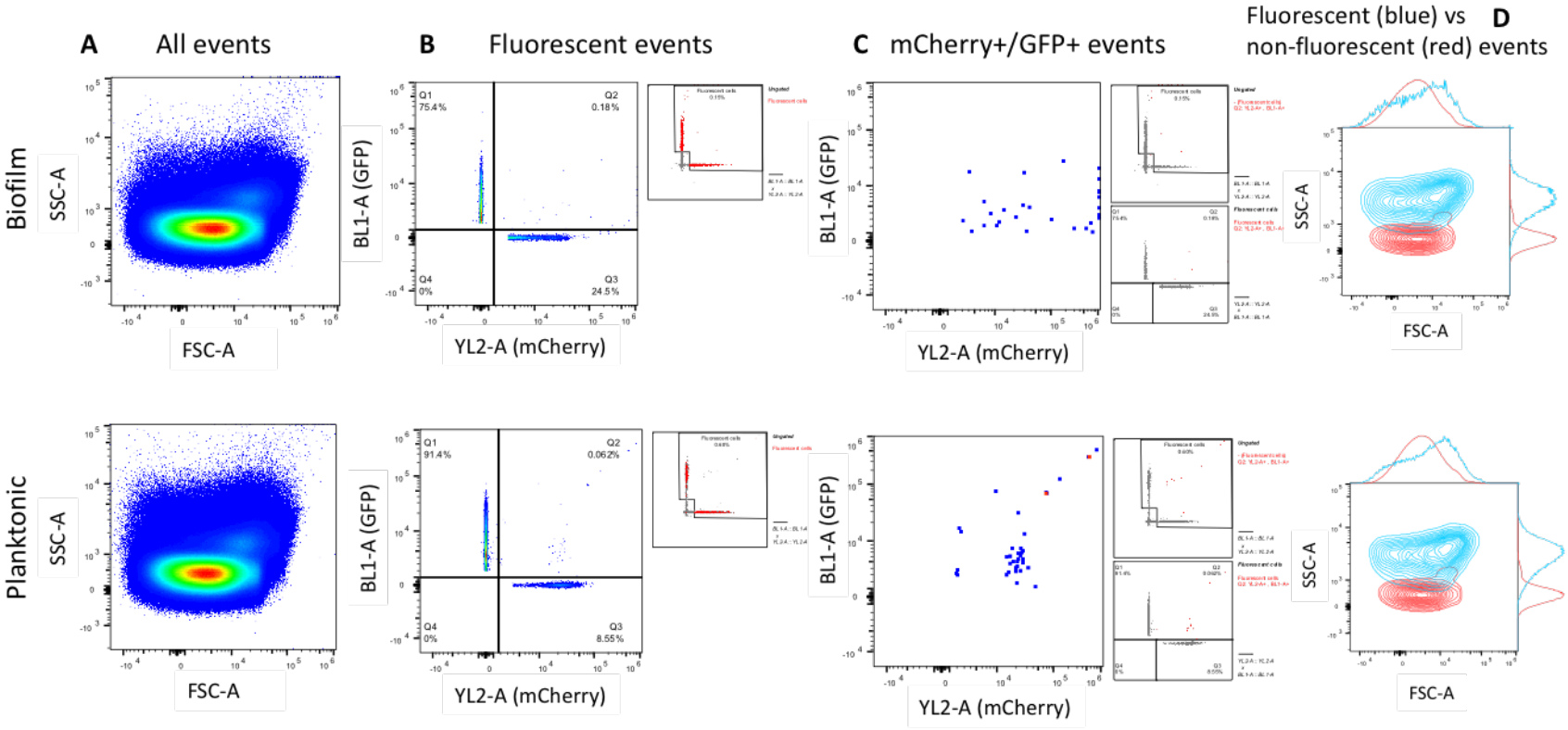

Figure S6: Using fluorescence profiles to direct 250 µL sample data analysis of planktonic and biofilm populations where donors contain pKpQIL*gfp* and recipients express *mcherry*. Gating strategy for selecting the fluorescent population from the total population for 6-well assay biofilms (top) and planktonic cells (bottom). Backgating is displayed in the small plots to indicate rationale. (A) 'All events' are displayed. (B) The 'fluorescent events' are selected from the total events. (C) The 'mCherry+/GFP+ events' are selected from the total fluorescent population. (D) 'Fluorescent (blue) and non-fluorescent (red) events' are superimposed. Example plots from a single biological replicate diluted 1:20,000 in PBS. Events acquired for 250 µL volume, rather than based on event number in the 'total bacteria' gate.

8.3 Appendix 3 - Chapter 4

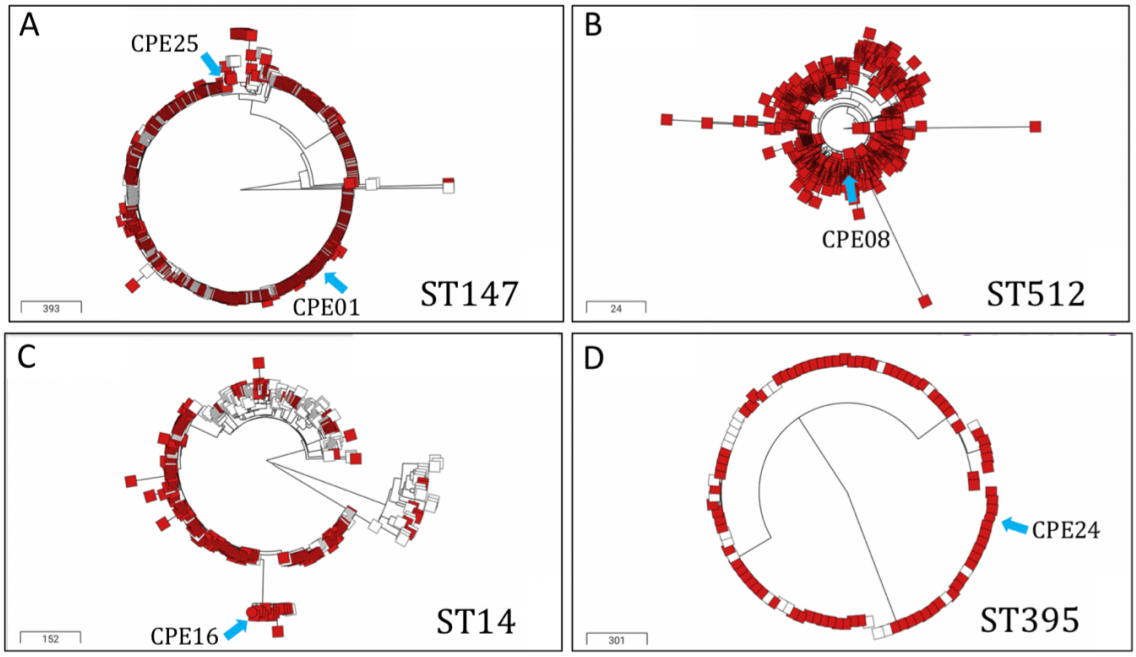

Figure S7: Phylogenetic trees (core-distance neighbour-joining; constructed by Pathogenwatch (https://pathogen.watch) using PhyloCanvas (https://www.phylocanvas.gl/) of CPE isolates and Sequence Type collections from Pathogenwatch (30/11/21 search for all available examples of each ST). Scales indicate nucleotide substitutions per site. (A) CPE01 and CPE25 alongside publicly-available examples of ST147. (B) CPE08 alongside publicly-available examples of ST512. (C) CPE16 alongside publicly-available examples of ST14. (D) CPE24 alongside publicly-available examples of ST395.

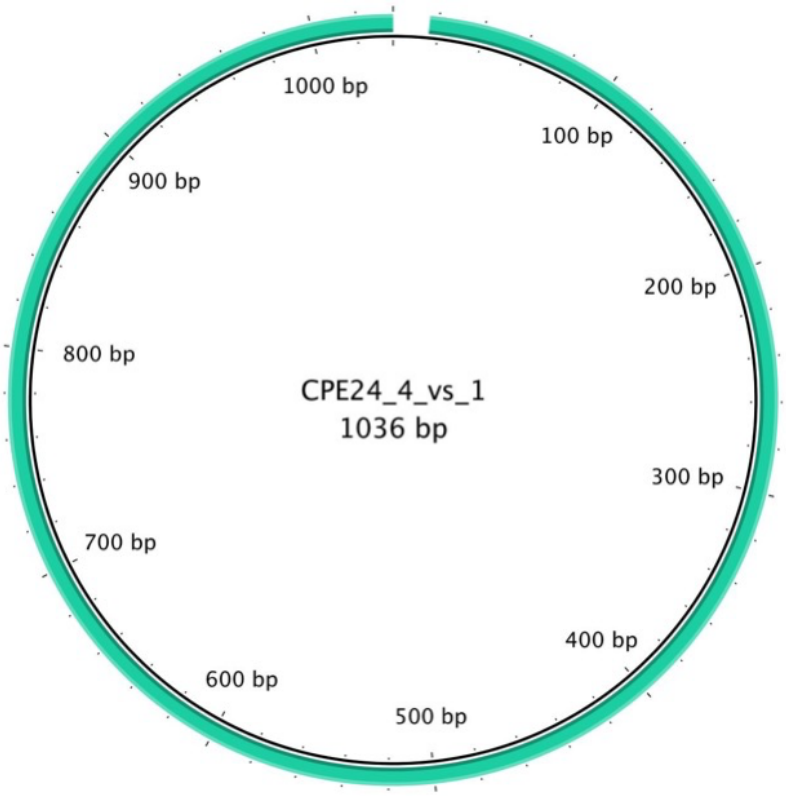

Figure S8: Region of CPE24 contig 1 (black line) corresponding to CPE24 contig 4 (green line, 100% identity on BLASTn). The break in the green line illustrates where there is no matching sequence of 100% identity. Image generated using BRIG (Alikhan *et al.*, 2011)

8.4 Appendix 4 - Chapter 5

Table S2: Reference versus measured MIC values for ATCC 25922 used as a control strain. All measured values were within one doubling dilution of the expected value. Reference values obtained from (Andrews, 2001). These represent the expected values for this strain. N/A indicates not applicable

Agent	**ATCC 25922 MIC (mg/L)**	
	Reference	**Measured**
Aztreonam	0.25	<0.25
Benzalkonium Chloride	N/A	32
Carbenicillin	N/A	16
Cefotaxime	0.06	0
Chloramphenicol	4	4
Ciprofloxacin	0.015	0
Clindamycin hydrochloride	N/A	128
Crystal violet	N/A	16
Erythromycin	N/A	64
Ethidium bromide	N/A	256
Fusidic acid	N/A	512
Gentamicin	0.5	<1
Meropenem	0.008	<1
Methylene Blue	N/A	>1024
Moxifloxacin	0.03	0
Nalidixic Acid	4	4
Novobiocin	N/A	32
Rhodamine 6G	N/A	1024
Rifampicin	N/A	8
Tetracycline disodium salt	2	1
Ticarcillin	N/A	16

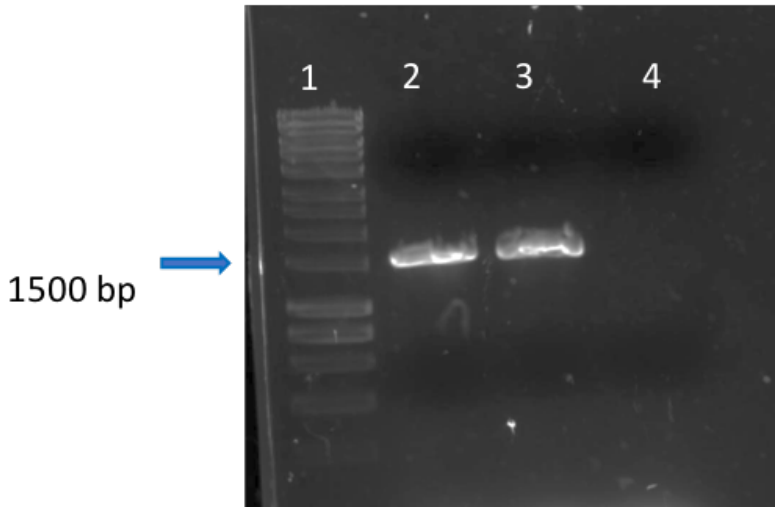

Figure S9: Check of amplified cassette from pSIM18. (1) Ladder (Hyperladder^{TM} 1 kb). (2-3) Candidate cassette DNA. (4) Negative control (no DNA). Expected band size 1483 bp. Arrow indicates ladder reference band.

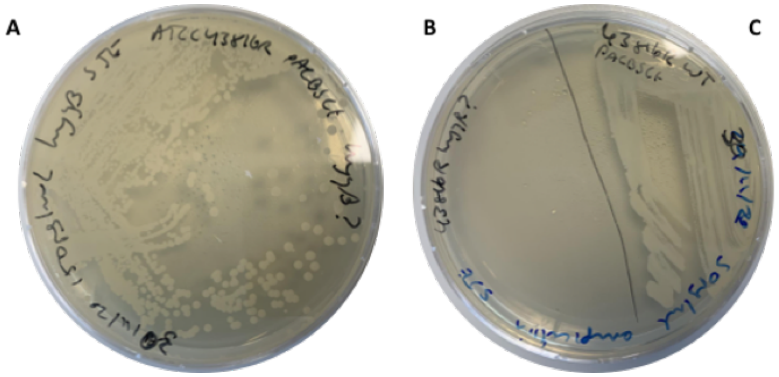

Figure S10: Growth of candidate KP20 colony and the WT strain KP1 on a selection of antibiotics. Comparison of susceptibility profiles of 43816R pACBSCE and candidate 43816R pACBSCE cassette containing colony on agar plates. (A) Candidate 43816R pACBSCE cassette-containing colony susceptibility to hygromycin B (150 µg/mL). (B) Candidate 43816R pACBSCE cassette-containing colony susceptibility to ampicillin (50 µg/mL). (C) 43816R pACBSCE susceptibility to ampicillin (50 µg/mL).

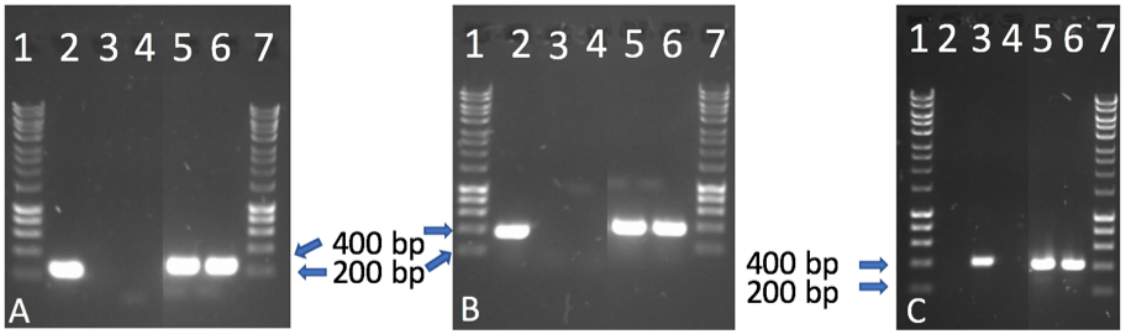

Figure S11: Biofilm KP20pCPE16 transconjugant validation. Colony PCR check of transconjugant colonies using primers targeting (A) a replicon on the pCPE16_3 carbapenem resistance plasmid (expected size 231 bp), (B) the NDM carbapenem resistance gene on pCPE16_3 (expected size 392 bp) and (C) the KP20 chromosome (expected size 413 bp). 1,7) Ladder (2) Donor control (3) Recipient control (4) Negative control (no DNA) (5,6) KP20pCPE16 colonies. Arrows indicate ladder reference band sizes.

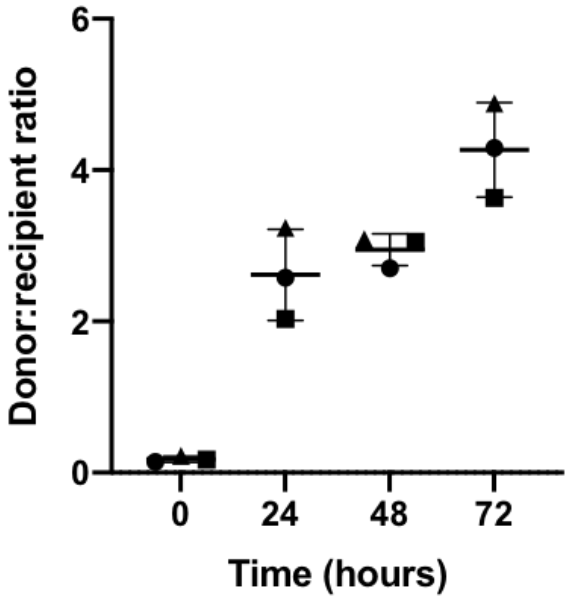

Figure S12: Mean donor:recipient ratios (CPE16:KP20) over time in biofilm conjugation assays. N = three experimental replicates, each the mean of four biological replicates. Error bars represent standard deviation from the mean.

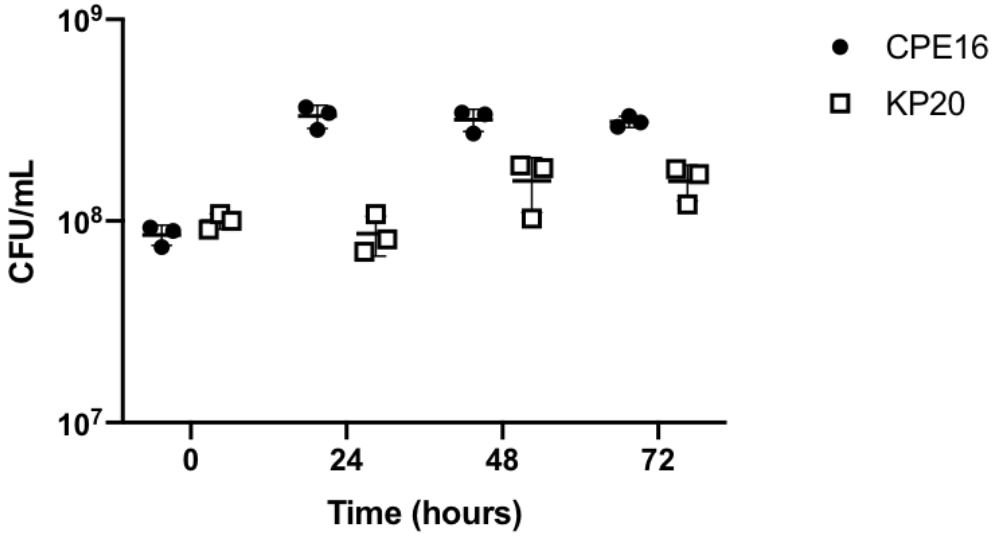

Figure S13: CPE16 and KP20 in mixed populations over time during the biofilm conjugation experiments. Mean CFU/mL for single strains at each time point during the assay. Comparing CPE16 and KP20 CFU/mL at 0 h, $P = 0.13$. By 24 h, $P = 0.0009$ for this comparison (unpaired t-test). N = three experimental replicates, each the mean of four biological replicates (apart from for 24 h in one replicate where three biological replicates of KP20 were plated). Error bars illustrate standard deviation from the mean.

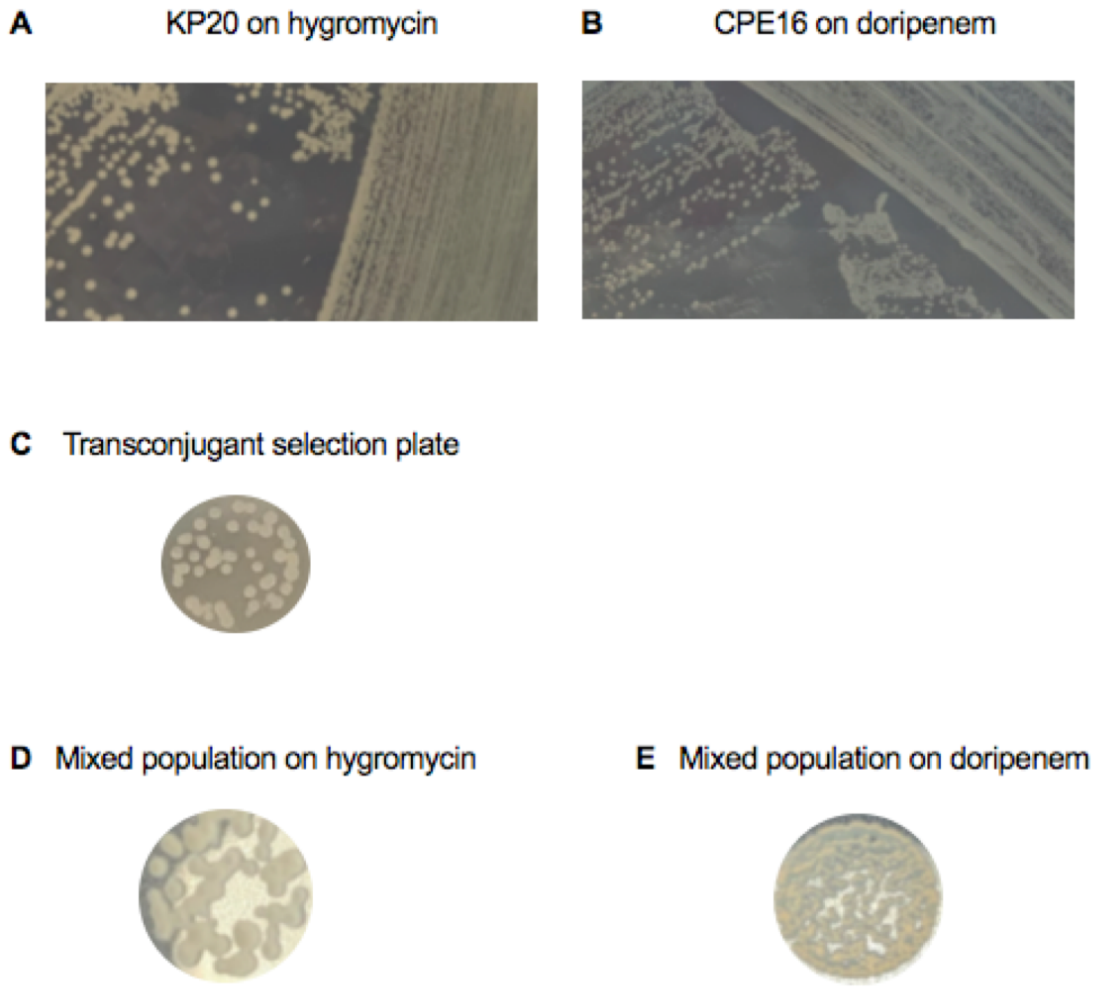

Figure S14: Morphology comparisons of the (A) KP20 recipient, (B) CPE16 donor, (C) putative transconjugant colonies and (D, E) the mixed population. Recipient colonies, putative transconjugants and the mixed population on hygromycin are all opaque, larger and not light-reflective when compared to the donor colonies and the mixed population on doripenem which are translucent and small.

8.5 Appendix 5 - Chapter 6

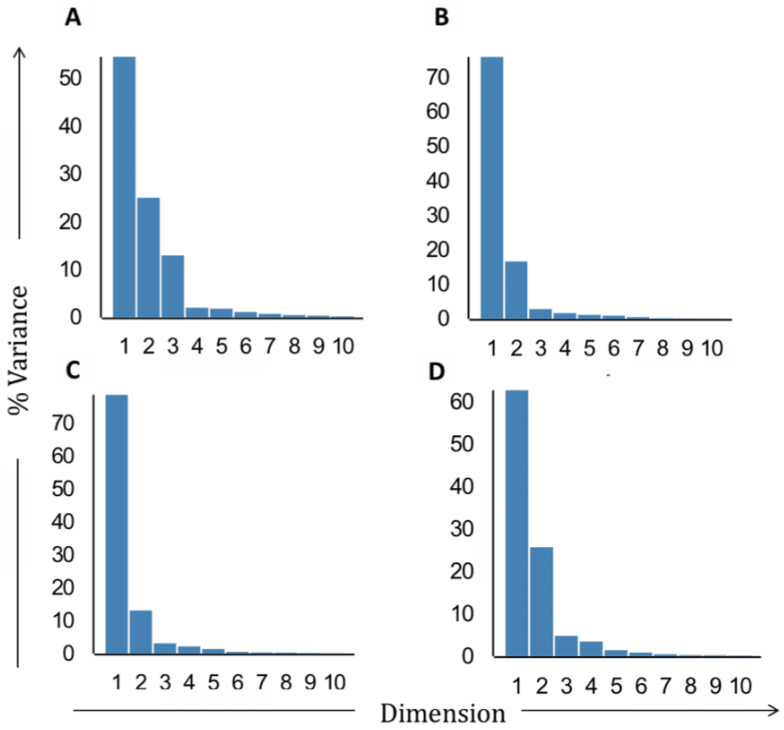

Figure S15: Percentage variance within MDS plot dimensions in Figure 1. (A) All samples, grouped by lifestyle, are compared to all other samples. (B) Planktonic exponential samples are plotted alongside planktonic 24 h samples. (C) Planktonic exponential samples are plotted alongside biofilm 24 h samples. (D) Planktonic 24 h samples are plotted alongside 24 h biofilm samples. Visualisation from Degust v4.1.1 (Powell, 2019).